The importance of IκBNS and Ca^{2+} signaling in DLBCL development

Dissertation

der Mathematisch-Naturwissenschaftlichen Fakultät
der Eberhard Karls Universität Tübingen
zur Erlangung des Grades eines
Doktors der Naturwissenschaften
(Dr. rer. nat.)

vorgelegt von
M. Sc. Marc Brändle
aus Sindelfingen

Tübingen
2017

Gedruckt mit Genehmigung der Mathematisch-Naturwissenschaftlichen Fakultät der Eberhard Karls Universität Tübingen.

Tag der mündlichen Qualifikation:	15.02.2018
Dekan:	Prof. Dr. Wolfgang Rosenstiel
1. Berichterstatter:	Dr. Stephan Hailfinger
2. Berichterstatter:	Prof. Dr. Klaus Schulze-Osthoff

Abstract

Diffuse large B-cell lymphoma (DLBCL) is an aggressive disorder of mature B-lymphocytes presenting with 40% of novel lymphoma cases worldwide the most common subtype of adult Non-Hodgkin lymphoma. DLBCL is characterised by a high degree of heterogeneity regarding clinical, pathologic and molecular genetic issues. Gene expression profiling revealed distinct molecular DLBCL subtypes resembling germinal centre B-cells (GCB DLBCL) and activated B-cells (ABC DLBCL). Despite advances in therapy, the 3-year progression free survival rates of GCB and ABC DLBCL upon immunochemotherapy are still at 74% and 40%, respectively. Consequently, there is an obvious need for identifying new molecular targets and biomarkers serving as starting points to develop new, more efficient therapeutic strategies especially of the adverse ABC DLBCL subtype.

In the present study we were able to demonstrate that IκBNS is constitutively expressed in ABC DLBCL cell lines and human biopsies, whereas IκBNS expression is absent in GCB DLBCL. We noticed that two IκBNS isoforms were detectable, the described p35 and a second larger IκBNS isoform exhibiting an additional N-terminal unstructured portion. Silencing of IκBNS led to a reduced growth of ABC DLBCL cell lines, suggesting an oncogenic function of IκBNS. Promoter studies suggested that IκBNS expression is under the control of NF-κB and NFAT signalling. Interestingly, we detected constitutive activation of NFAT in DLBCL cell lines, which was necessary to drive the expression of IκBNS in ABC DLBCL. Calcineurin inhibitors, which decrease the activity of NFAT proteins, did not only impair the expression of IκBNS, but also induced cell death in multiple ABC DLBCL cell lines. The expression of the pro-survival cytokines IL-6/-10 was markedly reduced by calcineurin inhibition, which might at least partially explain their toxicity in ABC DLBCL cell lines. With the help of phosphoproteomics, we identified several new calcineurin substrates in ABC DLBCL, including CD79, suggesting a more central role of calcineurin in tumorigenesis.

Taken together, these results provide first insights into the essential function of IκBNS in the development of ABC DLBCL. Furthermore, we suggest IκBNS as a promising biomarker to discriminate ABC from GCB DLBCL. Finally, we propose that calcineurin inhibitors could have therapeutic potential for the treatment of aggressive ABC DLBCL.

Zusammenfassung

Das diffus großzellige B-Zell-Lymphom (DLBCL) ist eine aggressive Erkrankung reifer B-Lymphozyten. Diese ist mit einem Anteil von bis zu 40% an allen weltweit neu auftretenden Lymphomen der am häufigsten auftretende Subtyp der adulten Non-Hodgkin Lymphome. DLBCL sind durch ein hohes Maß an Heterogenität hinsichtlich klinischer, pathologischer und molekular genetischer Aspekte charakterisiert. Genexpressionsanalysen haben verschiedene molekulare DLBCL Subtypen aufge-deckt, die Keimzentrums-B-Zellen (GCB DLBCL) und aktivierten B-Zellen ähneln (ABC DLBCL). Trotz Fortschritten in der DLBCL-Therapie, liegt das 3-Jahres progressionsfreie Über-leben nach einer Immunchemotherapie noch immer bei 74% für GCB DLBCL und lediglich 40% für ABC DLBCL. Es besteht somit ein offensichtlicher Bedarf an der Identifizierung neuer therapeutischer Ziele und Biomarker, die als Ausgangspunkt der Entwicklung neuer Behandlungsstrategien vor allem des ungünstigeren ABC DLBCL Subtypes dienen.

Diese Arbeit zeigt, dass IκBNS ausschließlich im ABC DLBCL Subtyp exprimiert ist. Interessanterweise konnten zwei IκBNS-Isoformen detektiert werden. Zum einen war die in der Literatur bereits beschriebene p35 Form zu sehen, zum anderen eine längere Isoform, die sich durch einen zusätzlichen unstrukturierten N-Terminus auszeichnet.

Wenn die Expression von IκBNS durch shRNA verhindert wurde, reagierten die ABC DLBCL Zelllinien mit einem verlangsamten Zellwachstum. Dies lässt eine onkogene Funktion von IkBNS vermuten. Mit Hilfe von Promotoranalysen konnte NFAT als essentieller Transkriptionsfaktor für die IkBNS Expression identifiziert werden. Überraschenderweise war eine konstitutive NFAT Aktivierung in allen DLBCL Zelllinien nachweisbar. Die Hemmung der NFAT Aktivität durch Calcineurin-Inhibitoren erniedrigte nicht nur die IkBNS Expression, sondern induzierte zudem Zelltod in mehreren ABC DLBCL Zelllinien. Die IL-6/-10 Expression, die das Wachstum der Krebszellen fördert, war durch Calcineurin-Inhibitoren stark erniedrigt.

Eine Analyse des Phosphoproteoms mit MS deckte neue Calcineurin-Substrate in ABC DLBCL Zellen auf. Unter anderem konnte CD79 identifiziert werden, was auf eine zentrale Rolle von Calcineurin in den onkogenen DLBCL Signalwegen impliziert.

Zusammenfassend bietet diese Arbeit erste Erkenntnisse über die Rolle des IκBNS Proteins in der Entwicklung von ABC DLBCL. Die IκBNS Expression in Tumorzellen könnte ein vielversprechender Biomarker sein, um GCB und ABC DLBCL histologisch einfach voneinander zu unterscheiden. Die gewonnenen Ergebnisse legen ferner nahe, dass die Anwendung von Calcineurin Inhibitoren eine nützliche Option in zukünftigen Behandlungsstrategien von ABC DLBCL mit bestimmten Mutationsmustern sein könnte.

Table of Contents

Abbreviations

aa	amino acid
ABC	Activated B-cell like
AKAP79	A-kinase anchor protein
ANK	Ankyrin repeat
AP-1	Activator protein-1
APC	Antigen Presenting Cell
APS	Ammonium persulfate
ARD	Ankyrin repeat domain
ARE	Antioxidant-response element
B2M	β2-microglobulin
BAD	Bcl-2-associated death promoter
BAFF	B cell activating factor
BAFF-R	B-cell activating factor receptor
BCAP	B cell adaptor for phosphoinositide 3-kinase
Bcl	B cell lymphoma
BCR	B-cell Receptor
BIRC	Baculoviral IAP repeat containing
BLK	B lymphoid tyrosine kinase
BLNK	B-cell linker protein
BSA	Bovine serum albumin
BTK	Bruton's Tyrosine Kinase
bZIP	Basic Leucine Zipper
C/EBPβ	CCAAT/enhancer binding protein β
CABIN1	Calcineurin-binding protein 1
CaM	Calmodulin
CBM	CARD11, BCL10 and MALT1
CC	Coiled-coil
CCL	CC-chemokine ligand
CCND1	CyclinD1
CD	cluster of differentiation
CD40L	Cluster of differentiation 40 ligand
ChIP	Chromatin immunoprecipitation
cIAP	Cellular inhibitor of apoptosis
CIITA	class II, major histocompatibility complex, transactivator
CIN85	Cbl-interacting protein of 85 kDa
CK1	Casein kinase1
CLIP	Class II-associated Ii peptide
c-Maf	v-Maf musculoaponeurotic fibrosarcoma oncogene homolog
CML	Chronic myelogenous (or myeloid or myelocytic) leukemia (CML)
cMyc	Avian myelocytomatosis virus oncogene cellular homolog
CnA/B	Calcineurin subunit A / B
COPD	Chronic pulmonary obstructive diseases
CRAC	calcium-release-activated calcium
CRE	cAMP-responsive element
CREB	cAMP response element-binding protein
CSP	Calcipressin
DAG	Diacylglycerol
dATP	2′-Deoxyadenosine 5′-triphosphate
DBD	DNA binding domain
DC	Dendritic cell
DD	Death-Domain
DLBCL	Diffuse Large B-cell Lymphoma
DMEM	Dulbecco's modified eagle medium
DMSO	Dimethyl sulfoxide
DNA	Deoxyribonucleic acid
dNTP	2'-Deoxynucleoside 5'-triphosphate
DOK	Downstream of kinase
DRiPS	Defective ribosomal products
dsDNA	Double-stranded deoxyribonucleic acid
dsRNA	Double-stranded ribonucleic acid
DTT	Dithiothereitol
DYRK	Dual-specificity tyrosine-phosphorylation regulated kinase
E2F	E2 Transcription Factor
EAE	Experimental allergic encephalomyelitis
ECL	Enhanced chemoluminiscence

ECM	Extracellular matrix
EDTA	Ethylenediaminetetraacetic acid
ELISA	Enzyme-linked immuno sorbent assay
ER	Endoplasmic reticulum
ERAD	ER associated protein degradation
ERK	Extracellular signal–regulated kinase
EZH2	Histone H3 lysine 27 methyltransferase enhancer of zeste homolog 2
FACS	Fluorescence-activated cell sorting
FCS	Fetal calf serum
FcγRIIB-1	Low affinity immunoglobulin gamma Fc region receptor II-b
FITC	Fluorescein isothiocyanate
FOXP	Forkhead box P
GADS	GRB2-related adaptor downstream of Shc
GAPDH	Glyceraldehyde-3-phosphate dehydrogenase
GCB	Germinal center B-cell like
G-CSF	Granulocyte colony-stimulating factor
GEF	Guanine nucleotide exchange factor
GM-CSF	Granulocyte macrophage colony-stimulating factor
GPCR	G protein–coupled receptor
GRB2	Growth factor receptor-bound protein 2
GRR	Gylcine rich region
GSK3β	Glycogen synthase kinase 3 beta
GST	Glutathione S-transferase
GTP	Guanosine-5'-triphosphate
HAT	Histone acetyltransferase
HDACs	Histone deacetylases
HEPES	4-(2-Hydroxyethyl)piperazine-1-ethanesulfonic acid
HLA	Human leukocyte antigen
HLH	Helix-Loop-Helix
HRP	Horseradish peroxidase
I	Ionomycin
IFNα/β/γ	Interferon α/β/γ
Ig	Immunoglobulin
IHC	Immunohistochemistry
IKK	IκB kinase
IL	Interleukin
IP	Immunoprecipitation
IP-10	Interferon gamma-induced protein 1
IP3	Inositol 1,4,5-trisphosphate
IRAK	IL-1R-associated kinase
IRF	Interferon Regulatory Factor
ITAM	Immunoreceptor tyrosine-based activation motif
ITIM	Immunoreceptor tyrosine-based inhibition motif
iTreg	Induced regulatory T cells
IκB	Inhibitor of κB/inhibitor of NF-κB
IκBNS	Nuclear factor of kappa light polypeptide gene enhancer in B-cells inhibitor, delta
JAK	Janus-associated kinase
JDP	Jun dimerization protein
JNK	c-Jun amino-terminal kinase
JNK/SAPK	c-Jun N-terminal kinases/ Stress-activated protein kinase
kDa	Kilo Dalton
LAT	Linker of Activated T-cells
LCK	Lymphocyte-specific protein tyrosine kinase
LPS	Lipopolysaccharide
LPS	Lipopolysaccharides
LTβ	Lymphotoxin β
LUBAC	Linear ubiquitin chain assembly complex
LYN	Lck/Yes novel tyrosine kinase
LZ	Leucine-Zipper
MAIL	Molecule possessing ankyrin repeats induced by lipopolysaccharide
MAPK	Mitogen-activated protein kinase
MARE	MAF-recognition elements
MCL	Mantle Cell Lymphoma
MCMV	Murine cytomegalovirus
MCP(-1)	Monocyte chemoattractant protein(-1)
M-CSF	Macrophage colony-stimulating factor
MDC	Macrophage-derived chemokine

MDM2	Mouse double minute 2
MEF	Mouse embyrionic fibroblast
MHCI	Major histocompatibility complex 1
MHCII	Major histocompatibility complex 2
MIP-1α	Macrophage Inflammatory Protein
MiR	microRNA
MS	Mass spectrometry
mTOR	Mammalian Target Of Rapamycine
MUM1	Multiple Myeloma Oncogene 1
MyD88	Myeloid differentiation primary response protein 88
NEMO	NF-κB essential modulator
NFAT	nuclear factor of activated T-cells
NF-κB	Nuclear factor kappa light chain enhancer of activated B cells
NHL	Non-Hodgkin-Lymphoma
NIK	NF-κB-inducible kinase
NLS	Nuclear localisation signal
NP-40	Nonidet P-40
NRON	Non-coding repressor of NFAT
P/I	PMA and Ionomycin
PAMP	Pathogen-associated molecular pattern
PAX5	Paired box protein 5
CARD11	Caspase recruitment domain-containing protein 11
PBS	Phosphate-buffered saline
PCR	Polymerase chain reaction
PD-1	Programmed cell death protein 1
PE	Phycoerythrin
PH	Pleckstrin homology domain
PI3K	Phosphoinositide 3 kinase
PIP2	Phosphatidylinositol 4,5-bisphosphate
PIP3	Phosphatidylinositol (3,4,5)-trisphosphate
PKC	Protein kinase C
PLC	Phospholipase-C
PMA	Phorbol 12-myristate 13-acetate
PMBL	Primary Mediastinal B-cell lymphoma
PPAR	peroxisome proliferator-activated receptors
PRDM1	PR domain zinc finger protein 1
PRDM1 (BLIMP-1)	PR domain zinc finger protein 1
PTEN	Phosphatase and Tensin homolog
PTM	Posttranslational modification
qPCR	Quantitative polymerase chain reaction
qRT-PCR	Quantitative reverse transcription-polyermase chain reaction
Rac/Rho	Ras homologue/ Ras-related C3 botulinum toxin substrate 1
RAF1	rapidly accelerated fibrosarcoma
RANKL	Receptor activator of nuclear factor κB ligand
R-CHOP	Rituximab-Cyclophosphamide,Hydroxydaunorubicin, Vincristine(Oncovin™), and Prednisone
RHD	Rel homology domain
RHD	REL homology domain
RING	Really interesting new gene
RNA	Ribonucleic acid
ROR	Related orphan receptor
ROS	Reactive oxygen species
RT	Reverse transcription
RTK	Receptor tyrosine kinase
RU	Relative units
S/T	Serine/Threonine
SD	Standard deviation
SDS	Sodium dodecyl sulphate
SDS-PAGE	Sodium dodecyl sulphate polyacrylamide gel electrophoresis
SEM	Standard error of the mean
SFK	Src-Family Kinase
SHIP	SH2 domain-containing inositol 5'-phosphatase 1
SHP	SH2 domain-containing phosphatase
SLP	SH2-domain-containing leukocyte protein
SOCE "	store operated Ca2+ entry
SOS	Son of sevenless
Src	Sarcoma
SRR	serine rich region

STAT	Signal transducers and activators of transcription
STIM	Stromal interaction molecule
SYK	Spleen Tyrosine Kinase
TAB	TAK1-binding protein
TAD	Transactivation domain
TAE	Tris acetic acid EDTA
TAK1	TGF-β-activated kinase 1
T-ALL	T-cell acute lymphoblastic leukaemia
TAP	Transporter associated with antigen processing
TBK1	TRAF family member-associated NF-κB activator TANK-binding kinase
TBS	Tris-buffered saline
TBS/T	Tris-buffered saline/polysorbat 20
TCR	T-cell Receptor
TEMED	Tetramethylethylenediamine
TGFβ	Transforming growth factor β
TIR	Toll/IL-1R
TLR	Toll-like receptor
TNFSFRs	Tumor necrosis factor superfamily receptors
TNF-α	Tumour necrosis factor-α
TonEBP	Tonicity enhancer binding protein
TOP	Thimet oligopeptidase
TRAF	TNF receptor-associated factor
TRAF	TNF-receptor-associated factor
TRAM	TRIF-related adaptor molecule
TRE	TPA-responsive element
Treg	Regulatory T cells
Tris	Tris(hydroxymethyl)aminomethane
Tween	Polysorbat 20
UTR	Untranslated region
VCAM	Vascular cell adhesion molecule
VEGF	Vascular endothelial growth factor
WT	Wild-type
XBP1s	X-box binding protein 1
ZAP-70	Zeta-chain (TCR) associated protein kinase 70 kDa
ZF	Zinc-Finger
κB site	NF-κB binding site

1. Introduction

The following chapters provide the required background knowledge of the topics that are relevant for the understanding of this study. Chapter 1.1 introduces the characteristics and molecular abnormalities of the different subtypes of diffuse large B-cell lymphoma (DLBCL) and mantle cell lymphoma (MCL). Moreover, it also covers the function and relevance of intracellular NF-κB inhibitors with a particular focus on the atypical NF-κB inhibitor IκBNS. The ensuing Chapter 1.2 focuses on the components, relevance, the molecular characteristics and signaling of transcription factor families that are involved in B-cell lymphoma genesis and are part of investigations conducted in this study. The subsequent chapter 1.3 describes the antigen-receptor signaling pathways of B- and T-cells. Lastly, Chapter 1.4 deals with MHCI and II molecules, their structure, assembly, function and what is known so far about their role in DLBCL.

1.1 B-cell lymphoid malignancies

1.1.1 Diffuse large B-cell lymphoma (DLBCL)

DLBCL account for 30% to 40% of all adult lymphoid malignancies world-wide and are therefore the most common form of Non-Hodgkin's lymphoma (The Non-Hodgkin's Lymphoma Classification Project, 1997; Coiffier et al., 1997). The disease can be observed at any age and is evenly distributed between genders (Armitage et al., 1998). The median age of onset is the seventh decade of life whereby 60% of patients are older than 60 years at diagnosis (Groves et al., 1995). Notably, there are considerable differences between ethnicities concerning the average age of disease onset, as African Americans in the United States are diagnosed at younger ages (Shenoy et al., 2011; Sinha et al., 2013). As the name "Diffuse large B-cell lymphoma" already implies it is a hematologic disorder of mature large B lymphoid cells (mean diameter ≥20 µm), growing diffusely. Most commonly the neoplastic B-cells eliminate the normal underlying lymph node architecture, thereby frequently causing rapidly swelling of lymph nodes. Up to 40% of patients exhibit extranodal primary lymphoma sites whereby the most common spots are the gastrointestinal tract, head and neck, skin and soft tissue and the genitourinary system (Hunt and Reichard, 2008; Castillo et al., 2014). Untreated, the median life expectancy of DLBCL patients is less than one year, indicating the aggressive nature of DLBCL (Sinha et al., 2013). The CHOP regime including Cyclophosphamide,

Hydroxydaunorubicin, Vincristine (Oncovin™) and Prednisone was first applied in the 1970s has been considered as the standard chemotherapeutic therapy approach for DLBCL. CHOP treatment was found to have an impact in only 40% to 50% of elderly DLBCL patients and results in an overall survival of 35% to 40% (Sonneveld et al., 1995). The CHOP based chemotherapy was complemented in 1997 by the introduction of the immunochemotherapeutic IgG1 monoclonal antibody Rituximab targeting the pan-B-cell marker CD20. The administration of the new R-CHOP therapy for initial DLBCL treatment improved complete response rates and prolongs progression-free and overall survival significantly in elderly DLBCL patients notably without excess of toxicity and is for these now the standard of care (Coiffier et al., 2002; Feugier, 2015). Despite this advance in treatment still nearly 40% of patients eventually die of relapsed or refractory DLBCL (Vaidya and Witzig, 2014). DLBCL are characterised by a high degree of heterogeneity in respect of clinical presentation and courses, pathology, morphology, molecular abberations and treatment response (Sinha et al., 2013; Carbone et al., 2014; Castillo et al., 2014). The wide spectrum of this single diagnostic category can be partially explained by the distinct molecular features of the tumors revealed by the investigation of DLBCL tumor samples using cDNA microarrays. Three distinct DLBCL disease entities were discovered by gene expression profiling (GEP) differing in their treatment outcomes after standard chemotherapy regimens, thus defining prognostic categories (Alizadeh et al., 2000). The newly established DLBCL subtypes seem to be derived from different stages in B-cell maturation as they exhibit gene expression patterns of non-transformed cells at different stages in B-cell differentiation. Alizadeh et al. used this distinctiveness in gene expression patterns to subdivide DLBCL and named the most common major DLBCL subtypes after the differentiation status of their cell of origin namely the germinal B-cell like (GCB) DLBCL subtype with accounting for 17% of B-cell malignancies, the activated B-cell like (ABC) DLBCL subtype making up 15% of B-cell malignancies. The primary mediastinal B-cell lymphoma (PMBL) accounting for 6% of B-cell malignancies, was defined as the third molecular DLBCL entity and named after the site of its manifestation.

1.1.1.1 GCB DLBCL

The germinal centre (GC) B-cell is the non-cancerous counterpart of the GCB DLBCL subtype. Patients suffering from GCB DLBCL show a drastically better 3-year overall survival rate with approximately 80% than patients diagnosed with the so called ABC DLBCL subtype with approximately 45% under R-CHOP regimen therapy (Lenz et al., 2008). On the molecular level the as GCB subtype classified lymphoma are characterised by the overexpression of several genes common for germinal centre B-cells such as the BCL6, LMO2 and the surface markers CD10 and CD38 (Schuetz et al., 2012; Alizadeh et al., 2000). For an overview of the molecular characteristics of GCB DLBCL see Figure 1. BCL6, a transcriptional repressor is expressed at high levels in mature B-cells within the germinal centre. BCL6 binds regulatory regions of several thousand genes in germinal centre B-cells and constitutes hence a well-established germinal centre marker. Hence, BCL6 is a master transcriptional regulator in germinal center B-cell differentiation and is constitutively expressed due to chromosomal translocation or mutations altering its promoter region in 45% of DLBCL cases that cause a deregulation of BCL6 expression (Lo Coco et al., 1994; Migliazza et al., 1995). For instance, BCL6 represses genes afflicted in inflammatory processes such as STAT1, important for interferon (IFN) response or the expression of the chemokines IL-10 and CCL3 (Toney et al., 2000). Moreover, BCL6 was revealed to have a crucial role in the regulation of apoptosis in GC B-cells. It acts as direct transcriptional of the anti-apoptotic BCL2 protein repressor by suppressing MIZ1 triggered BCL2 expression. However, this repressor function of BCL6 over BCL2 was found to be lost in DLBCL due to promoter mutations and chromosomal translocations of BCL2 and the deregulation of MIZ1 (Saito et al., 2009; Ci et al., 2009). Furthermore, BCL6 was reported by Phan et al. (2004) to be an active repressor of p53 expression in germinal center B-cells by binding to two specific sequences within the p53 promoter. Consequently, high levels of BCL6 as present in germinal center B-cells were found by Phan et al. to protect the cells from DNA-damage induced apoptosis by functional inactivation of p53. Thus, deregulated BCL6 expression as in GCB DLBCL contributes considerably to lymphomagenesis by the inactivation of p53. Additionally, important for cancerogenesis as well, is the property of BCL6 to repress pivotal cell-cycle regulators such as the cyclin-dependent kinase (CDK) inhibitors p21 and p27kip1. With this, BCL-6 enables unregulated cell-cycle progression

(Shaffer et al., 2000; Phan et al., 2005). The histone H3 lysine 27 methyltransferase enhancer of zeste homolog 2 (EZH2) is highly upregulated in GC derived B-cells and thus constitutively activated in GC-derived NHL. Morin et al. (2010) discovered a recurrent somatic EZH2 missense mutation in 21, 7% of investigated cases GCB DLBCL in exon 15 of the EZH2 gene exchanging tyrosine 641 for a histidine. The mutation is located in the catalytic component of the enzyme and responsible for adding methyl groups to substrates. The Y641H amino acid substitution is leading to reduced enzymatic turnover in vitro. Functionally, EZH2 cooperates with BCL6 by regulating the BCL6 repressor function on a subset of target genes in GC B-cells, probably mediating the GC B-cell phenotype and under aberrant conditions inducing lymphomagenesis of GC origin such ach GCB DLBCL (Caganova et al., 2013). Moreover, EZH2 impairs GC responses and silences BLIMP1 a major factor for terminal maturation to plasmocytes. Béguelin et al. (2013) proved in mice bearing DLBCL xenografts and in primary human DLBCLs that the combinatorial administration of BCL6 and EZH2 inhibitors synergistically kills DLBCL. The chromosomal translocation t(14; 18)(q32; q21) is reported to be associated with the GCB gene expression profile and CD10 expression and thus present in roughly 30% to 40% of all GCB DLBCL cases. This chromosomal abnormality brings the locus of the anti-apoptotic gene BCL2 under the regulatory control of the heavy-chain locus leading to BCL2 overexpression and simultaneous relieve of BCL6 repression (Zhang et al., 2011). The BCL2 gene was also found to be the most commonly mutated gene in GCB DLBCL. GC B-cells and their malignant counterparts of the GCB DLBCL subtype show only very minor activity of NF-κB due, in part, to the overexpression of the NF-κB negative regulator BCL2 and the fact that BCL6 inhibits the expression of p50 and was also observed to colocalise with RelA unfolding repressive transcriptional activity on various NF-κB target genes (Grimm et al., 1996; Shaffer et al. 2001; Li et al., 2005; Schuetz et al., 2012). Also contributing to GCB DLBCL pathogenesis is the frequent heterogeneous deletion of PTEN in ~10% and the complete loss of PTEN expression in 55% of GCB DLBCL as revealed by IHC (Pfeifer et al., 2013). The PTEN phosphatase is the major negative regulator of the PI3K/AKT pathway, is inversely correlated with p-AKT levels and was described to be crucial for growth, proliferation and survival of a subset of GCB DLBCL. Cells exhibiting PTEN loss were found to be addicted to PI3K/AKT signaling. Moreover, also the proto-oncogene MYC plays a crucial role

in GCB DLBCL. The loss of PTEN in GCB DLBCL and the subsequent constitutive PI3K/AKT signaling lead by the inhibition of GSK3β to the up regulation of MYC which is important for proliferation. Thus, the ectopic expression of PTEN in PTEN-deficient GCB DLBCL induced toxicity as PI3K/AKT signaling is consequently diminished and MYC expression reduced. Therefore, GCB DLBCL showing PTEN loss are suggested to be vulnerable to PI3K/AKT inhibition (Pfeifer et al., 2013; Roschewski et al., 2014). Noteworthy as well, for understanding GCB DLBCL lymphomagenesis is the microRNA cluster miR-17-92 which is amplified and overexpressed in 12,5% of GCB DLBCL cases but never in ABC DLBCL. miR-17-92 expression results in elevated MYC and related targets expression (Lenz et al., 2008). Murine cells expressing miR-17-92 also display down modulation of PTEN in turn leading to enhanced PI3K/AKT signaling and the repression of p21 altogether leading to promotion of cell growth and anti-apoptotic signaling (Xiao et al., 2008; Inomata et al., 2009; Olive et al., 2009).

a

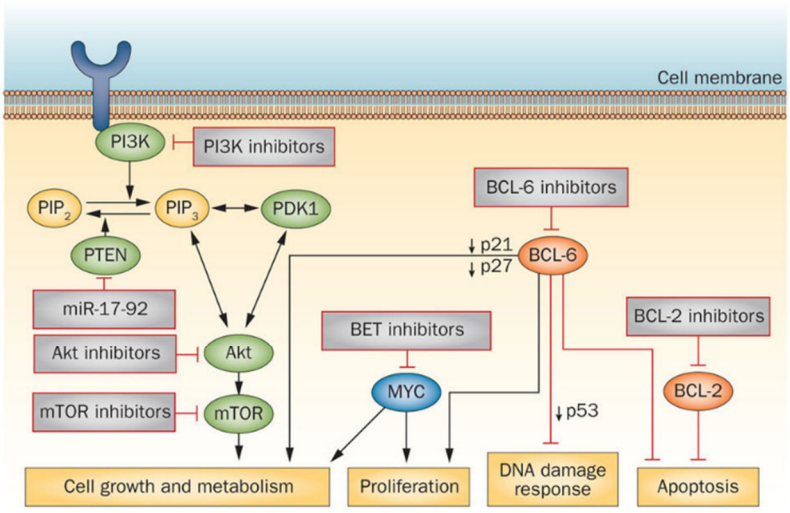

b

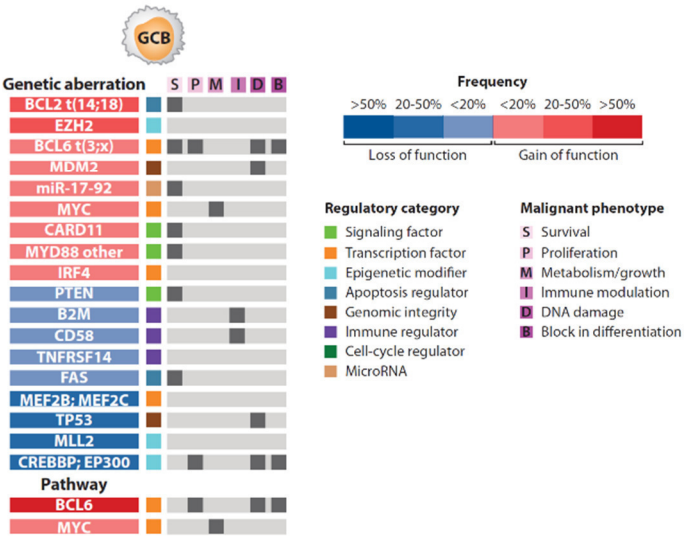

Figure 1. Overview of key signaling pathways affected and characteristic genetic aberrations involved in GCB DLBCL pathogenesis. **(a)** Signaling pathways afflicted in the pathogenesis of GCB DLBCL. Illustrated are possible targets for therapy approaches of GCB DLBCL by small molecule inhibitors (Figure adapted from: Roschweski et al., 2014). **(b)** Summary of recurrent genetic aberrations and deregulated pathways found in GCB DLBCL. Depicted on the right-hand site, the frequency of the distinct molecular abnormalities, if they are loss or gain of function, in which regulatory category they belong and to what kind of malignant phenotype they lead (Figure adapted from: Shaffer et al., 2012).

1.1.1.2 ABC DLBCL

ABC DLBCL derive from B-cells at the plasmablastic differentiation stage. This DLBCL entity shows a more aggressive behaviour than the GCB subtype, thus exhibiting a distinctly inferior cure rate of 40% in 2015 (Roschweski et al., 2015). The major molecular hallmark of ABC DLBCL subtype is the constitutively active classical NF-κB signaling sustaining viability, proliferation and anti-apoptotic signaling contributing to the lymphoma's aggressiveness and poor outcome of therapeutic approaches (Frick et al., 2011). An overview of recurrent genetic aberrations and signaling pathways such as NF-κB that are implicated in ABC DLBCL lymphomagenesis is depicted in Figure 2. As found by Davis et al. in 2001, the transduction of a dominant negative IκBα or IKKβ inhibiting NF-κB signaling is selectively toxic for ABC DLBCL cell lines what was indicating an addiction of ABC DLBCL to NF-κB activation. The permanent NF-κB activity is achieved by multiple molecular mechanisms in upstream signaling (Figure 2). A participation of B-cell receptor (BCR) signaling in the pathomechanistic context of ABC DLBCL was first revealed by an RNAi screen showing a toxic impact of shRNAs directed against CARD11, BCL10 and MALT1, the core components of the CBM complex (Ngo et al., 2006). The ternary complex serves as a signaling hub and is required to activate IKKβ downstream of the BCR, thus relaying signals from the BCR to the classical NF-κB pathway (Ngo et al., 2006). Hence, the CBM complex is critical for antigen receptor induced activation of classical NF-κB signaling. CARD11, also known as CARMA1, is a multidomain protein adapter. It functions as a signaling scaffold in the CBM complex, coordinating the activation of the NF-κB positive regulator IKKβ (Rawlings et al., 2006). Approximately 10% of ABC DLBCL cases harbour somatic activating mutations of CARD11 such as G1116S and L244P leading to increased NF-κB pathway activity independent from upstream BCR signaling (Lenz et al., 2008). The linear ubiquitin chain assembly complex (LUBAC) is associated with the CBM complex.Single nucleotide polymorphisms in the LUBAC subunit RNF31, especially enriched in ~8% of ABC DLBCL augment the ability of LUBAC to attach linear ubiquitin to IKKγ, thereby enhancing NF-κB signaling and consequently promoting the survival of the ABC DLBCL (Yang et al., 2014). Since IKKγ ubiquitination is required for IKK activation the knock down of LUBAC complex components is fatal for ABC DLBCL (Yang et al., 2014; Dubois et al., 2014). A RNA interference screen conducted by Davis et al. (2010) proved the Bruton's tyrosine

kinase (BTK) as an essential element for survival of ABC DLBCL with wild type CARD11 proteins. Moreover, the study also revealed that the shRNA mediated knockdown of the heavy and light chain of BCR, the components of the BCR co-receptor heterodimer CD79A/B and downstream BCR signaling key signaling molecules SYK, BLNK, PLCγ2, PKCβ results in the death of wild-type CARD11 bearing ABC DLBCL cell lines. In addition to that, Davis et al also identified CD79A/B ITAM sequences to be mutated in 21, 1% of ABC DLBCL and only in 3,1% in GCB DLBCL cases. In 18% of investigated ABC DLBCL biopsies, CD79B was mutated in the membrane-proximal ITAM tyrosine (Y) residue, whereas CD79A mutations occurred rarely in only 2,9% of examined biopsies. For instance, the ABC DLBCL model cell lines HBL-1 and TMD8 harbour a heterozygous missense mutation affecting the first tyrosine of the CD79B ITAM Y196F and Y196H, respectively. The ITAM mutations were shown to reduce the activity of the BCR signaling negative regulator LYN and to promote increased BCR surface expression. Together with the finding of the vital importance of more distal BCR signaling elements such as BTK or PKCβ these findings suggest that chronic active BCR signaling is a key mechanism in ABC DLBCL with wild type CARD11 resulting in constitutively active NF-κB signaling. Besides BCR signaling, a second signaling pathway was uncovered to contribute to constantly active NF-κB. Ngo et al. (2011) describe the dependence of ABC DLBCL cell lines on MYD88 which was observed to be mutated in 39% of ABC DLBCL, and the associated kinases IRAK1/4. MYD88 is a signaling adapter downstream of toll like receptors (TLRs) activating NF-κB upon ligand engagement of TLRs. Among the ABC DLBCL MYD88 mutations, the Ngo group describes an ABC DLBCL exclusive gain-of-function driver mutation. With a frequency of 29% this single amino acid exchange, L265P, located in the MYD88 Toll/IL-1 receptor domain, constitutes the most common MYD88 mutation in ABC DLBCL cases. Functionally, this particular L265P mutation led to promoted cell survival by IRAK1/4 assembly and activation in turn leading to NF-κB signalling, IFN-β production and by JAK/STAT3 mediated signaling the secretion of IL-6, IL-10 and. Notably, 34% of ABC DLBCL cases harbouring a MYD88 L265P mutation also exhibited a coincident mutation of CD79B/A and in some cases the MYD88 L265P mutation was coincident with CARD11 mutation. Thus, MYD88, CD79A/B and CARD11 mutations are not exclusive and can be observed in one tumor or the respective model cell lines like HBL1 (MYD88 L265P;

CD79B Y196F), TMD8 (MYD88 L265P; CD79B Y196H) or OCI-LY3 (MYD88 L265P; CARD11 L244P). Furthermore, Ngo et al. observed that the knock down of MYD88 in addition to shRNA mediated knockdown of CD79B or CARD11 in ABC cells lines, addicted to chronic active BCR signaling enhanced the killing of cells harbouring a combination of the earlier described mutations. This suggests a non-redundant synergising effect of aberrant BCR and MYD88 signalling in order to maintain ABC DLBCL survival. Additional NF-κB signaling promoting factors reported in the ABC DLBCL subtype is for instance the inactivation of the NF-κB negative regulatory, ubiquitin editing enzyme A20. Roughly 30% of ABC DLBCL patients exhibit biallelic A20 inactivation by mutations and/or deletions and epigenetic silencing of the A20 encoding gene (Compagno et al., 2009). Moreover, the TAB2-associated TGF-β-activated kinase (TAK1) was described to be mutated in the ABC DLBCL cell line U2932 and in 5% of patient derived samples (Compagno et al., 2009; Fontan et al., 2012). TAK1 is recruited and activated by TAB1 which in turn is recruited by TRAF6 upon TLR stimulation and subsequent MYD88 and IRAK1/4 activation. TAK1 promotes cell survival through activation of NF-κB signaling downstream of the CBM complex and the adaptor protein MYD88 by the phosphorylation of IKKβ and is therefore an essential mediator of proliferation and cytokine secretion (Wang et al., 2001; Sun et al., 2004 Moreno-García et al., 2013; Ansel et al., 2014).

Apart from NF-kB signaling there are several other proteins and signaling pathways afflicted in the molecular pathogenesis of ABC DLBCL. As already mentioned, ABC DLBCL derive from B-cells that are in the transition to become plasma cells. This maturation is blocked by several genetic aberrations in ABC DLBCL that for instance finally lead to the inactivation of the PRDM1 gene and its expression product BLIMP-1 (Rosenwald et al., 2002; Frick et al., 2011; Shaffer et al., 2012). Roughly one quarter of ABC DLBCL samples show inactivating truncations, nonsense and splice site mutations, deletions or epigenetically silencing of the PRDM1 gene encoding one master regulator of further cell differentiation, “the transcriptional repressor and plasmacytic differentiation driver B lymphocyte-induced maturation protein-1” (BLIMP-1) (Pasqualucci et al. 2006; Tam et al. 2006). This transcription factor orchestrates the transformation into plasma cells by shutting down mature B-cell gene expression programs for example the expression of PAX5 and SPIB and the exit of cell cycle (Shaffer et al., 2002). SPIB and its DNA binding

partner IRF4 are both highly expressed in ABC DLBCL and critical for ABC DLBCL survival as revealed by an RNAi screen (Yang et al., 2012). Also BCL6 which is a BLIMP-1 repressor as well, is found to be affected by translocations observable in 25% of ABC DLBCL patients (Iqbal et al., 2007; Tunyaplin et al., 2004; Shaffer et al., 2000). The ETS family transcription factor SPIB which is repressed by BLIMP-1 is highly expressed in ABC DLBCL and represses in turn BLIMP-1 constituting a negative feedback loop (Shapiro-Shelef et al., 2005; Lenz et al., 2008; Schmidlin et al., 2008). Together, SPIB and its DNA binding partner IRF4 which is highly expressed since it is induced by constitutively active NF-κB signaling are crucial for the expression of CARD11 (Young et al., 2015). In this manner NF-κB signaling, IRF4/SPIB and CARD11 shape a positive feedback loop pivotal for ABC DLBCL survival (Shaffer et al., 2012; Young et al., 2015). Furthermore, they act together in repressing cell cycle arrest and apoptosis promoting type I interferon response secretion in ABC DLBCBL that is induced by MYD88 signaling (Stark et al., 1998; Yang et al., 2012).

a

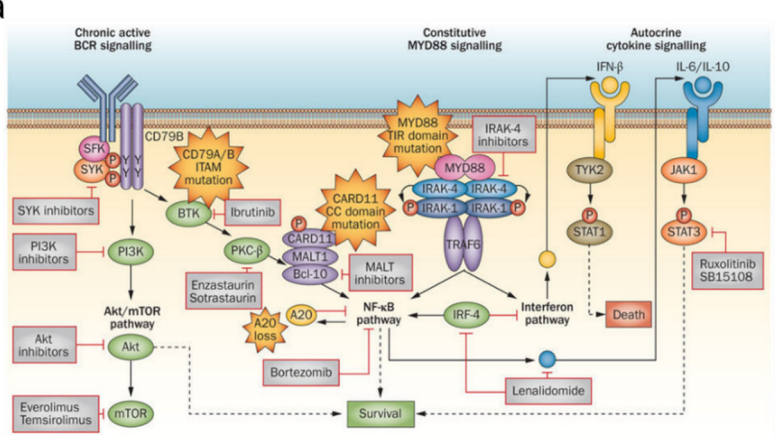

b

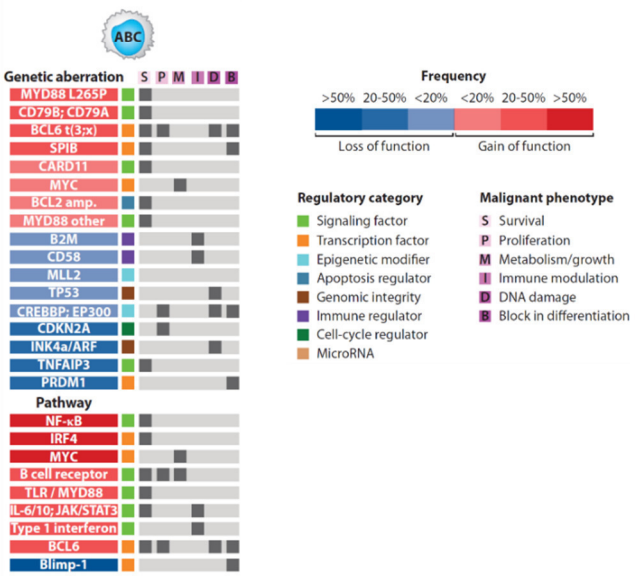

Figure 2. Overview of key signaling pathways affected and characteristic molecular aberrations involved in ABC DLBCL pathogenesis. (a) Signaling pathways afflicted in the pathogenesis of GCB DLBCL. Depicted in yellow stars, protein mutations leading to constitutively active NF-κB signaling. Illustrated are possible targets for therapeutic approaches of GCB DLBCL by small molecule inhibitors (Figure adapted from: Roschweski et al., 2014). **(b)** Summary of recurrent genetic aberrations and deregulated pathways found in ABC DLBCL. Depicted on the right-hand site, the frequency of the distinct molecular abnormalities, if they are loss or gain of function, in which regulatory category they belong and to what kind of malignant phenotype they lead (Figure adapted from: Shaffer et al., 2012).

1.1.1.3 PMBL

PMBL arise from a rare subset of B-cells residing in the thymus and is a clinically aggressive lymphoma (Dunleavy and Wilson, 2015; Shaffer et al., 2012). The malignancy predominantly affects adolescents and young adults with a median age of onset between 30 to 35 years, much earlier than the GCB and ABC DLBCL subgroups (Swerdlow et al., 2008). According to Rosenwald et al., (2003) the 5-year survival rate was with 64% relatively favourable after anthracycline multiagent based chemotherapy with some patients receiving radiation therapy. The clinical presentation and molecular characteristics are different from the other DLBCL subtypes and resemble “nodular sclerosing Hodgkin Lymphoma”. Notably, over one third of genes expressed in PMBL were also characteristic for Hodgkin Lymphoma (Dunleavy and Wilson, 2015; Rosenwald et al., 2003). PMBL exhibit a B-cell phenotype as they express CD20 and CD79A and show surface expression of GC-markers such as CD10, BCL6 and CD23 (Möller et al., 1987; Calaminici et al., 2004; Salama et al., 2010). A genetic hallmark found in PMBL are gains/amplifications in the p24 region of chromosome 9 (Joos et al., 1996; Lenz et al., 2008). The molecular characteristics of PMBL involved pathogenesis are summarised in Figure 3. The 9p24 chromosomal region encodes JAK2 the activator of STAT6 which was shown to transcriptionally repress BCL-6 (Ritz et al., 2013). Moreover, also in the 9p24 region located are the genes coding for the ligands for the inhibitory PD-1 receptor on the surface of T-cells, PDL1 and 2 which are rearranged at a frequency of 20% in PMBL, indicating a mechanism of immune evasion of PMBL (Green et al., 2010; Steidl et al., 2011; Twa et al., 2014). All genes in this 9p24 region JAK2, PDL1 and 2 are highly expressed in PMBL whereby PDL2 is according to Rosenwald et al. (2003) the best discriminator for PMBL. Epigenetic abnormalities seem to play a key role in the pathogenesis of PMBLs since the histone H3K9 demethylase “JMJD2C” which is also located in the 9p24 region cooperates with the earlier mentioned JAK2 in decreasing heterochromatin throughout the whole genome (Rui et al., 2010). Due to this JAK2/JMJD2C mediated epigenetic alterations, many genes are induced in PMBL such as MYC. Knockdown of JMJD2C and JAK2 resulted in the epigenetically silencing of MYC as a consequence of heterochromatin formation (Rui et al., 2010). Noteworthy 38% of PMBL show a translocation of CIITA, the master transactivator of MHC class II genes (Steidl et al., 2011). This translocation inactivates one CIITA gene copy leading to decreased MHCII on the cell surface and augmented immune

evasion and thus to inferior survival of PMBL patients. Alike ABC DLBCL, PMBL are addicted to constitutive activity of the NF-κB pathway (Lam et al., 2005; Rosenwald et al., 2003; Savage et al., 2003). One putative reason could be the inactivation of the deubiquitinating enzyme A20 (Schmitz et al., 2009).

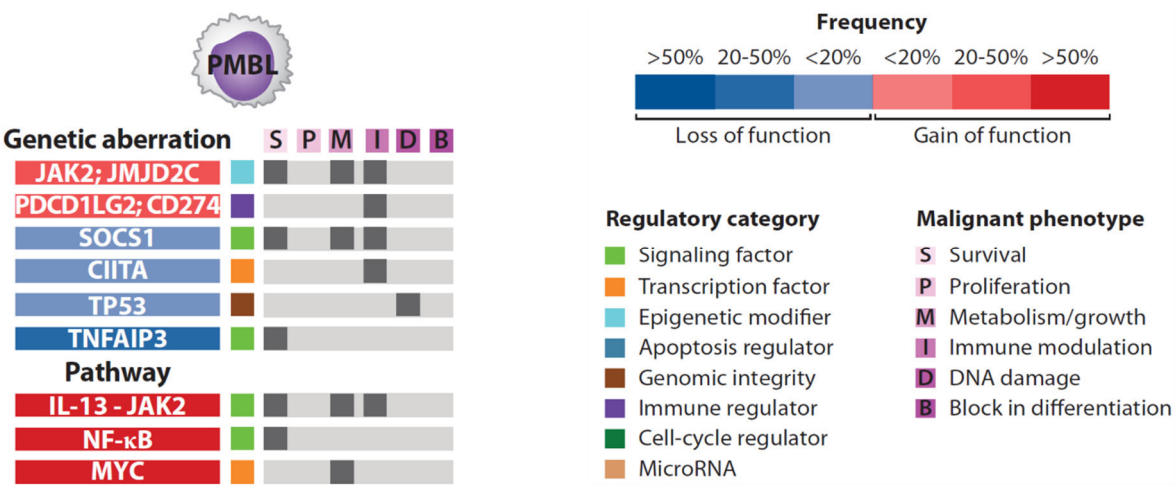

Figure 3. Overview of recurrent genetic aberrations and dysregulated signaling pathways involved in PMBL lymphomagenesis. Shown are the frequencies of the distinct molecular abnormalities, if they are loss or gain of function, in which regulatory category they belong and to what kind of malignant phenotype they lead (Figure adapted from: Shaffer et al., 2012).

1.1.2 Mantle cell lymphoma (MCL)

MCL were first described in 1975 by K. Lennert. MCL account for 3 to 10% of all NHL in the western world, predominantly affecting men (Anderson et al., 1998; Zhou et al., 2008). MCL describe an aggressive neoplasm of mature B-cell deriving from cells surrounding the germinal centres. In the early stages the neoplastic cells replace the mantle zone pattern of the lymph node (Tiemann et al., 2005). In more advanced stages MCL show a rather diffuse growth pattern (Bertoni et al., 2007). The median age of diagnosis is ≤ 60 years and the median overall survival lies between 3 to 5 years, thus exhibiting the poorest long-term survival among B-cell lymphoma (Zucca et al., 1995; Herrmann et al., 2009). So far, conventional chemotherapy approaches are not curative and MCL show a high frequency of remissions up to 90% in a short time range of 1 to 2 years. The normal counterpart of the malignant MCL cell seems to be the pre-germinal center B-cell (Pérez-Galán 2011). MCL display mature B-cell markers on their cell surface such as IgM and CD20 (Ghielmini et al., 2009; Pérez-Galán 2011). Molecularly, MCL share the expression of BCL2, CD5 and the hallmark chromosomal translocation the t(11,14)(q13;q32) bringing the CCND1 gene under the transcriptional control of the

Ig heavy chain promoter leading to an overexpression of the MCL prototypic oncogene cyclin D1 (Ghielmini et al., 2009; Pérez-Galán et al., 2011). A summary of genetic aberrations implicated in MCL lymphomagenesis is depicted in Figure 4. Observed as well in MCL were frequent deletions or the epigenetically silencing of the INK4a/arf locus that is coding for p16 and $INK4^{arf}$ that block the cell cycle and activate p53 (Rosenwald et al., 2003; Beà et al., 2001). HDM2 and HDM4, both negative regulators of p53 that synergistically promote proteasome-mediated p21 and p53 degradation were found to be overexpressed. HDM4 also inhibits the p53-mediated transcriptional activation of p21 a negative cell-cycle regulatory protein and inhibitor of cyclin D1 leading to the promotion of cell-cycle progression (Liang et al., 2010). Also DNA damage response pathways are afflicted in MCL pathogenesis since recurrent chromosomal deletions in chr.11q22-23 affect the functionality of the p53 upstream kinase ATM by gene truncation or missense mutations. By large scale pharmacological profiling Rahal et al. (2014) identified a subset of MCL cell line models that are sensitive to BCR signaling inhibitors ibrutinib (targeting BTK) and sotrastaurin (targeting PKC). They revealed that inhibitor sensitive MCL cell lines exhibit constitutively active BCR-signaling driven classical NF-κB signaling in contrast to resistant cell lines that show activation of the non-canonical NF-κB signaling. Moreover, the group also unveiled recurrent mutations in TRAF2 and BIRC3, proteins involved in the non-canonical NF-κB pathway in 15 % of examined patient samples by transcriptome sequencing. TRAF2 and 3 interact with BIRC2 and 3 in order to downregulate NIK which fosters the transition of the p100 precursor into the active mature p52 protein. RNAseq data obtained from MCL cell line models identified a TRAF2 nonsense mutant, $TRAF^{W114*}$ and a biallelic TRAF3 deletion. These mutations impair TRAF2 and 3 inhibitory properties on non-canonical NF-kB signaling. Furthermore, when they conducted targeted sequencing of key elements implicated in non-canonical NF-kB signaling in primary MCL samples they found frequent mutations of TRAF in 6% and BIRC3 in 10% of cases. Two patient derived BIRC3 mutant variants, the nonsense mutation S441* and the missense mutation C560S were investigated in more detail. The coexpression of NIK with $BIRC3^{S441*}$ or $BIRC3^{C560S}$ resulted in less efficient NIK destabilisation and increased p52 production compared to wild type BIRC3 coexpression. This result was confirmed when both BIRC3 mutant proteins were expressed in a cell line exhibiting low p52 levels. $BIRC3^{S441*}$ or $BIRC3^{C560S}$ expression in this cell line clearly

led to an increase of p100 cleavage to p52 whereas expression wild-type BIRC3 did not affect steady state p52 protein levels. In addition to that, inhibitor insensitive MCL cell lines with alterations in non-canonical NF-kB signaling were found to be addicted to NIK activity in vitro and in vivo. Also in this B-cell lymphoma malignancy, the NF-kB negative regulatory ubiquitin editing enzyme A20 is commonly inactivated by deletions, mutations or its transcription is epigenetically dampened by increased promoter methylation (Honma et al., 2009). Moreover, MCL were found to be addicted to IRF4 and SYK as revealed by knock down approaches (Friedberg et al., 2009; Shaffer et al., 2012). Several more secondary genetic alterations were discovered contributing to MCL lymphomagenesis including prosurvival and proliferative pathways like the PI3K/AKT/mTOR pathway, the WNT and Hedgehog pathway (Pérez-Galàn et al., 2011), critical cell-cycle regulating genes and DNA damage response and repair genes, indicating the MCL's unique biology.

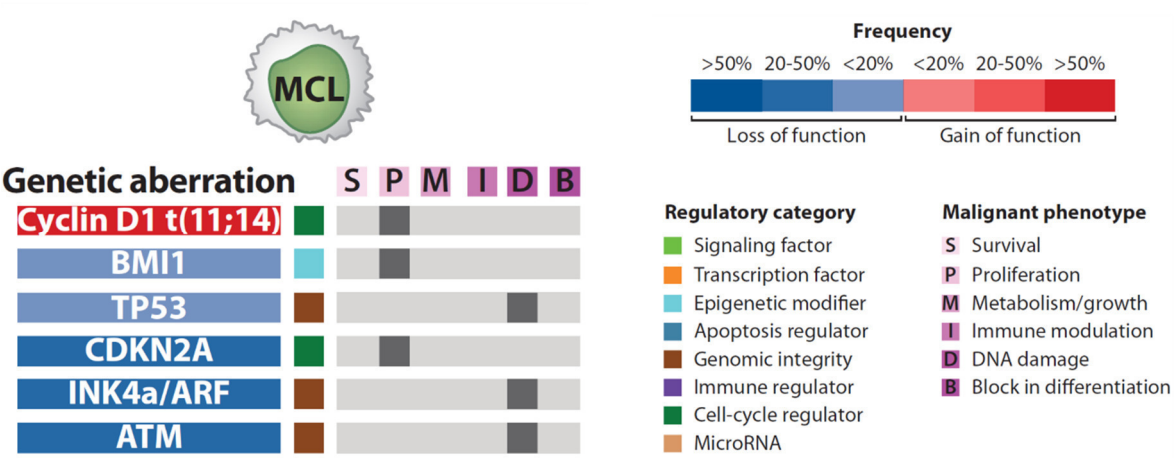

Figure 4. Overview of recurrent genetic aberrations involved in MCL lymphomagenesis. Shown are the frequencies of the distinct molecular abnormalities, if they are loss or gain of function, in which regulatory category they belong and to what kind of malignant phenotype they lead (Figure adapted from Shaffer et al., 2012).

1.2 Transcription factor families involved in B-cell lymphomagenesis

1.2.1 The NF-κB family

The nuclear factor kappa-light-chain-enhancer of activated B-cells (NF-κB) was discovered in 1986 and described as a constitutive nuclear B-cell specific inducible transcription factor regulating the expression of the Ig kappa light chain (Sen et al., 1986). As result of intensive research during the last decades it was revealed that NF-κB is present in all cells and that the NF-κB family of transcription factors consists of five members termed p65/RelA, RelB and c-Rel. All NF-κB family members (depicted in Figure 5) are encoded by a distinct gene, *RELA*, *RELB* and *REL* (Gerondakis et al., 1999). They all share the presence of an N-terminal structural domain, the conserved 300 amino acid (aa) Rel homology domain (RHD). This protein motif comprises a sequence for DNA binding, a nuclear localisation signal (NLS) and a site for the interaction with other REL proteins for homo- and heterodimerization or NF-κB inhibitors (IκBs) (Baeuerle and Henkel., 1994; Baldwin, 1996). Each of the NF-κB subunits has a unique DNA binding domain and therefore exhibits its own characteristic DNA binding affinity, as well. Thus, every subunit contributes to the overall DNA binding affinity of a NF-κB dimer leading to different dimer specific DNA binding consensus sequences (Wang et al., 2003; Siggers et al., 2011; Wong et al., 2011).Only RelA/p65, c-Rel and RelB exhibit a C-terminal transcriptional activation domain (TAD) which is necessary for the recruitment of coactivators and thus the transcriptional positive regulation of a certain NF-κB target gene (Hayden and Ghosh, 2012). As indicated earlier, NF-κB members form homo- and heterodimers that bind NF-κB consensus sites (κB sites) within promoters/enhancers of a target gene (Pahl, 1999; Hayden and Ghosh, 2004). For this reason only NF-κB dimers including either at least one RelA, c-Rel or RelB subunit are able to act as transcriptional inducers. In most cell types, the predominant dimer in NF-κB signaling is the RelA/p50 heterodimer (Li and Verma, 2002; Oeckinghaus and Ghosh, 2009). Noteworthy, RelB does not homodimerize and only forms dimers with p100, p52 or p50 whereas the other NF-κB subunits are being found in all possible hetero-or homodimer combinations (Ryseck et al., 1992; Bauerele et al., 1994; Bobrzanski et al., 1994). Unlike RelA, c-Rel or RelB, the N-terminal proteolytic cleavage products of p105 and p100, p50 and p52,

respectively lack a TAD. As a consequence of this, NF-κB homodimers consisting of p50 or p52 can only function as transcriptional repressors of their respective target gene.

Those transactivation incapable dimers can negatively regulate transcription by constitutively occupying κB sites in a NF-κB responsive promoter sequence until they are displaced by a competitive TAD comprising NF-κB dimer. In this manner, p50 and p52 homodimers can establish an activation threshold of a NF-κB target gene (Hayden and Gosh, 2012). Moreover, p50/p52 dimers were also shown to act as epigenetic modifiers by recruiting gene-silencing proteins such as histone deacetylases (HDACs) to inhibit transcription (for review see Chen and Greene, 2004). Taking into account the different NF-κB dimer compositions acting as gene inducers and repressors, distinct DNA binding site specificities depending on dimer combination, the large number of IκB sites in the genome and the multitude of NF-κB target genes makes the NF-κB transcription family and the regulated downstream signaling network highly complex and versatile.

1.2.2 NF-κB signaling

The induction of transcriptionally active NF-κB dimers by NF-κB signaling is classified into two main pathways termed as the canonical (classical) NF-κB pathway and the noncanonical (alternative) NF-κB pathway (pathways are schematically shown in Figure 6) (Sun, 2012). Both NF-κB inductive pathways share the activation of differently composed IκB kinase complexes and lead to the liberation of distinct NF-κB dimers. The activation of the pathways is under the control of a wide range of soluble and membrane-bound extracellular ligands originating from various extracellular sources (Hayden and Ghosh, 2012). Regarding the immune system, the NF-κB family coordinates various genes that control immune responses to a multitude of immune system stimulating agents for instance proinflammatory cytokines or pathogen derived substances recognised by pattern-recognition receptors such as LPS, peptidoglycans, lipoproteins, unmethylated bacterial DNA or dsRNA of viral origin (Li and Verma, 2002). Therefore, NF-κB signaling plays an important role in regulating the innate and adaptive immune system. Noteworthy, NF-κB activity was shown to be required for the rapid expression induction of acute-phase antimicrobial defence genes as response to invading pathogens. In adaptive immune system it plays a role in T-cell

development and function, Ig class switch of B-cells, germinal center formation or proper B-cell maturation (Gerondakis et al., 1998). Moreover, NF-κB signaling is also crucial for an appropriate response that is followed upon ligand binding of antigen-receptors implicated in the immune system like for example those of B- and T-cells (Schuster et al., 2012). In addition to that, there are also multiple intracellular pathways activating and regulating NF-κB activity such as DNA damage response, ionizing radiation, intracellular pattern recognition receptors and a plethora of other physical and chemical stresses (Li et al., 2001; Mohan and Meltz, 1994; Gilmore, 2008).

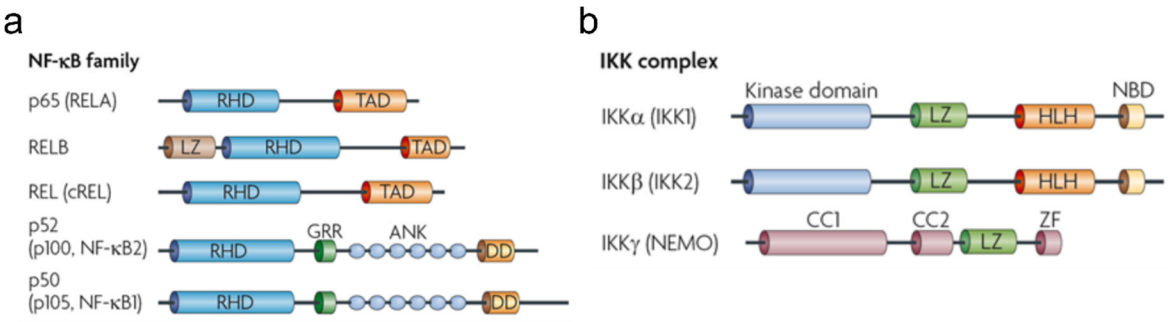

Figure 5. Molecular structures of members of the NF-κB family and the ternary IKK complex. (a) NF-κB family with indicated characteristic protein domains. p100 and p105 have dual role in NF-κB signaling as they exhibit IkB properties and when proteolytically processed to p52 and p50 they can act as activating NF-κB members. **(b)** Subunits of the high molecular IKK complex with indicated protein domains. ANK, ankyrin-repeat; CC, coiled-coil; DD, death domain; GRR, glycine-rich region; HLH, helix–loop–helix; IKK, IκB kinase; LZ, leucine-zipper; NBD, NF-κB-essential-modulator-binding domain; RHD, REL homology domain; TAD, transactivation domain; ZF, zinc-finger. Figure adapted from Ghosh and Hayden, 2008.

1.2.3 Canonical or classical NF-κB signaling

The canonical or also called classical NF-κB pathway is activated by signals emanating from of a variety of structurally diverse membrane bound receptors upon ligand binding. Among them are tumor necrosis factor super-family receptors (TNFSFRs), interleukin receptors (ILRs), pattern recognition receptors (PRRs) such as Toll-like receptors (TLRs) or antigen receptors like the B- or T-cell receptor (Hyaden and Ghosh, 2012). Receptor ligation is followed by the recruitment of receptor proximal specific adapter protein complexes. In canonical signaling these are mostly RIP (receptor interacting protein) and TNF-receptor-associated factor (TRAF) family member protein complexes generally in conjunction with the TGFβ-activated kinase-1 (TAK1) that is required as IKK kinase (IKK-K) for further

downstream signaling to the IκB kinase (IKK) (Hayden and Ghosh, 2008). Whereas TRAF proteins are utilised by both NF-κB pathway inducing pathways, RIP family members are exclusively used in the canonical signaling pathway Hayden and Ghosh, 2012). Receptor signaling culminates in the activation of IKKβ which is part of the trimeric cytoplasmic IKK complex consisting of the catalytic subunits IKKα and IKKβ, and the regulatory IKKγ (NEMO) subunit (Hacker and Karin, 2006). The activation of this ternary kinase complex requires the phosphorylation of IKKβ and the ubiquitination of IKKγ. Once activated, IKKβ in turn phosphorylates IκB proteins. The 37 kDa protein IκBα, the prototypical IκB is bound to the RHD of a NF-κB protein. IκBα mainly binds and thus regulates RelA/p50 or c-Rel/p50 heterodimers in the resting state by its repetitive ankyrin repeats thereby masking the NLS of either RelA or c-Rel. The p50 precursor protein p105 is constitutively processed through a cotranslational mechanism which is regulated by a glycine rich region (GRR) (Lin and Gshosh, 1996; Orian et al., 1999). On the other hand, also p105 phosphorylation at certain C-terminal serine residues by IKKβ was reported that was followed by inducible procession to p50. The NLS of p50 is still accessible as unveiled by crystallographic investigations (Huxford et al., 1998; Jacobs and Harrison, 1998; Malek et al., 2001, 2003). In combination with the impact of nuclear export signals (NES) within the protein sequences of RelA, c-Rel and IκBα, the p50 NLS accessibility is leading to the capability of the RelA/p50 or c-Rel/p50 complexes to shuttle between nucleus and cytoplasm under steady state conditions. But the masking of the RelA and c-REL NLS and the NES of IκBα results in the predominantly cytoplasmic localisation of NF-kB in the steady-state (Johnson et al., 1999; Huang et al., 2000). This dynamic balance of cytosolic and nuclear localisation is shifted towards the nucleus by the activation of NF-kB signaling. Upon the activation of canonical NF-κB signaling, IκBα is phosphorylated by IKKβ at two conserved N-terminal serine (S) residues 32 and 36 within the so-called destruction box (aa-sequence: D<u>S</u>GXX<u>S</u>). These phosphorylated serines are subsequently recognized and IκBα gets K48-linked polyubiquitinated by the E3 ubiquitin ligase $SCF^{\beta TrCP}$ leading to proteasomal degradation of IκBα (Hayden and Ghosh, 2008; Henkel 1993; Chen, 1995; Yaron, 1997). In this way, the NLS is of RelA/p50 or c-Rel/p50 is accessible again and the sequestration of the NF-κB dimers in the cytoplasm is ceased. Upon release, the NF-κB factors migrate to the nucleus where

they accumulate and bind DNA, recruit cofactors and so activate the transcription of NF-κB responsive target genes (Hayden and Ghosh, 2004, 2008).

1.2.4 Non-canonical or alternative NF-κB signaling

The second NF-κB inducing signaling pathway, the Non-canonical or alternative NF-κB signaling displays distinct kinetics and regulatory components (Razani et al., 2011). In contrast to the canonical NF-κB signaling this pathway is induced by a rather small variety of stimuli. A subset of TNFSFRs comprising lymphotoxin β receptor (LTβR), B-cell activating factor receptor (BAFF-R), OX40L (CD134), receptor activator of NF-κB (RANK), Fn14, and CD27 were revealed to induce non-canonical NF-κB signaling (Claudio et al., 2002; Coope et al., 2002; Dejardin et al., 2002; Novack et al.,2003; Ramakrishnan et al., 2004; Saitoh et al., 2003). The central regulatory mechanism in non-canonical NF-κB signaling involves the degradation modulation of the key kinase in this pathway, the NF-κB-inducing kinase (NIK) (Sun, 2011). Under steady state conditions, NIK is recruited to a cytosolic complex made up of TRAF2/3-cIAP1/2. NIK is brought together with the ubiquitin ligase cIAP1/2 by TRAF2/3. NIK K48-linked ubiquitination by cIAP1/2 results in constant NIK proteasomal degradation (Zarnegar et al., 2008). As soon as for instance TNFSFRs engage their respective ligands, receptor dimerization is induced as in the case of CD40 and the TRAF2/3-cIAP1/2 is recruited to the intracellular portion of the receptor. Ensuing downstream signaling is best characterised for CD40, and LTβR as follows. In CD40 proximal signaling instead of NIK, TRAF3 is now due to TRAF2 mediated K63 ubiquitination, the new target of the K48 ubiquitin ligase activity of cIAP1/2. In this fashion, newly synthesizes NIK proteins are not degraded anymore and can accumulate. Enriched and activated NIK then phosphorylates and activates IKKα kinase activity which prevails in a homodimeric complex. The active IKKα dimer then phosphorylates p100 C-terminal serine residues which in turn results in the recruitment of the ubiquitin ligase complex $SCF^{\beta TrCP}$. K48-linked ubiquitination of a distinct C-terminal lysine in p100, targets the protein C-terminus for proteolytic cleavage in which a GRR in close proximity to the ubiquitination plays an important role. This proteolytic processing of p100 ends up in leaving an N-terminal portion, named p52. NF-kB dimers that are generated as the end-product of this signaling cascade, consist of p52 and RelB. Full length p100 binds RELB which needs this association for stability. Prior to the

formation of mature p52, the NLS sequences of both subunits are hidden intra-molecularly by C-terminal p100 ankyrin repeats that are structurally homologue to those of IκBs, establishing the C-terminal part of p100 as IκB. In the course of p52 generation, also the NLS masking p100 ankyrin repeats are eliminated. Thus, the IκB-like function of p100 is abrogated and NF-kB dimers composed of RelB and p52 are not sequestered in the cytoplasm anymore and can translocate in the nucleus, initiating the positive transcriptional regulation of corresponding target genes. (For noncanonical NF-kB signaling review see Bonizzi and Karin et al., 2004; Oeckinghaus, Hayden & Ghosh, 2011, Razani et al., 2011; Sun et al., 2012)

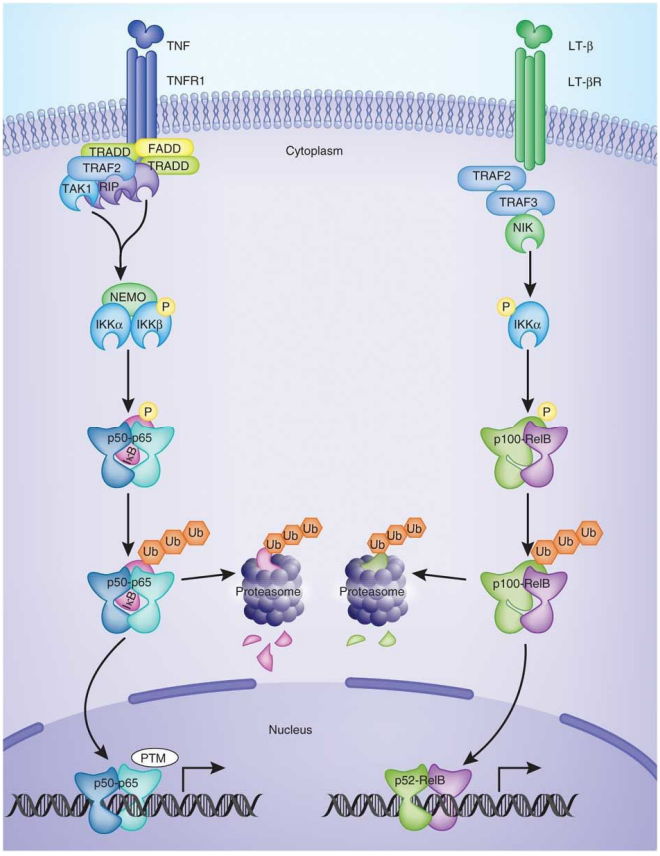

Figure 6. Exemplary TNF and LT-β triggering of canonical (classical, left) and noncanonical (alternative, right) NF-κB signaling. In canonical signaling, NF-κB dimers are bound by IκB proteins masking their NLS and thus, sequestering them in an inactive NF-κB state in the cytoplasm. Upon stimulus induced receptor, the IκB kinase (IKK) complex, consisting of the kinases IKKα, IKKβ and the regulatory IKKγ-subunit (NEMO), phosphorylates the IκB and targeting it for ubiquitination and eventual proteasomal degradation. NF-κB dimers are subsequently liberated and can migrate to the nucleus to bind transcription regulatory sites of NF-κB responsive genes. The canonical pathway (left) is triggered by a multitude of stimuli, represented here by TNFR1 signaling. TNF binding of TNFR1 results in the binding of TRAD, providing a platform for FADD and TRAF2 assembly. TRAF2 in turn associates with RIP1 to activate the IKK complex which phosphorylates IκBα in an IKKβ-and NEMO-dependent manner. In most cases p65-containing heterodimers are then released and translocate to the nucleus. NF-κB activity is further fine-tuned by modifying subunits with different PTMs. The noncanonical pathway, is induced by only certain TNF

family cytokines like CD40L, BAFF and as represented here, by lymphotoxin-β (LT-β). Upon receptor triggering, a complex consisting of TRAF3, TRAF2 and additional ubiquitin ligases regulates the stabilisation of NIK. This kinase phosphorylates IKKα which in turn phosphorylates p100 that is associated with RelB. This leads to proteolytic cleavage of p100 and the generation of p52 that pairs with RelB, generating active NF-κB dimers that migrate to the nucleus to exert transcriptional regulation of NF-κB target genes. (Figure taken from Oeckinghaus, Hayden & Ghosh, 2011)

1.2.5 Inhibitors of NF-κB signaling

NF-κB is critical for the regulation of multiple physiological processes such as cell differentiation, survival and proliferation. Moreover, the NF-κB signaling network is also a key player of more comprehensive mechanisms including embryonic development, the functionality of innate and adaptive immune system and tissue homeostasis (Annemann et al., 2016). For this reason, a fine-tuned regulation of NF-κB activity is essential for the regular functioning of intracellular and superior mechanisms of the human body. This task is achieved by intracellular inhibitors of NF-κB signaling, the IκB proteins. The NF-κB regulatory "IκB protein family" is according to structural and deduced functional properties subdivided into the classical and a distinct group of atypical (also referred to as the BCL-3 subfamily) NF-κB inhibitors (an overview of classical and atypical IκBs is shown in Figure 7). All IκB proteins, no matter from which subfamily, are characterised by the presence of an ankyrin repeat domain (ARD), containing six to eight ankyrin repeats (ANK), a 33 amino acid structural motif exhibiting a helix-loop-helix conformation (Hinz et al., 2012). The ARD of an IκB regulates protein stability and mediates protein-protein interaction with the RHDs of NF-κB dimers (Annemann et al., 2016).

1.2.5.1 Classical NF-κB inhibitors

In resting cells, classical IκB proteins bind NF-κB dimers mediated by their ARD and functionally inactivate the dimers by retaining them in the cytoplasm as a consequence of the molecular masking of their NLS located within the RHD (Hinz et al., 2012). In this fashion, the binding of NF-κB dimers to κB DNA sequences in enhancers or promoters of target genes is prevented. The protein family consists so far of five cytoplasmic (classical) IκBs, namely the prototypic IκBα, IκBβ, IκBε, p105 (NF-κB1) and p100 (NF-κB2). In mice, all members are quite ubiquitously expressed exhibiting specific elevated levels for IκBα and IκBβ in spleen, IκBβ and IκBε in testis, IκBα in thymus, and IκBε in lung (Thompson et al., 1995; Li et al., 1997; Whiteside et al., 1997; Lernbecher et al., 1994). IκBε primarily expressed in

hematopoietic cells (Hayden and Ghosh, 2008). p105 and p100 can be proteolytically processed to p50 and p52 by the cleavage of a C-terminal portion that serves as IκB, sequestering the NLS of a Rel protein, thus preventing the translocation of a NF-κB dimer to the nucleus (Bours et al., 1992; Beinke and Ley., 2004; Sun, 2012). Accordingly NF-κB1 and NF-κB2 exhibit both, a NF-κB and a cytoplasmic IκB functionality (Hinz et al., 2012). Structurally, classical IκBs are defined by exhibiting six ANK and share an unfolded structure N-terminal to the ARD (Hinz et al., 2012). This unfolded aa-stretch comprises a degron motif also called "destruction box", which includes two serines that are stimulus-dependent phosphorylated by IKKβ, namely S32 and S36 of IκBα, S19 and S23 of IκBβ and S157 and S161 for IκBε (Brown et al., 1995 ;DiDonato et al., 1996; Shirane et al., 1999; Hinz et al., 2012). The phosphorylated residues are recognised and polyubiquitinated by the E3 ligase $SCF^{\beta TrCP}$, followed by rapid the proteasomal degradation of the IκBs and release of NF-κB dimers (Henkel, 1993; Chen, 1995; Yaron, 1997; Winston1999; Ben-Neriah, 2002). Exclusive for IκBα and IκBβ is the presence of a region termed PEST, a peptide sequence rich in proline (P), glutamic acid (E), serine (S), and threonine (T) mediating fast protein turnover (Hinz et al., 2012). Regarding NF-κB signaling modulation, IκBs influence the transcriptional specificity of differently composed NF-κB dimers by their ability to preferentially associate with certain members of the NF-κB family. For example, the RelA/p50 heterodimer which is involved canonical NF-κB signaling is predominantly, albeit not exclusively, regulated by IκBα (Hayden and Ghosh, 2008). Classical IκB proteins also seem to have redundant functions. For instance the combined depletion of IκBα, IκBβ and IκBε resulted in an only minor increase of nuclear RelA levels (Tergaonkar et al., 2005). It is suggested that the inhibitory function of the three IκB was compensated by p105 and p100. Furthermore, IκBβ replacing the genomic IκBα was found to serve analogously to IκBα (Hayden and Ghosh, 2008 and 2012). On the other hand, studies in mouse embryonic fibroblasts (MEFs) investigating NF-κB responses upon knocking out one, two or all three of IκBα, IκBβ or IκBε revealed that the inhibitors have distinctive unique functions even within one signaling pathway (Hayden and Ghosh, 2008). Hoffmann et al. (2002) postulate that the distinct functional features of IκBα, IκBβ and IκBε are the consequence of differences in their degradation and resynthesis. The degradation and resynthesis of IκBε for instance occurs with remarkable delayed kinetics in comparison to that

of IκBα (Kearns et al., 2006). Cell type and temporal specific degradation of for example IκBε suggests that different IκBs also have unique functions in regulating NF-κB responses (Hayden and Ghosh, 2008). In this regard, the major physiological feature of the classical NF-κB inhibitor IκBα is its capability to rapidly but strictly transiently induce a NF-κB mediated response to a canonical NF-κB pathway specific stimulus. This characteristic suggested that IκBα constitutes an autoregulatory feedback loop with NF-κB in which activated NF-κB drives the synthesis of IκBα that in turn inhibits the activity of NF-κB by regulating predominantly, but not exclusively RelA/p50 dimers. This hypothesis was promoted by the finding that the IκBα promoter was found to comprise κB sites within its sequence (Ito et al., 1994). Moreover, Mice, knock-out for IκBα show a significantly delayed termination of NF-κB signaling in response to canonical stimuli as for example TNF-α, substantiating the existence of this negative feedback loop (Gerondakis et al., 2006; Pasparakis et al., 2006). Thus, due to this negative feedback mechanism, IκBα is able to facilitate the maintenance of the transient effect induced by multiple agents on the transcription of NF-κB responsive genes. Obviously, the duration of the NF-κB response relies heavily on the kinetics of the feedback pathway determined by a distinct IκB, demonstrating the importance of the NF-κB response regulation by classical IκB proteins.

1.2.5.2 Atypical NF-κB inhibitors

In 1990, the (B-cell lymphoma 3 protein) BCL-3 was initially identified by Ohno et al. as rearranged proto-oncogene expressed in patients suffering from B-cell chronic lymphocytic leukemia that is characterised by a specific chromosomal translocation. Two years later in 1992 the seven ANK of BCL-3 were found to be closely related to those common in classical IκB proteins and shown to mediate complex formation with NF-kB dimers by binding the dimerization domain of NF-κB. Further, BCL3 was proven to bind p50 and p52 homodimers and to be co-localised with those in the nucleus. These observations and further findings such as the capability of BCL3 to inhibit p50 DNA binding and the reversal of p50 homodimer-mediated transcription inhibition, revealed the protein as the first founding member of the atypical IκB family or also called BCL-3 subfamily (Franzoso et al., 1992; Hatada et al., 1992; Wulczyn et al., 1992; Nolan et al., 1993). Today, Bcl-3, IκBζ, IκBNS, IBη and IκBL belong to the group of atypical NF-κB inhibitors (Handel-Fernandnez et al., 1999; Kitamura et al., 2000; Fiorini et al., 2002; Yamauchi et al., 2010).

The atypical IκBs can be distinguished from classical IκBs by several distinct characteristics. In contrast to classical NF-κB inhibitors this protein group shows a completely different subcellular localisation as they are located predominantly in the nucleus where they exert their various functions by interacting with different NF-κB dimers in contrast to classical IκB which mainly bind NF-κB in the cytoplasm. However, the interaction of atypical IκB with different NF-κB dimers seems to be cell specific and dependent from the type of NF-κB stimulus or posttranslational modifications of the atypical IκBs. Furthermore, atypical IκB exhibit different activation and degradation kinetics. In detail, upon the induction of NF-κB signaling by extrinsic stimuli or antigen receptor derived signaling the expression of atypical nuclear IκBs is induced whereas classical IκB are initially degraded. Therefore, nuclear IκBs generally mediate their effects late in the transcriptional response or during secondary responses. The most important hallmark of the atypical IκBs that discriminates them from their classical relatives is their ability to either enhance, TAD sequences were found in BCL-3 and IκBζ, or diminish the transcriptional activity of target genes by the interaction with transcriptionally active DNA-associated NF-κB dimers. In contrast to the cytoplasmic IκBs, that can only act as negative regulators of NF-κB activity (for review see Schuster et al., 2013; Hinz et al., 2012; Annemann et al., 2016). These mechanism are not the only differences between the two NF-κB inhibitor classes. Atypical IκBs not only act as NF-κB repressors but are also known to fine tune NF-κB activation and transcriptional response in the nucleus. This occurs for instance by adding post translational modifications to NF-κB subunits such as acetylation, phosphorylation and ubiquitination. These modifications regulate NF-κB dimer exchange on the DNA, stabilise DNA associated NF-κB dimers or recruit and displace histone deacetylases (HDACs) and histone acetyltransferases (HATs) to epigenetically alter target gene expression (for review see Mankan et al., 2001 Cheng and Greene, 2004). Most atypical IκBs are part of a negative feedback loop to limit the duration of NF-κB signaling. Bcl-3, IκBε, IκBζ and IκBNS are transcriptional targets of NF-κB except for IκBη that is regulated almost independently of NF-κB. Additionally, Bcl-3 and IκBζ mRNA translation was found to be negatively regulated by microRNAs miR-125b and miR-124a, respectively (Guan et al., 2011; Lindenblatt et al., 2009). The knockout of a sole atypical IκB in mice was observed to be not lethal and results in normal growth after birth. However, the mice show multiple defects in organ

structures and immune system functions. Therefore, atypical IκB knockout mice suffer from autoimmune diseases and are for instance not able to mount proper defences against invading pathogens. Bcl-3 for example was shown to be important for correct splenic architecture, and the pathogen specific humoral immune response since knockout out mice are incapable of clearing listeria monocytogenes, streptococci pneumonia and toxoplasma gondii infections (Franzoso et al., 1997; Schwarz, 1997; Tassi et al., 2015). This impaired response to pathogens is in this case partially based on reduced IL-12p70 and IFNγ levels that are caused by the increased production of anti-inflammatory IL-10 by macrophages (Riemann et al., 2005). On the other hand, mice lacking Bcl-3 are more susceptible to diabetes type I, display higher levels of IL-17 and do not show signs of autoimmunity (Ruan et al., 2010). On the contrary, adult mice lacking IκBζ expression develop various symptoms of autoimmunity such as atopic dermatitis and chronic conjunctivitis. 90% of IκBζ deficient mice do not survive embryogenesis but the remaining fraction grows regularly after birth. IκBζ plays also an important role in adaptive immunity since it binds together with RORγ or RORα, to the IL-17a locus, promoting TH17 cell development. Together with its function to positively regulate IL-6 production upon LPS exposure, the previous finding establishes IκBζ as proinflammatory IκB (Okamoto et al., 2010). In contrast to that, the proinflammatory TNFα transcription is suppressed by IκBζ and knockout mice are more resistant to experimental autoimmune encephalomyelitis (EAE) due to the impairment of TH17 cell development and susceptible to MCMV infection (Motoyama et al., 2005; Miyake et al., 2010; Okamoto et al., 2010). These examples of the dual IκBζ function in pro- and anti-inflammatory mechanisms and processes clearly illustrates the versatile and complex role of atypical IκBs in the regulation of immune homeostasis and reaction. To sum it up, in this context atypical IκBs were revealed during the last decades to regulate the expression of surface markers, chemokines, cytokines and other effector proteins such as antibodies of immune cells, thus consequently regulating their maturation, differentiation and activation (for further review see Beg and Baldwin, 1993; Gosh et al., 1998; Li and Verma, 2002; Hayden and Gosh, 2004; Hayden and Gosh, 2008; Hinz et al., 2012; Hayden and Gosh, 2012; Schuster et al., 2013; Annemann et al., 2016).

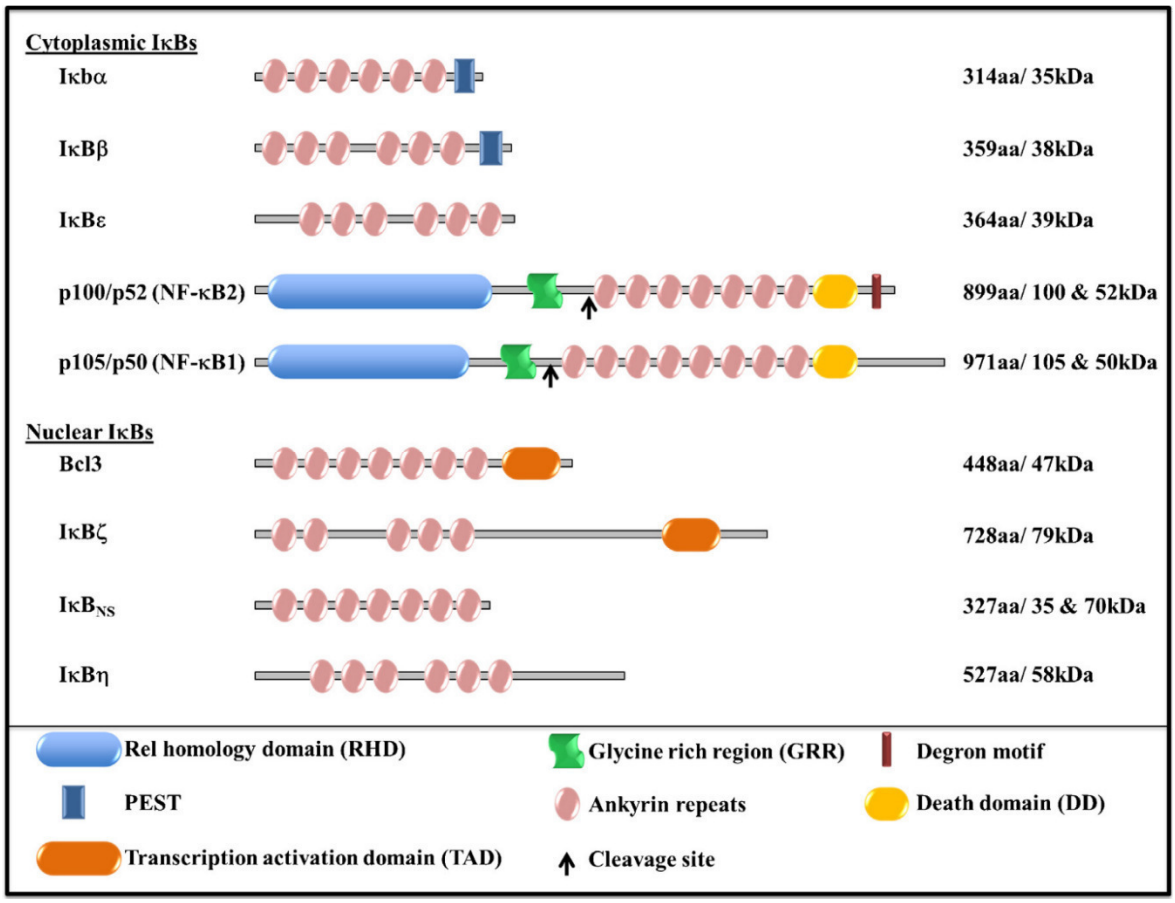

Figure 7. Schematic overview of the molecular structure of murine cytoplasmic and nuclear IκB proteins. IκBs are characterised by the presence of an ankyrin repeat domain consisting of six to eight ankyrin repeats (ANK). IκBNS belongs to the nuclear or atypical IκB subfamily and consists of 6 ankyrin repeats and short N-terminal and C-terminal tails. Figure taken from: Annemann et al., 2016.

1.2.5.3 The atypical NF-κB inhibitor IκBNS

IκBNS, also called TA-NFKBH and NFKBID is encoded on chromosome 19q13.12 in the *Nfkbid* gene and consists of 313 aa (human) or 327 aa (mouse). The protein comprises in human and mice six ANK for protein-protein interactions and short N-and C-terminal portions. IκBNS was first identified by Fiorini et al. in 2002 by investigating genes that are induced upon antigen induced negative selection of T-cells, bearing auto-reactive TCRs in the thymus. Soon afterwards it revealed to be inducibly expressed in several cell types. It was shown to be induced by stimuli like LPS, IL-10, CD40 and antigen ligands activating BCR and TCR signaling. IκBNS interacts with several NF-κB family members depending on the cell type. By conducting pulldown experiments with GST-IκBNS fusion proteins, Fiorini et al. (2002) have also shown the interaction of IκBNS with cytoplasmic and nuclear p50, as well as nuclear p52, p65, RelB and c-Rel in stimulated N14 TCR transgenic

thymocytes. In RAW264.7 macrophages overexpressed IκBNS interacts with p50 but not with RelA (Hirotani et al., 2005). Co-IPs using nuclear extracts from fractionised P/I stimulated regulatory T-cells (Tregs) cell lysates, Schuster et al. (2012) revealed strong interaction of endogenous IκBNS with p50 and mild interaction with c-Rel. IκBNS-deficient mice breed and grow regularly. They do not show signs of spontaneous autoimmunity and are like IκBζ knockout mice more resistant to TH17-dependent EAE (Kobayashi et al., 2014). Furthermore, they found decreased expression of IL17A, IL-17-related genes and RORγt in response to Transforming Growth Factor (TGF-β1) and IL-6 stimulation in IκBNS deficient T-cells. TH17 cells depend on the expression of RORγt as the driving transcription factor of the TH17 phenotype which is also primarily characterised by the production of IL-17 (Ivanov et al., 2006). Considering the results described by Kobayashi et al., IκBNS negative T-cells are thus impaired in differentiating in proinflammatory TH17 cells in response to TGF-β1 and IL6. For this reason, Kobayashi et al. concluded that IκBNS plays a crucial role in the generation of TH17 cells and in the control of TH17-dependent EAE. These results are in accordance with the findings of Annemann et al., 2015. They found IκBNS to be required for TH17 cell differentiation during gut inflammation and to regulate the expression of multiple key TH17 cytokines such as IL-17A, IL17-F; IL-2, IL-10, GM-CSF, and MIP-1α. The requirement of IκBNS for the TH17 key cytokine IL-17 production was also observed by Jeltsch et al. by using a shRNA mediated knockdown approach in mouse $CD4^+$ T-cells. Jeltsch et al. (2014) also demonstrated that Roquin and Regnase-1 repress mRNA encoding IκBNS, thereby inhibiting the expression of IκBNS and as a result of this also impair TH17 cell differentiation. Moreover, Annemann et al. (2015) report further that IκBNS exhibits increased binding to the IL-10 gene locus in stimulated TH17 cells in comparison to unstimulated TH17 cells. Therefore, the authors assume that IL-10 is a direct target of IκBNS expression and that IκBNS partially regulates TH17 differentiation by direct transcriptional control over TH17 phenotype determining cytokine expression. Furthermore, they reveal that IκBNS expression is not restricted to a specific T-cell subset, but drives besides TH17 also the development of TH1 cells in vitro. Consequently, they could observe reduced amounts of TH17 and TH1 cells, as result of a proliferation defect in IκBNS deficient mice. The group also describes that IκBNS mice display an impaired TH17 development. TH17 cells are required for the clearance of *Citrobacter rondentium*

infections in the gut, which induce a strong TH17 response. Thus, as IκBNS was found to be indispensable for proper TH17 development it is consequently required for restricting Citrobacter rondentium infections in the gut and IκBNS knockout mice were unveiled to be highly susceptible to Citrobacter rondentium infections. The knockout proved IκBNS also not to have a considerable role in thymic negative selection, as indicated by the results obtained by Fiorini et al. (2002), since $CD4^+$ and $CD8^+$ T-cell numbers were not altered between wild-type and knockout mice. Alike IκBζ, IκBNS exhibits a dual role as negative and positive regulator of NF-κB target genes. T-cells lacking IκBNS produce significantly less IL-2 and IFN-γ and exhibit slightly impaired proliferation upon anti-CD3/28 stimulation, demonstrating its ability to act as transcriptional inducer (Touma et al., 2007). In contrast, stimulation of bone marrow-derived dendritic cells (DCs), lacking IκBNS with LPS show clearly increased and longer expression of the MYD88 dependent genes IL-6, IL-12p40 and IL-18. This result indicated that IκBNS is needed for termination of NF-kB activity at certain gene promoters such as in case of IL-6 (binding of IκBNS-p50 complexes) and IL-12p40 that are induced late after TLR stimulation (Kuwata et al., 2006). The investigated knockout mice of this study were also highly susceptible to intestinal inflammation and LPS-mediated endotoxin shock. This outcome led to the conclusion that IκBNS is a regulator of inflammatory responses by inhibiting TLR-induced genes via the modulation of NF-kB activity. B-cell development and function are affected by IκBNS deficiency as well, since knockout mice exhibit for instance a complete absence of their peritoneal B1 B-cell repertoire and reduced mature B-cell numbers in the marginal zone of the spleen (Arnold et al., 2012). Furthermore, Touma et al. (2011) also describe that IκBNS deficient B-cells show a decreased proliferation upon LPS and anti-CD40 exposure whereas proliferation was not affected upon BCR-stimulation. Moreover, also the effector function of B-cells in the humoral immune response was impaired by the absence of IκBNS. In addition to the observation of impaired in vitro plasma cell differentiation, IgG3 class switch was defective, the amount of serum IgM and IgG3 was significantly diminished. Although B-cells of IκBNS deficient mice exhibit higher surface IgM levels. Also antigen-restricted antibody production in response to influenza A virus was decreased. As already mentioned earlier, IκBNS expression can be induced by IL-10. In this regard Fujita et al., showed high expression of IκBNS in mouse regulatory DCs in comparison to their conventional counterparts.

Those, regulatory DCs exhibit high levels of IL-10 but reduced levels of proinflammatory cytokines upon LPS exposure. This suggests that IκBNS participates in the suppression of the NF-κB-mediated production of proinflammatory cytokines. Schuster et al. showed in 2012 that IκBNS drives the expression of Forkhead box P3 (Foxp3) in mouse cells, the key transcription factor controlling development and phenotypic maintenance of the immunosuppressive regulatory T-cell (Treg) phenotype. IκBNS binds together with p50 and c-Rel to the Foxp3 the promoter and a conserved non-coding sequence in the Foxp3 locus. Noteworthy, IκBNS expression is in turn suppressed by Foxp3 upon its induction, establishing a negative feedback loop (Marson et al., 2007). As a consequence of this, IκBNS positive regulation of Foxp3 expression, the loss of IκBNS in mice results in a substantial decrease of ~ 50% in mature Treg cell numbers due to an impairment of precursor $Foxp3^-$ Treg cell development in the thymus. Moreover, IκBNS also critically regulates induced Treg (iTreg) cell development during gut inflammation, and prevents IL-2 secretion of Treg cells (Schuster et al., 2012). Taken together, IκBNS has versatile roles in regulating immune homeostasis and response and is therefore an important player within the innate and adaptive immune system. Since IκBNS carries out functions in immune system activating as well as in immune suppressive mechanisms, it cannot be specified as pro- or anti-inflammatory signaling protein.

1.2.6 The NFAT family

The nuclear factor of activated T-cells (NFAT) was first identified by Shaw et al. in 1988 as a rapidly inducible transcription factor that switches on interleukin-2 expression by binding to the IL-2 promoter in activated T-cells. Research in the following years revealed several more members of the NFAT family, it became obvious that NFAT expression is not restricted to T-cells but is expressed in almost all cell types, including other cells of the immune system, as well. The NFAT family now includes five members that are evolutionary related to the Rel/NF-κB family: NFAT1 (NFATc2/NFATp), NFAT2 (NFATc1/NFATc), NFAT3 (NFATc4), NFAT4 (NFATc3/NFATx) and NFAT5 (tonicity enhancer binding protein TonEBP) (Hogan et al., 2003; Miyakawa et al., 1999). Almost every cell type expresses one of the NFAT family members, including cells of hematopoietic and non-hematopoietic origin (Rao et al., 1997; Hogan et al., 2003; Graef et al., 2001; Crabtree and Olson,

2002). In general, the majority of NFAT proteins in lymphocytes, however, make up NFAT1 and NFAT2 (Rao et al. 1997). Research on NFAT proteins uncovered their regulatory roles in the central nervous system such as axonal guidance, angiogenesis, heart (e.g. cardiac valve formation), kidney, pancreas, skin, bone homeostasis, skeletal and smooth muscle development, the hematopoietic system, inflammatory response and the development and function of the immune system (Hogan et al., 2003; Graef et al., 2001; Crabtree and Olson, 2002; Kiani et al., 2004; Heit et al., 2006; Horsley et al., 2008; Pan et al., 2013). In more detail, in the context of lymphocyte development NFAT family members are expressed in peripheral lymphocytes except for NFAT3 which is primarily expressed outside of the immune system. NFAT1 is predominantly expressed in single positive thymocytes whereas NFAT2 is mainly expressed in double negative thymocytes and B-cells. In contrast to NFAT4 which is preferentially found in double positive thymocytes (Oukka et al., 1998; Amasaki et al., 1998). NFAT5 is expressed in almost all cells and is activated as response to osmotic stress. For instance it regulates the expression of cytokines such as TNF-α and LTβ in lymphocytes under osmotic stress (Miyakawa et al., 1999; Lopez-Rodriguez et al., 2001). NFAT1-4 are regulated by calcium signaling whereas NFAT5 exhibits a truncated NFAT homology region (NHR) and thus lacks the calcineurin binding site (in 2.4.2 more about NFAT protein structure). For this reason, this certain NFAT protein is insensitive to calcium and calcineurin.

1.2.6.1 Transgenic mice

Studies of mouse models deficient in various NFAT members unveiled diverse phenotypes indicating unique roles of the different NFAT proteins. NFATc1 knockout mice for instance, exhibit a lymphoproliferative disorder and TH2-like responses (Ranger et al. 1998b; Yoshida et al., 1998). Mice with a NFATc2 loss, show modestly increased immune responses with TH2 characteristics (Hodge et al., 1996; Xanthoudakis et al., 1996; Kiani et al., 1997; Schuh et al., 1998). NFATc3 deletion results in increased lymphocyte apoptosis, hyperactive peripheral T-cells and the loss of CD4/CD8 double positive thymocytes (Oukka et al., 1998). Animals with a NFATc2 and NFATc3 double knockout exhibit spontaneous differentiation of T-cells into TH2 cells, overshooting IgE secretion, lymphadenopathy and the TH2-predominant syndrome comprising allergic blepharitis and pneumonitis (Ranger et al., 1998c). As NFATc1 and NFATc2 exhibit the same DNA binding specificity, they were expected to be redundant in function. To figure this out, Peng et al. (2001)

reconstituted irradiated RAG2-deficient host mice with fetal livers taken from NFATc1/c2 double knockout mice. By doing this they confirmed the redundancy of NFATc1 and c2. They also investigated lymphocyte functions of NFATc1 or c2 deficient animals. Peng et al. found that NFATc1 and c2 are indispensable for the activation of certain cytokine encoding genes since lymphocytes did not produce any IL-2, IL-4 or TNF-α and reduced IL-5 levels. Mice harbouring a constitutively active NFATc1 mutant show a global inflammatory response without affectation of thymocyte development (Pan et al., 2007).

1.2.6.2 Common protein structure of NFAT proteins

Structurally, all NFAT classified proteins share a moderately conserved regulatory N-terminal NFAT homology region (NHR) (~300 aa) that includes a potent transactivation domain, a NLS, serine rich regions (SRR1, 2), KTS and SPXX-repeat motifs (SP1-3), whereby X denotes any amino acid. Furthermore, the NHR also comprises the docking sites for calcineurin (SPRIEIT), the casein kinase1 (CK1) (FSILF) and for further NFAT kinases (Müller and Rao, 2010). Together, these kinases regulate the activation of NFAT by determining the phosphorylation status of the many serine residues in the SRRs and SP motifs that are contained by the NHR protein domain. Moreover, the NFAT proteins have in common a highly conserved DNA binding domain (DBD) that shares high homology with the Rel homology domain found in Rel/NF-κB proteins, therefore also termed RHD (Chen et al., 1998). The RHD contains points of contact for the interaction with the activating protein-1 (AP-1) transcription family members FOS and JUN. Each NFAT protein has two or more isoforms that are can be distinguished by their length variable N-and C-terminal tails (Luo et al., 1996; Imamura et al., 1998; Park et al., 1996; Chuvpilo et al., 1999). Noteworthy, there are existing three isoforms of NFAT1 (called A, B, C) and six of NFAT2 (called αA, βA, αB, βB, αC, βC) and four of NFAT4 (called 1, 2, 3 and 4). These isoforms are generated by alternative splicing or by the usage of different promoter sites. The functional difference between the isoforms can be for instance the constitutive or inducible expression as in the case of NFAT2 (NFATc1) which encompasses five permanently expressed and one isoform (αA) induced by T- or B-cell stimulation (Macian, 2005).

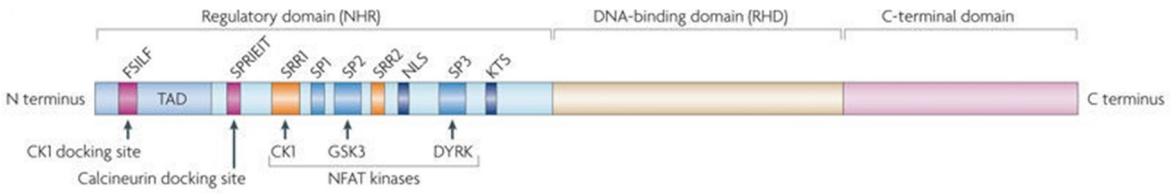

Figure 8. Schematic illustration of the common NFAT family protein structure. NFAT family proteins exhibit a characteristic N-terminal regulatory NFAT homology region (NHR), a DNA-binding domain which is due to its high similarity called REL-homology domain RHD and a C-terminal domain which is variable in length and that specifies isoforms. The NHR contains a transactivation domain (TAD) and docking sites for casein kinase 1 (CK1), termed FSILF, and calcineurin, termed SPRIEIT. The NHR includes as well multiple serine-rich motifs (SRR1, SP1, SP2, SRR2, SP3 and KTS) that provide phosphorylation sites for controlling NFAT activity and a nuclear localization sequence (NLS). Figure adapted from Müller and Rao, 2010.

1.2.6.3 Ca^{2+} signaling and NFAT activation

The activation of receptor tyrosine kinases (RTKs), G-protein coupled receptors (GPCRs), immunoreceptors such as antigen specific T-cell and B-cell receptors and Fc receptors on mast cells, monocytes and NK cells result in the initiation of a signal transduction cascade which leads to an increase of the intracellular Ca^{2+} concentration. Receptor engagement and thus activation leads to the activation of phospholipase C-γ (PLC-γ1 in T-cells and mast cells; PLC-γ2 in B-cells). PLC-γ in turn hydrolyses phosphatidylinositol-3,4-bisphosphate (PIP2) to generate the second messengers inositol-1,4,5-trisphosphate (IP3) and diacylglycerol (DAG). IP3 then binds to IP3 receptors located in the endoplasmic reticulum (ER) membrane inducing the release of ER stored calcium. This Ca^{2+} storage depletion is sensed by the high-affinity ER calcium sensors “stromal interaction moelcule1 or 2” (STIM1 or 2) which are then activated. STIM1 proteins subsequently form oligomers and migrate to the contact site between ER and the cytoplasma membrane. STIM1 oligomers bind then to specialised store-operated calcium-release-activated calcium (CRAC) channels crossing the plasma membrane, including ORAI1. This STIM1-CRAC channel binding triggers a conformational change and ensuing opening of CRAC channels such as ORAI1 in the plasma membrane. The described mechanism provides sustained Ca^{2+} influx into the cell (also called “store operated Ca^{2+} entry” (SOCE)) and maintenance of increased intracellular calcium. Calcium ions bind the Ca^{2+}-sensor calmodulin (CaM), which in turn binds and activates the serine-threonine (S/T) phosphatase calcineurin. Calcium binding by the calcineurin

regulatory B subunit (CnB) under increased intracellular Ca^{2+} conditions leads to the exposure of the calmodulin-binding site on the catalytically active calcineurin A (CnA) subunit. Together, both events result in the release of an autoinhibitory peptide in the catalytic pocket of CnA and the S/T phosphatase calcineurin is now capable of converting substrates such as the calcium/calcineurin signaling dependent NFAT family members NFAT1-4. In order to effectively dephosphorylate NFAT proteins, calcineurin has to bind to a specific peptide motif within the NHR that is highly conserved in the NFAT family and exhibits the consensus aa-sequence "PXIXIT" (X designates any aa). This main calcineurin binding site on NFAT proteins was also exploited to create a specific with calcineurin for NFAT binding competing peptide. This competitive inhibitor mimics the calcineurin NFAT binding site and thus blocks NFAT activation by calcineurin mediated dephosphorylation. The competitive peptide is termed VIVIT according to its aa-sequence. In studies VIVIT was found to prolong xenograft survival in mice and attenuating the invasion of breast cancer cells (Noguchi et al., 2004; Jauliac et al., 2002). The catalytic activity of calcineurin is tightly regulated since it is not only controlled by calcium and CaM but also by other negatively regulating inhibitors like the calcineurin-binding protein 1 (CABIN1), the A-kinase anchor protein AKAP79 and the calcineurin inhibitor family of calcipressins (CSPs). In resting cells, NFAT proteins are present in a hyperphosphorylated, inactive conformation in the cytoplasm. NFAT proteins exhibit 20 serine phosphorylation sites from which the regulatory region NHR comprises 18 in the SSR1 and SP1-3 motifs. The dephosphorylation of the SP2, SP3 and SRR1 motif serine residues by calcineurin unmasks the NFAT NLS, consequently resulting in the nuclear import of the NFAT protein (Macian, 2005). Moreover, in the nucleus calcineurin also sustains the dephosphorylated state of NFAT. In the nucleus, NFAT then cooperates with members of other transcription factor families (described later in more detail) such as AP-1 or NF-κB. These transcription factor families are activated downstream of DAG which induces the MAPK signaling pathway and PKC pathways, to regulate the transcription of target genes. Termination of NFAT transcriptional activity is achieved by its nuclear export and cytoplasmic relocation and accumulation. Responsible for this were found several regulating mechanisms as for example the inhibition of calcineurin activity. The inhibition of the calcineurin S/T phosphatase activity prevents NFAT transcriptional impact on target genes

because NFAT cannot migrate into the nucleus anymore and is also no longer retained there.

1.2.6.4 Pharmacologic inhibitors of NFAT signaling

Cyclosporin A (CsA, a cyclic peptide) and tacrolimus (FK506, macrolid lactone) are immunosuppressive drugs and function as pharmacological inhibitors of calcineurin which is their primary target. Both compounds are structurally unrelated but form complexes with intracellular immunophilins cyclophilinA and FRKBP12 (McCaffrey et al., 1993; Liu et al., 1991). These complexes in turn competitively inhibit calcineurin S/T phosphatase activity by binding to a hydrophobic groove between the catalytic (CnA) and regulatory subunit (CnB), thereby preventing substrate access to the active centre. Consequently, by inhibiting calcineurin, CsA and FK506 act as well as inhibitors of NFAT signaling which is necessary for T-cell mediated immunity as it is indispensable for inducing interleukin (IL)-2 transcription and T-cell activation. CsA is due to its potent immunosuppressive abilities commonly used in the clinic to prevent immune-mediated transplant rejection and in therapy of autoimmune diseases. However, in cancer chemotherapy both calcineurin/NFAT inhibitors are not applied yet because of non-proven effectiveness.

1.2.6.5 NFAT activity modulators

Also multiple cytoplasmic and nuclear NFAT targeting S/T kinases modulate NFAT transcriptional activity. These distinct NFAT kinases precisely maintain the subcellular localisation of NFAT proteins and with this their function as transcription factors. The kinases act as either maintenance or export kinases by sequestering NFAT in the cytoplasm by keeping NFAT fully phosphorylated or assist in NFAT nuclear export by rephosphorylating NFAT. A kinase that exhibits both functionalities is the casein kinase 1 (CK1) that phosphorylates the SRR1 motif. An example for an export kinase is the constitutively active glycogen synthase kinase 3 (GSK3) which phosphorylates the SP2 motif of NFAT1 and the SP2 and SP3 motifs of NFAT2. Another class of NFAT kinases, modifying the subcellular localisation of NFAT are the dual specificity tyrosine phosphorylation-regulated kinases (DYRKs). The family members DYRK1 and 2 phosphorylate the SP3 motif of NFAT1, providing the prerequisites for the phosphorylation of SP2 and SRR1 by GSK3 and CK1. DYRK1 facilitates the nuclear export of NFAT, whereas DYRK2 phosphorylates NFAT in the cytoplasm, thereby preventing it from migration to the

nucleus, thus acting as maintenance kinase. Moreover, also JNK and p38 MAPKs can phosphorylate SSRs of NFAT1 and 2. Phosphorylations are not the only kind of NFAT post-translational modifications and mechanism determining the subcellular localisation and with this NFAT transcriptional activity. Sumoylation for instance was described to result in nuclear relocalistation of NFAT1 and 2 (Terui et al., 2004; Nayak et al., 2009). Yoeli-Lerner et al. (2005) report that in breast cancer cells, NFAT1 is ubiquitinated and thereby targeted for degradation by the E3 ubiquitin ligase MDM2. Furthermore, the cytoplasmic proteins HOMER2 and 3 were found to compete with calcineurin for NFAT binding, thus preventing NFAT dephosphorylation and nuclear translocation. In addition to that, a non-coding RNA was discovered called non-coding repressor of NFAT (NRON) that was identified as specific inhibitor of NFAT nuclear trafficking (Willingham et al., 2005).

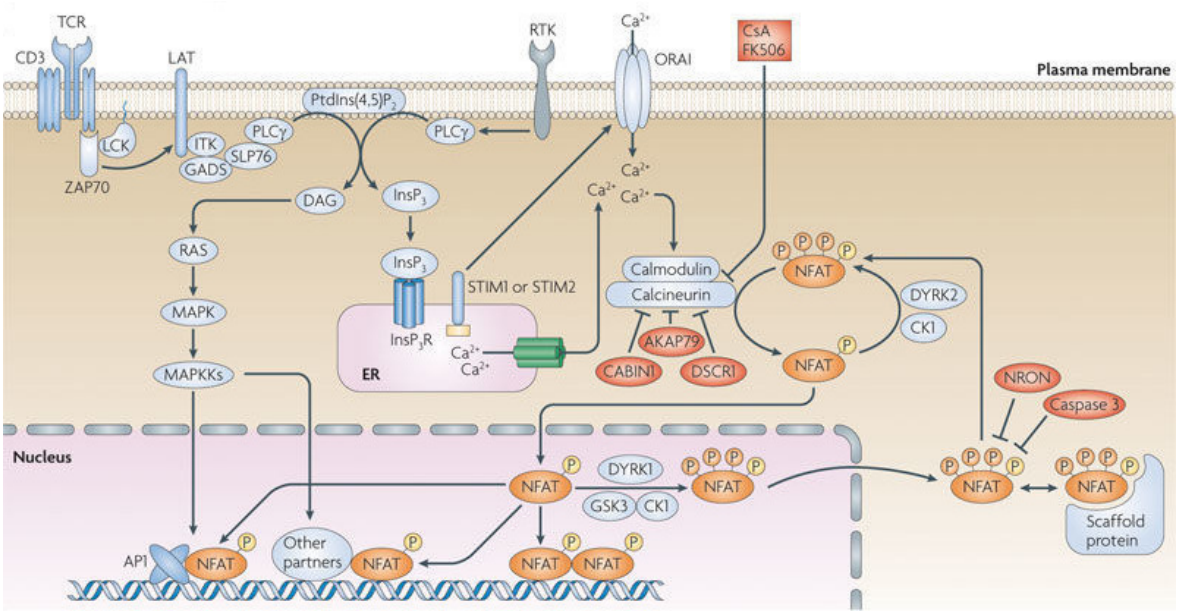

Figure 9. Schematic overview of Ca^{2+} - NFAT signaling. Ligand binding of immunoreceptors such as T-and B-cell receptors and receptor tyrosine kinases (RTKs) lead to the activation of phospholipase Cγ (PLCγ). PLCγ in turn hydrolyses phosphatidyl-4, 5-bisphosphate (PIP2) to generate diacylglycerol (DAG) and inositol-1, 4, 5-trisphosphate (InsP3). InsP3 binds to the InsP3 receptor in the endoplasmic reticulum (ER) membrane and induces the depletion of the ER $Ca2^{+}$ store. Stromal interaction molecule 1 or 2 (STIM1 or STIM2) subsequently detect the emptying of the ER Ca^{2+}storage and form small clusters. STIM1 and 2 interact with the calcium-release-activated calcium ion channel (CRAC) protein ORAI in the plasma membrane to trigger store-operated Ca^{2+} entry (SOCE). Calmodulin as calcium sensing protein binds $Ca2^{+}$ and activates calcineurin. Calcineurin in turn dephosphorylates NFAT, which then translocate to the nucleus where NFAT can cooperate with various transcriptional partners such as AP1 to regulate gene expression of target genes. Activation of transcriptional partners is controlled by for instance MAPK signaling and other pathways. Multiple NFAT kinases mediate the inactivation of NFAT proteins by rephosphorylating them. These are for example the glycogen-synthase kinase 3 (GSK3), Casein kinase1 (CK1) and the

dual-specificity tyrosine-phosphorylation regulated kinase 1 (DYRK1) and DYRK2. Calcineurin phosphatase activity is regulated by endogenous calcineurin inhibitors like calcineurin-binding protein 1 (CABIN1), A-kinase anchor protein 79 (AKAP79) and Down's syndrome critical region 1 (DSCR1). Cyclosporin A (CsA) and FK506 are efficient pharmacological inhibitors of calcineurin. Endogenous negative regulators of NFAT signaling are the Non-coding repressor of NFAT (NRON) and caspase 3. Different scaffold proteins were shown to participate in NFAT regulation. Abbreviations: GADS, GRB2-related adaptor protein; ITK, IL-2-inducible T-cell kinase; LAT, linker for activation of T cells; Lck lymphocyte-specific protein tyrosine kinase; MAPK, mitogen-activated protein kinase; MAPKK, MAPK kinase; SLP76, SH2-domain-containing leukocyte protein of 76 kDa; TCR, T cell receptor; ZAP70, ζ-chain-associated protein kinase of 70 kDa. Figure adapted from Müller and Rao, 2010.

1.2.6.6 NFAT transcriptional activity

Once entered the nucleus, active NFAT members interact with DNA as homodimers or heterodimers and the DNA binding domain is able to cooperate with those of other transcription factors families in the nucleus to enable functional synergies (Giffin et al., 2003). The interaction of NFAT with members of other transcription families is also needed to execute transcription regulation as NFAT exhibits only weak DNA binding properties. For example, the binding of NFAT and AP-1 to neighbouring DNA binding sites results in an ~ 20-fold increase in the stability of the NFAT-AP1-DNA complex in comparison with binding of NFAT to its DNA binding site alone (Jain et al., 1993). The interaction of NFAT proteins with other transcription factors is feasible thanks to a highly flexible linker region located between the RHD and the C-terminal domain that has contact only with the phosphate backbone of the DNA (Stroud and Chenpark, 2003). NFAT interacts with several transcription factors as for instance AP-1, GATA4, IRF4, MEF2, NF-kB, PPARγ, EGR, and FOXP2 & 3 (Yang et al., 2000; Molkentin et al., 1998; Crabtree and Olson, 2002; Rengarajan et al., 2002; Hogan et al., 2003; Macian et al., 2001; Macian, 2005; Pham et al., 2005; Wu et al., 2001; Hu et al., 2002; Hermann-Kleiter and Baier, 2010, Müller and Rao, 2010). This versatile cooperation of NFAT members with other transcription factors makes it possible to combine different signaling pathways in turn to activate specifically rendered gene programmes leading to different phenotypes and specific responses to various stimuli. The best characterised example is the interaction of NFAT with AP-1 members. Fos-Jun dimers form quaternary complexes with NFATs and DNA on corresponding NFAT-AP1 sites to regulate the transcription of diverse inducible genes. This NFAT-AP1 cooperation complex is needed in T-cell activation and integrates to main signaling

pathways of T-cell stimulation. Namely calcium signaling leading to NFAT activation and the MAP-kinase pathway inducing FOS and JUN expression (Chen et al., 1998; Jain et al., 1992). AP1 proteins are thus the main transcriptional partners of NFAT during T-cell activation and together they are inducing a distinct gene program that characterises the activated T-cell phenotype (Macian et al., 2001; Jain et al., 1992). Among the NFAT transcription factor family, NFAT5 is the only protein that is not capable to form cooperative complexes with AP-1 members on composite DNA elements. NFAT5 does not require a nuclear partner for its activity (Lopez-Rodriguez et al., 1999; Macian et al., 2001; Pan et al., 2013). Interestingly Macian et al. (2002), found that under conditions where AP-1 is not activated and NFAT-AP1 cooperation is not taking place, NFAT activity alone in T-cell activation leads to the activation of a different gene set resulting in lymphocyte anergy a completely opposing genetic program than the productive activated state mediated by NFAT-AP-1 complexes. Also a cooperation between NFAT and NF-κB was observed by several groups. Sica et al. (1997) for instance describe coordinate activities of NFAT and RelA/p50 NF-kB dimers binding at same site within the IFN-γ promoter in order to enhance IFN-γ transcription, the TH1 defining cytokine. Another study proves NFAT and NF-κB to act synergistically to activate IL-4 gene expression in T-cells (Li-Weber et al., 2004). Moreover, NFAT is also implicated in cooperation with different partners from different transcription factor families in the regulation of multiple other genes playing an important role in the regulation of the immune system. This includes for instance the cytokines IL-2, IL-3, IL-5, IL-6, IL-13, TNF-α and GM-CSF, the chemokines IL-8 and Mip-1α, the surface proteins Igk, CD5, CD25, CD40L and CD95L (Rao et al., 1997; Macian et al., 2001).

Thus, it is likely that NFAT signaling has a significant impact on chemokines in cells that are part of the tumor environment. This is from interest since leukaemia and lymphoma mouse models were revealed to harbour hyperactive NFAT as a result of paracrine signalling in the tumor environment (Medyouf et al., 2007; Pham et al., 2005).

1.2.6.7 Role of NFAT in B-cells

Regarding B-cells, mice lacking NFAT2 exhibit a complete loss of splenic and peritoneal B-1 cells. In contrast, NFAT1 deficient mice showed a normal repertoire of B-1a cells. Winslow et al. (2006) describe a more indirect role of NFAT in B-cell function. The group was investigating mice with a B-cell specific deletion of the

regulatory subunit B of calcineurin. As a consequence of this, the mice showed decreased plasma cell development, fewer immunoglobulin production, reduced numbers of B1a cells and a B-cell proliferation defect downstream of the BCR.

1.2.6.8 NFAT in solid cancers

NFAT signaling participates in the regulation of growth, survival, differentiation and development of many cell types and organ systems. Due to this, abnormalities in NFAT proteins and/or the dysregulation of NFAT signaling are potent to be associated with the development of neoplasms originating from various tissues. Indeed, aberrant NFAT signaling, mostly overexpression and/or hyperactivity, was documented to play roles in malignant transformation, tumor angiogenesis, invasive migration, and therefore in the development and pathogenesis of solid neoplasms. This is the case for instance in breast cancer (NFAT1, 5), pancreatic cancer (NFAT2), melanoma (NFAT2, 4), prostate cancer and endometrial cancer (Robbs et al., 2008; Mancini and Toker, 2009; Yoeli-Lerner et al., 2005 and 2009; Buchholz et al., 2006; Koenig et al., 2010; Flockhart et al., 2009; Lehen'kyi et al., 2007; Sales et al., 2009 and 2010).

1.2.6.9 NFAT in hematopoietic malignancies

NFAT family members and thus $Ca^{2+/}$NFAT signaling were also revealed by multiple studies to be implicated in the pathogenesis of haematological malignancies like B- and T-cell lymphoma (Pham et al., 2005; Fu et al., 2006; Glud et al., 2005; Medyouf et al., 2007). An immunohistological evaluation of almost 300 lymphoma samples conducted by Marafioti et al. in 2004 found NFAT2 to be overexpressed in most lymphoid neoplasms. Moreover, NFAT2 exhibiting a nuclear localisation was observed in 30% of DLBCL and 70% of Burkitt lymphoma samples, indicating in vivo activation of the NFAT pathway in those malignancies. Other studies report that in patient samples derived from DLBCL and T-All NFAT2 nuclear localisation or dephosphorylation of NFAT2 and 1 were observed (Fu et al., 2006; Medyouf et al., 2007). In line with this, another study conducted by Pham et al (2005) reports that NFAT is constitutively activated in LBCL. Moreover, they demonstrate that NFAT2 and c-Rel cooperatively bind at the CD154 promoter at similar binding sites. Thereby, they directly interact and synergistically regulate CD154 transcription in lymphoma B-cell lines. This result was supported by the finding from Srahna et al. (2001). They report an additive effect of NF-κB inhibitors and the NFAT inhibitor CsA

in inhibiting the expression of CD154 (CD40L) on both, the mRNA and protein level upon P/I mediated T-cell stimulation. In DLBCL and MCL it was found that NFAT2 regulates the expression of B-cell survival factors like CD40L (CD154) and B-lymphocyte stimulator (BLYS) (Pham et al., 2005; Fu et al., 2006). Mouse T-cell acute lymphoblastic leukemia (T-ALL) models that were treated with calcineurin inhibitors exhibited reduced proliferation and induction of apoptosis of leukemic blast cells, fast tumor clearance and consequently prolonged survival (Medyouf et al., 2007). Notably, NFAT2 was found to play an important role in cancer therapy resistance as the activation of Ca^{2+}-NFAT signaling was associated with the acquired resistance of chronic myeloid leukemia (CML) towards tyrosine kinase inhibitors (Gregory et al., 2010).

1.2.6.10 NFAT signaling summary

In summary, taking into account the almost ubiquitous expression of NFAT, the number of NFAT family members and their distinct isoforms, the multitude of NFAT binding partners from other transcription families on target genes, the abundance of NFAT activity modulators and the involvement of NFAT signaling in the regulation of a wide range of genes and physiological processes makes NFAT signaling to a complex and vital component of human cell organisation. Therefore, NFAT signaling constitutes a promising subject for further research in order to develop therapy approaches for a variety of malignancies.

1.2.7 The AP-1 family

The activator protein 1 (AP-1) transcription factor was discovered in 1987 as DNA binding protein in HeLa nuclear extracts that recognises a distinct DNA element (TGACTCA) within the promoter and enhancer region of the SV40 and metallothionein IIA gene (Lee et al., 1987) Today, the AP-1 transcription factor family comprises dimeric complexes made up of over 20 different protein subunits that are functionally and structurally related and categorised in five subfamilies termed JUN (v-Jun, c-Jun, JUNB and JUND), FOS/FRA (v-Fos, c-FOS, FosB, Fra1, Fra2), JDP (JDP1/2), ATF/CREB (ATF1, ATF2, ATF3/LRF1, ATF4, ATF5, ATF6a, ATF6b, ATF7, B-ATF; ATFa0, CREB) and MAF (v-Maf, c-Maf, MafB, MafF, MafG, MafK, Nrl). These subunits can form a multitude of homo- and heterodimeric combinations that exhibit different DNA binding specificities and affinities towards gene expression regulatory elements within promoters and enhancers of AP-1

responsive genes. The dimers also exhibit partially redundant functions and are differently regulated. Thus, the manifold dimer combinatorial possibilities determine the range of regulated genes. For instance, Jun containing dimers preferentially bind the AP-1 DNA recognition element also called the TPA-responsive element (TRE). But besides TRE there are several more different AP-1 responsive sequences that are preferentially bound by distinct dimer pairs. Some are favoured over others or are exclusively bound by a specific dimer composition. These are the cAMP-responsive element (CRE) which is preferentially bound by ATF proteins, the MAF-recognition elements (MAREs I/II) and the antioxidant-response elements (AREs). c-Jun homodimers for instance, favour TRE over CRE site binding whereas c-Jun/ATF4 heterodimers exclusively bind to CRE sites and c-FOS/MAFB/F/G/K heterodimers bind only to MARE I/II responsive elements (Eferl and Wagner, 2003). Such AP-1 binding elements were among others found in regulatory regions of genes that are induced during T-cell activation. This led to the assumption that proteins of the AP-1 transcription factor family could consequently regulate the expression of those genes. Promoter analysis of such a gene, the human IL-2 gene, encoding interleukin-2 an important growth factor for B-cells and critical for T-cell proliferation, differentiation and mounting of a T-cell dependent immune responses was identified to harbour two AP-1 responsive sites. Furthermore, the IL-2 promoter was also shown to bind partially purified AP-1 proteins and mutation of one of those sites resulted in diminished or abrogated induction of IL-2. The functionality of this AP-1 responsive site within the IL-2 promoter was validated by a cotransfection of IL-2-chloramphenicol acetyltransferase encoding plasmid together with c-FOS and/or c-Jun leading to an enhanced induction of IL-2-chloramphenicol acetyltransferases activity (Jain et al., 1992). In accordance with this, transgenic mice, overexpressing c-FOS exhibit enhanced IL-2 gene expression and cytokine production. Whereas mice expressing a dominant negative form of the CRE-binding protein (CREB) that is known to induce various AP-1 encoding genes show less IL-2 production with simultaneous decreased c-Jun, c-FOS, Fra2 and FosB mRNA levels (Ochi et al., 1994; Barton et al., 1996). Thus, AP-1 plays a pivotal role in the transcriptional regulation of the IL-2 gene. AP-1 members can also form complexes with non-bZIP proteins likeNF-κB and NFAT (Stein et al., 1993; Jain et al., 1992). AP-1 and NFAT were found to bind cooperatively to composite DNA binding sites and from stable complexes. This is the case for instance at the murine IL-4 promoter.

Together, NF-κB and NFAT bind at a composite site within the sequence of the IL-4 promoter. Therefore, AP-1 is together with the transcription factor NFAT critical for full activity of the murine IL-4 promoter. IL-4 is involved in the differentiation of precursor T-helper (TH) cells into the TH2 phenotype. Depending on the investigated T-cell line, c-FOS, Fra-2, Fra-1, c-Jun, JunB, and JunD were found to be involved in the transcriptional regulation of this leukocyte modulatory interleukin 4 (Le Gros et al., 1990; Chuvpilo et al., 1993; Rooney et al., 1995; Li-Weber et al., 1997). Consequently, loss of JunB in TH2 cells in vitro results in deregulated TH2 cytokine expression and the expression of TH1 characteristic key regulators (Hartenstein et al., 2002). Moreover, also IL-10 expression of TH2 cells is positively controlled by JunB/AP-1, c-Jun/AP-1 transcription complexes. In contrast to that, Meixner et al., 2004 found reduced IL-4 levels in JunD overexpressing lymphocytes and consistently with that higher IL-4 and IL-10 expression in JunD negative TH2-cells. This suggests that JunD unlike its relatives JunB and c-Jun suppresses TH2 differentiation and the expression of TH2 specific cytokines. The cooperation between AP-1 and NFAT was also observed in controlling the induction of IL-5. In the gene promoter of this cytokine which is predominantly produced by TH2 cells, a DNA element was found to which NFAT and c-FOS/c-Jun dimers bind cooperatively (Lee et al., 1995; Wang et al., 1994; Karlen et al., 1996). Furthermore, also in the promoters of IL-3 and IL-9 AP-1 sites were identified. Thus, AP-1 was reported to enhance the expression of an IL-3 reporter construct and c-FOS/c-Jun were found to bind to the IL-3 promoter in stimulated T-cells (Mathey-Prevot et al., 1990; Park et al., 1993). A mutational analysis revealed that AP-1 enhances IL-9 promoter activity in T-cells (Zhu et al., 1996). Moreover, also IFN-γ and TNF-α were described to be regulated by AP-1 proteins in cooperation with other transcription factors. For instance, in Jurkat T-cells AP-1 was found by Barbulescu et al. (1997) to be pivotal for the induction of IFN-γ expression. In line with this, an AP-1 heterodimer consisting of c-Jun and ATF2 was shown to interact and transactivate IFN-γ promoter constructs in T-cells (Penix et al., 1996). Additionally, AP-1 family members were reported to induce the macrophage inflammatory protein-1β (MIP-1β) and upon IL-1β stimulation of endothelial cells in cooperation with RelA/p50 the chemoattractant protein-1 (MCP-1) (Martin and Dorf, 1991). In calcium stimulated T-cells, an AP-1 dimer consisting of c-Jun/ATF-2 cooperates with NFATc2 to bind to a CRE site in order to induce TNF-α expression, whereas in LPS

stimulated THP-1 cells, c-Jun comprising AP-1 complexes cooperate with RelA/p50 dimers to increase TNF-α transcription (Tsai et al., 1996; Yao et al., 1997).
AP-1 family members were also reported to act as transcriptional repressors especially those exhibiting weak transactivation capacities such as JunB and JunD, Fra1 and Fra2. These AP-1 proteins can competitively out bind AP-1 subunits of transcriptionally active AP-1 dimers binding at the same DNA promoter site as they do. The Jun and Fos AP-1 subfamilies are the major AP-1 proteins. Notably, Jun proteins homo- and heterodimerize whereas FOS members are incapable of homodimerisation but pair stably with Jun proteins and some ATF family members. FOS proteins possess negatively charged residues adjacent to their leucine zipper domain leading to an electrostatic destabilisation of FOS homodimers, therefore favouring instead the formation of Jun-Fos heterodimers (Halazonetis et al., 1988). AP-1 proteins are composed of basic leucine zippers (bZIPs), heptad repeats of leucine residues. For this reason, AP-1 members are referred to as bZIP proteins. The bZIP forms an amphipathic α-helix and is associated with the leucine zipper of the second AP-1 member within the dimer in a coiled-coil arrangement facilitating the dimerization of the AP-1 subunits. Furthermore, AP-1 proteins comprise another α-helical region that includes several basic amino acid residues responsible for the interaction of the transcription factor with the phosphate backbone of the DNA. Moreover, AP-1 proteins also contain a transactivation domain called delta domain, determining transcriptional activation. AP-1 is activated by a wide array of different stimuli such as ligand engagement of BCR, TCR or TLRs, cellular stress, radiation, growth factors, neurotransmitters, peptide hormones, pathogens and cytokines. Hence, AP-1 signaling is involved in several cellular processes like apoptosis, inflammation proliferation, cellular migration, wound healing, survival and differentiation. Depending on the stimulus, different AP-1 subfamilies are induced by different upstream signaling pathways. Antigen receptor activation for instance results in the induction/activation of Jun (c-Jun, JunB), FOS (c-FOS) and ATF (ATF2, ATF3) proteins. Growth factors for example, induce AP-1 transcriptional activity by the activation of the S/T kinases mitogen-activated protein kinase (MAPK) subgroup of extracellular signal-regulated kinase (ERK) proteins which migrate to the nucleus where they activate ternary complex factors which in turn bind FOS promoters. The MAPK family members c-Jun N-terminal kinase (JNK) and p38 mainly activate AP-1 as response to pro-inflammatory cytokines, genotoxic stress

and some mitogenic signals. JNK which encompasses at least ten isoforms encoded by three different genes (JNK1, 2, 3) regulates the expression and activity of Jun family proteins. Subsequently to their nuclear translocation, JNK isoforms phosphorylate c-Jun, JUNB, JunD and less efficiently also ATF2 which then trigger the activation and formation of AP-1 dimers. For instance, JNK phosphorylation of c-Jun and ATF2 increases their transcriptional activity, stability and induces their heterodimerization. c-Jun/ATF2 heterodimers can then bind different sites in the c-Jun promoter. On the other hand, under non-stimulated conditions, phosphorylation inactive JNKs were shown by Fuchs et al. (1998) to degrade c-Jun and ATF2. As soon as the JNK phosphorylation enzyme activity is turned on, c-Jun and ATF2 degradation is abolished (Musti et al., 1997). AP-1 induction by p38 is facilitated by direct phosphorylation and activation of ATF2 and MEF2C.

In order to reveal whether c-Jun is essential for lymphocyte function, Chen et al. (1994) injected c-Jun deficient mouse embryonic stem cells into blastocysts derived from RAG2 lacking mice that do not develop mature lymphocytes. The resulting chimeric mice showed altered thymus structure and changes in the ratios of thymocyte populations but produced T-and B-cells exhibiting normal phenotypes. For this reason, c-Jun was not supposed to be required for lymphopoiesis. Moreover, also c-FOS deficient mice did not display any obvious differences in T-cell activation and proliferation (Jain et al., 1994). On the other hand, FosB2 (lacking a transactivation domain) overexpressing mice display strong alterations in thymic structures and composition. Furthermore, in comparison to their wild-type counterparts these mice show elevated amounts of αβ-TCR expressing thymocytes and reduced fractions of DP thymocytes. Research in c-FOS and c-Jun negative murine cells suggests that those proteins are not necessary for proper induction of apoptosis. This assumption was further strengthened by the occurrence of apoptosis in mouse embryos deficient in either c-FOS, c-Jun or both c-FOS and c-Jun (Roffler-Tarlov et al., 1996). Moreover, also splenic and thymic primary cultures from c-FOS knockout mice showed inducible apoptosis in cell culture experiments (Gajate et al., 1996). In contrast, a study conducted by Colotta et al. (1992) suggests that AP-1 plays a role in growth factor withdrawal-induced apoptosis of lymphoid cells.

It was reported that several FOS and JUN members associate alone or in conjunction with other transcription factors such as NFAT with the promoters of

genes coding for cytokines characteristic for TH1 and TH2 cells. Both T-cell subtypes were shown to express several AP-1 members upon activation (Rincon et al., 1998). TH1 cells express c-FOS and c-Jun whereas TH2 cells exhibit high levels of c-FOS, c-Jun and also of JunB. This indicates that different AP-1 expression patterns result in a distinct cytokine expression. AP-1 members also participate in hematopoietic differentiation as c-FOS was revealed with the aid of c-FOS deficient mice to be a unique regulator of bone marrow macrophage differentiation (Grigoriadis et al., 1993). The regulatory role of c-FOS in macrophages is also illustrated by c-FOS deficient macrophages that were found to produce higher IL-12 levels upon LPS stimulation than c-FOS positive controls (Roy et al., 1999).

Regarding B-cell biology, surface immunoglobulin (mIg) crosslinking was unveiled to induce several AP-1 family proteins in a primarily PKC dependent manner. For instance, c-FOS expression was induced in primary B-cells and model B-cell lines (Klemsz et al., 1989). Moreover, elevated levels of the AP-1 proteins JunB, FosB and JunD were observed as well in mIg stimulated primary B-cells (Tilzey et al., 1991; Tanguay et al., 1994; Huo and Rothstein, 1995 and 1996; Amato et al., 1996). On the other hand, also a predominantly PKC independent induction of the AP-1 proteins c-FOS, JunB and JunD by CD40 was observed (Huo and Rothstein, 1995; Francis et al., 1995; Kawakami et a., 1992). Unlike in other cell types, the induction of AP-1 DNA binding in B-cells was described not to increase AP-1 transactivation or cell-cycle progression. For instance, in the murine B-cell lymphoma line BAL-17.7.1 (BAL-17) which is a model for primary B-lymphocyte responses, induced AP-1 proteins did not transactivate a transiently transfected TRE binding site containing human collagenase gene promoter (Chiles and Rothstein, 1992). Kobayashi et al. (1997) report that in splenic B-cells derived from IFNα, β inducible c-FOS transgenic mice the cell cycle was arrested in the G1-phase as a consequence of IFNα/β application within half a day after anti-IgM stimulation. From this observation they concluded that induced c-FOS overexpression in the G1-phase interferes with the activation of cell cycle regulating mechanisms. In further investigating this, they found that IFN induced c-FOS overexpression in anti-IgM stimulated B-cells is responsible for preventing the down regulating of p27 as a result of abolished CDK2 kinase activity in late G1 phase. From this they drew the conclusion that c-FOS is able to negatively affect cell cycle regulatory mechanisms in anti-IgM stimulated B-cells (Kobayashi et al., 1997). Moreover, AP-1 dimers also

seem to be involved in antibody production as they were found to transcriptionally induce the kappa light chain and the Ig heavy chain gene (Schanke et al., 1994; Grant et al., 1995). In this respect, transgenic mice overexpressing c-FOS under the control of the H-2k^{b} promoter showed abnormalities in Ig class switch, an inability to produce primary IgG antibodies in response to antigens and no generation of memory B-cells in the spleen (Takao et al., 1991).

Members of the AP-1 family were observed to be frequently overexpressed in lymphoma such as c-jun, JunD, JunB and c-FOS in B-cell NHL of the splenic marginal zone. c-Jun and JunB were found to be overexpressed in primary and cultivated tumor cells of cHL patients and in anaplastic large cell lymphoma. JunB was also described to be overexpressed in cutaneous lymphoma and in an array of CD30^{+} lymphoma (Trøen et al., 2004; Mathas et al., 2002; Rassidakis et al., 2005). Regarding DLBCL, Blonska et al. (2015) have shown that c-Jun is frequently activated. By conducting a DNA microarray they revealed a number of c-Jun positively regulated genes that were coding for signaling and adhesion molecules, surface receptors, enzymes and cytokines. Thus, c-Jun knockdown resulted in decrease of cell adhesion to extracellular matrix (ECM) components, down regulation of ABC DLBCL (OCI-Ly3 and OCI-Ly10 cell lines) released cytokines such as macrophage-derived chemokine (MDC), interferon-inducible protein 10 (IP-10), IL-6, IL-10 and IL-12. Furthermore, c-Jun knockdown led to a reduction of tumor growth and cell invasiveness into the bone marrow of a mouse DLBCL xenograft model. Moreover, in cell lines classified as the ABC DLBCL subtype derived from patients in an advanced disease stage, they observed elevated c-Jun expression levels. In accordance with this study, Juilland et al. (2016) revealed that ABC DLBCL exhibit constitutively upregulated CARMA1 and MYD88 mediated expression of the AP-1 proteins c-Jun, JunB and ATF3. By conducting chemical cross-linking experiments, the indicated JUN family members were revealed to form constitutive dimers with ATF2 and ATF7 in both GCB- and ABC DLBCL cell lines. In contrast, ATF3 was found to be expressed exclusively in ABC DLBCL cell lines where it formed dimeric complexes with c-Jun, JunB and JunD. The group also reports that the usage of a competitive AP-1 inhibitor had an impairing effect selectively on ABC DLBCL viability. An additional shRNA mediated silencing approach of either ATF2, ATF3 or ATF7 in the ABC DLBCL cell line HBL-1 showed that ATF2 and ATF3 expression is pivotal for ABC DLBCL survival, whereas ATF7 silencing had only little

impairing effects on survival. Moreover, the analysis of 350 DLBCL patient samples by immunohistochemistry unveiled a strong nuclear presence of ATF3 in nodal ABC DLBCL samples, identifying ATF3 expression as a hallmark of the ABC DLBCL subtype. These results are consistent with observations made by Ruland et al. (2015). The group generated a mouse model expressing the human DLBCL derived CARD11 (L225LI) gain-of-function mutant that was uncovered by Ruland et al. to induce CBM dependent simultaneous NF-κB and JNK signaling in purified splenic B-cells. In line with the induced JNK signaling activity, they could observe high amounts of the phosphorylated AP-1 JNK substrates c-Jun and ATF2 in nuclear extracts of transgenic CARD11 (L225LI) expressing murine splenic B-cells. When they conducted gel mobility shift assays with these nuclear extracts, they found markedly increased NF-κB and AP-1 DNA binding activity in CARD11 (L225LI) expressing transgenic B-cells compared to wild-type B-cells. Furthermore, transfection of the mature B-cell lymphoma line Bal-17 with CARD11 (L225LI) led to increased nuclear c-Jun, RelA, c-Rel and p50 levels. Moreover, in order to figure out if the results that were obtained by the transgenic mouse model would also hold true for human DLBCL cases, they performed an immunohistochemistry based analysis to check for the presence of activated JNK in 67 human primary DLBCL samples patients. Indeed, in more than 55% of the investigated ABC DLBCL cases they found phosphorylated JNK indicating a constitutive JNK enzyme activity, whereas no GCB DLBCL classified cases were found to exhibit active JNK. Consequently, they tested established human ABC DLBCL model cell lines for the presence of phosphorylated i.e. activated JNK and revealed three of four cell lines to harbour constitutively phosphorylated JNK. Constitutive active JNK in these DLBCL could be further substantiated by conducting an *in vitro* kinase assay with the JNK AP-1 substrate c-Jun. In addition, alike in the murine Bal-17 cell line the transduction of the GCB DLBCL cell line BJAB with the CARD11 (L225LI) mutant caused the besides NF-kB also the activation of JNK as proven by p-JNK detection and JNK kinase activity assays. Finally, they treated ABC DLBCL with a JNK inhibitor and unveiled that all cell lines exhibiting JNK activity died upon JNK inhibitor treatment in a dose-dependent manner, indicating the relevance of the JNK pathway and associated AP-1 signaling for the survival of ABC DLBCL subtype.

1.3 Antigen receptor signaling: B-cell receptor (BCR) and T-cell receptor (TCR) signaling

B- and T-lymphocytes are central elements of the adaptive immune system. Both lymphocyte subsets bear highly diverse antigen receptors on their surfaces with each lymphocyte possessing its own unique antigen receptor namely the B-cell receptor (BCR) or the T-cell receptor (TCR) which a single antigen specificity. Therefore, the abundance of this receptor class enables the immune system to recognise a wide range of different pathogens. Whereas T-cells play a central role in cell-mediated immunity by killing cancerous or infected cell and activating other immune cells, the correct activation of B-cells is substantial for mounting an effective humoral immune response. The terminal effector cells of the B-cell lineage are plasma cells and memory B-cells emerging from mature activated B-cells that underwent a highly regulated differentiation process. Plasma cells are capable to neutralise invading pathogens such as bacteria and viruses by secreting high-affinity antigen specific immunoglobulins. Memory B-cells confer long-lasting protection against recurrent infections. B-cell activation begins with the engagement of the correspondent antigen by the B-cell antibody receptor (BCR) (for an overview of BCR-signaling see Figure 10). The BCR is a multiprotein complex made up of the ligand binding membrane bound immunoglobulin (mIg) heavy and light chains and an associated disulfide-linked heterodimer consisting of Igα (CD79A) and Igβ (CD79B) that are capable of transducing downstream signaling. The T-cell receptor (TCR) on the other hand, consists of the highly variable heterodimer forming antigen recognition chains TCRα and TCRβ. Moreover, the accessory CD3 complex is associated with the antigen-recognising portion by electrostatic interactions between aa-residues within their transmembrane domains. The CD3 complex comprises several invariant proteins, one CD3γ, one CD3δ and two CD3ε chains that consist of an extracellular Ig-like structure and cytoplasmic tails bearing one ITAM each. Further, the complex is associated with two ζ chains representing a mainly intracytoplasmic disulfide-linked homodimer bearing six ITAMs in total, responsible for TCR downstream signaling. Monovalent ligands binding to the BCR of mature B-cells are not able to activate the BCR. Instead, in order to properly active the BCR and ensuing downstream signal cascades, ligand engagement has to crosslink BCRs resulting in the formation of BCR aggregation clusters (Küppers, 2005). However, some studies report that in the absence of antigens, BCRs are

present on the surface of resting cells in oligomers that exhibit an autoinhibitory confirmation and are dissolved as a result of antigen binding (Fiala et al., 2013; Yang and Reth, 2010). The first step of signal propagation upon mIg antigen ligand binding is the phosphorylation of the CD79A/B immunoreceptor tyrosine-based activation motif (ITAM) tyrosins. Each CD79 subunit harbours a single ITAM in its cytoplasmic domain that incorporates two tandem tyrosines that are phosphorylated by the B-cell predominantly expressed LYN and also FYN, BLK or LCK kinases of the src family. Phosphorylation of the TCR associated CD3 invariant chains and the ζ-chains in T-cells is conducted by LCK. The phosphorylated ITAM tyrosines of CD79 (CD3 invariant chains and ζ-chains in TCR signaling) bind and activate the spleen tyrosine kinase also known as SYK (ZAP-70 in T-cells) as the dually phosphorylated ITAMs of the signaling chains provide a specific, spatially defined binding site for the SYK SH2 domains. SYK in turn is critical for coupling the BCR to downstream signaling events. Activated SYK autophosphorylates (ZAP-70 however is activated by LCK in T-cells) and in turn creates docking sites for further distal signaling proteins. SYK also interacts with and phosphorylates various proteins like the phospholipase Cγ2 (PLCγ2), the Tec-family protein Bruton's tyrosine kinase BTK, BCAP and the B-cell linker protein (BLNK; also known as SH2-domain-containing leukocyte protein SLP65). In TCR-signaling, ZAP-70 phosphorylates LAT and SLP76 (LCP2) to which SLP65 has strong sequence homologies. BLNK contains a SH2 domain and more than five sites for tyrosine phosphorylation that were unveiled to bind SH2 domains of effector molecules (Chiu et al., 2002). Thus, BLNK functions as a molecular scaffold for the coordinated formation of a signalosome in which BLNK provides the platform for the assembly of signaling proteins that spread BCR signaling into distinct signal transduction pathways. This signalosome consists besides SYK and BLNK of several signaling molecules like Vav, BTK, PI3K and PLCγ2. The BCR co-receptor CD19, an integral transmembrane protein that positively modulates CD79 signaling by recruiting and activating LYN, PI3K, BTK and VAV is phosphorylated in its cytoplasmic tail by Lyn in a BCR activation dependent manner (Buhl and Cambier et al., 1999; Fujimoto et al., 2000). CD19 phosphorylation by LYN provides a binding site for the PI3K p85 subunit. Together with the adaptor protein BCAP, CD19 localises the PI3K to the cytoplasma membrane where PI3K generates phosphatidylinositol-3,4,5-trisphosphate (PIP3), a docking site for BTK. Subsequent to the recruitment in the

signalosome, BTK gets activated and together with SYK it activates PLCγ2 (PLCγ1 in T-cells) by phosphorylation and recruits it to the cytoplasma membrane where PLCγ2 can bind phosphoinositides by its pleckstrin (PH) homology domain. PLCγ2 hydrolyses phosphatidylinositol-4,5-bisphosphate (PIP2) in order to generate the second messengers inositol triphosphate (IP3) and diacylglycerol (DAG). IP3 binds to IP3 receptors in the ER membrane leading to emptying the intracellular Ca^{2+} storage what in turn leads to the influx of extracellular calcium into the cell. Elevated intracellular Ca^{2}+ levels and DAG activate protein kinase C beta (PKCβ), in T-cells the isoform PKCθ (Isakov and Altman et al., 2002). The phosphorylation of CARD11 (also known as CARMA1) by PKCβ or PKCθ releases the intramolecular inhibitory interaction between the linker and the coiled-coiled domain of CARD11 and leads to the recruitment of BCL10 and MALT1 and consequently the formation of the CBM complex that triggers canonical NF-kB signaling (1.3.3). Another subset of proteins that is activated through BCR signaling is the mitogen activated protein kinase (MAPK) family with the subfamilies of extracellular signal regulated kinase (ERK), c-Jun NH2-terminal kinase (JNK/SAPK) and p38 MAPKs. These protein families in turn activate ETS-1, c-MYC and members of the transcription factor family AP-1 (2.5). There are several proposed mechanisms how BCR signaling facilitates the integration of MAPK signaling. For instance, Vav a Rac/Rho-specific guanine nucleotide exchange factor and adaptor for GRB2/SOS associates as well with phosphorylated BLNK, thus part of the signalosome, is able to activate the RAC and RAS MAPK family pathways. Furthermore, RasGRP3 phosphorylation by PKCβ promotes the formation of RAS-GTP which in turn activates RAF1 and subsequently the MAP kinases ERK1/2. Furthermore, it was also suggested that BCR ITAM tyrosine phosphorylation recruits the adaptor protein SHC which in turn associates with GRB2 and SOS. This ternary complex is proposed to activate the RAS/RAF/MEKK cascade (D'Ambrosio et al., 1996; Nagai et al., 1995). Conventionally, SYK was attributed to phosphorylate SHC. However, Pao et al. (1998) suggest an SYK independent pathway in which mono-phosphorylated CD79 binds SHC leading to its phosphorylation. This indicates that SRC-kinases are implicated in this mechanism. Also JNK activation was shown to require SYK and to a lesser extent BTK, whereas Lyn activity is not needed (Chan et al., 1998; Ishiai et al., 1999). Also PLCγ2 and the generation of IP3 were shown to be involved in the BCR mediated activation of JNK and p38 MAPK (Hashimoto et al., 1998).

In T-cells linking TCR signaling to MAPKs is facilitated by the adaptor protein GADS, a homologue of GRB2 which is recruited by phosphorylated LAT. GADS in turn uses SOS to recruit RAS. The serine/threonine kinase AKT is a further signaling protein that is integrated by downstream BCR signaling (Datta et al., 1997; del Peso et al., 1997). AKT is known to regulate transcription factors and other proteins that are involved in controlling apoptosis. Due to its PH domain, AKT is recruited by the generation of PIP3 to the cytoplasma membrane. This results in a conformational change through which serine and threonine residues can be phosphorylated that are necessary for full activation of the enzyme. A substrate of AKT kinase activity is BAD, a pro-apoptotic BCL-2 family protein promoting apoptosis by binding and thereby neutralising the anti-apoptotic BCL-XL. The phosphorylation of BAD by AKT leads to the dissociation from BCL-XL and the subsequent binding of AKT to 14-3-3 proteins ceasing BAD mediated BCL-XL neutralisation. AKT directly regulates several more transcription factors such as NF-kB, E2F and CREB and the forkhead transcription family (Brennan et al., 1997; Brunet et al., 1999; Kane et al., 1999; Kops et al., 1999; Plas and Thompson et al., 2003). Moreover, also GSK3 a kinase that participates in cell-cycle regulation and NFAT signaling as nuclear export kinase was found to be negatively regulated by AKT (Beals et al., 1997; Cross et al., 1995; Ikeda et al., 1998). Another transcription factor family that is activated by proximal BCR signaling is NFAT which is linked to BCR signaling through the increase of the intracellular Ca^{2+} concentration and the followed activation of the S/T kinase calcineurin (reviewed in 2.4.).

Negative modulators are an important component of BCR and TCR signaling as their loss usually results in self-reactive lymphocytes instead of anergy or deletion leading to the abrogation of tolerance and autoimmunity (Cornall et al., 1998; Cyster and Goodnow, 1995 and 1997). The group of negative regulators includes CD22, LYN, SH2 domain-containing phosphatase 1 and 2 (SHP1,2), SH2 domain-containing inositol 5'-phosphatase 1 (SHIP1) and the Fc receptor for IgG (FcγRIIB-1). Upon BCR aggregation, the src-family kinase LYN which has also a positive regulatory role, phosphorylates the three immunoreceptor tyrosine-based inhibitory motifs (ITIMs) located in the cytoplasmic tail of the inhibitory coreceptor CD22. The negative impact conferred by CD22 to BCR signaling is partially caused by its recruitment of SHP-1 (Blasioli et al., 1999). SHP-1 is a protein tyrosine phosphatase that removes phosphates that were previously added by tyrosine kinases.

Substrates of SHP-1 include CD79A, CD79B, SYK, VAV, BLNK and CD22 (Mizuno et al., 2000; Tamir et al., 2000; Wu et al., 1998). FcγRIIB-1, a low affinity IgG receptor also harbours regions that are phosphorylated in a LYN-dependent fashion. Upon ITIM phosphorylation, FcγRIIB-1 primarily recruits SHIP1 which removes the 5'phosphate group from PI(3,4,5)P3 to generate PI(3,4)P3 thereby preventing PI(3,4,5)P3 accumulation and hampering further BCR proximal signaling (Scharenberg et al., 1998; Fong et al., 2000). In vitro data suggest also an association of FcγRIIB-1 with SHP1 and SHP2 (Famiglietti et al., 1999; Hippen et al., 1997; Nakamura et al., 2000). FcγRIIB-1 was also observed to colligate with the BCR and subsequently to cause early termination of PIP2 hydrolysis and thus Ca^{2+} signaling. Moreover, SHIP can also recruit the adaptor protein downstream of kinase (DOK) that acts in inhibiting more proximal pathways such as RAS/ERK. The initiation of BCR signaling is fine-tuned regulated by two antagonistic non-BCR associated proteins namely CD45 and the C-terminal src tyrosine kinase (CSK). CD45 or also well-established as the pan B-cell marker B220, is a transmembrane glycoprotein with tyrosine phosphatase activity. CD45 is capable of removing inhibitory phosphate groups form src-family kinases thus acting in a BCR signaling promotive manner. For instance in CD45 deficient mice, LYN was shown by Pao et al. (1997) to be hyperphosphorylated at the C-terminal inhibitory tyrosine residue and was thus predominantly present in its inhibited conformation. The expression of a hyperactive CD45 variant by Majeti et al. (2000) resulted in autoimmunity and neoplasma growth. In contrast, CSK which is already constitutively active in resting cells, phosphorylates the C-terminal inhibitory tyrosine of src-family kinases promoting their inhibited state even when the kinases are already phosphorylated at their activating tyrosine. This mechanism was proven by the hypophosphorylation of the C-terminal tyrosine residue of LYN in CSK negative cells (Hata et al., 1994). (For further review see Dal Porto et al., 2004)

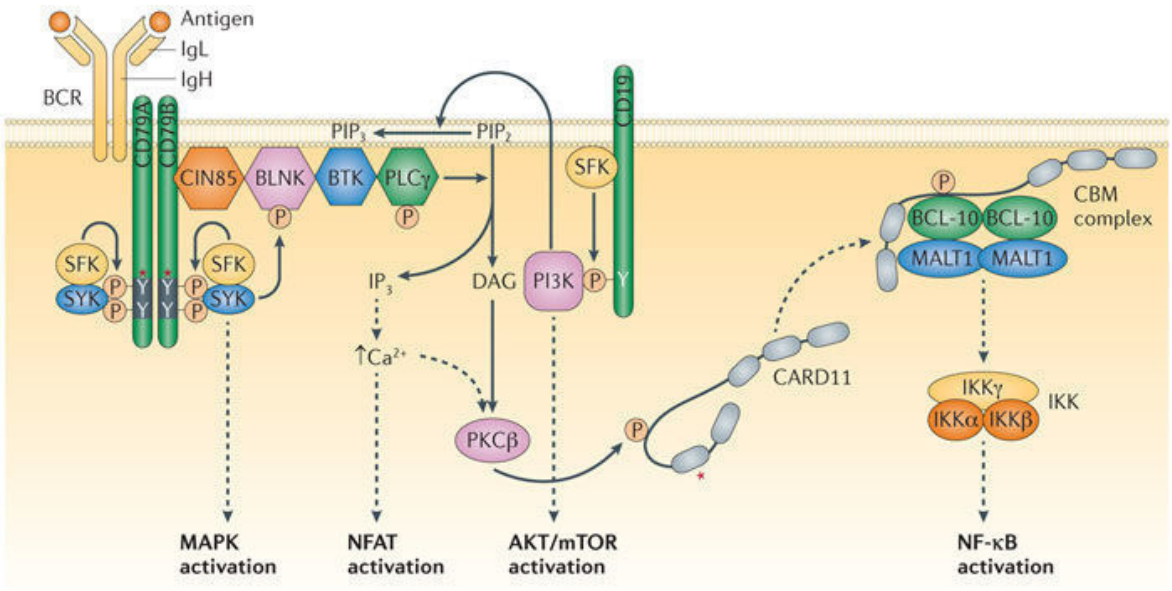

Figure 10. Schematic overview of BCR signaling and integrated proximal pathways. For a more detailed description see continuous text. The red asterisks designate protein domains commonly affected by mutations in human lymphoid malignancies. Abbreviations: BLNK, B-cell linker protein; BTK, Bruton's tyrosine kinase; CARD11, caspase recruitment domain-containing protein 11; CBM, CARD11–BCL-10–MALT1; CIN85, Cbl-interacting protein of 85 kDa; DAG, diacylglycerol; IKK, inhibitor of NF-κB kinase; IgH, immunoglobulin heavy chain; IgL, immunoglobulin light chain; IP3, inositol trisphosphate; MALT1, mucosa-associated lymphoid tissue lymphoma translocation protein 1; MAPK, mitogen-activated protein kinase; mTOR, mammalian target of rapamycin; NF-κB, nuclear factor-κB; NFAT, nuclear factor of activated T cells; PI3K, phosphoinositide 3-kinase; PIP2, phosphatidylinositol-4,5-bisphosphate; PIP3, phosphatidylinositol-3,4,5-trisphosphate; PKCβ, protein kinase Cβ; PLCγ, phospholipase Cγ; SFK, SRC family kinase. Figure and caption adapted from Young and Staudt, 2013.

1.4 The major histocompatibility complex (MHC)

The major histocompatibility complex (MHC) are cell surface glycoproteins that are a vital component in the responses of the adaptive immune system towards invading pathogens. The membrane bound glycoproteins are subdivided into two different classes termed MHC class I and II (MHCI and MHCII) molecules, exhibiting distinct subunit compositions and tissue expression patterns. MHCI and MHCII molecules originate from one gene locus, share high levels of polymorphism and similar spatial structure (Neefjes et al., 2011). Furthermore, both MHC classes bind and present pathogen-derived peptide fragments and antigens from self-proteins on the cell surface. A MHC-complex is made up of either a MHCI or II molecule and a pathogen derived peptide. Together, these components constitute a ligand that is intended to be recognised by the antigen receptors of $CD8^+$ and $CD4^+$ T-cell subsets and as consequence of this, to induce T-cell proliferation and to activate the T-cell's distinct

effector function. MHC class I molecules are present on the surfaces of all nucleated cells and most highly expressed on cells of the hematopoietic lineage. In contrast, the expression of MHC class II proteins is restricted to a comparatively small subset of professional antigen-presenting cells (APCs) such as monocytes/macrophages, dendritic cells and B-cells. Moreover, in humans MHCII expression was also observed to be expressed on activated T-cells and epithelial cells of the thymus (TECs) that are critical in the generation of $CD4^+$ T-cells. MHCII expression is also known to be induced in a couple of other cell types such as fibroblasts, epithelial cell and keratinocytes by IFN-γ stimulation (Pober et al., 1983; Glimcher and Kara, 1992; Pattenden et al., 2002). The MHCI molecules consist of two peptide chains, a polymorphic heavy α-chain which is non-covalently bound to a non-polymorphic smaller light chain called β2-microglobulin (B2M). The whole MHCI complex is subdivided into four domains. Three of which make up the heavy α-chain (α_{1-3}) and the fourth is contributed by B2M. Only the α-chain) exhibits a transmembrane domain (α_3) and thus anchors the whole MHCI complex in the cytoplasma membrane. The other α-chain domains, 1 and 2 together form the peptide-binding groove which includes the major differences between the different polymorphic MHCI α-chains. Peptides bound by MHCI molecules usually consist of 8 to 10 aa and are accommodated deeply within the peptide binding cleft which is closed at its ends by conserved tyrosine residues (Matsumura et al., 1992; Bouvier et al., 1994; Zacharias and Springer, 1994). The bound peptide within the groove stabilises the complex. Without a peptide ligand MHCI proteins are stabilised by ER chaperons like calreticulin, ERP57, PDI and tapasin. In humans, the heavy α-chain is encoded by three polymorphic genes named HLA-A, HLA-B and HLA-C located on chromosome 6p21 whereas the light chain (B2M) coding gene is situated on chromosome 5q (MHC sequencing consortium,1999; Roberts et al., 2006). HLA-A and -B usually exhibit higher expression levels compared to HLA-C which is sparsely expressed as it is (post-) transcriptionally controlled by microRNAs (Neefjes and Ploegh, 1988; Kulkarni et al., 2011). MHCII is categorised in 3 classical and 2 non-classical molecules that are encoded by genes located in the same gene locus as MHCI genes. Classical MHCII molecules that are responsible for antigen-presentation, are encoded by the three polymorphic HLA-DR, HLA-DQ and HLA-DP genes from which HLA-DR is the most highly expressed in humans (Cresswell, 1994; Landsverk et al., 2009). The expression of classical, non-classical MHCII and

several associated genes like CD74, stands under the coordinated control of a master transcriptional regulator the “class II major histocompatibility complex transactivator” (CIITA). In general, CIITA regulates the maturation dependent permanent expression of genes implicated in antigen presentation (Steimle et al., 1993; Wright et al., 2006). The activity of this MCHII transactivator in turn, is controlled by post-translational modifications such as phosphorylation and monoubiquitylation and other elements predominantly found to be active in cells belonging to the immune system. Structurally, a MHCII molecule is a heterodimer composed of two membrane anchored peptide chains, termed α and β, each consisting of two domains α 1, 2 and β 1, 2. In MHCII molecules the peptide binding groove, which encompasses the major polymorphism sites, is formed by aas of the two different peptide chains, α1 and β1. The MHCII peptide binding groove exhibits open ends. Therefore, the N-and C-terminal tails of a bound peptide-antigen are not buried within the MHCII molecules as their MHCI counterparts and accommodated peptides have a length of 13 to 25 residues (Wieczorek et al., 2017). Whether a peptide is suitable to be accommodated in the binding groove of MHCI and MHCII molecules is determined by the correct length and particular aa-residues at certain sequence positions (p), p2 or p5/6 of MHCI peptides and p1, 4, 6 and 9 of MHCII peptides. These aa-residues do not have to be identical but related in structure and characteristics. They occupy defined pockets in the MHC molecules and anchor the peptide antigen to the MHC backbone. Thus, these aa-residues are called anchor residues. The 2 non-classical MHCII molecules called HLA-DM, HLA-DO and the invariant chain (Ii), also known as CD74 (located on chr.5q32) are required as accessory proteins in the proper loading of MHCII molecules with peptides. HLA-DM is not present at the cell surface and does not bind antigenic-peptides itself. Instead, it catalyses the dissociation of the CLIP peptide, which is generated by the degradation of CD74, from the peptide binding groove of MHCII molecules. Furthermore, HLA-DM binds to and stabilises the peptide-free MHCII state. HLA-DM also acts as peptide editor and selects for antigenic-peptides that bind stably to MHCII molecules by promoting the dissociation of inappropriate peptides. The other non-classical MHCII molecule HLA-DO was found to be expressed in thymic epithelial cells, dendritic cells and B-cells (Liljedhal et al., 1996; Douek and Altmann, 1997). HLA-DO is as HLA-DM not present on the cell surface and seems not to bind antigens. It functions as HLA-DM negative regulator by associating with

HLA-DM and thereby inhibiting its catalytic peptide exchange activity. The HLA-DO inhibitor function was proven by the transfection of HLA-DO lacking but HLA-DM/-DR3 and Ii endogenously expressing cells with cDNA constructs coding for HLA-DO. This resulted in higher amounts of MHCII molecules still associated with Ii, a decreased number of antigenic peptide loaded MHCII complexes and thus reduced antigen presentation to T-cell clones (van Ham et al., 1997). MHCI and II exhibit different pathways of antigen processing to achieve surface antigen-peptide presentation to the immune system (a schematic overview of both pathways is depicted in Figure 11.). MHCI surface complexes of nucleated cells present antigenic peptide fragments originating from intracellular i.e. cytosolic and nuclear localised proteins which are degraded by 26S proteasomes. A large share (30% to 70%) of intracellular proteins is degraded ensuing translational synthesis just prior to the formation of operational proteins due to failures in transcriptional or translational processes. These degradation products are called defective ribosomal products (DRiPS) and explain why for instance viral proteins are presented on cell surfaces and recognised by T-cells in only a few hours after the infection (influenza virus antigens in ~ 90 minutes) independent from the natural half-life of a certain protein (Khan et al., 2001). The proteasomally generated peptide fragments of 8 to 16 aa length are translocated by the transporter associated with antigen presentation (TAP) into the endoplasmic reticulum (ER) where MHCI molecules are waiting for peptides (Parcej and Tampe, 2010). The MHCI molecules in the ER are folded by the chaperon tapasin which can also function as peptide editor in the same manner as HLA-DM in MHCII antigen loading. The ER transporter TAP also serves as platform for the binding of several tapasin proteins (Wearsch and Cresswell., 2008). Two more proteins, the chaperons calreticulin and ERp57 participate in the folding and stabilisation of MHCI molecules in the ER. Together, these ER-located chaperons form the so called peptide-loading complex (PLC) which facilitates the loading of peptides onto MHCI molecules and is released when peptide loading is accomplished. Before peptide fragments can be loaded by the PLC onto MHCI molceules, some of them first have to undergo N-terminal trimming by the ER aminopeptidases ERAP1 and ERAP2 in humans or the ER aminopeptidase associated with antigen processing (ERAAP) in mice (Serwold et al., 2002; Saveanu et al., 2005; Saric et al., 2002). ERAAP is known to shorten peptides down to minimally 8 aa (Schubert et al., 2000). In case these N-terminally

processed peptides do not bind a MHCI molecule, they are transported back into the cytosol by ER associated protein degradation (ERAD). In the cytosol, these peptides are eliminated by cytosolic aminopeptidases like the thimet oligopeptidase (TOP), the tripeptidyl peptidase II (TPPII) or the proteasome. Some peptides however, reenter the ER by TAP mediated transport and search again for a suitable MHCI molecule (Roelse et al., 1994; Koopmann et al., 2000). Successfully peptide loaded MHCI complexes are allowed to leave the ER. Consequently, the MHCI complexes detach from the ER and are subsequently mediated by the Golgi apparatus transported to the cytoplasma membrane to display their peptide antigens to $CD8^+$ cytotoxic T-cells. This $CD8^+$ T-cell subset kills cells presenting foreign antigens derived from intracellular pathogens or altered self-peptides for instance from mutated cancerous proteins. This process constitutes an important defense mechanism of the immune system in order to prevent the spread of infection and cancer. The already mentioned TCR coreceptor CD8 is a disulfide-inked heterodimer composed of an α- and β-chain. Additionally to the TCR, CD8 interacts with the MHCI molecule on a nucleated cell. In particular, CD8 binds to a conserved site in the α3-domain and also residues in the α2-domain of MHCI. These additional interactions stabilise the conjunction between the MHCI bearing cell and the T-cell and are thus essential for generating an effective immune response directed against the presented antigen and its origin. MHCI complexes present on the cell surface are quite stable and targeted for degradation by MARCH family proteins from which MARCH4 and 9 were described to regulate MHCI half-life by ubitquitylation (Bartee et al., 2004). This protein modification catalyses the internalisation and subsequent lysosomal degradation of MHCI molecules.

MHCII molecules are mainly expressed by professional APCs and were shown to assemble in the ER. In this organell, MHCII proteins also associate with the trimeric CD74 chaperon. Each of the three CD74 subunits binds to a single MHCII heterodimer. Since a stretch of the CD74 protein lies within the peptide binding groove of MHCII, CD74 prevents premature binding of antigenic peptide fragments to the cleft. For this reason, Bodmer et al. (1994) were able to show that in CD74 deficient mice, the fraction of endogenous-derived peptide fragments presented by MHCII is increased. Ensuing, the formed MHCII heterodimer translocates in a CD74 guided fashion, through the Golgi directly or by taking a detour via plasma membrane to a late endosomal compartment termed MHC class II compartment

(MIIC). Here, CD74 is digested in several serial steps by acid proteases such as the cysteine proteases cathepsin-S and-L (Hsing and Rudensky, 2005). The proteases leave a remaining short class II-associated Ii peptide (CLIP) which is still bound in the MHCII peptide binding cleft. Afterwards, the chaperon HLA-DM facilitates the exchange of CLIP for a suitable antigenic peptide fragment destined to be accommodated in the MHCII peptide binding groove in order to form a stable MHCII complex (as described earlier in more detail). HLA-DM also prevents aggregation and degradation of MHCII molecules before they bind their respective antigenic peptide (Kropshofer et al., 1996). MHCII molecules that do not bind a peptide after the release of CLIP are not stable within the low-pH MHCII environment upon the fusion with lysosomes and are thus degraded. In contrast to MHCI, MHCII molecules bind peptides derived from proteins that originate from exogenous sources and are degraded in the endosomal pathway upon their internalisation. Once MHCII molecules bound an appropriate peptide fragment, they are released from the MIIC and transported in vesicles to the plasma membrane where they can present their peptide antigen to $CD4^+$ T-cells. The release of peptide loaded MHCII containing vesicles from the MIIC was found to be dependent from several factors such as kinases, GTPases, cholesterol and cytosolic pH. The activation of the $CD4^+$ T-cell population by this MHCII dependent mechanism is important for the coordination and regulation of effector cells. CD4 is a monomeric protein that comprises 4 Ig-like domains (D1-D4). CD4 binds MHCII molecules displayed on the cell surface of a professional APC at a hydrophobic cleft between the α2 and β2 domain by the lateral site of the D1 domain. The simultaneous binding of the MHCII complex to the TCR and its CD4 co-receptor present on the T-cell surface enhances the signal triggered within the T-cell and furthermore, increases the T-cell's sensitivity towards the presented antigenic-peptide. Alike MHCI, MHCII molecules are quite stable complexes that do not degenerate on the cell surface and exhibit cell type dependent half-lives. Similarly to MHCI also MHCII molecules can be ubiquitinated by MARCH proteins, in particular MARCH1, thereby being targeted for endocytosis and proteasomal degradation (de Gassart, A. et al., 2008). Thibodeau et al. (2008) demonstrate the direct interaction of MHCII and MARCH1 proteins by immunoprecipitation experiments. MARCH1 expression was found to be strongly induced by IL-10 in human primary monocytes. Furthermore, siRNA mediated MARCH1 knockdown was observed to abrogate the IL-10 mediated down regulation

of surface MHCII levels in primary monocytes. Together, these experiments explain the mechanism behind the interfering impact of IL-10 on MHCII antigen presentation. It is also assumed that MHCII molecules are just degraded in usual lysosomal proteolysis. As already described earlier, MHCI complexes display antigenic peptides from intracellular sources whereas MHCII complexes present peptide fragments originating from extracellular proteins. However, this attribution of peptide sources to MHCI and II molecules is not static and it is therefore possible that cells can present antigens derived from extracellular origins on MHCI molecules. Furthermore, also endogenous antigenic protein fragments can be presented by MHCII complexes in case there were generated by autophagy under certain conditions. This link between MHCI and MHCII antigen presentation is termed antigen cross presentation. One purpose why endogenous proteins are exclusively presented by MHCI molecules is that healthy cells that have absorbed proteins of viral or tumorous origin derived from diseased cells in the close proximity do not get killed by $CD8^+$ cytotoxic T-cells. On the other hand, naive $CD8^+$ cytotoxic T-cells have to be activated by professional APCs before they can execute their lethal effector function. In case endogenous proteins would be exclusively restricted to be displayed on the surface of professional APCs by MHCI complexes, intracellular pathogens for instance that do not infect professional APCs, impair the endogenous antigen presentation or when a neoplasm does not originate from APCs, the only way to activate naïve $CD8^+$ cytotoxic T-cells by APCs is to present exogenous-derived antigens on MHCI molecules (Kurts et al., 2010).

Regarding B-cell malignancies, a loss of MHCI and MHCII expression was generally found to be associated with poor survival outcome and a more aggressive clinical behaviour of the neoplasms under CHOP or R-CHOP treatment (Guy et al., 1986; Moller et al., 1986; Riemersma et al., 2000; Booman et al., 2008; Momburg et al., 1987; Amiot et al., 1998, Wilkinson et al., 2012). In the context of DLBCL pathogenesis and prognosis, decreased MHCII expression for example of HLA-DRA surface expression was found to be associated with less tumor infiltrating $CD8^+$ T-cells and reduced patient survival, indicating impaired immunosurveillance (Rimsza et al., 2004). In addition, Rimsza et al., 2007 demonstrated that the expression of classical MHCII, non-classical MHCII and CD74 correlates with the expression of CIITA in DLBCL. In line with this, Cycon et al. (2009) found the expression of MHCII genes in the GCB DLBCL cell lines SU-DHL-4 and SU-

DHL-6 to be coordinately reduced and the extent of their expression was correlated with CIITA expression. The group found varying MHCII levels when they investigated the surface MHCII expression of several DLBCL model cell lines. They report that the ABC DLBCL cell line OCI-LY10 does not exhibit any HLA-DR and HLA-DQ surface protein levels due to homozygous deletions found in the MHCII locus. Furthermore, they also describe a dyscoordinated downregulation of the MCHII β-chain in the ABC DLBCL cell line OCI-LY3 resulting in dramatically decreased surface MHCII levels. An IHC-based study conducted by Rimsza et al. (2007), comprising 97 paraffin embedded tissue samples from MACOP-B regimen treated DLBCL patients revealed a loss of HLA-DR expression in 37% of investigated cases. MHCII gene expression loss was also reported to be common in rare cases of DLBCL arising in immune privileged sites such as eyes, brain, testes or ovary. It was shown that this type of DLBCL exhibits a loss of MHCII gene expression in more than 50% of cases in which the primary tumor was found in brain or testis. It is also described that the loss of MHCII expression was often accompanied by the homo- or heterozygous deletion of the MHCII locus in the above mentioned immune-privileged DLBCL cases. Whereas in 5% other DLBCL the loss of MHCII expression was not accompanied with abnormalities within the chr. 6p MHC gene locus (Riemersma et al., 2000; Jordanova et al., 2002). Moreover, the DLBCL subtype PMBL was also reported to exhibit a loss of MHCII proteins frequently. Furthermore, PMBLs showed significantly lower average expression of all individual MHCII genes except for CD74 compared to the GCB-DLBCL subtype whereas not to the ABC DLBCL subtype. This difference could probably be explained by the fact that GCB- and ABC DLBCL react differently to IL-4 exposure. IL-4 is known to encompass the MHCII genes as target genes. If this difference is also true for in vivo behaviour of DLBCL, this could be a reason for higher MHCII gene expression in GCB DLBCL.

In addition, also poor patient survival in PMBL cases was found to be correlated with decreased MHCII expression levels. Wilkinson et al., 2012 investigated the relationship between the loss of MHCII and the B-cell differentiation state as the plasmacytic differentiation of non-cancerous B-cells is known to be linked to the loss of MHCII surface expression. Accordingly, MHCII gene expression fluctuates within B-cell differentiation. Thus, MHCII gene expression is absent in pro-B-cell populations but is highly present in mature B-cells and further maturation to plasma

cells abolishes MHCII expression by the down regulation of the transcriptional regulator CIITA (Benoist et al., 1990). Indeed, the Wilkinson group was able to show that GCB exhibit significantly higher MHCII levels than the ABC DLBCL subtype. In accordance with this, they also revealed a negative correlation between the mRNA levels and the protein expression of MHCII (HLA-DR) molecules and classical plasmacytic markers such as MUM1, BLIMP1 and XBP1s. (For further review see Neefjes et al., 2011)

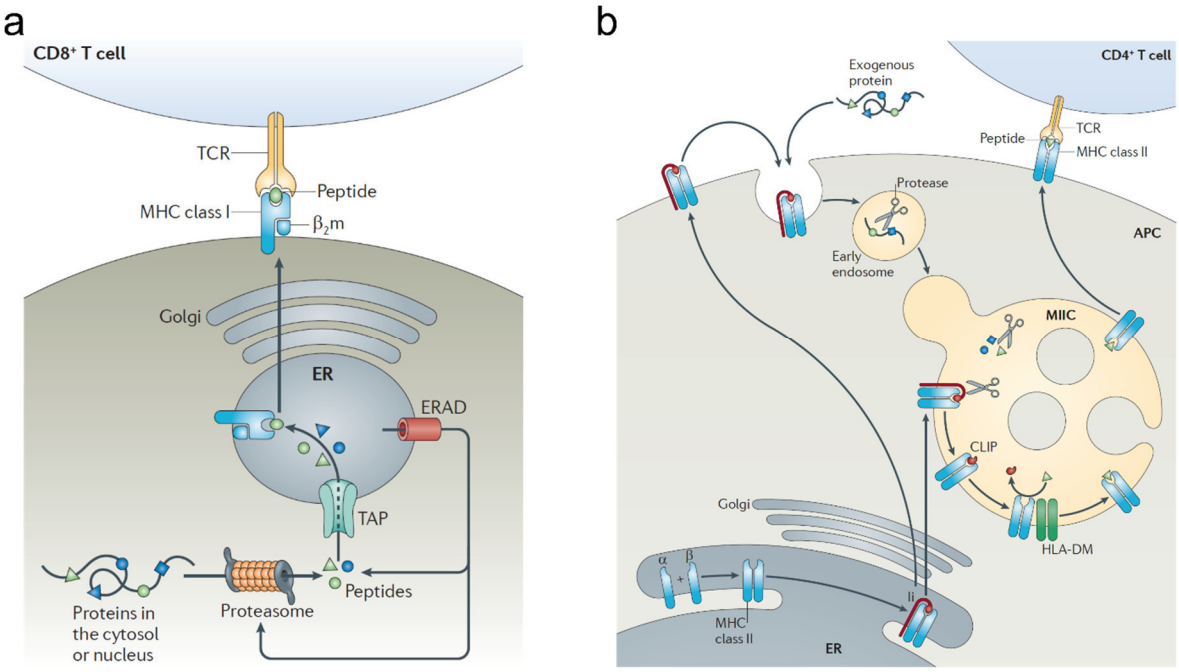

Figure 11. Schematic illustration of the basic events in the (a) MHCI and the (b) MHCII antigen presentation pathway. (a) The MHCI pathway begins with the generation of peptide fragments by the proteasome from cytosolic or nuclear proteins. These antigenic peptides are then translocated via the ABC transporter TAP into the ER. In the ER lumen MHCI proteins are loaded with suitable peptides. The resulting MHCI-peptide complexes are subsequently released from the ER. Through passing the Golgi apparatus they get to the cytoplasma membrane where they present their peptide cargo to the antigen receptor of $CD8^+$ cytotoxic T-cells. In case, a MHCI molecule does not bind a peptide in the ER it is transported back into the cytosol where it is degraded or alternatively, enters again via TAP the ER in order to find an appropriate MHCI molecule to bind. **(b)** The α-and β-chain of MHCII molecules is assembled in the ER of a professional APC. The trimeric invariant chain (li; CD74) then binds to three MHCII molecules in order to prevent premature peptide binding and to target the MHCII complex to be transported to the late endosomal compartment MIIC. This occurs either in a direct manner or via a detour to the cytoplasma membrane. In the MIIC the invariant chain is serially degraded by proteases. Also peptide fragments derived from endocytosed proteins from extracellular sources are generated here. The remaining fragment of the invariant chain which is called CLIP still binds the peptide-binding groove until it is exchanged for an appropriate antigenic-peptide. This exchange occurs in assistance with the auxiliary non-classical MHCII molecule and chaperon HLA-DM. Ensuing, antigen loaded MHCII molecules are transported to the cytoplasma membrane where they display their respective antigen to the TCR

of a $CD4^+$ T-cell. Abbreviations: APC, antigen presenting cell; TAP, transporter associated with antigen presentation; ER, endoplasmic reticulum ERAD, ER-associated protein degradation; TCR, T-cell receptor; β2m, β2-microglobulin; MIIC, MHC class II compartment; CLIP, class II-associated li peptide. Figure adapted from Neefjes et al., 2011.

2. Material and Methods

2.1 Materials

2.1.1 Providers

Providers	
Abcam	Abcam plc, Cambridge, U.K.
Agilent	Agilent Technologies GmbH, Böblingen, Germany
Ambion	Life Technologies GmbH, Darmstadt, Germany
AppliChem	Applichem GmbH, Darmstadt, Germany
BD	BD Biosciences, Heidelberg, Germany
BioLegend	BioLegend, San Diego, U.S.A.
Biorad	Bio-Rad, Hercules, U.S.A
Cayman Chemical	Biomol GmbH, Hamburg, Germany
Cell Signaling	New England Biolabs, Inc., Ipswich, U.S.A.
Corning	Corning, Inc., Tewksbury, U.S.A.
Eppendorf	Eppendorf AG, Hamburg, Germany
Eurofins MWG GmbH	Ebersberg, Germany
GE Healthcare	GE Healthcare Lifesciences, Dornstadt, Germany
Genaxxon	Genaxxon Bioscience GmbH, Ulm, Germany
Gibco	Gibco/Invitrogen Cell Culture, Carlsbad, U.S.A.
Gilson	Gilson, Inc. Middleton, WI,USA
IBA	IBA GmbH, Göttingen, Germany
Immunotools	ImmunoTools GmbH, Friesoythe, Germany
Invitrogen	Life Technologies GmbH, Darmstadt, Germany
KapaBiosystems	KapaBiosystems, Wilmington, Massachusetts U.S.A.
Macherey-Nagel	Macherey-Nagel GmbH & Co. KG, Düren, Germany
Merck	Merck KGaA, Darmstadt, Germany
NEB	New England Biolabs, Inc., Ipswich, U.S.A.
PAA	PAA Laboratories GmbH, Cölbe, Germany
PEQLAB	PEQLAB Biotechnologie GmbH, Erlangen, Germany
Pineda	Pineda – Antikörper service, Berlin, Germany
Promega	Promega Corp., Madison, U.S.A.
Qiagen	Qiagen GmbH, Hilden, Germany
Roche	Roche GmbH, Basel, Switzerland
Roth	Carl Roth GmbH & Co. KG, Karlsruhe, Germany
Santa Cruz	Santa Cruz Biotechnology, Santa Cruz, U.S.A.
Selleckchem	Selleckchem, Munich, Germany
Sigma	Sigma Aldrich, Buchs, Switzerland
Tecan	Tecan Group, Ltd., Crailsheim, Germany
Thermo	Thermo Fisher Scientific, Karlsruhe, Germany

TPP Techno Plastic Products AG	Trasadingen, Switzerland
VWR	VWR International GmbH, Darmstadt, Germany

2.1.2 Chemical reagents

Reagent	Provider
2% Bis-acrylamide	AppliChem
2-propanol	Merck
2x HeBS pH 7.5	Self made
40% Acrylamide	AppliChem
50 mM MgSO4	Invitrogen
Ammonium peroxodisulphate (APS)	Roth
Ampicillin	Sigma
Bradford	Biorad
Bromphenol blue	Biorad
BSA	PAA
$CaCl_2$	Merck
CHX	Sigma
cOmplete™, Mini, EDTA-free Protease Inhibitor Cocktail Tablets	Roche
Cyclosporin A	Merck
Dithiothreitol (DTT)	Roth
DMEM	Sigma
DMSO	Sigma
dNTPs	Thermo Scientific
DPBS	Thermo
EDTA	Roth
FCS	PAA
FK506	Selleckchem
GenAgarose LE	Genaxxon
Glacial acetic acid	AppliChem
Glycerol	AppliChem
Glycine	AppliChem
HEPES	AppliChem
IMDM	Sigma
Ionomycin	Sigma
Isopropanol	Merck
Kanamycin	Sigma
KCl	Sigma
LB-agar	Roth
LB-medium	Roth
L-glutamine, 200 mM	Sigma
Luminol enhancer solution	Promega
MgCl2	AppliChem
Na3VO4	AppliChem
Na4P2O7	AppliChem
NaCl	AppliChem
NaF	AppliChem
NaN3	AppliChem
Nonfat dried milk powder	Applichem
Nonidet P-40 (NP-40)	Applichem
nuclease-free water	Ambion

Orange G	Applichem
PBS (1x)	PAA
Penicillin, 10000 units/ml	Sigma
Peroxide solution	Promega
Plasmocin	Invitrogen
PMA	Sigma
Polysorbat 20/Tween 20	Merck
RPMI	Sigma
Triton-x-100	Merck
Sodium dodecyl sulphate (SDS)	Merck
Streptomycin	Sigma
Sucrose	Merck
SYBR ™ safe DNA gel stain	Invitrogen
Tetramethylethylenediamine (TEMED)	Roth
Tris base	AppliChem
β-mercaptoethanol	AppliChem

2.1.2 Commonly used Buffers and Solutions and their composition

Buffer / Solution	Compounds
Cell lysis	
Lysis buffer 1% triton X-100	150 mM NaCl 50 mM tris, pH 7,4
Lysis buffer 1% triton X-100 complete	10 ml lysis buffer 1% triton X-100 50 mM NaF 10 mM $Na_4P_2O_7$ 10 mM Na_3VO_4 1 tablet protease inhibitor
Agarose gel electrophoresis	
50x TAE buffer	242.2 g tris in 600 ml H2O 57.1 ml glacial acetic acid 100 ml 0,5 M EDTA, pH 8 ad 1 l H2O
5x DNA Sample Buffer	30 % (v/v) glycerol 0.2 % (w/v) orange G
SDS – Polyacrylamide gel electrophoresis	
10% acrylamide for resolving gel	125 ml 40% acrylamide 49 ml 2% bis-acrylamide 125 ml 1.5 M tris-HCl, pH 8.8 ad 500 ml H_2O
25% acrylamide for resolving gel	312 ml 40% acrylamide 17 ml 2% bis-acrylamide 125 ml 1,5 M tris-HCl, pH 8.8 ad 500 ml H_2O
10x migration buffer	60.6 g tris 288 g glycine

	20 g SDS ad 2 l H_2O
Sample buffer for SDS-PAGE	7,5 ml 1 M tris, pH 7.4 2.4 g SDS 12 mg bromphenol blue 30% glycerol 4 ml 14.3 M β-mercaptoethanol ad 100 ml H_2O adjust to pH 6.8 with HCl
2X urea sample buffer:	50mM Tris HCl pH 6.8 1.6% SDS 7% glycerol 8M urea 4% β-mercaptoethanol 0.016% bromophenol blue
Stacking gel	31.25 ml 40% acrylamide 16.25 ml 2% bis-acrylamide 31.25 ml 1M tris-HCl, pH 6.8 ad 250 ml H_2O

Western Blot

10x blot buffer	238 g glycine 50 g tris
1x blot buffer	1 l 10x blot buffer 1.7 l methanol 7.3 l H_2O
Western wash buffer: 1x PBS/T	1 l 10x PBS 50 ml tween 9 l H_2O
Blocking solutions: 5% milk / PBS/T	25 g nonfat dried milk powder ad 500 ml PBS/T
5% BSA / PBS/T	25 g BSA ad 500 ml PBS/T
Ponceau Rouge	10 g Ponceau 15 ml trichloroacetic acid 150 g sulfosalicylic acid ad 500 ml H_2O
ECL	1:1 luminol enhancer solution : peroxide solution

Cell fractionation

Buffer C	10 mM HEPES, pH 7.9 1.5 mM $MgCl_2$ 300 mM sucrose 0,25% / 0.5% NP-40 10 mM KCl 0,5 mM DTT added at the last minute complete protease inhibitor

Buffer N	20 mM HEPES pH 7.9 100 mM NaCl 0,2 mM EDTA 20% (v/v) glycerol 100 mM KCl 0,5 mM DTT added at the last minute complete protease inhibitor
Cell stimulation	
PMA/Ionomycin (P/I)	10 ng/ml PMA, 1 µM ionomycin in DMSO
PMA	10 ng/mL in DMSO
Ionomycin PMA	1 µM ionomycin in DMSO

2.1.3 Pharmacological inhibitors

Inhibitor	Description	Provider
CyclosporinA	Calcineurin inhibitor in complex with the immunophilins CyclophilinA.	Merck
FK506 (Tacrolimus)	Macrolidlacton calcineurin inhibitor in complex with the immunophilins FKBP12.	Selleckchem
JAK-1 inhibitor	Reversible, cell permeable, ATP – competitive Inhibitor witch a IC_{50} of 15nM. Soluble in DMSO (5 mg/ml)	Calbiochem
p38 MAPK inhibitor (SC204157)	Potent p38 MAPK inhibitor with a C50 = 35 nM; soluble in DMSO (25 mg/ml).	Santa Cruz
Sotrastaurin (STN) Synonym: AEB071	Potent and selective panPKC-inhibitor. Mostly for PCK θ with a Ki of 0, 22 nM. PKCβ1 Ki: 0, 64 nM. Inactive to PKCζ. Soluble in DMSO at 25°C: (87 mg/ml).	Selleckchem
Sulfosuccinimidyl Oleate (SSO)	Irreversible CD36 inhibitor which does not permeate the cytoplasma membrane.	CaymanChemical Chemical
z-LVSR-fmk	Tetrapeptide; MALT1 inhibitor. Based on “LVSR85” sequence in the MALT1 substrate RelB.	Margot Thomé

2.1.4 Enzymes

Designation	Description	Provider
Pfu DNA polymerase, recombinant	Highly thermostable DNA polymerase from Pyrococcus furiosus	Agilent
Platinum™ Pfx DNA polymerase	Higher fidelity than Pfu.	Thermo

	Hot start polymerase. Provided in inactive state due to antibody binding.	
Restriction endonucleases	Cuts DNA strands at enzyme specific palindromic recognition sequences	Thermo, NEB
T4 DNA Ligase	Joins DNA fragments by the formation of phosphodiester bonds between blunt and cohesive end DNA termini	Thermo, NEB
FastAP	Thermosensitive Alkaline Phosphatase. Catalysis the release of 5' and 3' phosphates from DNA, RNA, nucleotides and from proteins.	Thermo

2.1.5 Media and buffers for cell culturing

Medium/Buffer	Compounds/Preparation
DMEM IMDM RPMI	Before usage media from providers were supplemented with 100 U/ml penicillin, 100 µg/ml streptomycin, 2,5 µg/ml plasmocyin and either 10% or 20% FCS
Cell wash buffer	1x PBS
FACS Buffer	1x PBS; 2% (v/v) FCS.
Freezing buffer	20 % (v/v) DMSO in FCS

2.1.6 Media for bacterial culturing

Medium	Compounds/Preparation
LB-agar	4 % (w/v) LB-agar diluted with ddH20; autoclave and cool to 60°C; pour plates and store them at 4°C
LB-selection agar suppl. with ampicillin	4 % (w/v) LB-agar diluted with ddH20; autoclave and cool to 60°C subsequently add 100 µg/ml ampicillin; pour plates and store them at 4°C
LB-selection agar suppl. with kanamycin	4 % (w/v) LB-agar diluted with ddH20; autoclave and cool to 60°C subsequently add 50 µg/ml ampicillin; pour plates and store them at 4°C
LB-medium	2 % (w/v) LB-medium; autoclave; store at 4°C
LB-selection medium suppl. with ampicillin	2 % (w/v) LB-medium; autoclave; cool down to ~ 60°C; add 100 µg/ml ampicillin and store at 4°C
LB-selection medium suppl. with kanamycin	2 % (w/v) LB-medium; autoclave; cool down to ~ 60°C; add 50 µg/ml kanamycin and store at 4°C

2.1.7 Kits

Product	Application	Provider
RNeasy Mini Kit	Isolation of RNA	Qiagen
QuantiTect Reverse Transcription Kit	2-step-reaction, gDNA digestion and cDNA synthesis	Qiagen
GeneJET Plasmid Miniprep Kit	Isolation of plasmid DNA	Thermo Scientific™
GeneJET Gel Extraction Kit	Purification of DNA from agarose gel	Thermo Scientific™
GeneJET PCR Purification Kit	Purification of DNA-fragments generated by PCR	Thermo Scientific™
NucleoBond Xtra Maxi Kit	Large-scale isolation of plasmid DNA	Macherey-Nagel
Dual-Luciferase® Reporter Assay System	Genetic reporter system to investigate eukaryotic gene expression and cellular physiology	Promega
eBioscience™ Human IL-2 ELISA Ready-SET-Go!™ Kit	Detection of IL-2 in the supernatant of human cells	Thermo Scientific™
eBioscience™ Human IL-6 ELISA Ready-SET-Go!™ Kit	Detection of IL-6 in the supernatant of human cells	Thermo Scientific™
eBioscience™ Human IL-10 ELISA Ready-SET-Go!™ Kit	Detection of IL-10 in the supernatant of human cells	Thermo Scientific™
KAPA SYBR® FAST qPCR Master Mix (2X) Kit	Ready-to use cocktail to conduct qRT-PCR assays. Comprises: 2X master mix with integrated antibody-mediated hot start polymerase, SYBR Green I fluorescent dye, MgCl2 , dNTPs, and stabilizers	KapaBiosystems
CellTiter 96® AQueous One Solution Cell Proliferation Assay	Colorimetric method to determine the portion of viable cells	Promega
LEGENDScreen™ Lyophilized Antibody Array Human PE Kit	Kit containing 361 PE-conjugated lyophilised antibodies directed against human cell surface markers and corresponding isotype controls.	BioLegend®

2.2 Biological material

2.2.1. Size markers for DNA and proteins

Product	Provider
O´GeneRuler 1 kb Plus DNA ladder, ready-to-use	Thermo Scientific
O'GeneRuler 100 bp Plus DNA Ladder, ready-to-use	Thermo Scientific
Spectra Multicolour Broad Range Protein Ladder	Thermo Scientific

2.2.2. Antibodies

According to the manufacturer's instructions antibodies were dissolved in respective dilutions either in 1xTBS/T supplemented with 5% (w/v) nonfat dried milk powder or 1xTBS/T supplemented with 5% (w/v) BSA. Additionally, NaN_3 in a dilution of 1:250 was added to prevent spoilage of Milk or BSA. The prepared dilutions were used several times and stored at 4°C or -20°C dependent on the antibody. Secondary antibodies were prepared freshly prior to use and dissolved 1:10.000 in 1xTBS/T supplemented with 5% (w/v) nonfat dried milk powder.

Protein	Mol. Weight	Species	Provider	Catalogue number
Primary antibodies				
A 20 (59A426)	90 kDa	mouse monoclonal	Santa Cruz	sc-52910
Bcl10 (H-197)	33 kDa	rabbit polyconal	Santa Cruz	sc-5611
BCL-XL	30kDa	rabbit monoclonal	Cell Signaling	2764
CYLD (D1A10)	108 kDa	monoclonal rabbit	Cell Signaling	#8462
ERK 2 (C14)	42kDa	rabbit polyclonal	Santa Cruz	sc-154
Flag (M2)	1 kDa	mouse monoclonal	Sigma	F1804
GAPDH (A3)	37 kDa	mouse monoclonal	Santa Cruz	sc-137179
IkB-α (L35A5)	39 kDa	mouse monoclonal	Cell Signaling	#4814
IκBNS	35 kDa & 70 kDa	rabbit polyclonal	abcam	ab182633
IκBNS p35/p70	35 kDa & 70 kDa	rabbit polyclonal	Pineda	Self-made against aa 105-120 and aa
IκBNS p70	70 kDa	rabbit polyclonal	Pineda	Self-made against aa 215-231
Lamin A/C	28 kDa	rabbit polyclonal	Cell Signaling	#2032
MALT1	90 kDa	rabbit polyclonal	Cell Signaling	#2494
NFAT c1 (7A6)	110 kDa	mouse monoclonal	Santa Cruz	sc-7294
p-BLNK (Y96)	68 kDa	rabbit polyclonal	Cell Signaling	3601
Phospho-IkBα (Ser32/36)	40 kDa	mouse monoclonal	Cell Signaling	#9246
Phospho-Stat3 (Thy705) (D3A7)	79, 86 kDa	rabbit polyclonal	Cell Signaling	#9145
Phospho-Tyrosine	total protein	mouse monoclonal	Cell Signaling	#9411
ß-Tubulin (H-235)	55 kDa	rabbit polyclonal	Santa Cruz	sc-9104
Stat3 (124H6)	79, 86 kDa	mouse monoclonal	Cell Signaling	#9139

StrepMAB-Classic	1,1 kDa	mouse monoclonal	Iba	2-1507-001
Syk (Tyr526)	70 kDa	rabbit polyclonal	Cell Signaling	#2704

Flow cytometry antibodies	Mol. weight	Colour	Provider	Catalogue number
CD36	53 kDa	FITC	ImmunoTools	21270363
CD90	18 kDa	FITC	affymetrix eBioscience	11-0909
CD108	75 kDa	FITC	ImmunoTools	21271083
CD274	33 kDa	APC	affymetrix eBioscience	17-5983
HLA-DR	29 kDA	FITC	ImmunoTools	21278993
secondary antibodies	**Description**		**Provider**	
anti-mouse IgG	HRP conjugated secondary antibody		Promega	W4021
anti-rabbit IgG	HRP conjugated secondary antibody		Promega	W4011

2.2.3 Oligonucleotides

All applied oligonucleotides were purchased from Sigma.

2.2.3.1 RNAi mediated gene expression knockdown:

Designation		Sequence 5' - 3'
shRNAs designed for IκBNS knockdown		
shRNA1	Sense:	GCC AGG AGA TCA AGA GCA ACA
	Antisense:	CCC GTG GGC CTT CAT GTT G
shRNA2	Sense:	CAA CAT GAA GGC CCA CGG G
	Antisense:	CCC GTG GGC CTT CAT GTT G
shRNA3	Sense:	CTG CGC AAC CTG GAG AAT G
	Antisense:	CAT TCT CCA GGT TGC GCA G
shRNA4	Sense:	CAG CTG TTG AAG AGG AGC C
	Antisense:	GGC TCC TCT TCA ACA GCT G
shRNA5	Sense:	GGG GAC TCC CAG GCC TGT G
	Antisense:	CAC AGG CCT GGG AGT CCC C
shRNA6	Sense:	CCC CAG GGC ATG GAG GCT G
	Antisense:	CAG CCT CCA TGC CCT GGG G
shRNA7	Sense:	CTG AGC ATC ACT CAA GCT C
	Antisense:	GAG CTT GAG TGA TGC TCA G
shRNA8	Sense:	GCA AAC CCA TGA TAAT GTA
	Antisense:	TAC ATT ATC ATG GGT TTG C
shRNA9	Sense:	CGG CAT ATG CTG CGG CTG A
	Antisense:	TCA GCC GCA GCA TAT GCC G
shRNA10	Sense:	ACA TGA AGG CCC ACG GGA A
	Antisense:	TTC CCG TGG GCC TTC ATG T
shRNA11	Sense:	ACT GAG ATC TTT CGG GTT C
	Antisense:	GAA CCC GAA AGA TCT CAG T

siRNA pools	Provider
IκBNS: SMARTpool: ON-TARGET plus NFKBID siRNA	Dharmacon™, GE Healthcare
MALT1: SMARTpool: ON-TARGETplus MALT1 siRNA	Dharmacon™, GE Healthcare
Control: ON-TARGETplus Non-targeting Pool	Dharmacon™, GE Healthcare

2.2.3.2 Oligonucleotides used in Crispr/Cas9 mediated gene expression knockout

Target gene		gRNA sequence 5' - 3'
Nfkbid	**fwd:**	GCT CAC GAA TGT CAA GAC GC
	rev:	GTT TAA AAA CTC GCG GGT ACC GG

2.2.3.3 Oligonucleotide primers applied in qRT-PCR experiments

Template mRNA		Sequence 5' - 3'	Length (bp)	Tm°C
CD36	fwd:	GGC TG TGA CCG GAA CTG TG	19	62,9
	rev:	AGG TCT CCA ACT GGC ATT AGA A	22	60,8
CD90	fwd:	ATC GCT CTC CTG CTA ACA GTC	21	61,3
	rev:	CTC GTA CTG GAT GGG TGA ACT	21	60,9
CD274	fwd:	TGG CAT TTG CTG AAC GCA TTT	21	62,0
	rev:	TGC AGC CAG GTC TAA TTG TTT T	22	60,4
ACADM	fwd:	ACA GGG GTT CAG ACT GCT ATT	21	60,5
	rev:	TCC TCC GTT GGT TAT CCA CAT	21	60,6
ACADVL	fwd:	ACA GAT CAG GTG TTC CCA TAC C	22	61,2
	rev:	CTT GGC GGG ATC GTT CAC TT	20	62,5
HADHA	fwd:	ATA TGC CGC AAT TTT ACA GGG T	22	60,4
	rev:	ACC TGC AAT AAA GCA GCC TGG	21	63,0
IκBNS	fwd:	GTG TAC CGG CGT CTT GAC ATT	21	62,7
	rev:	GTG AGG CCC TCG AAG TCT CT	20	62,8
SDHA	fwd:	CAA ACA GGA ACC CGA GGT TTT	21	60,7
	rev:	CAG CTT GGT AAC ACA TGC TGT AT	23	60,9

2.2.3.4 Oligonucleotide primers used for sequencing of plasmids

Sequencing Primer	Sequence 5' - 3'
BGH Reverse	TAG AAG GCA CAG TCG AGG
EF-1α Forward	TCA AGC CTC AGA CAG TGG TTC
GLprimer2	CTT TAT GTT TTT GGC GTC TTC CA
SP6	ATT TAG GTG ACA CTA TAG
T7	TAA TAC GAC TCA CTA TAG GG

2.2.4 Bacterial strains

Product	Provider
NEB 5-alpha competent E.coli	NEB
One Shot™ Stbl3™ Chemically Competent E. coli	Thermo

2.2.5 Continuous human cell lines

Cell Line	Lymphoma (Sub-)Type	Medium	% Supplemented FCS
DLBCLs			
BJAB	GCB	RPMI	10
SU-DHL-4	GCB	RPMI	10
SU-DHL-6	GCB	RPMI	10
OCI-LY1	GCB	IMDM	10
OCI-LY7	GCB	IMDM	10

OCI-LY19	GCB	IMDM	10
HBL-1	ABC	RPMI	20
U2932	ABC	RPMI	20
TMD8	ABC	RPMI	20
OCI-LY3	ABC	RPMI	20
OCI-LY10	ABC	IMDM	20
MCLs			
Granta 519	MCL	DMEM	10
Z138	MCL	RPMI	10
Rec-1	MCL	RPMI	10
Jeko-1	MCL	RPMI	10
JVM2	MCL	RPMI	10
UPN1	MCL	RPMI	10
Others			
Jurkat	Adult T-cell Leukemia/ Lymphoma (ATLL)	RPMI	10
Raji	Burkitt's Lymphoma	RPMI	10
Ramos	Burkitt's Lymphoma	RPMI	20
HEK293T	Human embryonic kidney 293 cells	DMEM	10

2.2.6 Plasmids

Plasmid	Backbone/ Description	Resistance	Source
Transient Expression Plasmids			
FLAG-RelA	pCR3	Amp	Margot Thomé
FLAG-NFKBID	pCR3	Amp	This study
STREP-NFKBID	pCR3	Amp	This study
V5-NFKBID Iso3	pCR3	Amp	This study
FLAG-DN-IkBa	pCR3	Amp	This study
VSV-MALT1	-	Amp	Margot Thomé
VSV-Bcl10	-	Amp	This study
StrepHA-MyD88 L265P (aa13-296)	-	Amp	Oliver Wolz
StrepHA-MyD88 wt (aa13-296)	-	Amp	Oliver Wolz
HA-CARMA1 WT	pTO_HA	Amp	Georg Lenz
HA-CARMA1 Mutant2 (L244P)	pTO_HA	Amp	Georg Lenz
HA-CARMA1 Mutant3 (G116S)	pTO_HA	Amp	Georg Lenz
NFATc1	pcDNA3	Amp	Georg Lenz
pSUPER empty	Intermediate vector for cloning shRNAs into pLVTHM or pAB286.1 (Rueda et al., 2007)	Amp	Margot Thomé; OligoEngine
Retroviral expression constructs			
V5-BIRC3 WT	pRetro_PG	Amp	Georg Lenz
V5-BIRC3 S441Stop	pRetro_PG	Amp	Georg Lenz
Lentiviral expression constructs			
V5-NFKBID Iso3	pRDI_292	Amp, Puro	This study
FLAG-NFKBID	pRDI_292	Amp, Puro	This study
FLAG-a-fos	pRDI_292	Amp, Puro	This study
pLVTHM	IRES GFP coupled shRNA expression	Amp	Addgene #12247

pLVTHM IκBNS shRNA1 and 8	IRES GFP coupled expression of shRNAs targeting IκBNS mRNA	Amp	
pAB286.1	Lentiviral expression of shRNA	Amp	Margot Thomé
pAB286.1 IκBNS shRNA1 to 11	Lentiviral expression of shRNA1 to 11 targeting IκBNS mRNA	Amp	
lentiCRISPRv2	Empty Crispr/Cas9 vector	Amp	Addgene #52961
lentiCRISPRv2 gRNA IκBNS	Comprises specifically designed gRNA to knock out IkBNS by Crispr/Cas9	Amp	This study
Helper plasmids to generate lenti-viral particles			
pCMV-VSV-G	CMV promoter-driven expression of VSV-G envelope	Amp	Addgene #8454
psPAX2	2nd generation lentiviral packaging plasmid.	Amp	Addgene #12259
Luciferase reporter plasmids			
Human IκBNS promoter in pGL3-basic	Construct of the human IκBNS promoter for testing its activity in response to transcription factor is luciferase assay.	Amp	Promega
pRL-TK Renilla Luciferase Control Reporter Vector	Transcription efficacy normalisation in luciferase assay.	Amp	Promega

2.3 Additional materials

Material	Provider
Filter Paper for Western Blotting	Thermo
Nitrocellulose membrane, protran BA 83, whatman	GE Healthcare
Ultra Cruz autoradiography film, blue	Santa Cruz
Tissue Culture Test Plates (6, 12, 24, 48 - well)	TPP
Tissue Culture Flask 500 ml	TPP
Cell Culture Flask 20 ml, 250 ml, 550 ml	Greiner
CELLSTAR® 96 well plates flat bottom, round bottom	Greiner
LightCycler® 480 Multiwell Plates 96, 384, white	Roche
Centrifuge tubes 15ml, 50 ml	VWR
Corning® large volume centrifuge tube, 500 ml	Sigma
VWR® Culture Tubes, Plastic, with Dual-Position Cap	VWR
VWR® PCR 8-Well Tube Strips; PCR Tubes and Caps	VWR
Safe-Lock Tubes, 1.5 ml;2,0 ml Eppendorf Quality™	Eppendorf
Pipetman Classic Pipettes P20, P200 and P1000	Gilson, Inc. Middleton, WI ,USA

2.3.1 Devices used for conducting experiments

Device	Provider
DMI6000 Microscope	Leica
Light Cycler 480 II	Roche
LSRII FACS Device	BD
Nanodrop 1000	Peqlab
Tecan Infinite M200	Tecan
Film processor for western blot films	Agfa
Gene Pulser Xcell™ Electroporation Systems	Biorad
Gene Pulser®/MicroPulser™ Electroporation Cuvettes, 0.4 cm gap	Biorad
PerfectBlue™ gel system Twin ExW S	Peqlab
Trans-Blot® Cell	BioRad

2.4 Methods

2.4.1 Experimental procedures in molecular biology

2.4.1.1 Isolation of whole cell RNA

Whole cell RNA was isolated using the Qiagen RNA mini Kit according to the manufacturer's instructions from frozen or freshly harvested supernatant-free GCB/ABC DLBCL cell line derived pellets. RNA was eluted in the final step from the column by using 35 µl nuclease free water. Until usage, isolated RNA was stored at -80°C.

2.4.1.2 Determination of nucleic acid concentrations and purity

DNA and RNA concentrations and purity was determined photometrically using the Nanodrop 1000 device as per manufacturer's protocols.

2.4.1.3 Reverse transcription of RNA

The QuantiTect Reverse Transcription Kit was used according to the manufacturer's instructions to reverse-transcribed 500 ng of isolated RNA (3.4.1.3) into cDNA in a final volume of 10 µl.

2.4.1.4 Quantitative RT-PCR

Quantitative RT-PCR was conducted in a LightCycler 480II. cDNA was diluted with H_20 to 50ng/µl. Per reaction 7,5 ng of cDNA was applied. When using a 96/384 well plate 15 µl/7,5µl of the KAPA Master mix (H20, KAPA SYBR® FAST qPCR Master Mix (2X) Kit, resolight, fwd/rev primers) plus 5 µl/2,5µl cDNA was used per well. Primer pairs were diluted 1:10 in H_20. mRNA levels were analysed by applying the following primer pairs: CD36 fwd/rev; CD90 fwd/rev; CD274 fwd/rev; ACADM fwd/rev; HADHA fwd/rev; ACADVL fwd/rev; IκBNS fwd/rev; SDHA fwd/rev. SDHA mRNA levels were determined in order to be used as house-keeping reference gene

in all qPCR analysis. Primer sequences as listed in 3.2.3.3 were obtained from the "PrimerBank - PCR Primers for Gene Expression Detection and Quantification database" (https://pga.mgh.harvard.edu/primerbank/). Relative Quantification of the reverse transcribed RNA was conducted using the ΔΔCP method:

$$\Delta CP = CP \text{ target gene} - CP \text{ reference gene (here: SDHA)}$$
$$\Delta\Delta CP = \Delta CP \text{ treatment} - \Delta CP \text{ control (solvent control)}$$
$$\text{Ratio} = 2^{-\Delta\Delta CP}$$

2.4.1.5 RNAseq analysis

For IκBNS knock-down, HBL-1 cells were lentivirally transduced with the empty pAB286.1 vector as control and pAB286.1 comprising IκBNS shRNA1. After 4 days of puromycin selection, cells were harvested and whole cell RNA was isolated as described in 3.4.1.1. RNA samples were sent to the group of Prof. Dr. med. Georg Lenz, Medizinische Klinik A – Hämatologie und Onkologie, UK Münster who conducted the RNAseq and subsequent analysis. For the characterisation of the second IκBNS isoform, deep sequencing analysis was performed in collaboration with the "Institut für Humangenetik", Münster

2.4.1.6 Digesting DNA strands with restriction endonucleases

In subcloning ,standard restriction endonuclease digestions were performed in a total volume of 20 µl including 2-3 µg of target or/insert comprising vector that were digested with corresponding restriction enzymes and buffers as to the manufacturer's instructions. Restriction enzymes were obtained from Thermo or NEB. 1,5 µl of FastAP was used to dephosphorylate DNA-ends in order to prevent self-ligation of vectors upon single enzyme digestion. Enzymatic digestion of vector DNA was incubated for 1 h at 37°C.

2.4.1.7 Agarose gel electrophoresis

Un-/Digested dsDNA originating from vectors or PCR-products was analysed by size separation using agarose gel electrophoresis. To this end, 1-2% (w/v) of GenAgarose LE was dissolved in 1xTAE buffer using a microwave. Subsequently, 4 µl SYBR Safe was added to the liquid agarose which was poured into a sealed gel casting frame and cooled down at RT in order to solidify. Before loading into agarose-gel pockets, DNA samples were mixed with 5x sample buffer. Electrophoresis was performed in 1xTAE buffer at 90-120V. As DNA molecular weight standards served the DNA ladders O´GeneRuler 1 kb Plus DNA ladder or

the O'GeneRuler 100 bp Plus DNA Ladder. Separated DNA fragments were visualised by an LED transilluminator, exciting the dsDNA intercalating SYBR Safe.

2.4.1.8 Extraction of DNA fragments from agarose

Desired DNA fragments were cut out from the agarose and purified from the gel using the GeneJET Gel Extraction Kit according to the manufacturer's instructions. The final DNA column elution step was performed with 40 µl ddH_2O.

2.4.1.9 Ligation

Ligation of appropriate cut and purified vectors and inserts was performed using the T4 Ligase. For this purpose 5 µl Insert, 3 µl vector and 1 µl each of T4 DNA Ligase and T4 DNA Ligase buffer were mixed and incubated at RT for at least 1h.

2.4.1.10 Transformation of competent *E.coli* bacteria

For transformation of non-viral expression vectors, NEB 5-alpha competent *E.coli* were used for transformation whereas for the transformation of viral expression vectors One Shot™ Stbl3™ Chemically Competent *E. coli* were used. Until usage, bacterial strains were stored at -80°C. For transformation they were thawed on ice and incubated for 20 – 30 minutes with 1 - 2,5 µl of the ligation reaction or 200 ng of plasmid. Subsequently, bacteria were heat-shocked at 42°C for 30 sec in case of NEB 5-alpha and for 45 sec. in case of Stbl3™ bacteria. Following 1 min on ice the bacteria were transformed with an ampicillin resistance bearing vector, were plated out immediately on selective agar plates and incubated over night at 37°C. Bacteria transformed with a kanamycin resistance bearing vector were incubated after heat shock with 200 µl of SOC-outgrowth medium and incubated for 1h at 37°C. Ensuing, bacteria were plated out on selective agar plates and incubated overnight.

2.4.1.11 Analytical plasmid preparation

On selection agar grown single bacterial colonies were picked with an autoclaved pipet tip. Subsequently, picked colonies sticking to pipet tips were transferred into 3 ml of selective LB- medium and incubated over night at 37°C and shaking (140 rpm). The next day, plasmid preparation from grown bacterial suspensions was conducted using the GeneJET Plasmid Miniprep Kit following the manufacturer's instructions. Plasmid DNA was eluted from the column with 40 µl of elution buffer.
In turn to validate if the isolated plasmids actually contain the desired insert, 15 µl of each isolated plasmid was digested with the appropriate restriction enzyme.

Ensuing, digested samples were analysed by agarose gel electrophoresis for the presence of the insert of interest.

2.4.1.12 Sequencing

In order to be certain that a distinct plasmid comprises the exact sequence of interest or in case of undirected cloning the insert in the correct orientation, 50-100 ng of a plasmid in 15 µl dH_2O were sent for sequencing to Eurofins MWG Operon. Depending on the vector and the availability of oligonucleotide primers provided by Eurofins, sequencing samples were additionally mixed with 10 nM of oligonucleotide primers in 2µl dH_2O resulting in a total volume of 17 µl.

2.4.1.13 Preparative plasmid isolation

NEB 5-alpha competent *E.coli* or One Shot™ Stbl3™ Chemically Competent *E. coli* were transformed with freshly isolated and via sequencing validated plasmid constructs. A single bacteria colony or a small amount of a frozen bacteria glycerol stock was picked by a pipette tip and transferred to 200 ml of LB-medium supplemented with the appropriate selection antibiotic and incubated over night at 37°C and shaking (140 rpm). For optimal growth, 3 ml pre-bacterial cultures from glycerol stocks were set up and incubated over day at 37°C and shaking (140 rpm). In the evening pre-cultures were inoculated in 200 ml of selective LB-medium and incubated over night at 37°C and shaking (140 rpm). The next day, plasmid DNA was prepared using the NucleoBond Xtra Maxi Kit for high-copy plasmids as per manufacturer's instructions. Deviating from that 100 – 250 µl ddH_20 were used to resolve the DNA pellet. Finally, the plasmid DNA concentration was adjusted to 1 µg/µl. Plasmid DNA solutions were stored at -20°C.

For long-time storage of back-up bacterial cultures bearing generated plasmid constructs, bacterial glycerol stocks were prepared. For this purpose, 500 µl of the overnight culture was added to 20% of glycerol and 30% of LB-medium. Bacterial glycerol stocks were stored at -80°C.

2.4.1.14 Polymerase chain reaction (PCR)

PCR was conducted in order to introduce restriction endonuclease recognition sites flanking the DNA sequences of inserts or to change start and stop codons. PCR reactions were performed using the Pfu DNA polymerase or the Platinum™ Pfx DNA polymerase according to the manufacturer's instructions. In a standard PCR reaction, 200 ng of template was used in a total volume of 50 µl.

2.4.1.15 Cloning of PCR fragments

Using the Pfx DNA Polymerase generates blunt end DNA fragments. Primers can be designed to yield PCR generated amplicons that are flanked by palindromic sequenced serving as restriction endonuclease recognition sites. The digested ends of the PCR fragment facilitates a ligation in an appropriately digested target vector. Subsequently to a PCR, the total reaction volume of 50 µl was analysed via agarose gel electrophoresis (3.4.1.7). The DNA fragment with the correct size was cut out of the gel and purified using the GeneJet gel extraction kit and eluted in 50 µl. 40 µl of the PCR product was taken to be subjected to restriction with the appropriate endonuclease digestion and afterwards purified again. In parallel, appropriate target vectors were digested with the same endonucleases and purified. Finally, the digested PCR fragment could be ligated with the appropriate cut target vector (3.4.1.9).

2.4.1.16 Generation of shRNA expressing vectors

shRNA sequences targeting IkBNS mRNA (3.2.3.1) were modified with flanking adaptor sequences to bear BglII and HindII target sites and in order to generate a 64-mer that constitutes the final duplex form with the 3'UU overhang, typical for siRNA:

5'-gatcccc-target sequence sense-ttcaagaga- target sequence antisense-ttttta-3'
5'-agcttaaaaa- target sequence sense-tctcttgaa- target sequence antisense-ggg-3'

The designed forward and reverse 64-mers were annealed and digested by BglII and HindII. The pSuper backbone is digested by BglII and HindII, as well. The digested pSUPER backbone and the annealed and digested insert can then be ligated as described in 3.4.1.9

For subcloning of the shRNA sequence into the lentiviral expression vector pAB286.1, pSUPER and the target vector were digested by BamHI and SalI followed by ligation.

For subcloning into the pLVTHM vector, pSUPER and the target vector had to be digested by EcoRI and ClaI, followed by ligation.

3.4.1.17 Generation of CRISPR/Cas9 expressing vectors

In order to clone the target gRNA sequence into the lentiCRISPRv2 backbone, two 25-mer oligonucleotides had to be generated in the following form (N designates any DNA nucleotide):

5‘-caccgNNNNNNNNNNNNNNNNNNN-3‘
3‘-cNNNNNNNNNNNNNNNNNNNcAAA-5‘

The gRNA sequence replacing “N” in order to target the *NFkBID* gene are listed under 3.2.3.2 Lentiviral backbone digestion, oligo-annealing and gRNA cloning into the digested vector were conducted according to the “Target Guide Sequence Cloning Protocol” established by the Zhang lab.

2.4.1.18 Luciferase IkBNS promoter reporter generation

The putative IkBNS promoter sequence with flanking restriction endonuclease recognition sites was chemically synthesized by Invitrogen GeneArt Gene Synthesis. Upon delivery, the received bacterial stab was cultured and the plasmid containing the synthesized promoter sequence was isolated. Subsequently, the IkBNS promoter sequence was cut out of its backbone and subcloned into the pGL3-basic luciferase reporter plasmid using XhoI and NheI. With the generation of this plasmid construct the IkBNS promoter activity could be investigated under different conditions by the Dual luciferase reporter assay (3.4.2.8).

2.4.2 Experimental procedures in cell biology

2.4.2.1 Determination of cell concentrations

Cell concentrations were determined by using Neubauer Chamber slides according to the manufacturer’s instructions.

2.4.2.2 Cryoconservation of cells

10^6 - 10^7 cells per mL were dissolved in 1,5 ml freezing buffer in cyroconservation tubes. Subsequently, cells were inverted several times and stored for a couple of days in Mr. Frosty™ freezing containers at -80°C. For long time storage, cells were stored in liquid nitrogen.

2.4.2.3 Thawing of cells

In liquid nitrogen frozen cells were thawed in a 37°C water bath and subsequently transferred into 50 ml of the cell line corresponding medium with the purpose to dilute the cell toxic DMSO. Cells were pelleted by centrifugation at 300 g for 4 min. The supernatant was decanted and cells were resuspended in 15 ml of the respective cell culture medium (3.1.5).

2.4.2.4 Culture of lymphoma cells

All cell lines used (3.2.5) were cultured in a humidified atmosphere under standard conditions comprising 5 % CO2, 20 % O_2 and a temperature of 37°C.

The GCB DLBCL cell lines BJBAB, SU-DHL-4, SU-DHL-6 were cultured using RPMI supplemented with Plasmocin, 100 U/ml penicillin/ 100 µg/ml streptomycin and 10% FCS. OCI-LY1, OCI-LY7, OCI-LY19 were cultured using IMDM supplemented with 2,5 µg Plasmocin, Pen/Strep and 10% FCS. The **ABC DBLCL cell lines** HBL-1, TMD8, U2932, OCI-LY3 were cultured using RPMI supplemented with 2,5 µg/ml Plasmocin, 100 U/ml penicillin/ 100 µg/ml streptomycin and 20% FCS. **OCI-LY10** was cultured using IMDM supplemented with 2,5 µg/ml Plasmocin, 100 U/ml penicillin/ 100 µg/ml streptomycin and 20% FCS. **MCL cell lines** Z138, Rec-1, Jeko-1, JVM2, UPN1 were cultured using RPMI supplemented 2,5 µg/ml Plasmocin, 100 U/ml penicillin/ 100 µg/ml streptomycin and 20% FCS except for Granta519 which was cultured using DMEM supplemented with Plasmocin, Pen/Strep and 10% FCS. **The Burkitt's lymphoma cell lines** Raji and Ramos were cultured using RPMI supplemented 2,5 µg/ml Plasmocin, 100 U/ml penicillin/ 100 µg/ml streptomycin 10% and 20% FCS, respectively. **The Adult T-cell Leukemia/ Lymphoma (ATLL)** cell line Jurkat was cultured using RPMI supplemented 2,5 µg/ml Plasmocin, 100 U/ml penicillin/ 100 µg/ml streptomycin and 10% FCS. **HEK293T cells** were cultured using DMEM supplemented with Plasmocin, 100 U/ml penicillin/ 100 µg/ml streptomycin and 10% FCS. Cells were kindly provided by Prof. Dr. Falko Fend, University of Tuebingen, Germany; Prof. Dr. Georg Lenz University of Münster, Germany and Prof. Dr. Margot Thomé Université de Lausanne, Switzerland.

2.4.2.5 Transfection of DNA by calcium phosphate precipitation

24 h prior to transfection, confluent HEK293T cells were splitted 1:10 with supplemented DMEM. In case adherent cells grown in 6-well plates were transfected, 125 µl nuclease free water was mixed with 12,5 µl of 2,5 M $CaCl_2$. For 10 cm culture dishes 500 µl nuclease free water and 50 µl of 2,5 M $CaCl_2$ were mixed. To this mixture, the respective plasmid DNA was added. Subsequently, 125 µl (6-well plate) or 500 µl (10 cm dish) of 2x HeBs (pH7,05) was added dropwisely to this mixture under vortexing followed by an incubation time of 10 min at room temperature. Ensuing, this mixture was added in small drops to the cells. The media of the transfected cells was exchanged 16 h later. 24 h - 48 h after transfection, cells

were harvested and lysed for usage in downstream methods such as western blot and luciferase assay.

2.4.2.6 Lentiviral transduction of DNA

HEK293T cells were seeded in 10 cm plates. 24h later HEK293T cells were transfected using calcium phosphate precipitation with the lentiviral helper plasmids pCMV-VSV-G (3 µg per sample) and psPAX2 (6,5 µg per sample) and an appropriate lentiviral expression vector (10 µg per sample). Another 24 h later, medium was sucked off the 10 cm plates and substituted by 6ml the appropriate target cell medium. 96 h after transfection, virus containing HEK293T supernatant of one plate (6 ml) was given to $2x10^6$ target cells in 6 ml medium by syringe driven filtration (0,45 µM). 48h after infection, medium was exchanged for puromycin containing selection medium. At least 48 h after exposure to selection medium, remaining antibiotic resistant cells can be harvested and checked for proper expression of the protein of interest by western blot.

2.4.2.7 Transfection of DNA by electroporation

Suspension cells were transfected by electroporation. Per sample, 6 to 10 million cells were pelleted and washed in DPBS supplemented with Ca^{2+}/Mg^{2+}. Subsequently, the cells resuspended in 350 µl DPBS. Ensuing, up to 30 µg plasmid DNA was added. Samples were then incubated for 15 min and then transferred to a 4 mm electroporation cuvette. Electroporation pulsing was conducted by BioRad Gene Pulser using the exponential protocol at 220-230 V, 950 µF and infinite resistance in cuvettes with 4 mm gap size. After pulsing, 1 ml of RPMI medium without supplements was added to the cells in the 4 mm cuvette. By using a transfer pipette, cells were transferred preferably without cellular debris to pre-warmed cell line corresponding culture medium. 24 h - 48h after transfection, cells were harvested and lysed for usage in downstream methods such as western blot or luciferase assay.

2.4.2.8 Dual luciferase reporter assay

For conducting the dual luciferase reporter assay, adherent HEK293T cells in 6 well plates were additionally transfected to the plasmids of interest with 0,125 µg of pGL3-basic comprising the putative human NFkBID promoter which was cloned upstream of a firefly luciferase coding gene and 0,0125 µg of a TK-Renilla expressing vector. Transfection was conducted using the calcium phosphate

precipitation method. 24 h – 48 h after transfection medium was sucked off the wells. Subsequently, cells were lysed using the provided 1x passive lysis buffer and incubated for half an hour under agitation. Ensuing, 5 µl of cell lysate was added to 50 µl of luciferase substrate in a FACS tube. By using a photometer, luminescence intensity of the expressed firefly luciferase was measured. After that, 50 µl stop and glow solution was added to the mixture and then the luminescence value for TK-Renilla was measured. The constitutive expression of TK-renilla and the resulting luminescence value was determined as efficacy control for transfection and thus for the normalization of samples in order to compare them equitably independent from different transfection efficacies. As negative control served a sample containing only the promoter to be investigated and the TK-renilla encoding plasmid. Samples were transfected as either duplicates or triplicates.

2.4.2.9 MTS Assay

In order to determine the number of viable cells upon the treatment of DBCL cells with calcineurin inhibitors, the colorimetric based MTS assay was performed using the Promega CellTiter 96® Aqueous One Solution Cell Proliferation Assay. The assay was conducted in 96-well plates according to the manufacturer's instructions with 1-2,5 x 10^5 cells. Absorbance at 490 nm was measured using the Tecan Infinite M200. As background values served wells filled with equal amounts of the corresponding medium. Samples were applied as triplicates to the 96 well plate each containing 1-2,5 x 10^5 untreated or treated cells dependent from the experiment.

2.4.2.10 Generation of protein lysates for Western Blot

For lysis, suspension cells were centrifuged down at 500g for 4 min. Subsequently, supernatant was discarded and cells washed with 1x PBS and transferred to a 1,5 ml reaction tube. The supernatant of adherent cells was discarded and cells were detached from culture plate with 1 ml of 1x PBS and transferred to a 1,5 ml reaction tube. After centrifugation, PBS was aspired and depending on the cell pellet double the volume of ice-cold Tris-NaCl lysis buffer (50 mM Tris, pH 7.4, 150 mM NaCl, and 1% Triton X-100) complemented with inhibitors of proteases (cOmplete™, Mini, EDTA-free Protease Inhibitor Cocktail Tablet) and phosphatases (50 mM NaF, 10 mM Na4P2O7, and 10 mM NaVO4) was added. After vortexing, cells dissolved in lysis buffer were incubated for 15 min of ice, interrupted by occasional vortexing.

Subsequent to incubation, cell debris was removed by centrifugation for 10 min at 14.000 g and 4°C. The cleared postnuclear cell lysate was finally transferred to another 1,5 ml reaction tube and stored at -20°C. The remaining cell debris was discarded.

3.4.2.11 Protein quantification

Protein concentration of cell lysates was determined calorimetrically using the Bio-Rad Protein Assay Dye Reagent Concentrate. The Concentrate was diluted 1:5 in a volume of 1 ml ddH_20 in 1,5 ml reaction tubes. In this dilution 0,5 µl of cell lysate was pipetted and the total volume was transferred into a cuvette. Protein concentration of lysate sample duplicates was finally determined using a photometer measuring absorbance at 595 nm.

2.4.2.12 Fractionation of cytosolic and nuclear proteins

10 to 20 million cells of the GCB DLBCL cell line BJAB and the ABC DLBCL cell lines U2932 and HBL-1 were harvested and washed once with ice-cold 1x PBS and centrifuge for 5 min at 300g at 4°C. The reductant DTT and a protease inhibitor was added to Buffer C before the resuspension of cells with 3-to 4-fold the volume of the cell pellet. After short vortexing cells were incubated in Buffer C on ice for 5 minutes. The cytosolic fraction and the nuclei were then separated by centrifugation at 9000 rpm for 45 sec. Subsequently, the generated supernatant i.e. the cytosolic fraction was now transferred to a fresh 1,5 ml reaction tube. The remaining pellet was then washed twice for 10 sec. with Buffer C. In order to crack the nuclei, dependent on pellet size two times the volume of Buffer N was added and the reaction tubes were frozen in liquid nitrogen and thawed in a 37°C water bath for 9 cycles. Subsequently, the samples were sonicated for 10 seconds. Ensuing, the cellular debris was separated from the nuclear fraction by centrifugation at 14.000g for 10 min. The supernatant i.e. the nuclear fraction was transferred to a new 1,5 ml reaction tube. To examine the subcellular distribution of the protein of interest and to verify the purity of fractions, samples were then separated by SDS-PAGE and analysed by immunoblotting.

2.4.2.13 Stimulation of cells

Cells were centrifuged down at 500g for 4 min in 15 ml falcons. The supernatant was discarded and cells were resuspended in 1-4 ml of corresponding supplemented cell medium. Cells were then incubated for 15 min in a pre-warmed water bath at 37°C. Finally, B- or T-cells were stimulated with either a mixture of PMA (10 ng/ml) and Ionomycin (1 µM) (P/I; 1:1000), PMA (10 ng/ml; 1:500) or Ionomycin (1 µM; 1:200) for different periods of time. As stimulation control, DMSO was applied in the same dilution as the cell stimuli.

2.4.2.14 Cycloheximide treatment of ABC DLBCL cell lines

To investigate the protein half-life of IkBNS isoforms, the ABC DLBCL cell lines HBL-1 and OCI-LY3 were treated with the protein biosynthesis inhibitor cycloheximide (CHX). Cells were harvested an resuspended in 3 ml RPMI medium supplemented with 20% FCS in 15 ml tubes. Tubes were then incubated for 15 min in a 37°C water bath. Subsequently, CHX was added to the cells to a final concentration of 20 µg/ml for 1, 2, 4 or 6h at 37°C. After that, cells were harvested and protein lysates were generated that were separated by SDS PAGE and analysed by western blot.

3.4.2.15 Stable isotope labeling by/with amino acids in cell culture

300 ml of densely grown HBL-1 were centrifuged down at 500g for 4 min. Cells were then resuspended in equal portions of 150 ml in light growth medium (RPMI 20% FCS) containing normal amino acids, medium heavy amino acids containing growth medium (RPMI 20% FCS), containing amino-acids labeled with non-radioactive isotopes and growth medium comprising amino acids labeled with stable heavy isotopes. Cells were splitted every other day and harvested after 12 days of incubation in corresponding medium. Five hours prior harvesting CsA (2,5 µM) and FK506 (5 µM) were added to differentially labeled cells that were previously resuspended in 50 ml of corresponding fresh SILAC medium. Subsequent to harvesting, cells were resuspended in lysis buffer provided by the Quantitative Proteomics & Proteome Center Tuebingen. Cells in lysates were stored at -20°C until given to MS analyses in order to assess calcineurin inhibition dependent changes in the phosphoproteom in the ABC DLBCL cell line HBL-1.

2.4.3 Immunobiological methods

2.4.3.1 Staining of lymphoma cell surface markers and analysis by FACS

Lymphoma surface marker expression was quantified by FACS analysis using an LSRII device. For this purpose, 4 ml of GCB and ABC DLBCL cell suspensions were harvested in FACS tubes by centrifugation at 500g for 4 min. Medium supernatant was discarded. Cells were subsequently washed with 4 ml of 1x PBS and resuspended in 200 µl FACS Buffer (1x PBS; 2% FCS) containing fluorochrome-conjugated anti-CD36, CD90, CD108, CD274 or HLA-DR in a dilution of 1:50 each. As control served the staining of cells line with appropriate fluorochrome-labelled isotype control antibodies. Following an incubation time of 30 minutes in the dark, cells were centrifuged at 500g for 4 min, supernatant was discarded and cells were washed once using 4 ml of FACS Buffer. Finally, cells were resuspended in 200 µl FACS of Buffer and subjected to FACS analysis.

2.4.3.2 Legend screen™

The BioLegend® LEGENDScreen™ Lyophilized Antibody Array Human PE Kit was conducted following the standard operating procedures provided by the manufacturer using the GCB DLBCL cell lines BJAB, SU-DHL-4 and SU-DHL-6 and the ABC DLBCL cell lines HBL-1, TMD8, U2932, and OCI-LY3.

2.4.3.3 ELISA

In order to detect the amounts of Jurkat secreted interleukin-2 and ABC DLBCL secreted interleukin-6 and -10 the eBioscience™ Human IL-2, IL-6 and IL-10 ELISA Ready-SET-Go!™ Kits were used. The respective interleukin containing supernatants of control samples and differently treated cell lines were harvested as triplicates and transferred into 1,5 ml reaction tubes that were subsequently stored at -80°C until usage. When conducting an ELISA, samples were initially thawed on ice. Samples were applied as duplicates to the 96-well pre-coated ELISA plate. The following ELISA was performed according to the manufacturer's instructions. Deviating from that, as controls served cell line corresponding media without supplements.

2.4.3.4 Sodium dodecylsulphate polyacrylamide gel electrophoresis (SDS-PAGE)

Proteins in generated cell lysates (3.4.2.10) were size separated using the denaturing sodium dodecylsulphate polyacrylamide gel electrophoresis (SDS-PAGE). The appropriate volume of lysate corresponding to the desired amount of protein was mixed with reducing 3x SDS sample loading buffer or 2x urea sample buffer. This mixture was subsequently boiled for 10 min at 95°C to denature the proteins. Afterwards, samples were loaded into polyacrylamide gels (acrylamide percentage depends on the size of the protein of interest), that were handcasted using the Peqlab PerfectBlue™ gel system Twin ExW S. As molecular weight standard, the Spectra Multicolour Broad Range protein ladder was additionally loaded. Samples were electrophoretically separated according to their size in the Peqlab PerfectBlue™ gel system chamber filled with 1x migration buffer. Initially, 80 V were applied. As soon as the samples ran out of the pockets of the stacking gel, SDS-PAGE was continued applying 120 V until the loading front ran out of the resolving gel.

2.4.3.5 Immunoblotting

Subsequent to the size dependent separation of lysate proteins by SDS-PAGE, proteins were transferred to a nitrocellulose membrane by tank blotting for 90 min at 100 V using the BioRad Trans-Blot® Cell filled with 1x blotting buffer. Optionally, in order to check regular protein transfer on membranes could be incubated for some minutes in Ponceau Rouge which could washed away using dH_2O. Hereafter, nitrocellulose membranes were incubated for 30 to 60 min in blocking solutions under shaking. Depending on the later applied primary antibody blocking solutions either contained 5% milk powder or 5% BSA dissolved in 1xTBS/T. After blocking, the primary antibody (3.2.2) either dissolved in 25 ml 5% milk powder/ 1xTBS/T or 25 ml 5% BSA/1xTBS/T was added to the membrane and incubated over night or longer at 4°C under shaking. The next day, membranes were washed three times for 5 minutes with 1xTBS/T. Ensuing, membranes were incubated for 2-4h in immunoblotting secondary antibody solution comprising HRP-coupled IgG secondary antibodies in a dilution of 1:10.000 depending on the primary antibody either from mouse or rabbit (3.2.2) After secondary antibody incubation, membranes were washed three times for 5 minutes with 1xTBS/T. Subsequently, ECL solution

was applied and specific protein bands were finally detected by exposing the nitrocellulose membranes to Ultra Cruz Blue autoradiography films.

For reprobing of membranes with another primary antibody, membranes were washed three times for 5 minutes with 1xTBS/T and blocked again for 30-60 min depending on the primary antibody with either 5% milk / PBS/T or 5% BSA / PBS/T. Additionally, 100 µl NaN_3 was added to the blocking solution to eliminate remaining HRP activity from the previous detection. Subsequent to blocking, another primary antibody was given to the membrane and incubated at least over night at 4°C.

3. Results

3.1 IκBNS regulation in lymphocytes

In turn to investigate how IκBNS expression is regulated in lymphocytes and moreover which transcription factor families (TF-families) might be implicated in this regulation we made use of a model T-cell line.

To figure out whether the AP-1 family or NF-κB could be the driving factors of IκBNS expression we lentivirally transduced the T-cell line Jurkat with either A-Fos, an inhibitory AP-1 construct preventing the binding of other AP-1 family members to DNA in a competitive manner (Olive et al., 1997) or with a FLAG-tagged, non-phosphorylatable dominant negative IκBa (DN-IκBa). Both TF-families are well known to positively regulate IL-2 secretion upon T-cell activation (Hoyos et al, 1989, Jain et al., 1995; Juilland et al., 2016). Therefore, we stimulated Jurkat cells for 16 h with P/I, a mixture of PMA (phorbol-12-myristate-13-acetate), activating PKC, and Ionomycin an ionophore produced by Streptomyces conglobatus, which is leading to raising intracellular Ca^{2+} levels. Subsequently, IL-2 was measured in the supernatants of the differently transduced Jurkat cells (Figure 12.a). In comparison to control cells, A-Fos and DN-IκBa transduced cells secreted considerably less IL-2 upon P/I stimulation, indicating the proper functionality of A-Fos and DN-IκBa. To further validate the functionality of the Flag-tagged DN-IκBa in B-lymphocytes and to see a putative effect on IκBNS induction, we lentivirally transduced the GCB-DLBCL cell line BJAB with the NFκB inhibitor. As a DN-IκBa functionality control, we blotted against A20, a negative regulator and target of NF-κB (Compagno et al., 2009). A20 expression was clearly diminished upon stimulation in DN-IκBa transduced cells compared to control cells (Figure 12.b). Expression of DN-IκBa was confirmed by staining against the FLAG-tag. Upon 16 h of P/I stimulation we did not observe any difference between IκBNS levels in control cells and DN-IκBa transduced BJAB cells (Figure 12.b), suggesting NF-κB not to be essential for IκBNS induction and expression maintenance.

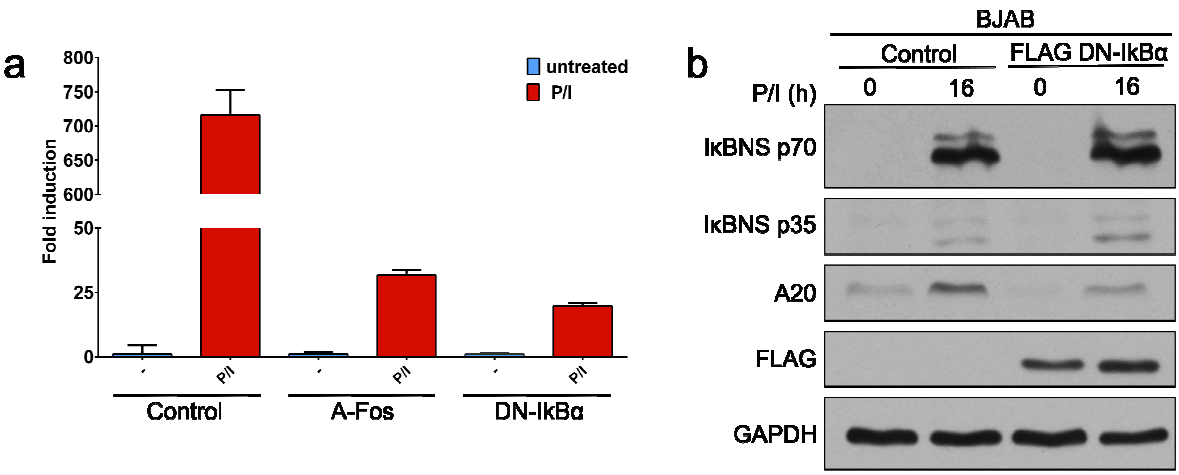

Figure 12. Proving functionality of A-Fos and DN-IκBα. (a) IL-2 ELISA made from supernatants of non-stimulated or P/I treated Jurkat cells that were lentivirally transduced with either a FLAG-tagged expression construct for A-Fos, DN-IκBα or an empty vector as control. **(b)** Immunoblot analysis of IκBNS, A20, FLAG expression levels in BJAB cells transduced with a FLAG-tagged expression construct for DN-IκBα or an empty vector as control. Cells were treated with P/I for 16 h or with solvent alone as control **(a, b)** GAPDH served as an indicator for equal loading.

To narrow down which TF-families are responsible for IκBNS expression, we again lentivirally transduced BJAB B-cells and Jurkat T-cells cells with either an empty control vector, A-Fos or DN-IκBa and the combination of A-Fos and DN-IκBa to exclude a redundancy of AP-1 and NF-κB TF-family members (Figure 13.a,b; 14a, b). Expression of the dominant negative inhibitors was validated by using an anti-FLAG antibody. The activation of B- and T-cells was confirmed by blotting against CYLD, a deubiquitinase and negative regulator of NF-κB (Brummelkamp et al., 2003). Upon B- and T-cells activation CYLD is cleaved C-terminally by MALT1 in a 40 kDa and 70 kDa fragment (Figure 13.a, b; 14a, b) and is therefore an indicator of B- and T-cell activation. To the different viral backgrounds of BJABs we additionally applied a p38-inhibitor and Cyclosporin A (CsA) (Figure 13.a, b, 14.a, b), an inhibitor of the phosphatase calcineurin and thus of the NFAT-family of TFs, as well. CsA was originally isolated from fungus Tolypocladium inflatum and is today an essential, commonly used immunosuppressive drug. Since IκBNS is not expressed in BJAB under steady state conditions, cells were initially pre-incubated for 20 minutes with the previously mentioned inhibitors and afterwards stimulated with P/I for the indicated periods of time to induce IκBNS expression. IκBNS was clearly detectable after 1 h of P/I stimulation. The IκBNS expression level reached its peak at 3 h and declined after 4 h of P/I mediated stimulation under all conditions. BJAB expressing A-Fos, DN-IκBa alone or the combination thereof did not show

any changes in their IκBNS induction behaviour upon P/I stimulation compared to the control (Figure 13.a). This finding is in line with the result of Figure 12.b which showed that NF-kB inhibition alone does not have an influence on proper IκBNS induction. When we treated the cells additionally to the expression of the dominant negative inhibitors with a p38-inhibitor we saw slightly diminished levels of IκBNS induction upon P/I treatment. This is most likely due to toxic side effects of this inhibitor. In contrast, when we added Cyclosporin A, IκBNS induction was tremendously hampered upon stimulation in all differently transduced cells compared to non-treated cells (Figure 13.b). Notably, the combined treatment with the NFAT-inhibitor Cyclosporin A and the expression of the NF-κB-inhibitor (DN-IκBa) led to the strongest impairment of IκBNS induction upon P/I stimulation. To further elucidate how IκBNS induction is regulated in lymphocytes we conducted the same experiment with Jurkat T-cells (Figure 14.a, b). To confirm the effect of CsA seen in Figure 13.b we also tested FK506 (tacrolimus), another calcineurin inhibitor, that is commonly used in immunosuppressive therapies. FK506 is a macrolid lactone originally produced by Streptomyces tsukubaensis and exerts its mechanism of action basically in the same manner as Cyclosporin A does (Haddad et al., 2006; Bonner and Boulianne, 2017). Using this second calcineurin inhibitory compound made it possible for us to exclude putative unspecific CsA effects and to further validate the observations previously made in BJAB. As in BJAB B-cells, Jurkat T-cells obviously expressed IκBNS 1 h upon P/I mediated stimulation, reached its peak at ~ 3 h but remained at the same expression level at 4 h, regardless the expression of the empty control vector, A-Fos, DN-IκBa or the combination of both. Moreover, the eventual expression levels of IκBNS were neither altered under AP-1, NF-κB inhibitory nor the combination thereof compared to empty control (Figure 14.a). However, as soon as we gave in the calcineurin inhibitors CsA or FK506, IκBNS induction was remarkably affected compared to non-treated controls. For FK506 treated samples, this effect was even more pronounced (Figure 14.b). Noteworthy, in Jurkat T-cells the strongest negative effect on IκBNS induction did not occur under the combination of CsA treatment and DN-IκBa expression compared to CsA only treated cells. The same applies to Jurkat cells, in which we combined calcineurin inhibition by FK506 and NF-κB inhibition (Figure 14.a, b). Hence, the induction of IκBNS in T-cells could be slightly differentially regulated as in B-cells.

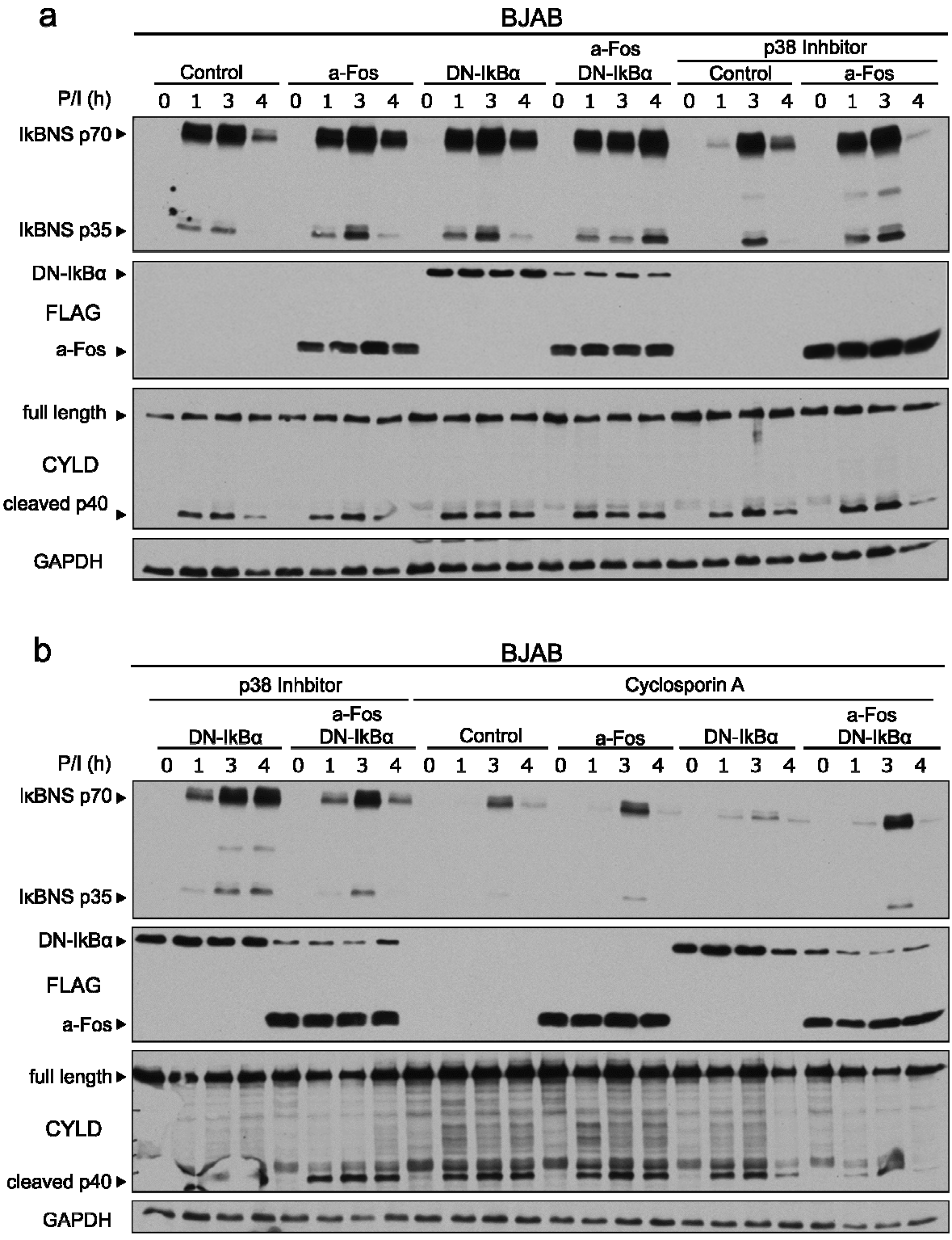

Figure 13. Investigating the TF-family dependency of IκBNS induction and expression maintenance in B-cells. Analysis of IκBNS protein expression by western blot in lysates of BJAB cells lentivirally transduced with either an empty control vector (Control), an expression construct for Flag-tagged A-Fos, DN-IκBα or the combination of thereof upon P/I stimulation for the indicated times. Cells were pre-incubated with p38 inhibitor or Cylcosporin A (2,5 μM) for 20 min ahead of P/I stimulation. FLAG-tag expression was assessed to validate expression of A-Fos and DN-IκBa. Proper B-cell stimulation by P/I was verified by determining CYLD cleavage. In a+b blotting for GAPDH served as a loading control.

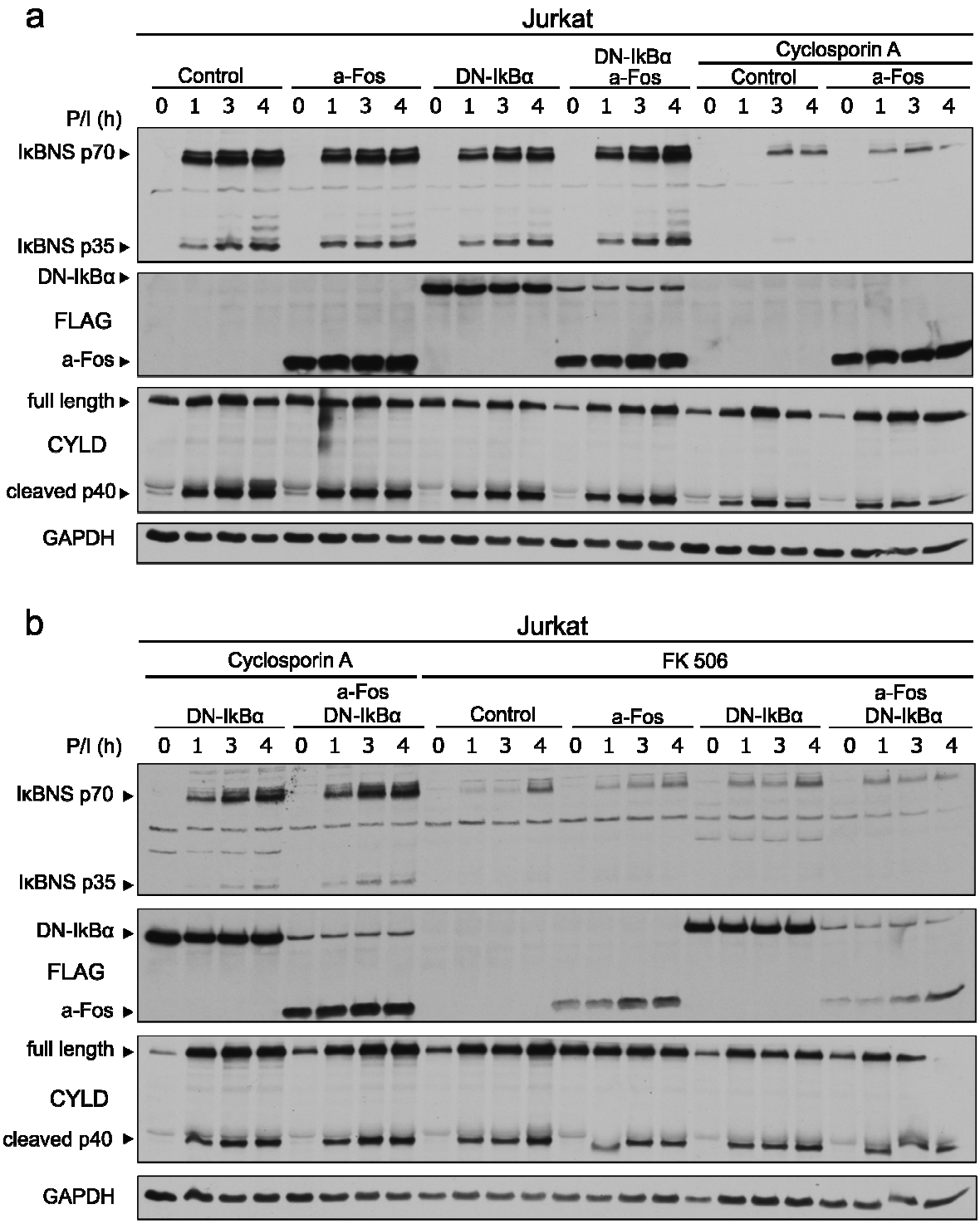

Figure 14. Investigating the TF-family dependency of IκBNS induction and expression maintenance in T-cells. Immunoblot analysis of IκBNS protein expression in lysates of Jurkat cells lentivirally transduced with either an empty control vector (Control), an expression construct for Flag-tagged A-Fos, DN-IκBα or the combination of thereof upon P/I stimulation for the indicated times. Cells were pre-incubated with calcineurin inhibitors Cylcosporin A (2,5 µM) or FK506 (5 µM) for 20 min ahead of P/I stimulation. FLAG-tag expression was assessed to validate expression of A-Fos and DN-IκBa. Proper T-cell stimulation by P/I was verified by determining CYLD cleavage. In a+b blotting for GAPDH served as a loading control.

To substantiate our previous findings of IκBNS regulation and to exclude unspecific CsA effects in B-lymphocytes as well, we also tested FK506 in BJAB. Cells were pre-treated with solvent only or with either one of the calcineurin inhibitors CsA or FK506 just before P/I mediated cell stimulation for the indicated times (Figure 15.a). Under solvent only (control) conditions IκBNS protein levels could be appreciably determined by western blot analysis after 1 h, raised at its highest level after 3 h and remained at the same level after 4 h of P/I stimulation. However, in CsA or FK506 pre-treated BJAB IκBNS induction was unambiguously impeded (Figure 15.a).

Collectively, these findings show that the indirect inhibition of NFAT by using calcineurin inhibitors CsA and FK506 lead to impaired IκBNS induction in both B-and T-lymphocytes. Moreover, when the NF-κB pathway is additionally blocked by a dominant negative approach this inhibitory effect is, at least in B-cells the strongest among all tested conditions. Taken together, the results suggest a synergistic role for NF-κB and NFAT TF-family members for the induction and maintenance of IκBNS in B-and T-lymphocytes.

So far, the effect of CsA or FK506 was only tested upon P/I meditated cell stimulation. Due to this, we wanted to assess next the effect of NFAT-inhibition by CsA and FK506 also on high steady state expression level of IκBNS. As we describe in chapter 4.2 in more detail, we noticed that ABC DBLCL cell lines express high levels of IκBNS under steady state conditions. Therefore, we treated the ABC DLBCL B-lymphocyte cell lines HBL-1 and U2932 for two days with CsA and examined the effect on IκBNS protein levels (Figure 4.b). CsA treatment clearly decreased the IκBNS levels in both cells lines compared to solvent controls (Co) even after one day of application and was also lasting at the same extend on day two (Figure 15.b). These findings are in accordance with the previously gained data and therefore strengthen the assumption that NFAT is likely to be important for the induction of IκBNS upon cell stimulation (Figure 13.a, b; Figure 14.a, b; Figure 15.a). Furthermore, as found in HBL-1 and U2932 (Figure 15.b) NFAT is also important for the maintenance of high level steady state IκBNS levels in ABC DLBCL.

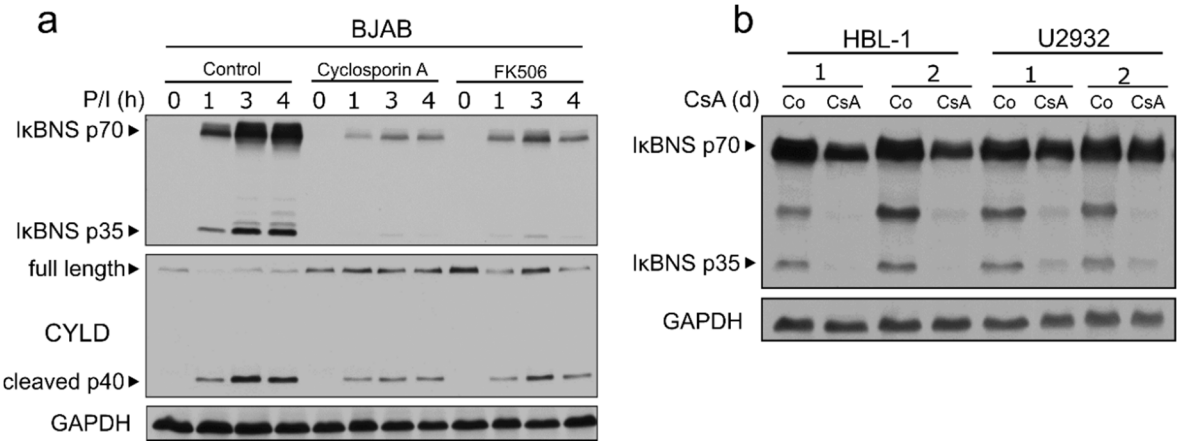

Figure 15. NFAT requirement for induction of IκBNS upon P/I stimulation and maintenance of high level steady state IκBNS protein levels in B-lymphocytes analysed by western blotting. **(a)** The GCB-DLBCL cell line BJAB was preincubated for 20 min with either solvent control (DMSO), CsA (2,5 µM) or FK506 (5 µM) and subsequently stimulated with P/I for the indicated times. **(b)** HBL-1 and U2932 ABC DLBCL lines were treated for 1 or 2 days with DMSO (Co) or CsA (2,5 µM). Blots were incubated with the indicated antibodies. GAPDH was blotted to show equal loading of samples in (**a, b)**.

Owing the fact that we have observed the strongest impairment of IκBNS induction upon P/I mediated B-cell stimulation when combining an NFAT inhibitor and an NF-κB inhibitor (Figure 13.b) we now ask ourselves what would be the outcome of single-treatment with either PMA or Ionomycin on IκBNS up-regulation compared to their combined treatment. PMA mimics diacylglycerol and therefore activates PKC and adjoining downstream pathways. Amongst others, NF-κB and AP-1 (Staudt and Young, 2013) but due to lacking Ca^{2+} mobilisation, NFAT is not activated hereby. In contrast, treating the cells only with Ionomycin gives rise to elevating intracellular Ca^{2+} levels that lead in turn to the activation of calcineurin and eventual nuclear translocation and activation of NFAT (Steinbach et al., 2007) but not NF-κB. In this manner we were able to distinguish between the effects of NFAT and NF-κB activity alone, compared to their synergistic impact on the induction of IκBNS (Figure 16.). PMA treatment of BJAB cells alone obviously led to IκBNS up regulation albeit very weak compared to P/I stimulation. After 1 h IκBNS expression was already detectable in western blot, reached its highest level at 3 h and was on the edge to decline after 4h of stimulation upon PMA treatment. Thereby, only IκBNS p70 was detectable most likely due to the anyway higher expression levels than IκBNS p35. However, the treatment of BJAB cells with Ionomycin alone did not lead to any detectable IκBNS (Figure 16.).

Taking into account the previously gained findings, this result was further approving the assumption that NF-κB and NFAT play a synergistic role to fully induce IκBNS expression levels as we could observe them upon stimulation in B- and T-lymphocytes and as well as under high steady state expression levels in representative ABC-DLBCLs. In detail, NF-κB alone is able of inducing only very little amounts of IκBNS whereas NFAT alone does not exhibit the capability to induce IκBNS at all (Figure 16.).

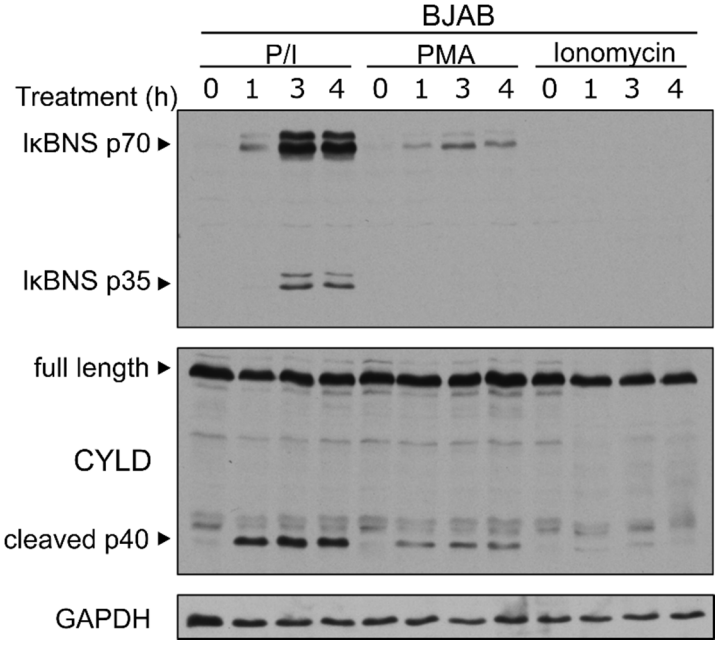

Figure 16. Distinguishing the inductive capabilities of NF-κB and NFAT solely and in synergy to up regulate IκBNS in BJAB B-lymphocytes analysed by immunoblotting. Cells were treated with either PMA, Ionomycin or their mixture for the indicated times. Protein levels, stimulation of B-cells and equal loading were determined with the indicated antibodies.

So far, all evidences suggested that NF-κB and NFAT together were the main drivers of proper Nfκbid gene induction and expression maintenance in B-lymphocytes. Thus, we had a closer look at the Nfκbid gene structure. CHIP data, published in the UCSC Genome Browser (http://genome.ucsc.edu) revealed a putative Nfκbid promoter region in intron one of the Nfκbid gene (Figure 17.a; framed in red; Figure 17.b nucleotide sequence of this chromosome stretch) with putative binding sites for NF-κB family members and NFATc1. Moreover, when we analysed the nucleotide sequence as shown in Figure 17.b for potential transcription factor binding sites by using a prediction tool, we actually found potential NF-κB (Figure 17., depicted in yellow and red) and NFAT (Figure 17., depicted in blue) binding sites.

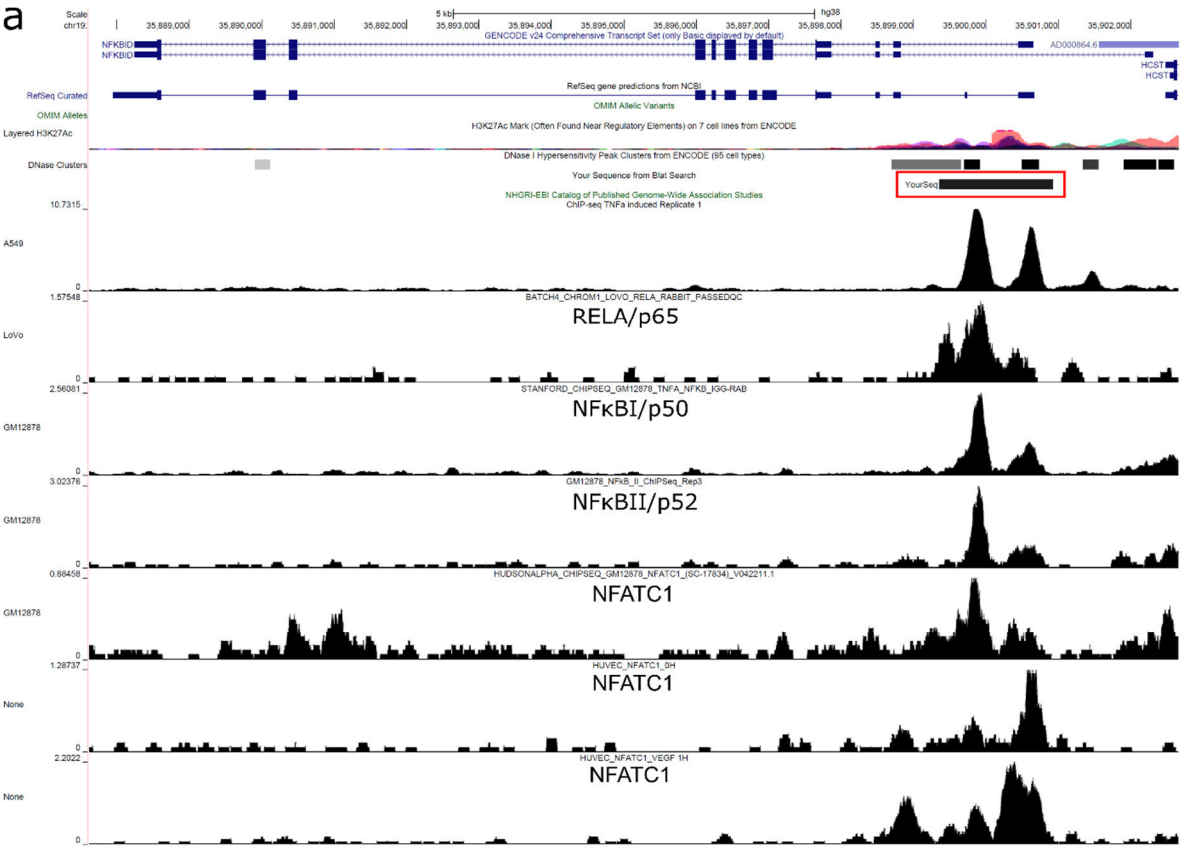

Figure 17. Putative promoter sequence of the Nfκbid gene. (a) CHIP-Seq data for different NF-κB family members and NFATc1 in the region of the Nfκbid gene on chromosome 19q13.12 in multiple cell lines. Framed in red: the sequence in intron one of the Nfκbid gene containing potential transcription factor binding sites as indicated by several peaks **(b)** Nucleotide sequence of the sequence framed in red in **(a)** which is covering the stretch of putative binding sites for NF-κB family members and NFATc1 in intron one of the Nfκbid gene. Depicted in 5'→3' direction. Highlighted in blue: potential NFAT binding site; in yellow and red: potential NFκB binding sites.

To investigate this Nfκbid promoter sequence further, we cloned the whole sequence as depicted in Figure 17.b upstream of a firefly luciferase encoding gene located in a reporter construct, with which we then transfected HEK293T cells. By measuring the activity of this firefly luciferase reporter, we had the tool to test for factors that would potentially activate the putative Nfκbid promoter (Figure 18. a, b).

When we added RelA as a potent NF-κB activator alone in a low amount (of plasmid DNA) we were able to induce the promoter up to ~ 7,5 fold compared to an empty vector control. However, when we applied the same amount of RelA and additionally treated the HEK293T cells 3 h before harvesting with Ionomycin we could double the promoter activity up to ~ 15,5 fold. The same was true of higher amounts of RelA leading to a luciferase activity that could be more than doubled by incubating the cells with Ionomycin (Figure 18.a). To figure out whether the promoter activity could be reduced by using a DN-IκBa approach, we also co-transfected steady amounts of RelA and two different amounts of DN-IκBa. This NF-κB inhibitory approach reduced promoter activity in a dose dependent manner down to the empty control background level. So far, it remains an open question why the lentiviral approach (Figure 13.a) in which DN-IκBa was expressed solely did not lead to a reduction of IκBNS levels. A possible reason for this could be that multiple pathways were switched on after the inhibition of classical NF-κB signaling by DN-IκBa that either substitute NF-κB activity or exert a redundant function like the related alternative NF-κB signaling on the IκBNS promoter. Conceivable as well is that the lentivirally transduced DN-IκBa inhibited NF-κB not completely resulting in low levels of NF-κB sufficient to induce IκBNS.

In the next step we wanted to explore the direct effect of an NFAT-transcription family member (NFATc1) on Nfκbid promoter activity (Figure 18.b). We co-transfected again RelA that led to a clear dose dependent induction of the Nfκbid promoter activity. Since the treatment of B-lymphocytes with Ionomycin only, did not induce any IκBNS expression (Figure 16.) we also co-transfected NFATc1. As anticipated, NFATc1 did not activate the IκBNS promoter. Moreover, we then also co-transfected NFATc1 additionally to RelA. This combination however, led to an even better induction of the luciferase activity compared to RelA alone. Taken together, the collected data suggest that the induction and expression of IκBNS is indeed driven by NF-κB and NFAT, acting in a synergetic manner. NF-κB and NFAT alone however, are only capable of inducing very low levels of IκBNS (NF-κB) or even unable to induce IκBNS (NFAT).

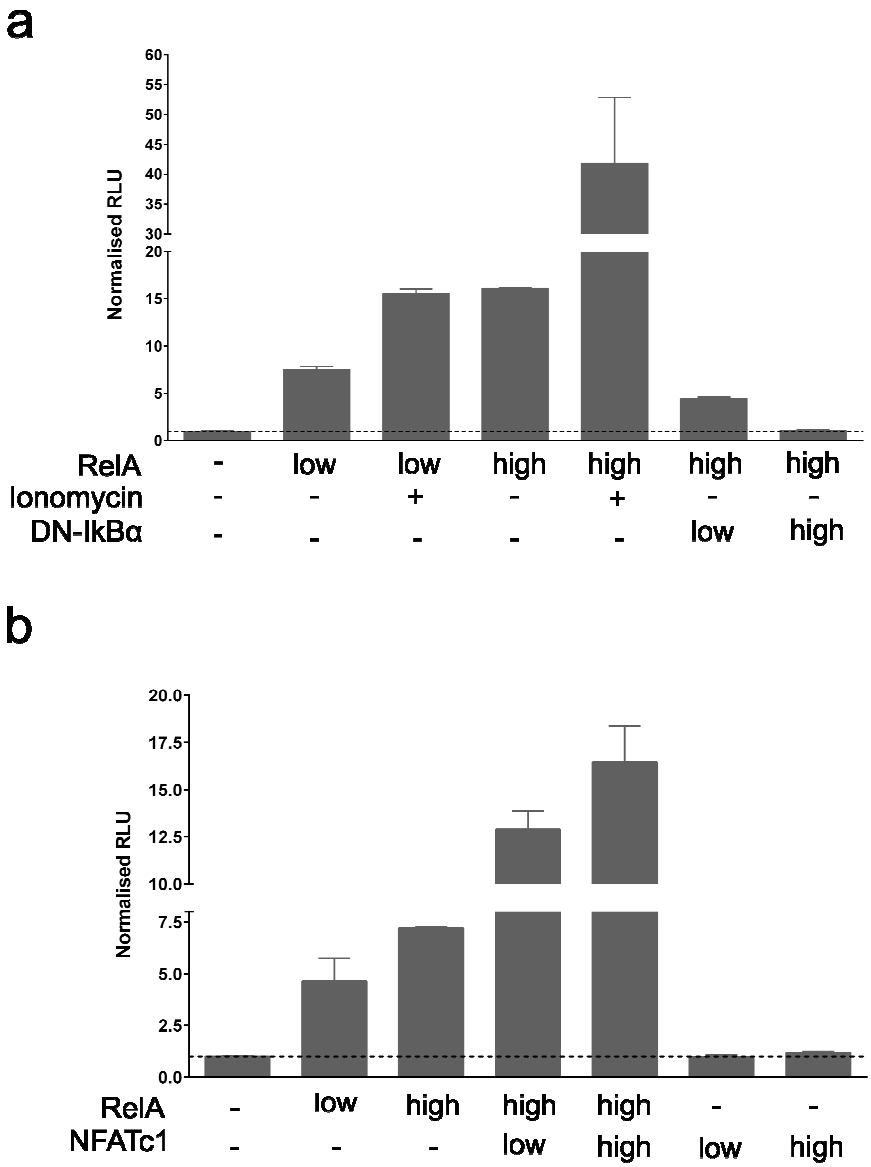

Figure 18. Luciferase reporter activity assay upon cloning of the putative Nfκbid promoter into a luciferase reporter construct. The promoter was then tested for being activated by different putative factors. (a, b) HEK293T were transfected with the Nfκbid reporter construct together with a renilla luciferase reporter, RelA, DN-IκBa, and NFATc1 at different amounts (low/high) of plasmid DNA. Ionomycin was added 3 h before harvesting HEK293T cells. Values were normalized against an empty vector control. RLU means Relative Luciferase Units. Bars represent means ± standard deviation.

Since our so far collected data suggest an important role for NF-κB in regulating the expression of IκBNS in B-lymphocytes, we next asked ourselves whether an interference in NF-κB upstream signaling would have an effect on IκBNS induction and expression. To this end, we pre-incubated BJAB cells with either LVSR or sotrastaurin just before addition of P/I and compared IκBNS levels to a solvent treated control at the indicated time points (Figure 19.a). LVSR acts as a peptide-based inhibitor of MALT1 paracaspase activity, which is activated upon B- and T-

cell stimulation (Hachmann et al., 2015; Rebeaud et al., 2008; Coornaert et al., 2008). As part of the CBM complex, MALT1 is a pivotal upstream-modulator of NF-κB activity (Lucas et al., 2001; Thome et al., 2010). Sotrastaurin (AEB071, Novartis) on the other hand is a pan-PKC inhibitor, thus blocking the activation of PKCβ (B-cell specific isoform) in the context of B-cell stimulation by e.g. proximal antigen-receptor engagement or artificially by PMA. PKCβ phosphorylates CARMA1, which is part of the CBM complex, essential for NF-κB activity (Shinohara et al., 2005; Sommer et al., 2005). Treatment of BJAB with LVSR or Sotrastaurin under concomitant P/I stimulation completely abolished IκBNS induction (Figure 19.a). To further verify the important role of NFκB signaling on IκBNS expression not only under stimulating conditions, we next conducted an siRNA mediated approach to knock-down MALT-1 levels in HBL-1 B-lymphocytes cells that constitutively express high levels of IκBNS (Figure 19.b). As a consequence of this, IκBNS protein levels were drastically reduced but not completely vanished compared to scramble control. This is most likely based on to the incomplete siRNA-block of detectable MALT1 expression, other unknown factors leading to NFκB signaling in HBL-1 and also the fact that IκBNS expression is according to our data a result of the interplay of NFκB and NFAT (Figure 12.-18.). Collectively these results fortify an important role for NFκB signaling in IκBNS induction upon P/I mediated stimulation and under high level steady state expression conditions.

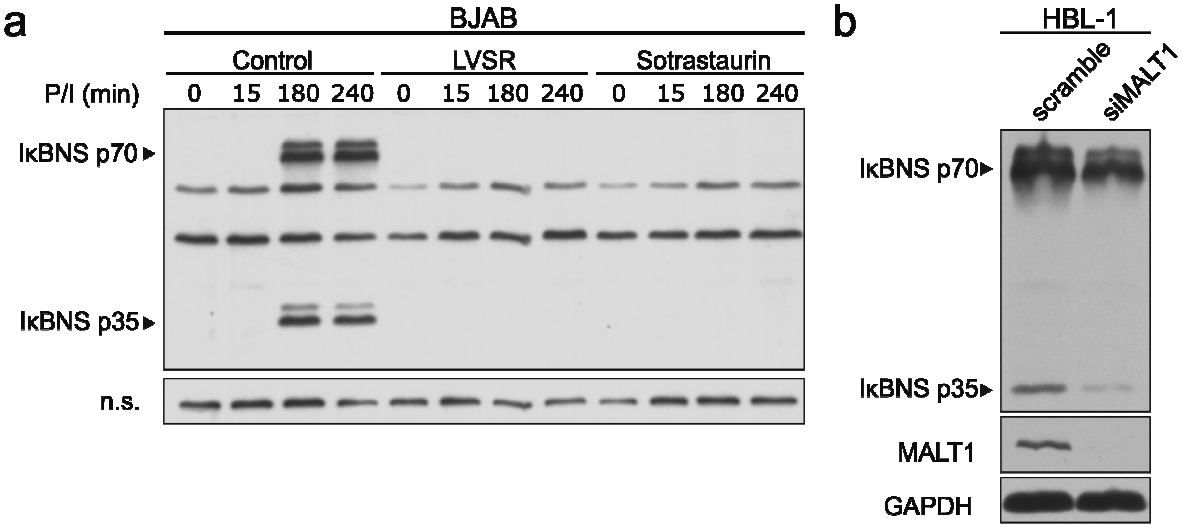

Figure 19. Determining IκBNS expression upon (a) direct pharmacological inhibition or (b) siRNA mediated knock-down of NFκB signaling up-stream elements MALT1 and PKC under P/I mediated B-cell stimulation in (a) BJAB or (b) under high level steady-state conditions in HBL-1 cells (b) by western blotting. (a) BJAB cells were pre-treated for 20 min with either DMSO as solvent control, the MALT1 peptide inhibitor LVSR (1 μM)

or the pan-PKC inhibitor Sotrastaurin (10 μM) and were subsequently stimulated by P/I for the indicated time points. Thereafter, cell lysates were analysed for IκBNS levels. A not specific band (n.s.) served as loading control. **(b)** HBL-1 cells expressing IκBNS under steady state conditions were electroporated with scramble as a control or siRNA targeting MALT1. Following cell lysis 48 h post-electroporation lysates were analysed for IκBNS levels and as a control for efficient siRNA mediated knockdown for the presence of MALT1. GAPDH served as a loading control.

To gain further and more detailed insights into the mechanisms of IκBNS regulation in B-lymphocytes we next had a closer look at another signaling pathway that could be implicated in this context. As IκBNS is a member of the atypical IκB-family and from these the murine IκBNS protein sequence is known to share its highest similarity with the murine IκBζ (43%) (their human counterparts 26 %) in this subgroup of nuclear NF-κB inhibitors (Fiorini et al., 2002), we presumed it to be highly likely that IκBζ and IκBNS could also share some aspects in regard to their regulation in B-lymphocytes. Nogai et al, 2013 found only very low levels of IκB-ζ mRNA expression in multiple myeloma and classical Hodgkin lymphoma compared to ABC DLBCL cell lines, even though their survival also depends on the activity of the NF-κB signaling network. Therefore, Krappmann comments on this finding that NF-κB activation could not be solely responsible for high IκB-ζ levels as observed in ABC DLBCL cell lines (Daniel Krappmann, Comment on Nogai et al, page 2242; Blood, 2013). It was reported that not only NF-κB is able to induce IκB-ζ but also the activation of STAT3 by JAK1 phosphorylation due to a pivotal autocrine feedback loop of IL- 6 and IL-10 in ABC DLBCLs (Lam et al., 2008; Okamoto et al., 2010; Okuma et al., 2013). This link between IκB-ζ that also positively regulates IL-6/-10 secretion and STAT3 phosphorylation suggests a positive feed-back loop that is supporting the malicious excessive IL-6/-10 production and NF-κB hyperactivity in ABC DLBCL. So far however, it was not shown, whether JAK1 inhibition would directly influence IκB-ζ (Daniel Krappmann, Comment on Nogai et al, page 2242; Blood, 2013). Taking everything into account, we were therefore interested to see if there would be an observable effect of JAK1 inhibition on steady state IκBNS expression levels in the ABC DLBCL cell line OCI-LY3 (Figure 20.). OCI-LY3 cells were incubated with the JAK1 inhibitor up to 6h. At all times indicated we could not observe any changes in IκBNS levels compared to solvent control or amongst treatment time points. The JAK1 inhibitor worked properly due to the complete disappearance of active phosphorylated STAT3 (Figure 20.). Taken together, the

expression of IκBNS seems to be independent from the JAK/STAT signaling pathway despite its relation to IκB-ζ.

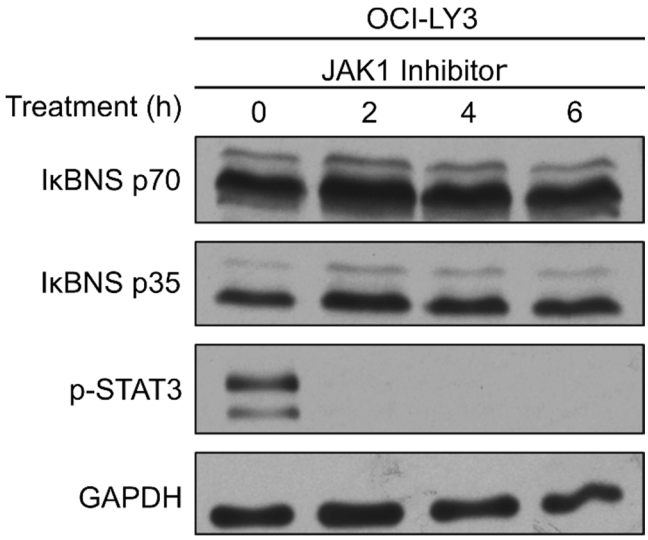

Figure 20. Revealing potential links between IκBNS expression and the JAK/STAT signaling pathway in the ABC cell line OCI-LY3 by western blot analysis. IκBNS expression levels were assessed at the indicated time points upon treatment with 5 µM of JAK1 inhibitor. Blotting for p-Stat3 levels served as proof of functionality of the JAK1 inhibitor. Loading of equal amounts of proteins was controlled by blotting for GAPDH.

Another yet in the literature undescribed aspect of IκBNS regulation in B-lymphocytes is concerning the half-life of the protein and whether there is a difference between IκBNS p35 and IκBNS p70. To investigate this, we took two ABC DLBCL cell lines that express high levels of IκBNS under state conditions. HBL-1 and OCI-LY3 cells were incubated for the indicated times in the presence of the antibiotic cycloheximide, an inhibitor of protein translation from *Streptomyces griseus*. IκBNS levels did not alter still within the sample with the longest incubation of cycloheximide for 6h in both cell lines. Thereby, we could not observe any difference between IκBNS p35 and IκBNS p70. For controlling the proper function of cycloheximide we were blotting against IκBα, which is known to have a rather short half-life (Fagerlund et al., 2015). IκBα clearly diminished over time in OCI-LY3 cells, and was almost completely vanished at 6 h of cycloheximide treatment. Surprisingly, in HBL-1 cells however, IκBα levels just began to decline at 6h of applying cycloheximide. Thus, IκBα seems to have a longer half-life in HBL-1 cells compared to OCI-LY3 cells. In summary, it can be stated that IκBNS has a rather long half-life of more than 6h in the ABC DLBCL cell lines HBL-1 and OCI-LY3.

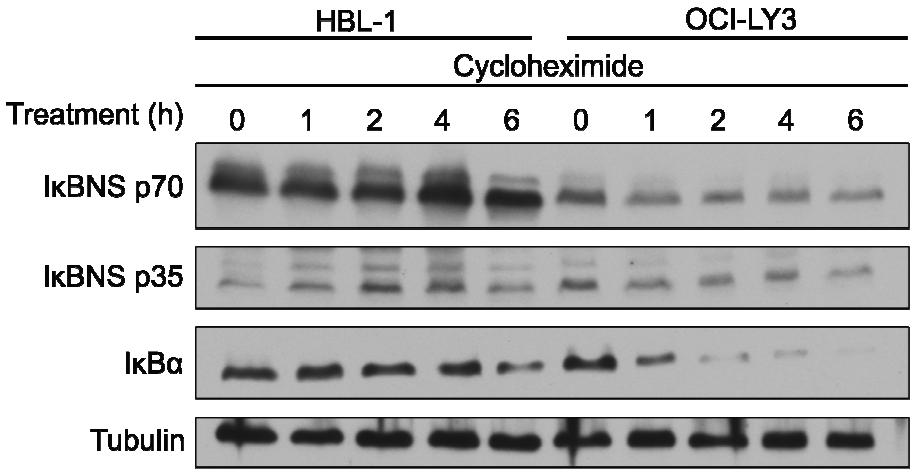

Figure 21. Determining the half-life of IκBNS in HBL-1 and OCI-LY3 cells under steady state conditions for the indicated time periods by the treatment with the protein synthesis inhibitor cycloheximide. IκBNS levels in lysates of HBL-1 and OCI-LY3 cells upon cycloheximide treatment were determined by western blot to estimate half-life of IκBNS and to see possible differences between IκBNS p35 and IκBNS p70 in this respect. Functionality of translation blockage by cycloheximide was assessed by blotting against IκBα. Tubulin levels were determined to check for evenly-loaded amounts of protein.

3.2 Role of IκBNS in ABC DLBCL

Gene expression profiling of the clinically heterogeneous DLBCL revealed three distinct subgroups of DLBCL (Alizadeh et al., 2000). This eventually led to their molecular classification into GCB/ABC DLBCL and PMBL. Those subtypes are highly different in their prognosis and their response to therapeutic approaches. Moreover, in 2001 Davis et al. unveiled the constitutive activity of the NF-κB pathway as a hallmark of ABC DLBCL. Furthermore, they also showed the dependency of this subtype on hyperactive NF-κB signaling by using a NF-κB super-repressive form of IκBα which was toxic for ABC DLBCL but not for GCB DLBCL. Since IκB-ζ, which like IκBNS belongs to the family of the atypical nuclear NF-κB inhibitors, was reported to be overexpressed in ABC DLBCL but not in GCB DLBCL (Nogai et al., 2013) and we previously found IκBNS induction and expression maintenance to be regulated by NF-κB, (chapter 3.1) we were interested in whether this expression pattern would be also hold true for IκBNS.

For this purpose, we screened a selection of GCB and ABC DLBCL model cell lines for their expression of IκBNS (Figure 22., 23a). Initially, we used a commercially available antibody to assess IκBNS protein levels (Figure 11.). In this panel we also included several representative mantle cell lymphoma (MCL) lines (Figure 22.). We chose this aggressive B-cell cancer type because MCL were shown to have

either chronic active BCR-driven classical NF-κB signaling (Jeko-1, Rec-1) like ABC DLBCL or NIK (MAP3K14) depended alternative NF-κB signaling (Granta-519, JVM2, Z-138) (Rahal et al., 2014). To estimate the size of IκBNS on a SDS-PAGE we also involved two lysates of HEK293T cells in the western blot, an empty control and a sample in which we overexpressed a FLAG-tagged IκBNS p35 (Figure 22.). Indeed, when we compared the IκBNS expression pattern of GCB and ABC DLBCL cell lines, IκBNS was exclusively expressed in ABC DLBCL cell lines, just as IκB-ζ, shown in Nogai et al., 2013. The MCL cell lines showed a rather mixed pattern of IκBNS expression, most likely depending on whether the classical or alternative NF-κB signaling pathway was predominantly activated, indicating that IκBNS is mainly induced by classical NF-κB signaling. In this experiment (Figure 22.) we also noticed a consistently with IκBNS p35 upcoming band running at approximately 70 kDa, labelled as IκBNS p70. We presumed it either to be an IκBNS p35 homodimer, posttranslational modification of IκBNS p35 or another IκBNS isoform. This issue will be further investigated in chapter 4.4.

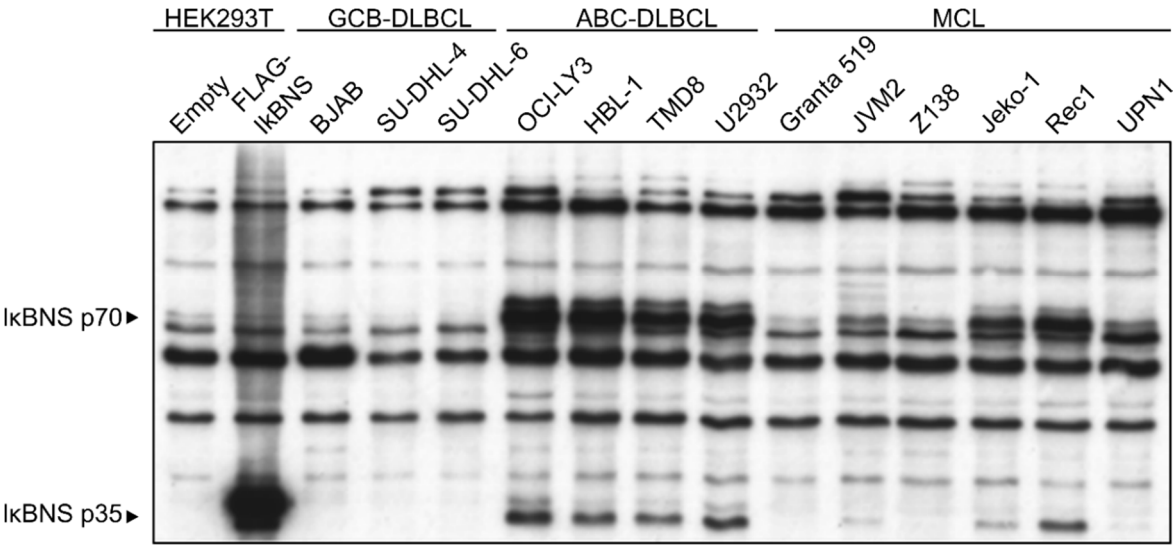

Figure 22. Determining IκBNS expression levels in GCB, ABC DLBCL and MCL by western blot analysis. Samples from HEK293T cells, either transfected with an empty vector or with a FLAG-IκBNS p35 construct served as a negative and positive control.

As the IκBNS antibody we used so far, displays plenty of unspecific bands (Figure 22.), we decided to generate an anti-IκBNS antibody ourselves. We used this self-made antibody to repeat the experiment depicted in Figure 22., comprising mostly the same GCB and ABC DLBCL model cell lines (Figure 23.a). This time were not only interested to assess IκBNS protein levels but IκBNS mRNA levels, as well (Figure 23.b). Using the self-made antibody confirmed IκBNS to be solely expressed

in ABC DLBCL compared to GCB DLBCL cell lines. An empty and a FLAG-tagged IκBNS overexpressing HEK293T sample served again as specificity controls to estimate at which size IκBNS p35 has on a SDS-PAGE. Also detected by the antibody was the IκBNS p70 band, which only appears when IκBNS p35 is detected, as well. As B-cell activation markers, we stained against CYLD and BCL-10. BCL-10 is like CYLD a substrate of MALT1 and part of the CBM complex, thus important for an appropriate NF-κB response upon B- and T-cell receptor engagement (Rebeaud et al., 2008; Ruland et al., 2003). As expected, only DLBCL of the ABC subtype exhibit MALT1 substrate cleavage of CYLD and BCL-10. The assessment of IκBNS mRNA levels reflects the protein levels (Figure 23.a, b). Relative to GCB DLBCL cell lines ABC DLBCL cell lines express abundant amounts of IκBNS mRNA (Figure 23.b), indicating that increased mRNA levels are translated into protein expression.

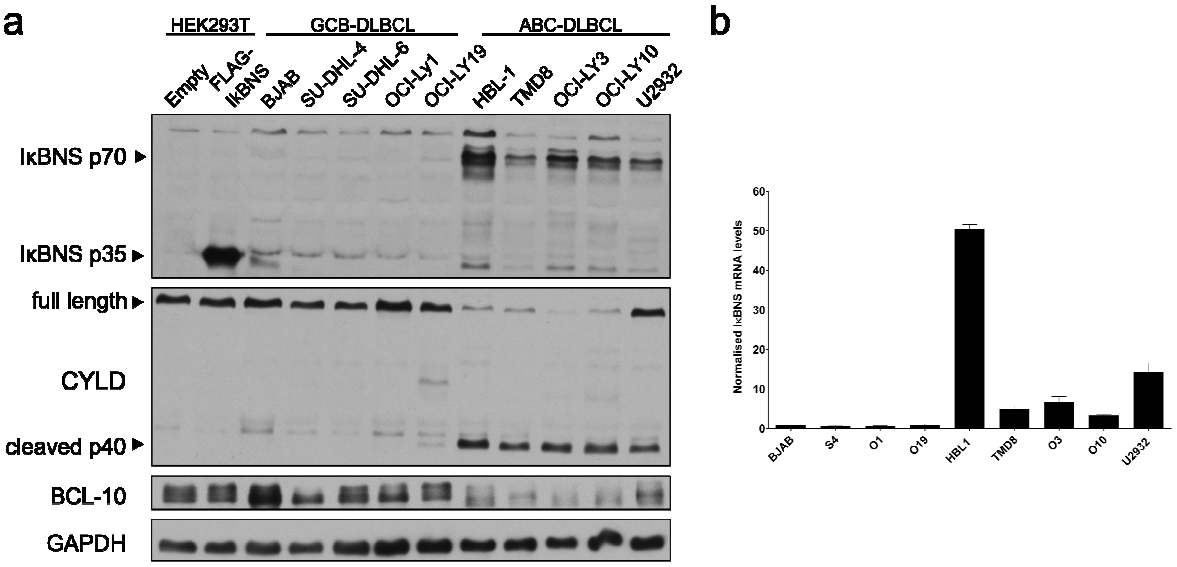

Figure 23. Assessment of IκBNS mRNA and protein levels in GCB and ABC DLBCL model cell lines. (a) IκBNS mRNA levels were determined by qPCR and normalized against the IκBNS expression level of the GCB DLBCL cell line BJAB. Bars represent means ± standard deviation. **(b)** IκBNS protein levels were detected by immunoblot using a self-made antibody. Lysates from HEK293T cells that were either transfected with an empty vector or with a FLAG-IκBNS p35 expression construct served as a negative and positive control. Blotting against CYLD and BCL-10 indicates B-cell activation status. GAPDH served as a loading control.

In summary, the atypical nuclear IκB IκBNS is expressed exclusively in the NF-κB signaling dependent ABC subtype of DLBCL what is reflected on both, the mRNA and protein level. Moreover, also MCL model cell lines that mainly exhibit chronic activation of BCR-driven classical NF-κB signaling express IκBNS. Furthermore, we

found a second correlating, presumably specific p70 IκBNS band additionally to IκBNS p35 that could represent a dimer, a posttranslational modification of IκBNS p35 modified or an unknown IκBNS isoform (further investigated in chapter 4.4). Taken together, these results underscore the regulation of IκBNS induction and expression maintenance by classical NF-κB signaling in the context of oncogenic signaling in DLBCL and MCL.

In order to shed some more light on IκBNS regulation within the framework of frequent mutations leading to oncogenic NF-κB pathway signaling in ABC DLBCLs, we next made us again of the already established NFκBID promoter sequence cloned into a luciferase reporter construct (Figure 17.). A number of different somatic mutations in positive and negative NF-κB regulator proteins have been found to contribute to chronically active NF-κB signaling in ABC DLBCLs including e.g. MYD88 and CARMA1/CARD11 (Lenz et al., 2008; Kato et al., 2009; Davis et al., 2010; Ngo et al., 2011;). Thus, we co-transfected several well-known proteins afflicted in ABC DLBCL in their wild type and representative mutant variants together with our luciferase reporter construct in HEK293T cells (Figure 24.a). NFκBID promoter activity was clearly induced by RelA and blocked upon adding DN-IκBa, reproducing results gained earlier (Figure 18.a, b). However, when we co-transfected NF-κB signaling regulatory proteins affected in ABC DLBCL in their wild-type version, mutant version or combinations of different mutants like they also occur in ABC DLBCL, luciferase activity was only slightly increased (Figure 24.a). This result suggests, that NF-κB upstream elements alone (wild type or mutant), that positively regulate the classical NF-κB pathway in ABC DLBCL, have only a minor impact on IκBNS induction. This is most likely due to the missing synergistic IκBNS inducible effect of Ca^{2+} mediated NFAT signaling in HEK293T cells under steady state conditions.

So far we were just examining if wild-type or mutant upstream elements of the classical NF-κB pathway like CBM complex members or MYD88 would induce the NFκBID promoter luciferase reporter. But also a BIRC3 missense mutation was recently described for the first time in DLBCL (Hatem et al., 2016). For these reasons, we were next investigating if also elements that are implicated in alternative NF-κB signaling would be capable of inducing or repressing the NFκBID promoter. For this purpose, we used a wild-type and a mutant variant of BIRC3 which is a key regulatory component of the non-canonical NF-κB pathway.

BIRC3 interacts with BIRC2 and TRAF2/3 in regulatory complex to down regulate NIK by constitutive ubiquitin-dependent degradation. NIK supports the transition of the cytosolic p100 precursor into the active p52, thereby activating alternative NF-κB signaling (Zarnegar et al., 2008; Zarnegar BJ et al.,2008; Vallabhapurapu et al., 2008.). Rahal et al. showed in 2014 that roughly 10% of MCL patient samples they collected, carry mutations in BIRC3 leading to genetically deregulated alternative NF-κB signaling. They revealed amongst others, two frequent mutants namely $BIRC3^{S441*}$ and $BIRC3^{C560S}$. They found those mutants to be less efficient in destabilizing NIK and to be affected to prevent p52 maturation. Moreover, they also showed $BIRC3^{S441*}$ and $BIRC3^{C560S}$ expression in a GCB DLBCL cell line to elevate p52 levels, thereby increasing alternative NF-κB signaling. Obviously, $BIRC3^{S441*}$ and $BIRC3^{C560S}$ lost their ability to suppress alternative NF-κB signaling. For this reason we were interested to examine what effect wild-type and the $BIRC3^{S441*}$ mutant would have on NFκBID promoter activity. When we co-transfected wild-type BIRC3, NFκBID promoter activity negligibly increased for yet unknown reasons. Albeit, when we co-transfected the non-sense mutation $BIRC3^{S441*}$ we observed a weak but dose-dependent increase in luciferase activity (Figure 24.b). That implies that IκBNS can also be induced by the alternative NF-κB pathway. Together, the results obtained from the experiments depicted in Figure 24.a, b indicate that IκBNS expression can be induced by both classical and alternative NF-κB signaling. In particular, the IκBNS promoter was also inducible, although weakly, by upstream wild-type but also mutant elements of classical NF-κB signaling regulation commonly found in the context of ABC DLBCL somatic mutation patterns. Also a typical negative regulator of the non-canonical NF-κB pathway that lost its suppressive function by a missense mutation, found in MCL and recently reported to be also found mutated in DLBCL, slightly induced IκBNS promoter activity.

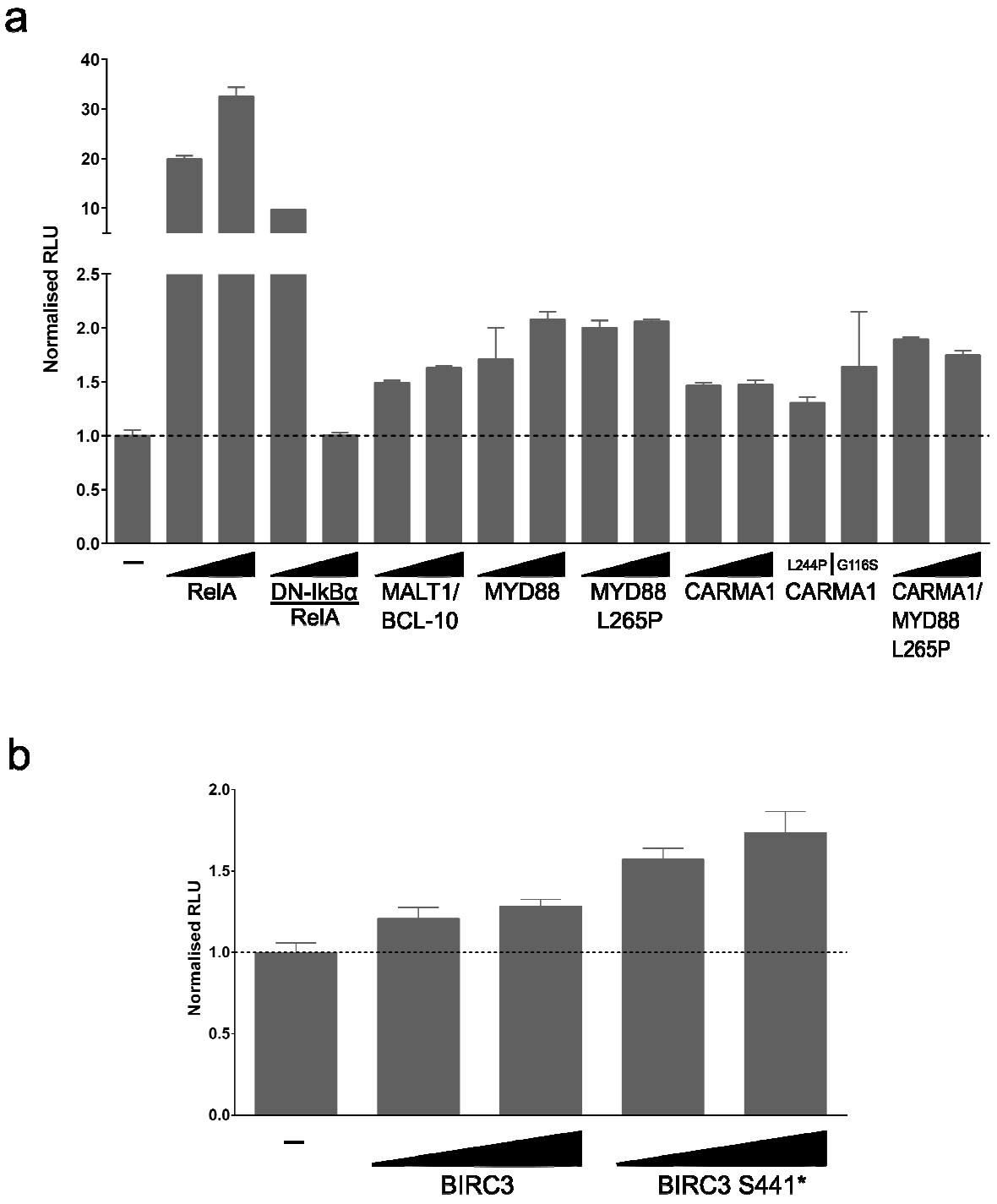

Figure 24. Examining the inducible abilities of classical and alternative NF-κB wild-type and in the context of ABC DLBCL pathogenesis commonly mutated NF-κB upstream elements on NFκBID promoter activity by luciferase assay. (a) Co-transfection of wild type and mutant variants commonly found somatically altered in the context of ABC DLBCL mutagenesis. RelA co-transfection and the inhibition of its induced NFκBID promoter activity by DN-IκBα served as a specificity control of induction **(b)** Co-transfection of the wild-type BIRC3 negative regulator of alternative NF-κB signaling and the loss of function variant missense mutated $BIRC3^{S441*}$. **(a, b)** Triangles indicate increasing amounts of plasmid DNA co-transfected to a constant amount of NFκBID promoter luciferase construct. RLU means Relative Luciferase Units Bars represent means ± standard deviation.

To strengthen the previous findings that were obtained based on the analysis of NFκBID promoter activity we subsequently wanted to figure out what would be the result of CARMA1^{L244P} and CARMA1^{G116S} overexpression in a GCB DLBCL (without constitutive NF-kB signaling) on the actual IκBNS protein expression (Figure 25.). Thus, we electroporated BJAB cells with either an empty vector as control, wild-type CARMA1 or the missense base substitution carrying mutant proteins CARMA1^{L244P} and CARMA1^{G116S}. These CARMA1 variants are both mutated in their coiled-coil domains and were discovered in the ABC DLBCL cell line OCI-LY3 (harbours a CARMA1^{L244P} mutation) and in an ABC DLBCL biopsy (CARMA1^{G116S}) (Lenz et al., 2008; Snow et al., 2012). Both mutants were shown to generate high levels of constitutive active NF-κB signaling without any extrinsic stimuli and introduction in BJAB resulted in the induction of NF-κB target genes (Lenz et al., 2008). Since our previous results suggest that IκBNS is also a NF-κB target gene, we assumed IκBNS to be induced also on the protein level upon introduction of CARMA1^{L244P} and CARMA1^{G116S} in BJAB cells. Indeed, the overexpression of CARMA1^{L244P} or CARMA1^{G116S} in BJAB led to a clear induction of IκBNS p35/p70 proteins in a comparable degree (Figure 25.). Moreover, also BJAB cells expressing wild-type CARMA1 showed a weak induction of IκBNS p35/p70 but considerably less pronounced compared to the mutant CARMA1 variants (Figure 25.) most likely due to its potent NF-kB activating properties.

Taken together, the weak induction of IκBNS p35/p70 protein levels upon introduction of ABC DLBCL derived CARMA1 mutants into the GCB DLBCL cell line BJAB is in line with the weak induction of the IκBNS promoter reporter upon co-transfection with common mutant ABC DLBCL NF-κB regulators (Figure 24.a). Additionally, this result validates IκBNS as NF-κB target gene and constitutive NF-κB signaling in ABC DLBCL to drive IκBNS expression. The only weak induction also indicates that NF-κB is capable of inducing IκBNS expression on its own but for full induction and high protein levels as seen in ABC DLBCL, it might require the synergistic signaling of NF-κB together with NFAT.

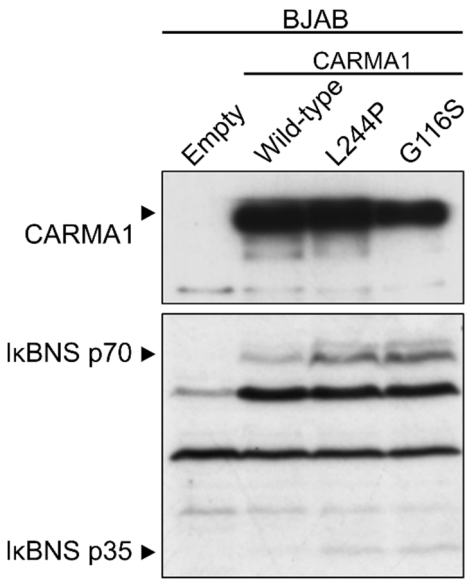

Figure 25. CARMA1 mutants induce the expression of IκBNS in the GCB DLBCL cell line BJAB as revealed by Western Blot analysis. Cells were either electroporated with an empty vector as control, wild-type CARMA1 or the missense base substitution carrying mutant proteins CARMA1^{L244P} or CARMA1^{G116S}.

To further elucidate the role of IκBNS and how important its steady state expression is for ABC DLBCL we now tried a shRNA mediated knock down approach targeting IκBNS. Therefore, we initially designed and screened for functional shRNA sequences (Figure 26.). For this, we lentivirally transduced BJAB cells, a cell line model of the GCB DLBCL subtype with constructs expressing the distinct shRNAs and assessed the suppressive abilities of the different shRNAs on IκBNS protein levels upon P/I mediated induction of IκBNS. Out of 11 different possible shRNA sequences we identified two suitable shRNA sequences (#1 and #8) that were sufficiently able to decrease IκBNS expression levels after 4 h of P/I stimulation compared to controls (Figure 26.).

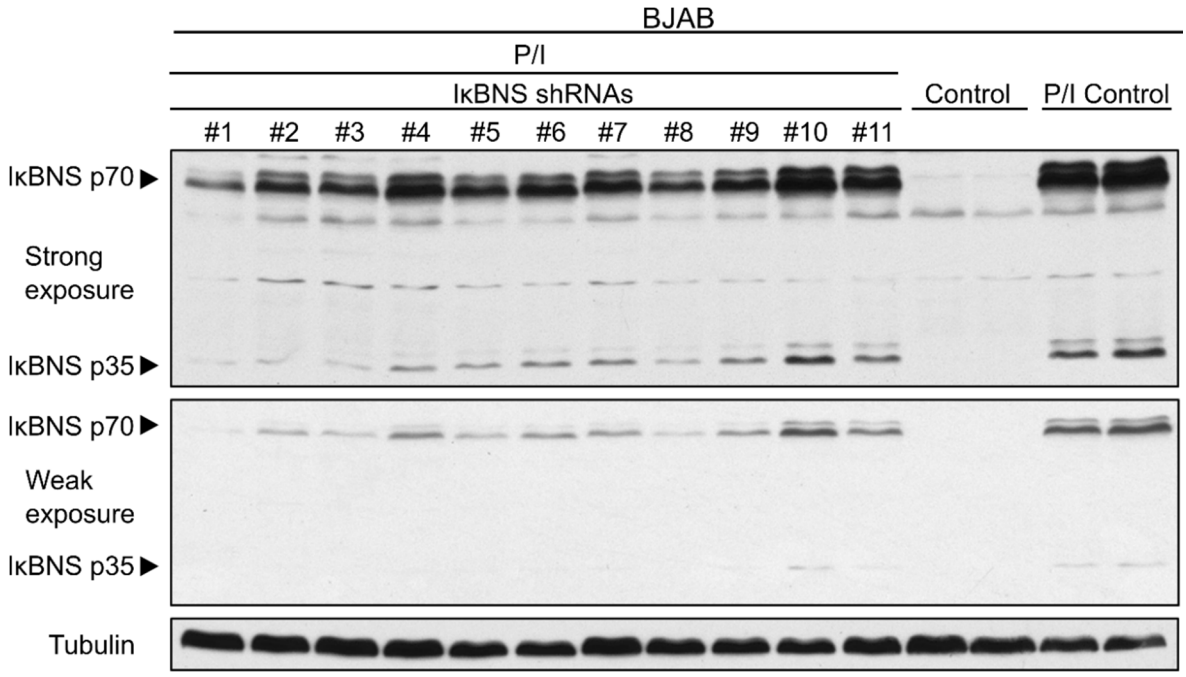

Figure 26. Screening for functional shRNA sequences to knock down IκBNS levels. BJAB cells were lentivirally transduced with shRNA sequences (#1 - #11) targeting IκBNS mRNA. Upon selection of shRNA expressing cells by puromycin cells were stimulated with P/I for 4 h to induce IκBNS expression. Suitable shRNA sequences should markedly diminish induced IκBNS protein levels induced by 4 h of P/I stimulation compared to stimulated controls. Two shRNAs #1 and #8 were identified to sufficiently decrease IκBNS on the protein level. Weak and strong exposures are shown to evaluate down regulations of IκBNS p35 and p70 due to differences in expression levels. Tubulin served as a loading control.

With IκBNS shRNA #1 and #8 we now had the appropriate tool to test the effect of IκBNS knock down on DLBCL. To this end, we lentivirally transduced DLBCL of the ABC and GCB subtype with the identified functional shRNAs (#1 and #8) targeting IκBNS. shRNA expression was coupled to the expression of GFP by an IRES-element, so that GFP served as a read-out for the survival rate of shRNA #1 and #8 expressing cells over the course of time.

IκBNS knock down by the two independent shRNAs #1 and #8 clearly induced toxicity in the group of IκBNS positive ABC DLBCL cell lines (HBL-1, TMD8, U2932, SU-DHL-2) after some days in case of shRNA #1 and after roughly one week for shRNA #8 after transduction (Figure 27.). This obvious time difference could be explained by the different efficiencies of both shRNAs to knock down IκBNS (Figure 26.). For instance the growth rate of TMD8 declined over the course of time down to 30% 17 days after transduction transduced with shRNA #1 and to less than 20% 23 days after transduction with shRNA #8. In contrast, the shRNAs did not affect the growth of the GCB DLBCL group (HT, SU-DHL-4, SU-DHL-6, OCI-LY1, OCI-LY7)

which exhibited little or no IκBNS mRNA levels and displayed no detectable IκBNS on the protein level, as well (Figure 22.; 23.a, b). This result suggests a selectively toxic effect of the IκBNS knock down to ABC DLBCL and furthermore an addiction of ABC DLBCL to the expression of IκBNS, indicating an essential role for growth.

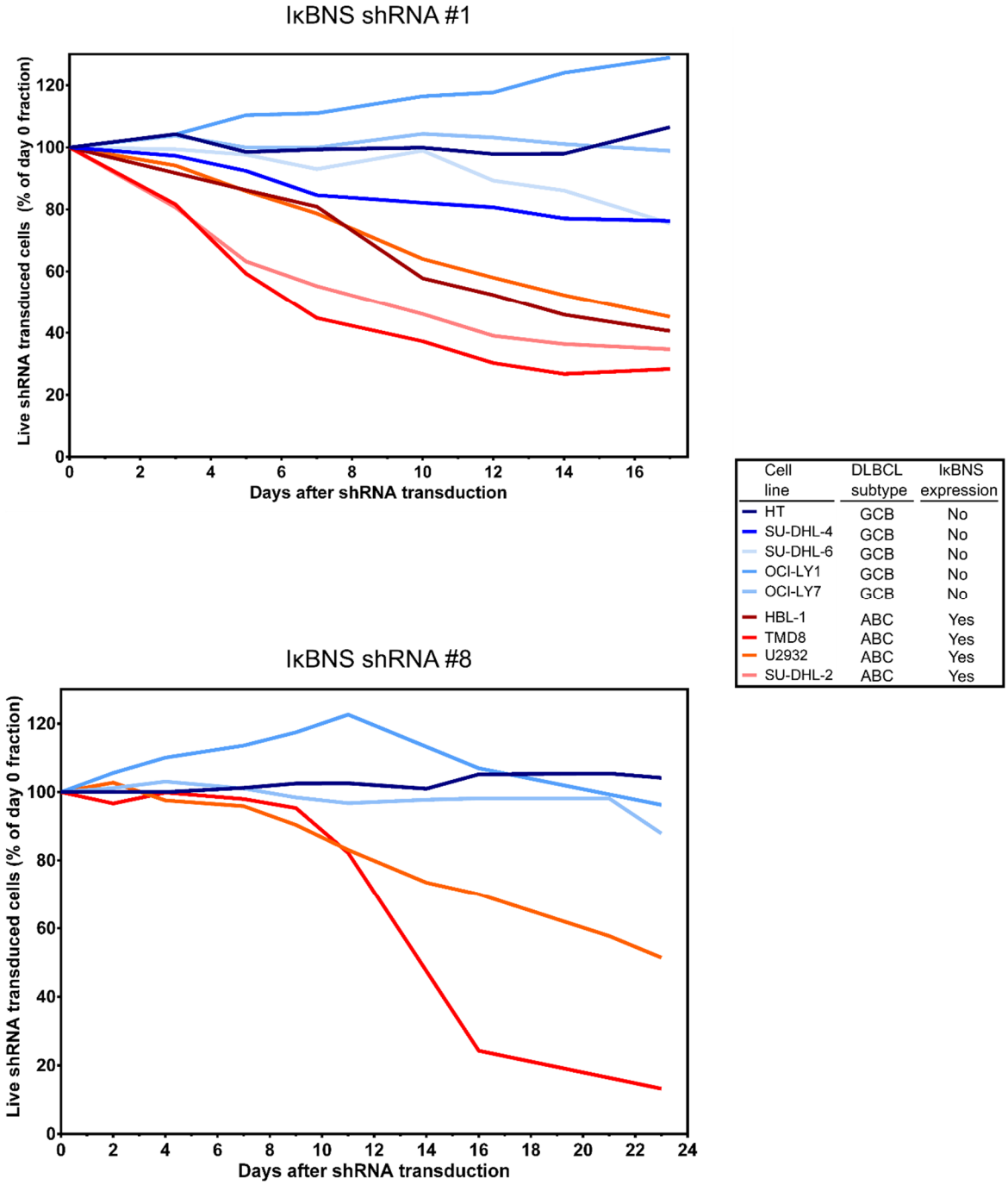

Figure 27. Investigating the effect on survival of IκBNS knock down mediated by two independent shRNAs. Cells of the GCB and ABC subgroup of DLBCL were lentivirally transduced by either shRNA #1 (upper panel) or # panel8 (lower) mediating the knockdown of IκBNS. shRNA expression was coupled to the expression of GFP by an IRES element. GFP served as a read out for the rate of living transduced cells in % of day 0 fraction over the course of time

measured by flow cytometry. Survival rates were assessed for 17 days after transduction for shRNA #1 and for 23 days after transduction for shRNA #8

As demonstrated, IκBNS knock down is exclusively toxic to the ABC subgroup of DLBCL (Figure 27.). We now addressed the question whether what would be the outcome of the vice-versa experiment, meaning the overexpression of IκBNS p35 in GCB and ABC DLBCL cell lines for a longer period of time. Thus, we lentivirally transduced a GCB cell line (BJAB) and two ABC cell lines (HBL-1 and U2932) with a GFP-tagged IκBNS p35. GFP served as the read out for the rate of living transduced cells over the next 14 days of measurement. As depicted in Figure 28., the overexpression of IκBNS p35 did not affect the growth of GCB and ABC DLBCL cell lines over a time frame of two weeks. Taken together, the overexpression of IκBNS p35 has neither a noticeable positive effect on the survival of IκBNS negative cells (BJAB) nor a negative effect on IκBNS positive ABC DLBCL cell lines (HBL-1,U2932) and vice versa, 14 days after IκBNS p35 transduction. This suggests, IκBNS p35 overexpression alone does not confer a survival advantage over non-transduced GFP^- cells. Furthermore, the high steady levels of IκBNS in ABC DLBCL does not seem to be vulnerable to a further increase in IκBNS p35 protein expression since no toxic effects on survival were observed.

In summary, IκBNS knockdown is selectively toxic to ABC DLBCL cell lines whereas the overexpression of IκBNS p35 does not affect the survival of both the GCB and the ABC subtype of DLBCL neither in a positive nor in negative manner in the time span of several weeks.

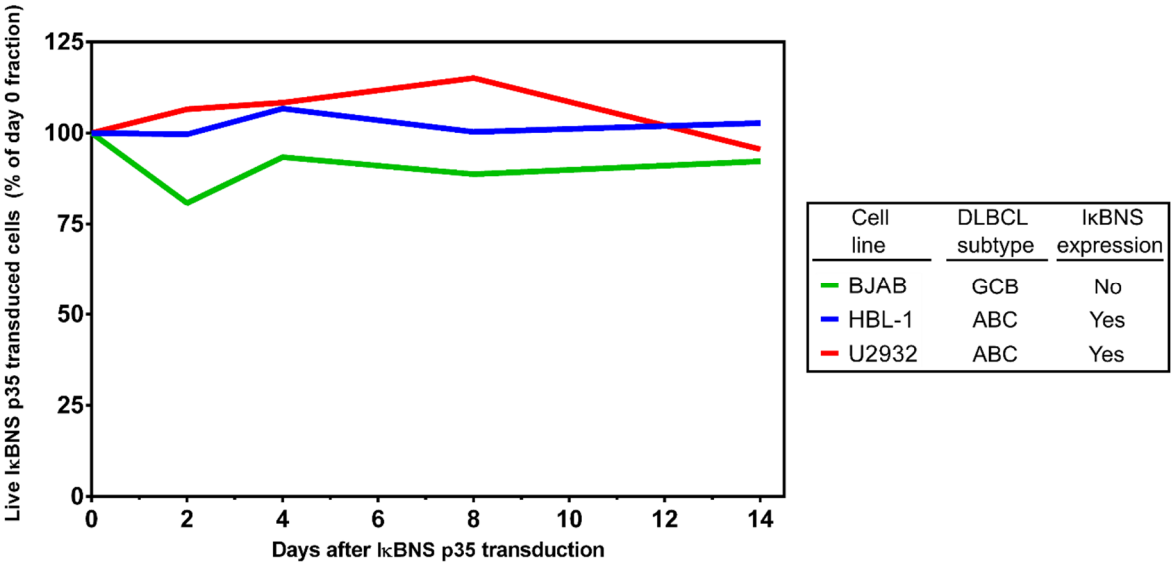

Figure 28. Impact of IκBNS p35 overexpression on the survival of GCB and ABC DLBCL cell lines. The IκBNS negative cell line BJAB (GCB DLBCL) and IκBNS positive cell

lines HBL-1, U2932 (both ABC DLBCL) were lentivirally transfected with a GFP-tagged IκBNS p35 expression construct. GFP expression served as a read out for the rate of living IκBNS p35 transduced cells in % of day 0 fraction measured by flow cytometry over a period of 14 days.

To substantiate the clinical importance of this study and to reaffirm the finding that IκBNS is expressed exclusively in the ABC but not in the GCB subtype of DLBCL also in a clinical context, we analysed patient samples from both DLBCL subtypes for the relative mRNA expression of IκBNS. Indeed, also clinical samples derived from GCB and ABC DLBCL patients show the same IκBNS mRNA expression pattern as the investigated DLBCL model cell lines (Figure 29.). Also in these patient derived samples IκBNS mRNA is significantly higher expressed in ABC DLBCL samples compared to GCB DLBCL samples confirming the results shown in Figure 23.b. The high background of IκBNS mRNA levels in both DLBCL subtypes is most likely due to infiltrating activated T-cells expressing high levels of IκBNS mRNA.

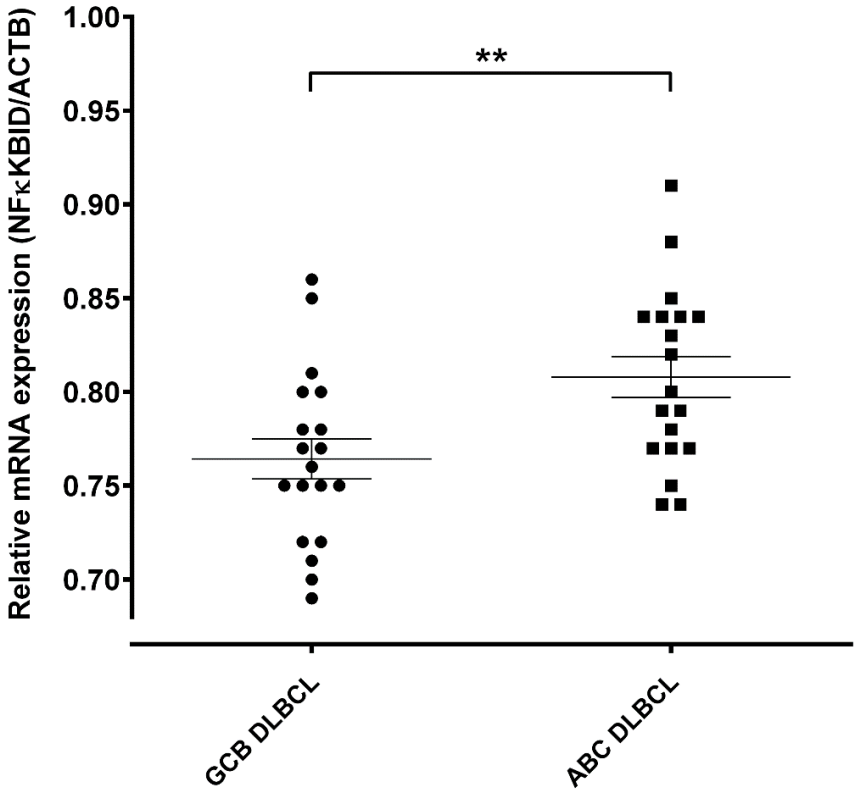

Figure 29. Comparison of relative NFκBID mRNA expression levels determined by qPCR in patient samples derived from DLBCL of the GCB and ABC subtype. NFκBID mRNA expression is depicted relative to the housekeeping gene ACTB coding for Actin Beta. Analysis was performed on 19 patient samples (n=19) for each DLBCL subtype. Each dot represents one patient sample. Shown is the standard error of the mean. The difference between the two groups was statistically significant with **p < 0, 05 (unpaired, two-tailed t-test). The experiment was performed in collaboration with Dr. Irina Bonzheim.

3.3 Role of calcineurin in DLBCL

As demonstrated earlier in this study, the induction of IκBNS expression upon stimulation of GCB DLBCL by P/I and the maintenance of IκBNS expression under steady state conditions in ABC DLBCL needs both, classical NF-κB signaling and NFAT signaling, together acting in a synergistic manner. Thus, we have also shown that it is possible to decrease IκBNS expression by applying the phosphatase calcineurin inhibitors Cyclosporin A (CsA) and FK506. This effect, we assume is most likely the consequence of NFAT signaling blockage by CsA and FK506. CsA and FK506 mediated calcineurin inhibition, prevents the cytosolic NFAT to be dephosphorylated. Thus, also its consecutive translocation in the nucleus is blocked where it would otherwise, cooperatively with other partners such as NF-κB direct transcriptional control over a multitude of target genes including IκBNS (Figure 15.a,b; 16. a,b; 17.a,b) (Fu et al. 2006; Pham et al. 2005; Steinbach et al., 2007; Gachet and Ghysdael, 2009). Due to this dependency of IκBNS expression to active NFAT signaling and because IκBNS was highly expressed in all investigated ABC DLBCL, we were interested to figure out the activation status of the calcium signaling responsive NFAT member NFATc1 in the DLBCL cell lines (Figure 30.). Therefore, we treated cells from the GCB subtype (BJAB, HT, SU-DHL-4) and the ABC subtype (HBL-1, TMD8, OCI-LY10, OCI-LY3, SU-DHL-2, U2932, RIVA) of DLBCL for 2 h with CsA and compared afterwards lysates from CsA treated cells with untreated cells in regard to their NFATc1 protein expression. Undoubtedly, all tested cell lines except for SU-DHL-4 exhibit active dephosphorylated NFATc1 species. Those hyperphosphorylated active NFATc1 isoforms could be identified by an obvious upward shift of NFATc1 bands to higher molecular weights on the blot, upon CsA treatment (Figure 30.). Notable were also the highly different NFATc1 expression levels amongst the DLBCL cell lines (Figure 30.).

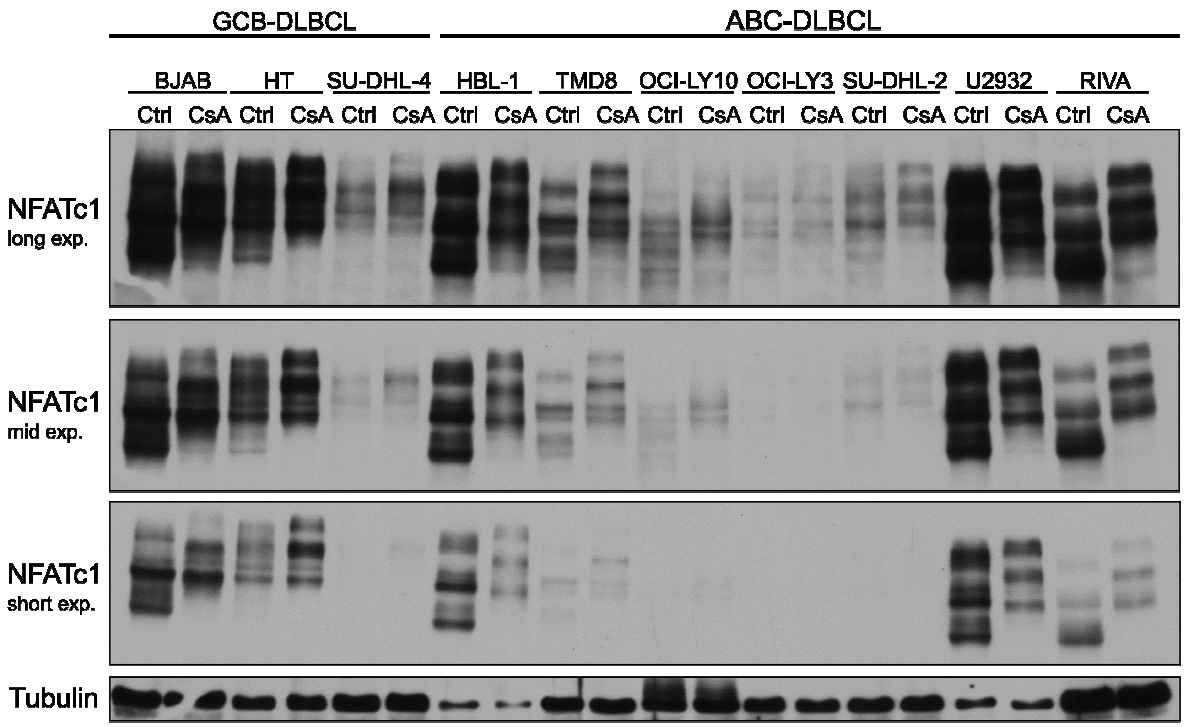

Figure 30. Assessment of NFATc1 phosphorylation and expression levels in DLBCL of the GCB and ABC subtype by western blot. Each cell line was either treated with solvent control (Ctrl) or 2,5 µM CsA for 2 h prior to lysis. Different NFATc1 blot exposures (long exp., mid exp., short exp.) are shown due to the different NFATc1 expression levels of the investigated DLBCL. Blotting for Tubulin served as loading control amongst untreated and CsA treated samples.

As shown in Figure 30., it turned out that NFAT signaling was active in all GCB and all ABC DLBCL cell lines tested except SU-DHL-4. In Figure 27., we have proven that the direct knock down of IκBNS by two independent shRNAs was toxic to all ABC DLBCL we tested but not to GCB DLBCL cell lines. We now asked ourselves what would be the impact on ABC and GCB DLBCL growth of indirect IκBNS protein expression knock down as shown in Figure 15.a,b by CsA and FK506 mediated inhibition of NFAT signaling. For this, we treated GCB (SU-DHL-4, BJAB, HT) and ABC (HBL-1, TMD8, OCI-LY3, U2932, RIVA, SU-DHL-2, OCI-LY10) DLBCL with either two different concentrations of CsA or FK506 (Figure 31.) and measured their growth by MTS assay on day six of calcineurin inhibitor treatment. Inhibitors were once reapplied on day two. In detail, the GCB DLBCL group (SU-DHL4, BJAB, HT) was completely unaffected by CsA or FK506 inhibitor treatment. However, some members of the ABC DLBCL group namely HBL-1 and TMD8 were severely impaired in their proliferation capabilities by the application of both inhibitors and concentrations. For instance, at the higher CsA or FK506 inhibitor concentration those cell lines show a reduction of growth up to 80 % or 60%

compared to respective solvent controls. Furthermore, U2932, RIVA, SU-DHL-2 and OCI-LY10 represent a group of ABC DLBCL that were clearly impeded in their proliferation by both inhibitors concentrations of CsA and FK506 but were less vulnerable than HBL-1 and TMD8. On the contrary, OCI-LY3 was the only ABC DLBCL cell line that entirely tolerated CsA and FK506 treatment.

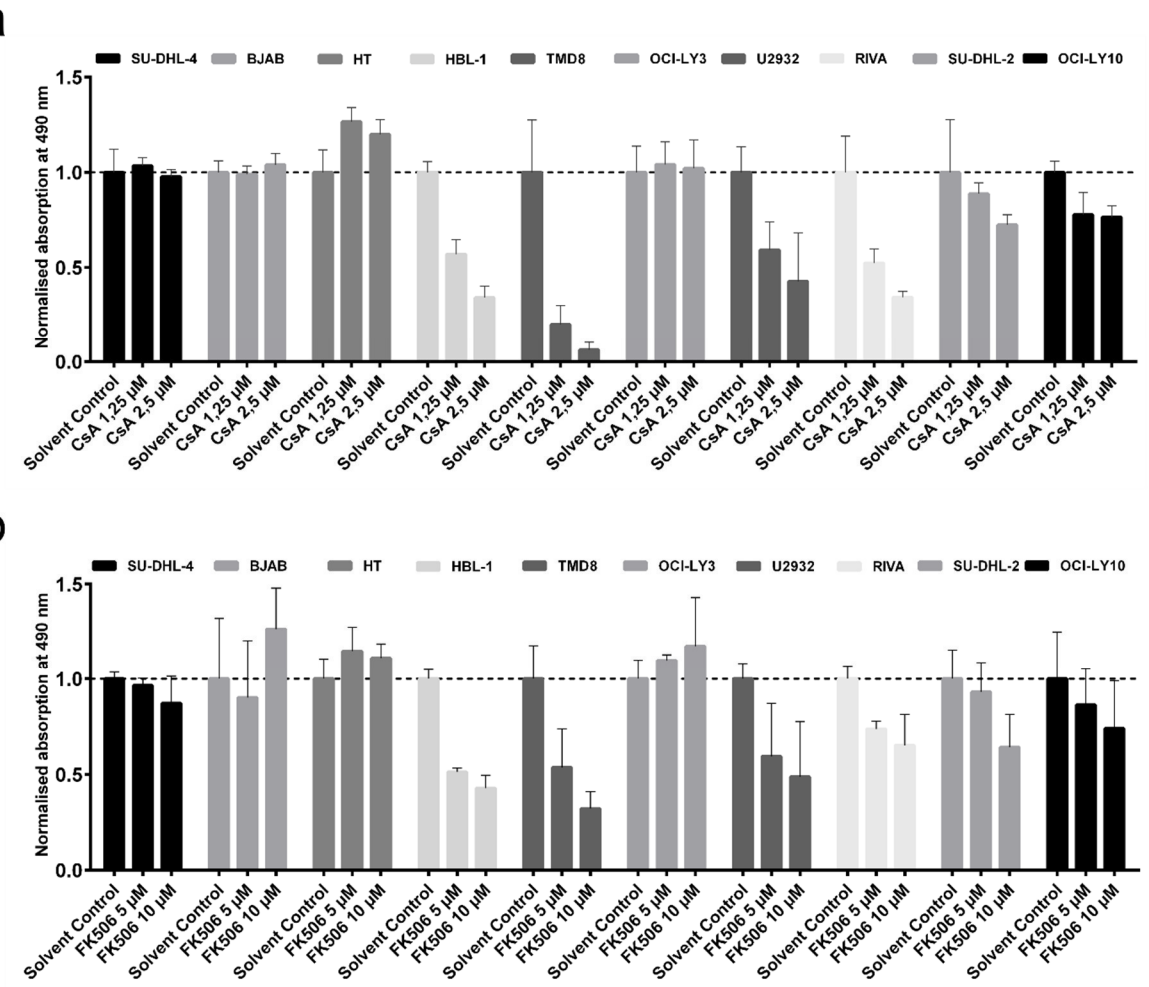

Figure 31. Indicated GCB and ABC DLBCL cell lines show different growth behaviours upon treatment with calcineurin inhibitors CsA and FK506. Cells were treated with either solvent as control **(a, b)** or two different concentrations of **(a)** CsA (2, 5 µM or 5 µM) and **(b)** FK506 (5 µM or 10 µM), respectively. Inhibitors were applied on day 0 and 2 of the experiment. Cell proliferation was determined on day 6 of inhibitor treatment by MTS assay. Bars represent means from 3 independent replicates ± standard deviation.

In order to exclude unspecific toxic side effects mediated by CsA and FK506 at µM concentrations and to validate our findings concluded from the results depicted in Figure 31. we selected four ABC DLBCL cell lines to test at lower CsA and FK506 inhibitor concentrations (Figure 32.). To this end, we decided to comprise one or more ABC DLBCL cell line representative of each distinct inhibitor susceptibility group. The most sensitive HBL-1 and TMD8, the intermediate

sensitive SU-DHL-2 and the resistant OCI-LY3 ABC DLBCL cell line. Treating the selected ABC DLBCL with considerably lower concentrations of CsA (250 nM and 500 nM) or FK506 (500 nM and 1000 nM) reproduced the results gained from higher concentrations (Figure. 31) albeit less pronounced (Figure 32.). Cell growth was again measured by MTS assay on day 6 of treatment. Cells were retreated with inhibitors on day 2, as well. HBL-1 and TMD8 were again the cell lines the most susceptible to inhibitor treatment whereas OCI-LY3 was also here not affected by inhibitor treatment. SU-DHL-2 however, that previously showed intermediate sensitivity to calcineurin inhibition seemed to be unimpressed by lower CsA and FK506 concentrations (Figure 32.). The less pronounced impairing effects on growth of HBL-1 and TMD8 cells and the unsuceptibility of SU-DHL-2 to CsA and FK treatment at lower concentrations can be attributed most likely to the short time span of treatment.

a

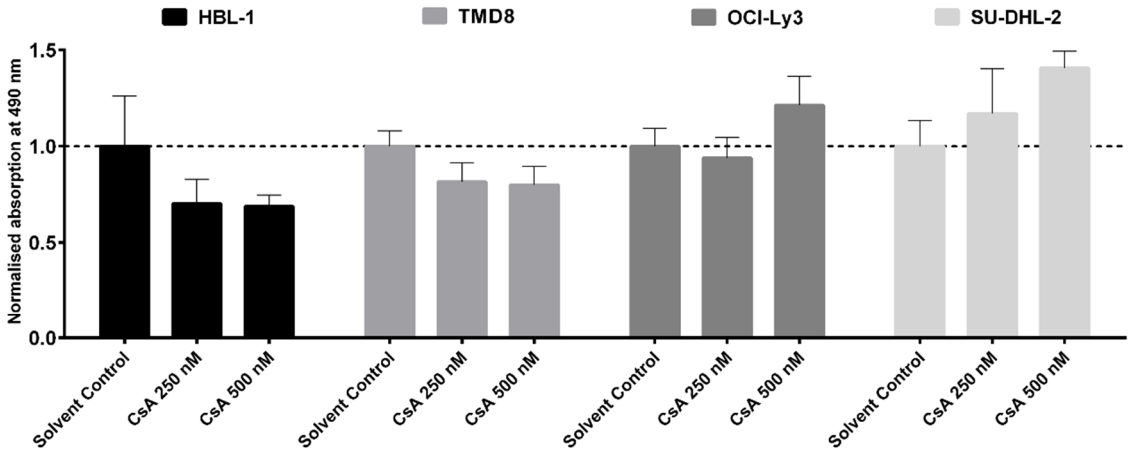

b

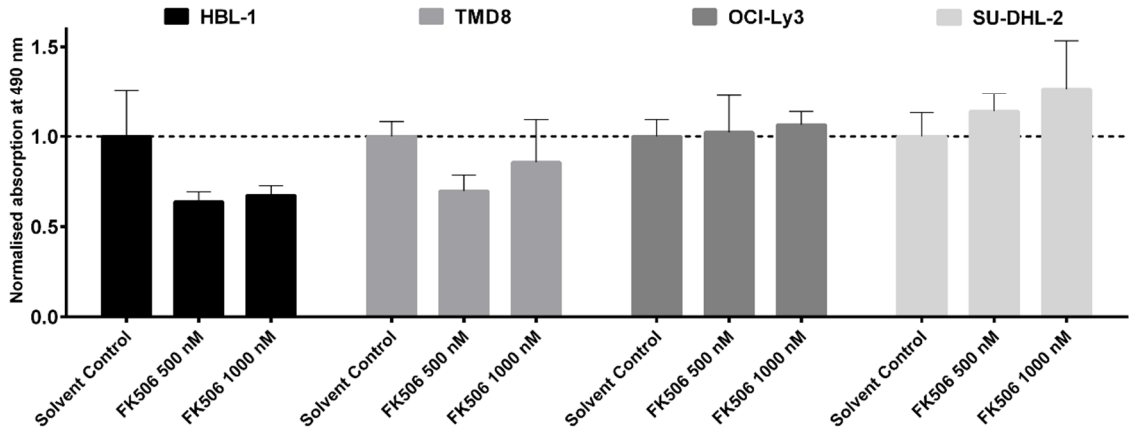

Figure 32. GCB and ABC DLBCL cell lines show different growth behaviours upon treatment with calcineurin inhibitors CsA and FK506 also at lower compound concentrations. Indicated cell lines were treated with either solvent as control **(a, b)** or two different concentrations of **(a)** CsA (250 nM or 500 nM) and **(b)** FK506 (500 nM or 1000 nM), respectively. Inhibitors were applied on day 0 and 2 of the experiment. Cell proliferation was determined on day 6 of inhibitor treatment by MTS assay. Bars represent means from 3 independent replicates ± standard deviation.

In summary, these results suggest calcineurin inhibition to be exclusively toxic to some ABC DLBCL cell lines at both, high and low inhibitor concentrations indicating calcineurin activity to be essential for the growth of certain ABC DLBCL cell lines. Hereby, we can differentiate between highly sensitive, intermediate sensitive and resistant ABC DLBCL cell lines in regard to calcineurin inhibition by CsA and FK506. In contrast, all tested cell lines of the GCB subtype of DLBCL were not prone to calcineurin inhibition, at all. Moreover, due to the usage of two independent calcineurin inhibitors these impairing effects on cell growth are highly likely to be specific. Besides this, the observed effects on cell growth could be independent from NFAT signaling that is blocked upon calcineurin inhibition, since NFAT is active in all investigated ABC DLBCLs. Taken together, taking into consideration all previous mentioned points the different outcomes of the ABC DLBCL growth upon calcineurin inhibition could be the result of a yet unknown calcineurin substrate that positively regulates pivotal chronic active BCR-driven classical NF-κB signaling of ABC DLBCL in its dephosphorylated state but loses this ability when calcineurin dependent dephosphorylation is blocked. Furthermore, the given circumstance of CsA/FK506 less or insensitive ABC DLBCL cell lines could be dependent from the distinct mutation patterns harboured by the ABC DLBCL cell lines, since the highly sensitive cell lines HBL-1 and TMD8 share mutations in the same protein CD79B quite upstream in BCR signaling (Davis et al., 2010). The toxic effect of calcineurin inhibition could be overridden by different common NF-κB positive regulating mutations that can be found in CsA and FK506 intermediate and insensitive ABC DLBCL downstream of this putative substrate. Such mutations in intermediate or non-sensitive cell lines include mutant CARMA1 and mutant/biallelic truncating mutation of A20 in SU-DHL-2 (Naylor et al., 2011, Ma et al., 2015); TAK1 mutation and A20 hemizygous deletion in U2932 (Fontan et al., 2012; Ma et al., 2015); mutant $CARMA^{L244P}$ and hemizygous A20 deletion in OCI-LY3 (Lenz et al., 2008; Naylor et al., 2011; Ma et al., 2015), possibly explaining the growth behaviour of those cell

lines. Upon obtaining the results shown in Figure 31. and 32. the question emerged what the general reason could be that leads to impaired growth of ABC DLBCL cell lines as result of CsA and FK506 treatment. As already described earlier, ABC DLBCL are addicted to classical NF-κB signaling. But moreover, this chronically active NF-κB signaling also induces the induction and subsequent secretion of the B-cell pro-proliferative cytokines IL-6 and IL-10 (Kishimoto, 2005; Moore et al., 2001). An autocrine/paracrine feedback loop of those cytokines then activates IL-6 and IL-10 receptor associated JAK kinases which subsequently phosphorylate STAT3. This phosphorylated STAT3 (p-STAT3) transcription factor accumulates in the nucleus and initiates target gene transcription, such as STAT3 itself, establishing a positive auto regulatory loop (Narimatsu et al., 2001). Therefore, ABC DLBCL that exhibit high NF-κB activity show also high IL-6 and IL-10 secretion in turn leading to elevated STAT3 and p-STAT3 levels (Lam et al., 2008). In addition to that, IL-6 and IL-10 secreting ABC DLBCL cell lines were killed by the inhibition of STAT3 signaling alone and combining JAK-1 and NF-κB inhibition actually led to synergistic toxicity, indicating ABC DLBCL to be addicted not only to NF-κB signaling alone but also to the mentioned autocrine/paracrine cytokine signalling loop consisting of IL-6 and IL-10 (Lam et al., 2008). For these reasons, we were interested to see whether p-STAT3 levels and therefore also the associated pivotal IL-6 and IL-10 secretion of ABC DLBCL would be affected in ABC DLBCL exposed to calcineurin inhibitors. To test this, we treated a GCB DLBCL cell line (BJAB) and four ABC DLBCL (HBL-1, TMD8, SU-DHL-2, RIVA) cell lines that were sensitive to calcineurin inhibition as shown in Figure 31.a,b; 32.a,b with 2,5 µM of CsA or FK506 for one or two days, respectively. Calcineurin inhibitors worked properly in all cell lines, indicated by the shift of NFATc1 bands (Figure 33.a-e). Indeed, when we treated the cells with either CsA or FK506 we observed clearly decreased p-STAT3 levels in all ABC DLBCL cell lines (Figure 33.b-e) just after one day of treatment, whereas STAT3 levels remained the same. Noteworthy, the CsA and FK506 highly sensitive cell lines HBL-1 and TMD8 and the intermediate sensitive cell line RIVA showed the most pronounced reduction in p-STAT3 when treated with the inhibitors. SU-DHL-2 cells that were shown to be intermediate sensitive for higher concentrations (Figure 31.a, b) and insensitive for lower concentrations of calcineurin inhibitors accordingly showed only a small decrease of p-STAT3 levels for CsA treatment and little, if any reduced p-STAT3 levels when treated with FK506 even after two days of treatment.

In comparison, the calcineurin inhibitor insensitive GCB DLBCL cell line BJAB was if, at most, only marginally affected in p-STAT3 levels. Also STAT3 levels remained the same upon treatment (Figure 33.a). We also included two well-known NF-κB targets, the antiapoptotic BCL-XL (Chen et al, 2000; Lee et al, 1999) and the NF-κB negative regulator A20 (Krikos et al, 1992) in our experiment to check whether NF-κB signaling in DLBCL would be affected. This was seemingly not the case for all DLBCL cell lines tested (Figure 33.a-e).

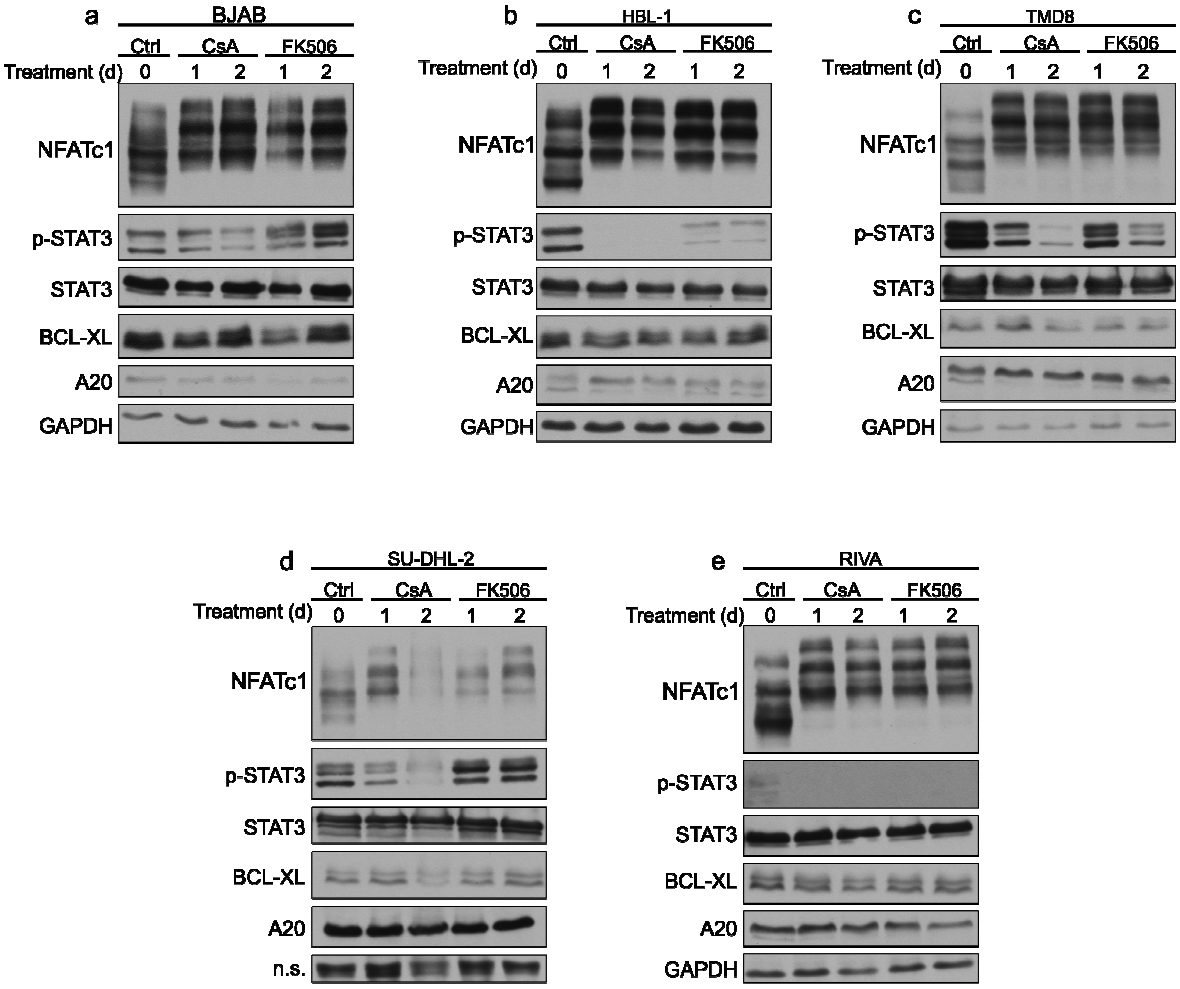

Figure 33. Assessing the impact of calcineurin inhibition of CsA and FK506 treatment on signaling in GCB and ABC DLBCL cell lines (a- e). Protein expression levels in GCB (BJAB) and ABC DLBCL (HBL-1, TMD8, SU-DHL-2, RIVA) cell lines was determined by western blot using the indicated antibodies. Cells were either treated with solvent control or calcineurin inhibitors CsA (2,5 µM) / FK506 (5 µM) for one or two days. Blotting against NFATc1 served as functionality control for CsA and FK506. In figure panels **(a, b, c, e)** blotting for tubulin served as a loading control, whereas in (**d)** a non-specific band indicates equal loading.

In turn to verify that the sensitivity of ABC DLBCL towards calcineurin inhibitors (Figure 31.a, b; 32.a, b) correlates with the extend of p-STAT3 level reduction upon CsA and FK506 application, we treated the highly sensitive ABC DLBCL cell line

HBL-1 (Figure 34.a, c) and the fully insensitive ABC DLBCL cell line OCI-LY3 with dilution series of CsA for 2 days and compared consequent p-STAT3 levels to untreated cells. We did this in a dilution series to learn whether the reductive effect on p-STAT3 levels is CsA dose dependent. As presumed, with increasing concentrations of CsA we observed reciprocally decreasing levels of p-STAT3 (Figure 34.a, b), indicating a CsA dose dependent effect. On the contrary, OCI-LY3 cells treated with a CsA dilution series did not show any changes in their p-STAT3 levels at all concentrations applied (Figure 34.b). Again, STAT3 expression remained at the same level in HBL-1 and was not altered in OCI-LY3 cells under all conditions, as well (Figure 34.a, b).

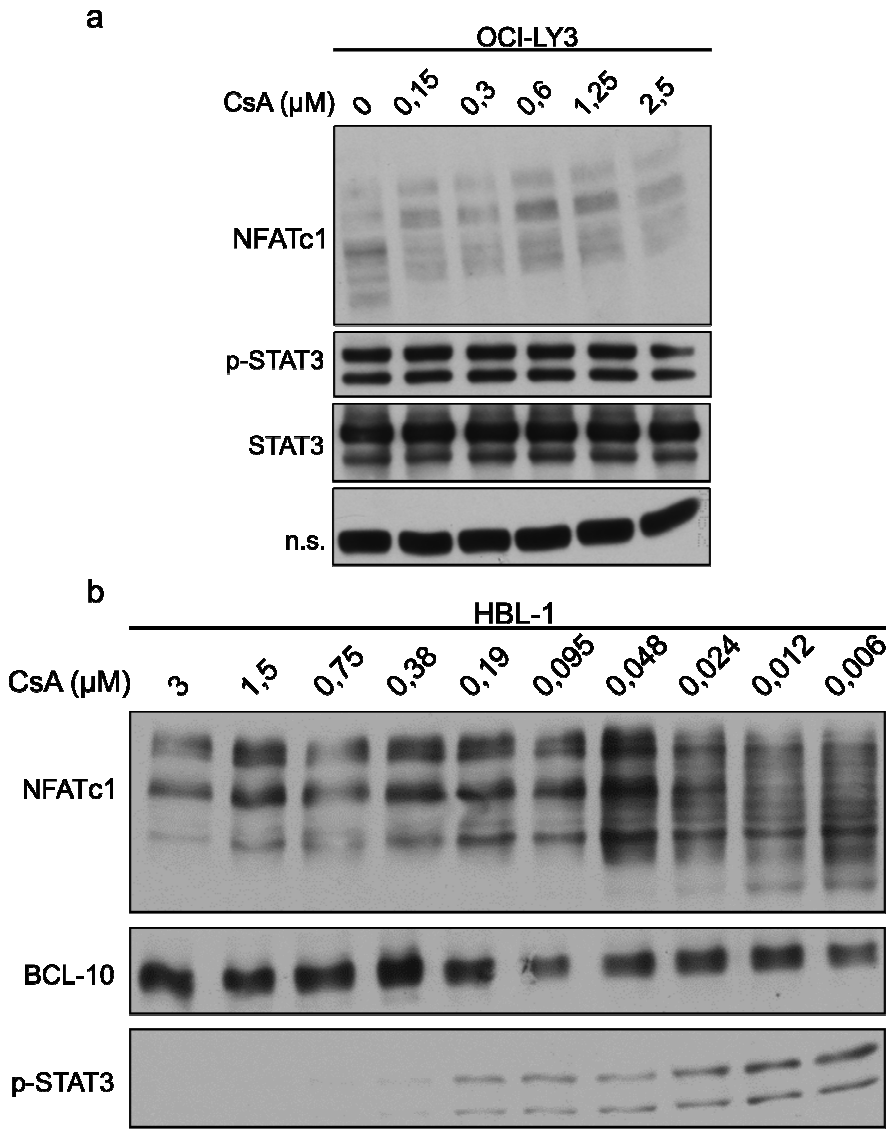

Figure 34. Verifying the decline of p-STAT3 levels in a dose-dependent manner as a result of a CsA dilution series treatment by western blotting. (a, b). Lysates were analysed by western blotting with anti NFATc1, anti-STAT3, anti p-STAT3, and anti-BCL-10 antibodies.

Cells were treated with solvent control or CsA applied at the indicated concentrations. In **(a, b)** a non-specific band served as a loading control. Equal loading in (**b)** is indicated by BCL-10.

In summary it can be said, therefore, that the different sensitivities of GCB and ABC DLBCL in respect of their growth towards the treatment with increasing concentrations of calcineurin inhibitors CsA and FK506 correlates with their observed reciprocal decrease in STAT3 phosphorylation as a consequence of CsA and FK506 application. Mentionable, this effect was dose-dependent at least for the investigated CsA treatment. Unphosphorylated STAT3 levels however, stayed the same at all times. Since we found lowering p-STAT3 levels upon CsA and FK506 treatment in only certain ABC DLBCL cell lines e.g. HBL-1 and TMD8 we supposed the secreted amounts of IL-6 and IL-10 (that bind their corresponding receptors distal from JAK1 mediated STAT3 phosphorylation) of solely those cell lines also to be reduced. On the other hand, we did not expect the secretion of IL-6 and IL-10 of OCI-LY3 cells to be reduced as result of CsA and FK506 treatment as p-STAT3 levels were not declined. Hence, we treated calcineurin inhibitor treatment highly sensitive ABC DLBCL cell lines HBL-1 and TMD8 and the unresponsive OCI-LY3 cell line with either a solvent as control or CsA and FK506 in a dilution series for two days and subsequently assessed relative IL-6 and IL-10 secretion levels in the supernatants.

In fact, we were able to reveal that secretion of both Interleukins, IL-6 and IL-10 by HBL-1 and TMD8 cells were clearly decreased when treating them for two days with calcineurin inhibitors (Figure 35.a, b). This was even the case for very low levels of 40 nM for CsA and 160 nM for FK506, respectively. Those cell line were also shown to have markedly lowered p-STAT3 levels when they were exposed to calcineurin inhibitors (Figure 33.b, c; 34.a). In contrast, the IL-6 and IL-10 secretion of OCI-LY3 cells was completely unaffected by calcineurin inhibitors (Figure 35.a, b) what is in agree with stable p-STAT3 levels upon CsA/FK506 treatment. Furthermore, already low CsA or FK506 concentrations had a strong impairing effect on IL-6 and IL-10 secretion. Moreover, higher compound doses did not improve the interleukin secretion inhibitory effect (Figure 35.a, b). Worth mentioning as well is the fact that IL-10 secretion is slightly more hampered compared to IL-6 secretion by usage of both calcineurin inhibitors (Figure 35.a, b).

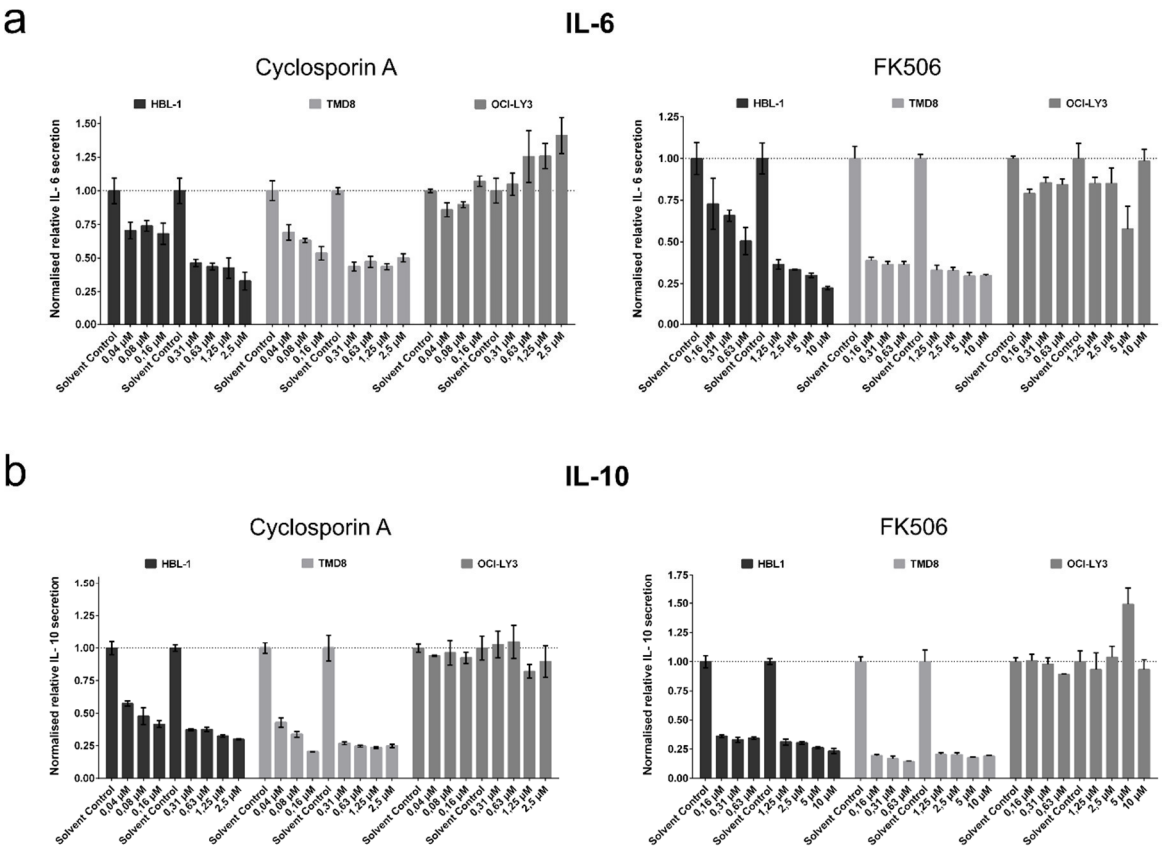

Figure 35. Determination of IL-6 and IL-10 levels in the supernatants of ABC DLBCL cell lines HBL-1, TMD8 and OCI-LY3 upon two days treatment of CsA and FK506 in dilution series. Cells were either treated with DMSO as solvent control, or the calcineurin inhibitors CsA and FK506 at the indicated concentrations. After two days of exposure, supernatants of cells were collected and subsequently measured for their levels of IL-6 and IL-10 by ELISA. Bars represent means from 3 independent replicates ± standard deviation.

To substantiate the finding of decreasing IL-6 and IL-10 secretion of ABC DLBCL cell lines that exhibit diminished p-STAT3 levels upon calcineurin inhibitor treatment the next experiment was performed including the CsA/FK506 resistant cell line SU-DHL-2 (at low concentrations; Figure 32.a,b). Cells were again subjected to CsA or FK506 treatment for two days before assessing IL-6 and IL-10 levels in their supernatants. As it was expected, IL-6 and IL-10 secretion upon inhibitor treatment was tremendously hampered in in samples derived from HBL-1 and TMD8 cells whereas the supernatants collected from OCI-LY3 and SU-DHL-2 showed unchanged (in case of CsA) or inconsiderably less (in case of FK506) IL-6 and IL-10 secretion (Figure 36.a, b). This finding correlates well with both, the remarkable decrease of p-STAT3 levels in HBL-1 and TMD8, the unaltered levels of p-STAT3 in OCI-LY3 and finally the only slightly decreased p-STAT3 levels in SU-DHL-2 when applying CsA or FK506 (Figure 33.b, c, d; Figure 34.a-c).

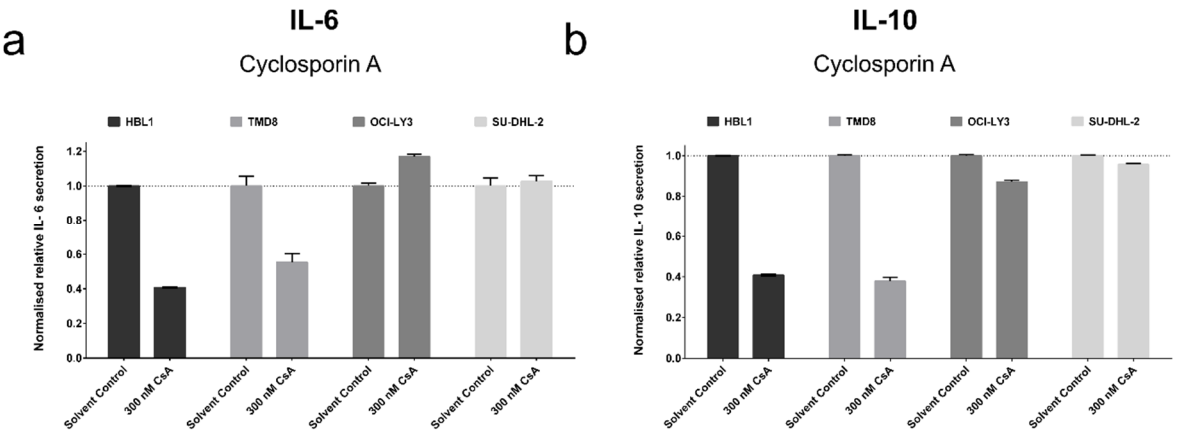

Figure 36. IL-6 and IL-10 secretion assessment of calcineurin inhibitor sensitive and insensitive ABC DLBCL cell lines treated with 300 nM CsA. (a, b). Cells were treated with DMSO as solvent control or a sole concentration of CsA (300 nM) for two days. Subsequently supernatants were taken to measure IL-6 and IL-10 levels by ELISA. Bars represent means from 3 independent replicates ± standard deviation.

Taken together, the demonstrated results suggest that the different growth outcomes of ABC DLBCL upon treatment with calcineurin inhibitors correlate with distinct secretion levels of the pro-proliferative interleukins IL-6 and IL-10, which act in a survival promoting autocrine/paracrine feedback loop, the cells are addicted to. These varying interleukin secretion properties are reflected by diverging amounts of p-STAT3. In summary, this means the higher the sensitivity towards calcineurin inhibitors of DLBCL with respect to their growth, the lower are secreted IL-6 / IL-10 levels as well as p-STAT3 levels. As already stated earlier, NFAT activity is shared by all ABC DLBCL tested and moreover all of them express high levels of IκBNS, as well. In addition to that, when we considered differences between the ABC DLBCL cell lines we concluded that they mainly differ, as previously mentioned, in exhibiting distinct mutant patterns. In this regard, we noticed that cell lines that were impaired the most by calcineurin inhibitor treatment in their ability to secrete IL-6 and IL-10, thus also affected severely in respect to proliferation, were mutated in the BCR associated signaling protein CD79. Taking this into account, we addressed the question what the molecular mechanism could be behind this selective toxicity. A recently published paper by Dutta and colleagues gave us an indication for a possible explanation. In their study they were investigating primary human $CD4^+$ T-cells and Jurkat T-cells. From their results they draw the conclusion that calcineurin is recruited to the TCR signaling complex, where it positively regulates the tyrosine kinase LCK by removing an inhibitory phosphorylation which is normally induced by TCR activation. Moreover, when they inhibited calcineurin activity by

different approaches such as the pharmacological inhibition by CsA or FK506 or siRNA mediated knock down, they observed increased TCR-mediated LCK inhibitory phosphorylation, impaired phosphorylation of ZAP-70 and various alterations of phosphorylation events in related TCR-proximal pathways. The T-cell and B-cell antigen receptor pathways share a multitude of common elements and other similarities such as the association of the antigen receptor to invariant ITAM bearing accessory proteins, the recruitment of Src-family kinases to the receptor complex, the involvement of proteins sharing strong sequence homologies such as BLNK and SLP-76 and the eventual activation of proximal signaling pathways converging in the activation of NF-κB, NFAT and AP-1 TF-families. These homologies are the reason why we thought that calcineurin could be not only implicated in TCR-signaling but also in BCR-signaling events by dephosphorylation of a yet unknown substrate as already earlier mentioned. This in turn would lead to positive regulatory effect on downstream BCR signaling. When we transferred this thought in the context of ABC DLBCL signaling it was justified to hypothesise that only CD79 mutated ABC DLBCL cells were vulnerable to CsA/FK506 mediated calcineurin inhibition because the more proximally mutated cell lines could override the loss of the positive regulation of BCR signaling upon calcineurin inhibition. To unveil this putative new calcineurin substrate whose dephosphorylation indirectly or directly leads to an enhanced BCR downstream signaling we performed a SILAC with subsequent phosphoproteom analysis by mass spectrometry (MS). For this, we treated HBL-1 cells for 5 h with either CsA or FK506 after being subjected to medium containing amino acids with differentially heavy isotopes. The frequency of phosphorylated peptides in calcineurin inhibitor treated samples was then compared to the abundance of the corresponding phosphorylation in peptides from the solvent treated control. SILAC revealed, that indeed proteins that are implicated in BCR-proximal signaling are present in a more phosphorylated state like CD79A and CD79B or in a less phosphorylated state as the adaptor protein BLNK (Table 1.). This result indicates that calcineurin could be indeed recruited to BCR downstream signaling where it dephosphorylates (a) certain substrate(s) leading directly or indirectly to a promotion of further BCR signaling events. As a specificity control for this SILAC experiment serves the finding of BCL-10 that is accordingly to our result roughly two times more phosphorylated at serine 138 (S138) when calcineurin is inhibited by either CsA or FK506. BCL-10 S138 is known to be an IKK2

phosphorylation target site and was identified by Zeng et al. (2007) as a T-cell receptor activation-induced phosphorylation site that is implicated in the induction of BCL-10 ubiquitination and subsequent degradation. Zeng et al. demonstrate that the prevention of BCL-10 phosphorylation at S138 inhibits T-cell activation induced BCL-10 ubiquitination and degradation and also causes sustained NF-κB signaling and enhanced IL-2 production. Palkowitsch et al. (2011) revealed calcineurin to constitutively interact with the CBM complex in T-cells and moreover CsA/FK506 inhibition and siRNA mediated knock-down of calcineurin led to increased levels of phosphorylated BCL-10, reduced CBM complex formation and consequently decreased NF-κB activity. Furthermore, based on their results, Palkowitsch et al. suggest BCL-10 S138 to be a calcineurin dephosphorylation site. In accordance with the Zeng study, Palkowitsch et al. suggest that the calcineurin mediated BCL-10 dephosphorylation at S138 is thus linked to a positive regulation of CBM complex assembly and therefore to antigen receptor induced NF-κB signaling, as well. Moreover, our results also revealed BCLAF1 as a new direct putative calcineurin substrate or at least indirectly regulated by calcineurin. According to the SILAC analysis BCLAF1 frequently appeared to be more phosphorylated upon calcineurin inhibition at several known and unknown putative phosphorylation sites (Table 1). So far, there is nothing known about the already noted phosphorylation sites, neither their function nor whether they have a positive or negative effect on BCLAF1 function. BCLAF1 fulfils diverse functions. It is known as inducer of apoptosis, autophagic cell death in myeloma cells and as repressor of transcription (Kasof et al., 1999; Liu et al., 2007; Lamy et al., 2013) and was moreover it was found as a target of NF-kB (Kong et al., 2011; Shao et al., 2016). Taken together, this result suggests an actual role of calcineurin in modifying BCR downstream signaling as we found BCR signaling elements under the top hits of peptides with altered phosphorylation rates by phosphoproteom analysis. Putative substrates thereby could be directly due to more phosphorylation CD79 or indirectly due to less phosphorylation BLNK. Since the inhibition of calcineurin impairs the growth of certain ABC DLBCL we have to assume a positively regulating role of calcineurin in BCR signaling. We found CD79B phosphorylation altered at serine 221 in close proximity to the CD79B amino terminal ITAM (aa185 - aa213) when calcineurin was inhibited. This suggests that the common heterozygous HBL-1 and TMD8 amino acid substitutions Y196F and Y196H, located in the middle of the CD79B ITAM,

could somehow enhance the negative effect of calcineurin inhibition on BCR downstream signaling compared to wild-type CD79B Y196. Moreover, MS based phosphoproteom analysis of isotope labelled samples also revealed CD79A to be more phosphorylated at multiple sites upon calcineurin inhibition. Those sites are situated closely to the CD79A ITAM except for S197 what lies in the middle of the CD79A ITAM. As OCI-LY10 exhibits a heterozygous deletion of aa191- aa208 affecting parts of the CD79A ITAM also this mutation could slightly strengthen the adverse effect on BCR downstream signaling upon inhibition of calcineurin causing their intermediate sensitivity towards calcineurin inhibition. This link between CD79A/B mutations in ABC DLBCL that somehow alter the outcome of calcineurin inhibition on BCR downstream signaling and calcineurin dephosphorylation sites in CD79A/B could also explain why the interleukin secretion and growth of wild-type cell lines such as GCB DLBCL or some ABC DLBCL are only minimally or not impaired by calcineurin inhibition.

In order to have an overview of the general changes in the patterns of phosphorylated tyrosines upon calcineurin inhibition we next stimulated the cell line Ramos for different time periods with anti-IgM antibodies with or without pre-incubation of CsA and had then a closer look at phosphorylated tyrosine residues by western blotting (Figure 37.). As GCB DLBCL are known to be stimulated by anti-IgM only very difficult we used the Burkitt lymphoma cell line Ramos for this experiment. Moreover, Burkitt lymphoma usually do not harbour mutations in BCR proximal CD79 signaling, just as GCB DLBCL. ITAMs are common for associated signaling chains of immunoreceptors such as CD79A / CD79B of the BCR and are phosphorylated at two invariant tyrosines upon activation of the corresponding immunoreceptor and critical for the intracellular signal generation by e.g. upon antigen engagement (Niemann and Wiestner, 2013). As tyrosine phosphorylation (p-tyrosine) is a common feature in BCR mediated signaling in B-cells, it is possible to recognise changes in the phosphorylation of ITAM tyrosines by using anti-p-tyrosine antibodies in western blotting.

Protein	aa	Position	Peptide with STY phosphorylation probabilities	Ratio M/L normalised by protein *CsA treatment*	Ratio H/L normal-ised by protein *FK506 treatment*
CD79A	S	197	LGLDAGDEY(0.001) EDENLY(0.079)EGLNLDD C**S**(0.609)MY(0.188) EDIS(0.123)R	1,85	3,78
	Y	210	GLQGT(0.002)**Y**(0.998)QV GS(1)LNIGDVQLEKP	1,74	2,09
	S	215	GLQGT(0.002)Y(0.998)QV G**S**(1)LNIGDVQLEKP	1,30	1,27
	T	209	GLQG**T**(0.748)Y(0.016)QV GS(0.236)LNIGDVQLEKP	1,25	1,05
CD79B	S	221	W**S**(1)VGEHPGQE	1,94	1,58
BLNK	S	129	SSQRH**S**(1)PPFSK	0,89	0,85
	S	213	**S**(1)PPPAAPSPLPR	0,74	0,76
	S	409	NHQH**S**(1)PLVLIDSQ NNTK	0,66	0,67
	S	270	QEAVQ**S**(1)PVFPPAQK	0,43	0,46
BCL-10	S	138	SN**S**(1)DESNFSEK	1,74	2,09
BCLAF1	S	196	DTFEHDPSE**S**(1)IDEFNK	2,21	2,72
	S	523	S(0.921)T(0.085)FREE **S**(0. 994)PLR	2,10	2,72
	S	395	QKFND**S**(1)EGDDTEE TEDYR	1,40	1,24
	S	387	AEGEWEDQEALDYFS(1) DKE**S**(1)GK	1,37	1,57
	S	383	AEGEWEDQEALDYF**S** (1)DK	1,33	1,23
	S	295	YS(0.965)PS(0.035)QN**S**(1)PIHHIPS(0.791)RRS(0.20 9)PAK	1,29	1,38
	S	529	STFREE**S**(1)PLRIK	1,23	1,04

Table 1. Peptides and their corresponding proteins that prevail in a more or less phosphorylated state upon CsA or FK506 treatment. "aa" for amino acid designates the abbreviation for a certain amino acid in its one letter code. **"Position"** means the amino acid's spot in the protein. "**Peptide with STY phosphorylation probabilities"** depicts the found peptide with the assigned probabilities of phosphorylation of the amino acids serine **(S)** threonine **(T)** or tyrosine **(Y)**. **"Ratio M/L" or "H/L" normalised by protein** represents the frequency of a certain phosphorylated peptide with medium heavy **(M)** or heavy **(H)** labelled isotopes in the CsA or FK506 treated sample divided by the frequency of this phosphorylated peptide labelled with normal, light isotopes **(L)** under untreated control conditions.

From the results obtained from this approach, we concluded no major changes in tyrosine phosphorylation patterns upon BCR signaling activation of Ramos cells in the presence of CsA compared to control conditions (Figure 37.). Anti-IgM stimulation itself was successful because unstimulated cells showed considerably fewer and less intensive p-tyrosine bands (Figure 37.). From this result it can be

claimed that upon BCR-mediated B-cell stimulation under calcineurin repressive conditions, tyrosine phosphorylation patterns are not appreciably changed, at least in B-cells deriving from Burkitt's Lymphoma. In summary, calcineurin seems to convey its positive influence on BCR signaling not indirectly by altering the phosphorylation of tyrosines as there was no obvious change in BCR upstream signaling p-tyrosine patterns. This conclusion is at least true for the Burkitt's Lymphoma cell line Ramos and cannot be handled as general and can be therefore different for DLBCL which show other mutation patterns.

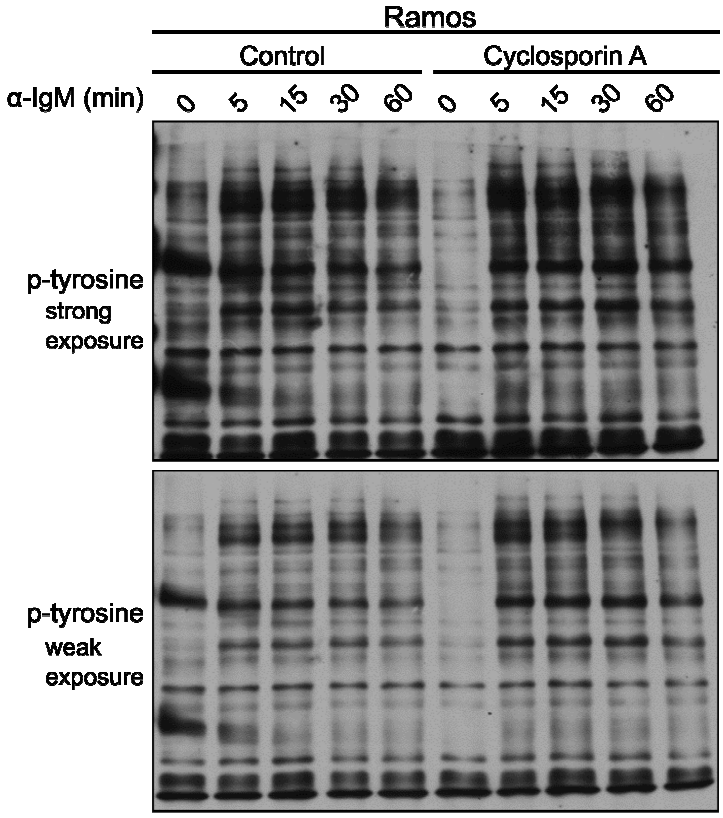

Figure 37. Detection of p-tyrosine residues by western blot in lysates from the Burkitt lymphoma cell line Ramos upon anti-IgM mediated BCR stimulation in the presence or absence of CsA. Ramos cells were either pre-incubated for 20 min with solvent as control or 3 µM CsA prior to 15 µg/ml anti-IgM mediated BCR stimulation for the indicated periods of time. Weak and strong exposure of p-tyrosine blots are shown to better assess the effects of calcineurin inhibition on tyrosine phosphorylation due to the difference in band thickness.

Following this, to further elucidate the potential influence of calcineurin on BCR proximal signaling we investigated the phosphorylation of additional proteins implicated in BCR signaling. The Ashwell lab recently published in the previously mentioned study by Dutta et al., which they found the activating Y493 within the activation loop of the tyrosine kinase domain of Zap-70 to be less phosphorylated

subsequently to the loss of calcineurin activity that was achieved by different approaches (Dutta et al., 2017). Since ZAP-70 is specifically expressed in T-cells and plays a role in TCR signaling we were thus interested in the BCR signal transduction analogous and structurally similar protein SYK (Chu et al.,1998). Alike ZAP-70, SYK is a protein tyrosine kinase and activated by the phosphorylation of Y525 and Y526 in the activation loop of its kinase domain. These site are therefore crucial for the proper function of SYK (Zhang et al., 2000). For this reason, Y493 of ZAP-70 and SYK Y525 and Y526 can be regarded equally in their respective function in the context of TCR and BCR signaling. Furthermore, Dutta et al. also showed that the phosphorylation of the ZAP-70 ensuing downstream signaling molecule SLP-76 at Y145, which facilitates the binding to ITK (Bunnell et al., 2000) was diminished by the CsA and FK506 mediated inhibition of calcineurin in T-cells. Due to that finding, we were also here interested in the B-cell homologous adaptor protein which is called BLNK or SLP-65. BLNK follows directly to SYK in the signal transduction chain. It is phosphorylated by SYK among others at Y96 which serves similar to p-Y145 of SLP-76 as docking site for signaling molecules as for instance PLCγ (Kurosaki and Tsukada, 2000; Ishiai et al., 1999). Consequently, also the phosphorylation sites Y145 from SLP-76 and Y96 from BLNK at are homologous in their function as ZAP-70 Y493 and SYK Y525 / Y526. For these reasons and because there were no commercially available antibodies against the phosphorylation sites we unveiled by SILAC for BLNK and CD79A/B as well, we examined the phosphorylation sites Y526 from SYK and Y96 from BLNK that are both important for BCR downstream signaling in a bit more detail (Figure 38.). For this purpose, we treated calcineurin sensitive ABC DLBCL cell lines TMD8 and HBL-1 with CsA or FK506 for 2, 5 and 5 and were keen to see if p-SYK^{Y526} or p-BLNK^{Y96} levels would change when calcineurin is inhibited. As control for CsA and FK506 function, we blotted once more against NFATc1. Both inhibitors worked regularly as indicated by NFATc1 shift. We did not recognise any changes in SYK and BLNK phosphorylation in neither CsA/FK605 insensitive nor sensitive cell lines (Figure 38.). Notably there were no detectable p-BLNK^{Y96} levels emanating from TMD8. In summary, the alterations of TCR signaling phosphorylation events upon calcineurin inhibition found by Dutta et al seem to be not true for the corresponding molecules and phosphorylation sites of BCR signal transduction, we investigated. This in turn suggests, a completely different mechanism or other phosphorylation

events in the same or other proteins to be the reason behind the calcineurin inhibition caused effects on B-cell signaling and their final impact on interleukin secretion and proliferation of certain ABC DLBCL. Hence, it is likely that calcineurin acts differently in BCR signaling compared to the mechanisms that were shown for the phosphatase in primary $CD4^+$ and Jurkat TCR downstream signaling by the Aswhell lab. As these mechanisms seem to differ, it is therefore not unlikely that the calcineurin mediated positive effect on BCR signaling is caused by the direct and indirect dephosphorylation of the newly by SILAC identified putative calcineurin affected amino acids in CD79A and/or CD79B or the indirect phosphorylation of BLNK at one or multiple sites (Table 1.), which are consequently less phosphorylated when calcineurin activity is blocked.

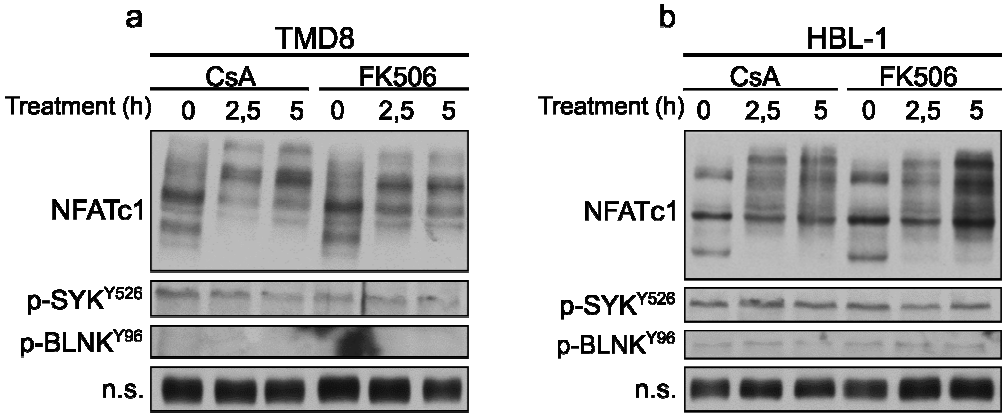

Figure 38. Revealing the effects of calcineurin inhibition on BCR downstream phosphorylation events in CsA and FK506 sensitive cell lines. (a, b). As indicated lysates derived from TMD8, HBL-1 were analysed for protein levels of NFATc1, p-SYK^{Y526} and p-BLNK^{Y96} by western blotting. Cells were treated with either a solvent as control (0 h), or for 2, 5 and 5 h with CsA (2, 5 µM) / FK506 (5µM). A non-specific band approves the equal loading of samples.

3.4 Expression of IκBNS isoforms in B and T-cell lymphoma cell lines

Western blot based analysis of IκBNS expression levels in a panel of ABC DLBCL cell lines and the P/I mediated stimulation of the GCB DLBCL cell line BJAB and Jurkat T-cells revealed a constantly with the predicted 35 kDa IκBNS signal correlated emerging band with a size of approximately 70 kDa. Furthermore, this 70 kDa signal always appeared to be stronger compared to the IκBNS p35 one. In turn to investigate if the 70 kDa protein is indeed another IκBNS specific gene product, we tried different IκBNS specific knock down or knock out approaches (Figure 39.a-d). For this purpose, we lentivirally transduced the GCB DLBCL cell line BJAB with

either an empty vector or a construct expressing shRNA #1 and subsequently selected for shRNA expressing BJAB cells. Because BJAB do not express IκBNS under steady state conditions we induced IκBNS expression in both cell populations by P/I mediated stimulation for different time periods (Figure 39.a). To figure out whether the experimental outcome would be the same for T-cells, we conducted the former described experiment with Jurkat cells, as well (Figure 39.b). Additionally, we also tried siRNA mediated IκBNS knock down under steady state IκBNS expression in the ABC DLBCL cell line HBL-1 (Figure 39.c). Moreover, we designed a CRISPR/Cas9 guide RNA (gRNA) for specific genomic knock out of IκBNS. Since the GCB DLBCL cell line BJAB does not depend on IκBNS expression under steady state conditions, we lentivirally transduced BJAB cells with the CRISPR/Cas9 construct comprising the gRNA targeting the genomic NFκBID sequence. For validation of CRISPR/Cas9 caused IκBNS knock out BJAB cells were stimulated by P/I for several time periods to induce IκBNS gene expression (Figure 39.d). P/I treated BJAB samples that were CRISPR/Cas9 transduced were then compared to stimulated empty vector transduced BJAB samples. In case the unknown 70 kDa protein should be indeed another IκBNS as well, the 70 kDa signal should vanish concomitantly with the p35 IκBNS band in all mentioned IκBNS knock down and knock out attempts. All cells transduced with an empty vector as a control, P/I treatment induced both, the IκBNS p35 and p70 signal in the expected ratio, regardless of B- or T-cell origin (Figure 39.a-d). Indeed, the shRNA and siRNA mediated knock down of IκBNS (Figure 39.a, b, c) and the CRISPR/Cas9 conducted knock out (Figure 39.d) of IκBNS which all targeted originally the p35 protein also affected the appearance of the 70 kDa band in the same manner as for p35 (Figure 39.a-d). Furthermore, also this result was true for both, the shRNA knock down of IκBNS in B- and T-cells. The correlation between the p35 and the p70 band could be monitored very nicely in the siRNA mediated knock down approach on steady state levels of IκBNS in HBL-1. Here, the strength of both, the p35 and p70 signal simultaneously and gradually increased when the siRNA mediated knock down of IκBNS ceased over time (Figure 39.c). Blotting against the MALT1 substrate CYLD served as control for B- and T-cell stimulation. Taken together, these results suggest that in addition to the already known IκBNS p35, there actually exists another IκBNS protein that could constitute for instance a posttranslationally modified IκBNS, an IκBNS homodimer or a different IκBNS isoform with a size of approximately 70 kDa,

afterwards designated as IκBNS p70. As our self-made antibody recognised IκBNS p70 and the shRNA, we applied, also targeted this IκBNS p70, both IκBNS proteins must share at least those stretches of amino acid sequences that are recognised by the antibody and the shRNA sequence. Since the CRISPR/Cas9 knock out approach that was designed with the ambition to target IκBNS p35 also led to the disappearance of the IκBNS p70 signal in immunoblot further indicates that both, the p35 and p70 IκBNS protein are indeed NFκBID gene products and are supposed to originate from the same gene locus in B- and T-cells.

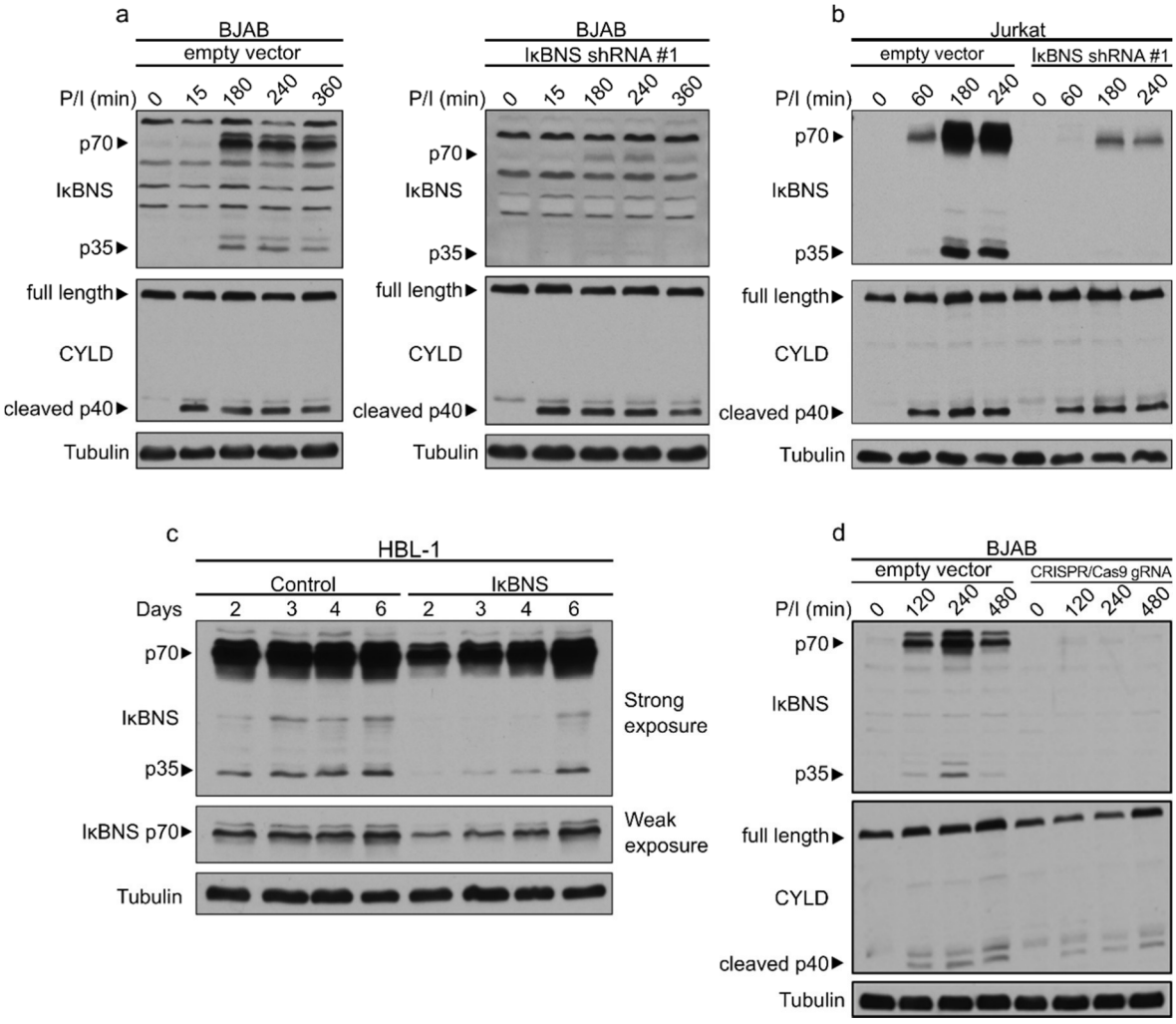

Figure 39. shRNA and siRNA mediated IκBNS knock down and CRISPR/Cas9 caused IκBNS knock out approach to elucidate whether the emerging p70 signal is a IκBNS specific band. (a) BJAB GCB DLBCL cells or **(b)** Jurkat T-cells were lentivirally transduced with either an empty vector as control or a construct expressing shRNA#1. Subsequent to puromycin selection, cells were stimulated with P/I for the indicated time periods. Induced IκBNS expression levels under empty vector and shRNA#1 expressing vector conditions were determined by Western Blotting. **(c)** HBL-1 cells were electroporated at 240 V with either a mixture of unspecific siRNA sequences as control or 300 pmol of siRNA targeting IκBNS. Lysates of HBL-1 cells electroporated with either control or siRNA targeting IκBNS were analysed by Western Blot for IκBNS p35 and p70 knock down for the indicated days following electroporation. Weak and strong exposure of

IκBNS p70 is shown due to different expression levels of IκBNS p35 and p70. **(d)** BJAB cells were lentivirally transduced with either a CRISPR/Cas9 encoding vector without gRNA (empty vector) as control or a construct bearing a gRNA sequence targeting the genomic sequence of NFκBID leading to a knock out. To verify the successful knock out of IκBNS p35 and p70 upon puromycin selection, levels of P/I induced IκBNS p35 and p70 in control cells and IκBNS knock out cells were compared by western blot analysis. In **(a, b and d)** CYLD cleavage validated cell activation by P/I. In all figure panels **(a-d)** Tubulin served as loading control.

Next, we wanted to shed some more light on the induction mechanisms of IκBNS p35 and p70. Since the stimulation of B-cells by their antigen receptor is more difficult to achieve compared to T-cells we decided to investigate this issue in a T-cell lymphoma model cell line. The acute T-cell leukemia derived cell line Jurkat showed the same stimulation behaviour in the up regulation and shRNA mediated knock down of IκBNS p35 and p70 as BJAB GCB DLBCL (Figure 39.a, b). For this reason, we chose the Jurkat T-cell line as model to investigate IκBNS up regulation. To study whether different fashions of T-cell activation would also result in diverse induction manners of whole IκBNS levels or in differences between the expression patterns of IκBNS p35 and p70 we stimulated Jurkat cells with either cross-linked stimulating monoclonal antibodies against the T-cell activation molecules CD3 and CD28 or P/I for different time periods. Subsequently IκBNS p35 and p70 expression was assessed by western blot. Anti-CD3/CD28 antibodies activate T-cells in a way that partly mimics physiological stimulation by antigen-presenting cells, whereas cell stimulation mediated by P/I acts more proximally in TCR signaling by inducing PKC activity and increasing Ca^{2+} mobilisation. Both stimuli led to the induction of high IκBNS p35 and p70 expression levels in the familiar ratios after 180 min of administration (Figure 40. a, b). Noteworthy, both the p35 and the p70 IκBNS signal appear as a lower strong and upper weak double band, indicating the existence of further modified IκBNS proteins. The only small distinction between the different kinds of T-cell stimulation regarding IκBNS induction was the non-long lasting T-cell stimulation intensity and as a consequence of this the earlier decline of IκBNS p35 and p70 levels after 360 min when cells were activated by anti-CD3/CD28 antibodies compared to P/I stimulated T-cells. This effect is caused most likely due to the fact that P/I seemed to stronger stimulate the cells in general and over a longer time frame in this experiment indicated by the higher portions of cleaved CYLD p40 of P/I stimulated cells compared to CYLD p40 levels in anti-CD3/CD28 stimulated cells. Furthermore, from this outcome we can draw the conclusion that there are neither noteworthy differences between whole IκBNS levels nor

observable changes in the ratios of p35 and p70 expression levels caused by the two fashions of T-cell stimulation. In summary, this result suggests that both IκBNS gene products, the p35 and p70 protein are also induced when T-cell receptors engage their antigens reflected by the physiological TCR activation by anti-CD3/CD28 antibodies. Taken together, we can state that T-cell stimulation is a potent functional inducer of IκBNS p35 and p70 expression.

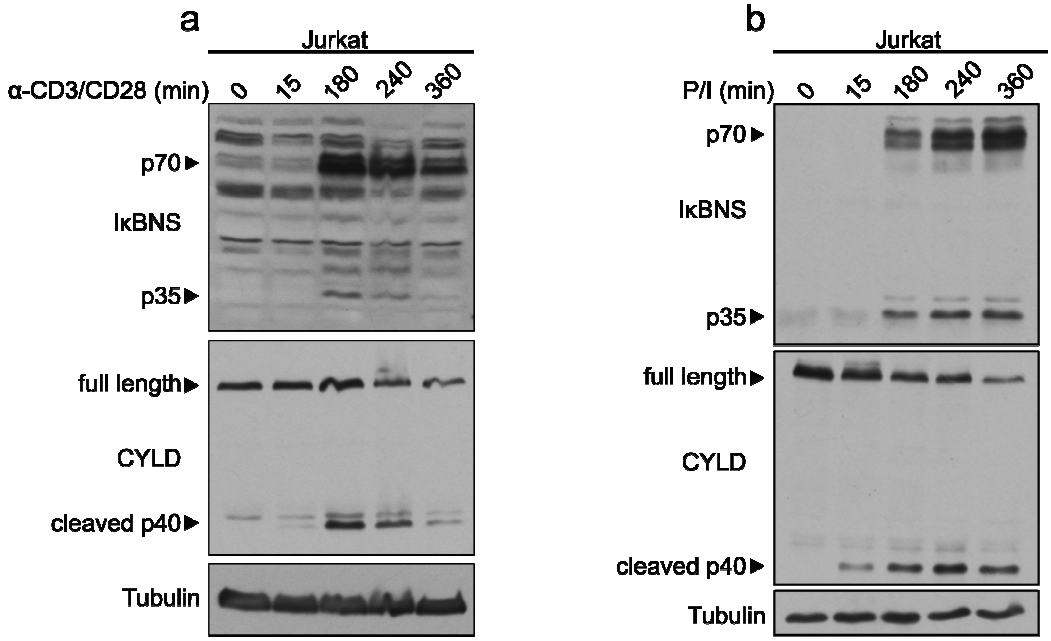

Figure 40. Investigating the potential differences of anti-CD3/CD28 antibody and P/I mediated T-cell stimulation on IκBNS p35 and p70 expression. (a) Jurkat T-cells were treated with 10 µg/µl cross-linked anti-CD3/CD28 antibodies or **(b)** P/I for the indicated periods of time. Lysates were analysed for IκBNS and CYLD expression levels by immunoblot. **(a, b)** CYLD cleavage by MALT1 reflects the antibody and P/I mediated activation of Jurkat T-cells. Tubulin served as an indicator for equal loading of samples.

Thanks to the previously conducted experiments we now had several lines of evidence that the p70 signal is indeed another additional IκBNS protein sharing amino acid sequence stretches with the predicted IκBNS p35. Moreover, by applying the CRISPR/Cas9 method, we proved that the two proteins arise from the same gene locus in human B-cells. Both IκBNS proteins were already observed in mouse conventional T-cells by Schuster et al. in 2012 and in mouse embryonic fibroblasts by Jeltsch et al. in 2014, as well. Schuster et al. also assumed p35 and p70 to emanate from a sole gene locus as stimulated mouse *Nfkbid*-deficient cells show no p70. Additionally, Jeltsch et al. claim IκBNS to produce specific signals at 35 and 70 kDa. However, the two of them did not show evidence that the 70 kDa signal arises indeed from another distinct IκBNS protein in mouse cells. Nevertheless, so

far, we did not know what exactly the additional IκBNS protein with a size of approximately 70 kDa was indeed. We speculated if the IκBNS p70 could be a second IκBNS isoform, a postranslationally modified p35 or a p35 homodimer. The latter possibility was the most obvious for us as the IκBNS protein of so far unknown genesis exhibits exactly double the size (70 kDa) of the predicted IκBNS with 35 kDa. For that reason, we next tried to figure out if the IκBNS p70 is just a seemingly SDS-stable homodimer of IκBNS p35. To this end, we tried different approaches to crack the putative IκBNS p70 homodimer in lysates derived from steady state IκBNS expressing cell lines OCI-LY3, HBL-1 and Rec1 by different modifications of our sample buffer (Figure 41.a,b). Kolodziejski et al. suggested to increase the concentration of protein reducing agents to destruct dimers. From this we considered combining 2-ME that is already included in our sample buffer with the other commonly used reductant DTT (Figure 41.a). Moreover, we also applied another strongly reductive sampler buffer (2x urea buffer) to lysates comprising 8 M urea plus either 8% of SDS or 6 M guanidine hydrochloride (Figure 41.b). We decided to include 8% SDS and 6 M guanidine hydrochloride concentrations according to Kolodziejski et al., 2003. All listed compounds are either strongly reductive agents such as 2-ME and DTT or strong protein denaturants like urea, SDS and guanidine hydrochloride (Wingfield, 2016) that should disrupt the putative IκBNS dimers of 70 kDa into two 35 kDa IκBNS monomers. As depicted in Figure 41.a, b, none of the different reductive and denaturising conditions successfully led to the disruption of the presumable 70 kDa homodimer. This is indicated by stable amounts of IκBNS p70 and no further increase in the amount of putative IκBNS p35 monomers (Figure 41.a) in comparison to sample buffer controls (sample buffer with 2-ME). HEK293T lysates derived from cells transfected with an empty vector or a FLAG-tagged IκBNS p35 expressing construct were included in Figure 41. to estimate the size at which IκBNS p35 runs on a SDS-gel. Taken together, this result suggests that IκBNS p70 is not an IκBNS p35 homodimer and favours instead the hypothesis of a further, larger IκBNS isoform or postranslationally modified IκBNS p35.

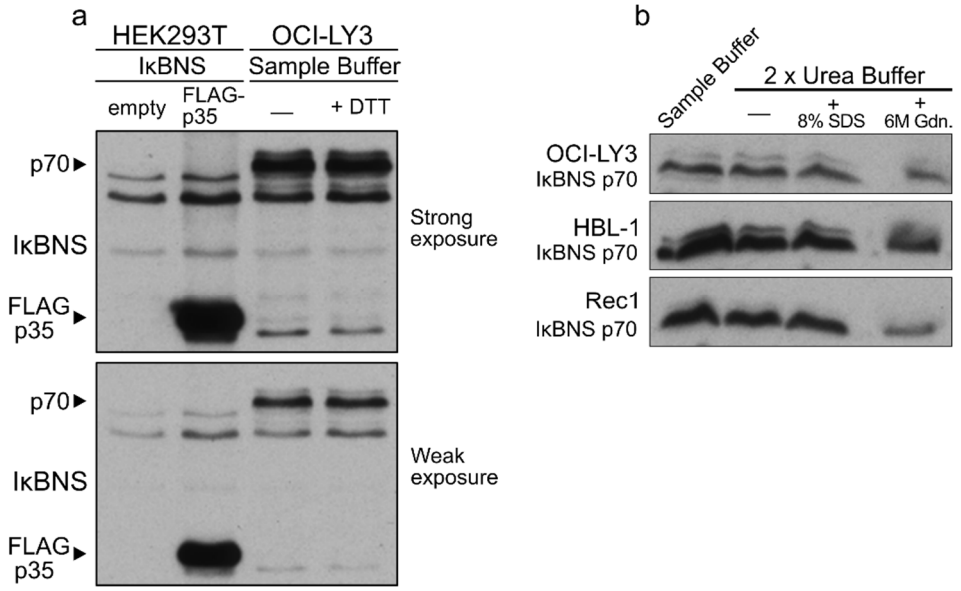

Figure 41. Pursuing the question whether IκBNS p70 is a SDS stable IκBNS p35 homodimer. (a) Lysates from OCI-LY3 cells expressing steady state levels of IκBNS p35 and p70 were treated with either our commonly used sample buffer or a modified variant containing 100 mM DTT. Expression levels of IκBNS were then assessed by western blotting **(b)** Western blot analysis of lysates from OCI-LY3, HBL-1 and Rec1 cells expressing steady state IκBNS p35 and p70 levels were exposed either to the commonly used sample buffer as control or 2 x Urea Buffer comprising either 8% SDS or 6 M of guanidine hydrochloride to disrupt the presumable 70 kDa IκBNS p35 homodimer.

To further elucidate if IκBNS p70 is indeed no dimer and no postranslationally modified p35, as well, we next overexpressed a FLAG-tagged IκBNS p35 in the ABC DLBCL cell line HBL-1 by lentiviral transduction. Both, IκBNS p35 and p70 are already expressed at high levels under steady state conditions in HBL-1 cells. The FLAG-tagged IκBNS p35 exhibits a slightly higher molecular mass than the endogenously expressed IκBNS p35. We assumed that in case the IκBNS p70 would be a homodimer, made up of two IκBNS p35 or a postranslationally modified IκBNS p35 then the artificially introduced FLAG-tagged IκBNS p35 should also exist either as a FLAG-tagged p70 IκBNS dimer or postranslationally modified FLAG-tagged p70 IκBNS. Due to the FLAG-tag these IκBNS p70 versions would then have a slightly higher molecular weight compared to their endogenously expressed counterparts and would therefore run higher on a SDS-gel, so that they could be easily distinguished from each other. Thus, the existence of those FLAG-tagged p70 IκBNS versions would strengthen the p35 dimer and posttranslational modification hypothesis. However, the outcome of this experiment as depicted in Figure 42. rejects the dimer and posttranslational modification thesis since the described

additional FLAG-tagged p70 IκBNS signals do not appear. In summary, we excluded the IκBNS p70 protein to be an IκBNS p35 homodimer by different disruption approaches (Figure 41.a,b). This result was approved by the overexpression of a FLAG-tagged IκBNS p35 in HBL-1 cells that did not lead to the generation of a FLAG-tagged IκBNS p70 that could easily be distinguished from the endogenous counterparts in immunoblot due to the slightly increased molecular weight. Moreover, the absence of those FLAG-tagged IκBNS p70 variants also proofs that IκBNS p70 is not just a posttranslationally modified IκBNS p35. Taken together, the obtained results suggest that the IκBNS p70 is most likely a further second, discrete IκBNS isoform originating from the same gene locus as IκBNS p35.

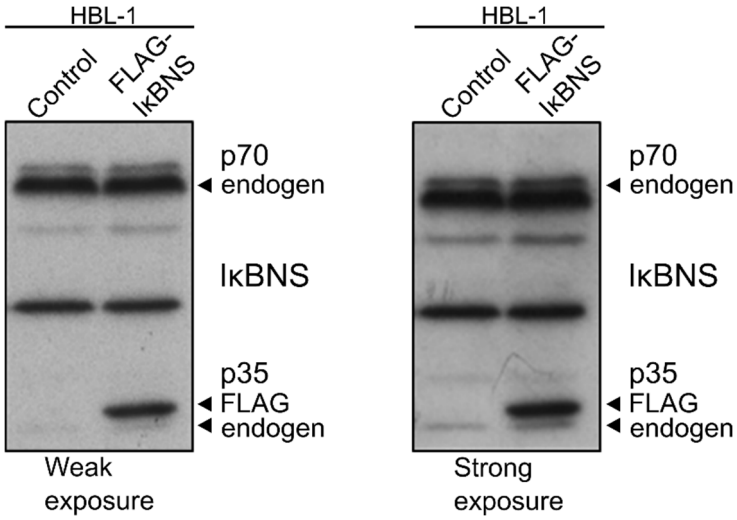

Figure 42. Exploring whether IκBNS p70 is an IκBNS p35 derived homodimer or a postrans-lationally modified IκBNS p35. The steady state endogenous IκBNS p35 and p70 expressing ABC DLBCL cell line HBL-1 was lentivirally transduced with either an empty vector as control or a FLAG-tagged IκBNS p35 expressing vector. HBL-1 lysates were analysed for IκBNS levels by western blotting. Due to the FLAG-tag, the lentivirally transduced IκBNS p35 exhibits a minimally higher size therefore running at slightly higher molecular weight on the western blot compared to endogenous IκBNS p35. As no FLAG-tagged IκBNS p70 band emerges upon expression of FLAG-tagged IκBNS p35 the theory of an IκBNS p70 consisting of two IκBNS p35 and an IκBNS p70 that is a posttranslationally modified IκBNS p35 was ruled out. Weak and strong exposures of blots are shown for a better impression of the different expression levels of IκBNS p35 and p70.

Since previous experiments strongly indicate IκBNS p70 to be a second distinct IκBNS isoform originating from the same gene locus as IκBNS p35, we next had a closer look at the transcribed NFκBID mRNA. In fact, deep sequencing conducted with samples from the ABC DLBCL cell line HBL-1, revealed that only one IκBNS mRNA is expressed. Furthermore, with the help of an ORF prediction tool, we found a second open reading frame consisting of 1716 nucleotides coding for a protein

comprising 572 aa with a resulting predicted molecular weight of 61 kDa, suggesting the expression of a second isoform (Figure 43.; IκBNS p70). This molecular weight was a bit less than expected, as we assumed a molecular weight of approximately 70 kDa due to the IκBNS p70 signal. In order to prove the presence of the predicted IκBNS isoform in B-cells

Figure 43. Schematic illustration of the IκBNS p35 and p70 isoform. The human IκBNS p35 consists of 313 aa and includes 6 ankyrin repeats (ANK; shaded in grey), important for protein-protein interactions. IκBNS p70 comprises 572 aa and exhibits an additional 259 aa N-terminal unstructured portion of unknown function (shaded in grey), and shares the complete IκBNS p35 sequence. The predicted molecular weight of IκBNS p35 is 33,5 kDa whereas IκBNS p70 is predicted to have a molecular weight of 61,1 kDa. aa, amino acid; NH_2, N-terminus; COOH, C-terminus.

In turn to examine this newly established isoform (Figure 43.; IκBNS p70) in more detail, we cloned a vector encoding the potential new IκBNS p70 isoform and conducted multiple experiments with this. First of all, we wanted to figure out at which size the presumable IκBNS p70 would actually run on a SDS gel compared to the endogenous IκBNS p70 counterpart to have a clue whether our sequence could be indeed identical to the endogenous one found in ABC DLBCL as well as in in GCB DLBCL and Jurkat T-cells upon P/I mediated stimulation. To this end, we transfected HEK293T cells with either an empty vector as control or with vector constructs expressing STREP-tagged IκBNS p35 or p70. In order to compare these STREP-tagged proteins with the size of endogenously expressed IκBNS p35 and p70 proteins we included several samples from ABC DLBCL cell lines (HBL-1, TMD8, OCI-LY3 and RIVA) in the experiment showing high endogenous expression levels of IκBNS p35 and p70. In contrast to that we also implicated multiple samples deriving from GCB DLBCL cell lines (SU-DHL-4, SU-DHL-6 and OCI-LY1) that are known to us to express no IκBNS. As shown in Figure 44.a, STREP-tagged IκBNS p35 was properly expressed in HEK293T and showed as expected a slightly higher molecular weight than the endogenous protein. Furthermore, western blot analysis also clearly revealed that the STREP-tagged IκBNS p70 expressed in HEK293T de facto exhibits a slightly higher molecular weight in the blot than the actual predicted size of 62 kDa including STREP-tag. This size was comparable with the

endogenous IκBNS p70 from ABC DLBCL (Figure 44.a). Moreover, the expression of the STREP-tagged IκBNS p70 led to the formation of several bands that were lying close to each other, resembling the band pattern observable in ABC DLBCL samples (Figure 44.a). Noteworthy as well, the expression of IκBNS p35 and p70 expressed in HEK293T cells closely resembled the pattern of IκBNS p35 and p70 endogenously expressed by ABC DLBCL. For these reasons, the IκBNS p70 protein sequence we found is likely to be same as the endogenous IκBNS p70 amino acid sequence found under steady state conditions in ABC DLBCL cell lines and upon stimulation of GCB DLBCL.

The following experiment we conducted to analyse what influence the ectopic expression of IκBNS p35 and p70 would have on endogenous IκBNS p35 and 70 levels that were induced by P/I mediated T-cell stimulation (Figure 44.b). In addition to that, we wanted to know, whether the expression of the IκBNS p70 isoform in T-cells would look the same as in HEK293T cells. For this purpose, we lentivirally transduced Jurkat T-cells with either an empty vector or plasmid constructs expressing either FLAG-tagged IκBNS p35 or the V5-tagged IκBNS p70 isoform. Once the successfully transduced cells were selected by puromycin treatment Jurkat T-cells were stimulated by P/I to induce endogenous levels of IκBNS p35 and p70. Samples were subsequently analysed for IκBNS expression by immunoblotting. Both IκBNS isoforms that were lentivirally transduced expressed well in Jurkat cells (Figure 44.b). As already observed in samples coming from HEK293T cells, the expression of lentivirally transduced V5-tagged IκBNS isoform p70 exhibits just a marginally higher size than the endogenously expressed IκBNS p70 caused by the V5-tag. For the same reason, also the FLAG-tagged IκBNS p35 shows a slightly increased molecular weight compared to its physiological correspondent. In this way it was possible to clearly distinguish between endogenous and lentivirally transduced IκBNS isoforms. Compared to the P/I induced IκBNS p35 and p70 levels of Jurkat cells transduced with an empty vector both, the expression of the FLAG-and V5-tagged lentivirally transduced IκBNS p35 and p70 isoforms resulted in remarkably decreased levels of endogenous IκBNS p35 and p70 that were induced by 4 h of cell stimulation by P/I (Figure 44.b). Noteworthy, the level of cell stimulation was equal amongst the samples, indicated by the amount of cleaved CYLD. This result suggests that IκBNS p35 and p70 act in a negative (auto inhibitory) feedback loop to restrict and down regulate their own

expression. By pull-down experiments in TCR transgenic thymocytes, IκBNS was shown to bind NFκB family members such as nuclear p50, p65, RelB and c-Rel. Moreover, IκBNS binds to transcriptional inactive p50 homodimer on the IL-6 promoter (Hirotani et al., 2006). In IκBNS deficient macrophages Kuwata et al. observed in 2006, the extended binding of the RelA/p50 heterodimer to the IL-6 promoter, indicating that IκBNS is able to act as a transcriptional repressor. Thus, it would be conceivable that this negative feedback loop could be conducted by the binding of IκBNS to NF-κB components such as a transcriptional inactive p50 homodimers, thereby preventing subsequent DNA binding of other active NF-κB and NFAT members to the NFκBID promoter. Also imaginable would be that IκBNS shortens the resting time of active RelA/p50 heterodimers by removing them from the NFκBID promoter. Taken together, these results suggest that the IκBNS p70 amino acid sequence we revealed is indeed equivalent to the endogenous IκBNS p70 protein sequence from B- and T-cells under steady state and P/I mediated induced IκBNS expression conditions. Furthermore, both IκBNS isoforms seem to work in a negative (auto inhibitory) feedback loop to limit and down modulate a surplus of IκBNS expression levels.

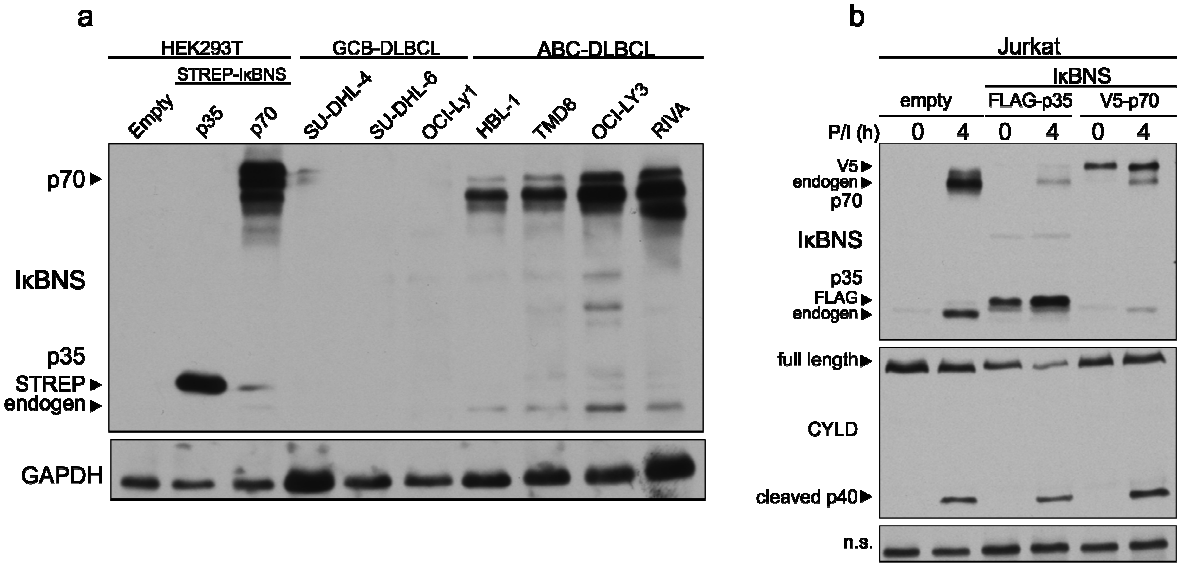

Figure 44. Expression of the revealed IκBNS p70 protein in comparison to steady state endogenous IκBNS p70 in ABC DLBCL cell lines and P/I induced IκBNS p70 in Jurkat T-cells. **(a)** HEK293T cells were transfected either with an empty vector as control or a vector expressing IκBNS p35 or p70. Lysates from indicated GCB and ABC DLBCL cell lines were analysed for IκBNS p35 and p70 expression in comparison to IκBNS p35 and p70 overexpressed in HEK293T cells. GAPDH served as a loading control especially for samples from GCB DLBCL cell lines that do not express IκBNS **(b)** Jurkat T-cells were lentivirally transduced either with an empty vector as control or one of the two IκBNS isoforms (FLAG-tagged p35 or V5-tagged p70) and stimulated for 4 h with P/I to induce endogenous IκBNS expression. CYLD cleavage was determined

to indicate T-cell stimulation by P/I. A not specific band (n.s.) served as indicator for equal loading of samples.

To further substantiate that the IκBNS p70 isoform sequence we established is really the one that can be found endogenously in DLBCL, we generated an IκBNS p70 isoform specific antibody that binds an antigen in the N-terminal portion unique for IκBNS p70. Thus, this antibody should not detect the shorter IκBNS p35 isoform. In order to test the anti-IκBNS p70 antibody, we stimulated the GCB DLBCL cell line BJAB for different periods of time with P/I what would cause the induction of both IκBNS isoforms. By western blot analysis we compared the IκBNS antibody recognising both isoforms (Figure 45. upper panel) with the antibody detecting exclusively the larger p70 IκBNS isoform. Indeed, the p70 isoform specific antibody detected a protein strongly appearing after 180 min of P/I mediated cell stimulation with the expected size of approximately 70 kDa. Unfortunately, this presumably specific IκBNS p70 signal was partly overlaid with another unspecific band. Thus, it was not possible for us to make further statements about the recognition capacities of the self-made anti-IκBNS p70 antibody and the pattern of bands specific for IκBNS p70. Moreover, the anti-IκBNS p70 antibody did not detect any IκBNS p35 isoform at all (Figure 45. middle panel) as it was the case for the anti-p35/p70 antibody (Figure 45. upper panel) that recognised an IκBNS p35 specific band in samples from BJAB cells that were stimulated with P/I for 180, 240 and 360 minutes. BJAB stimulation by P/I was confirmed by assessing the cleavage of the MALT1 substrates BCL-10 and CYLD. In summary, this result strengthens the assumption that the endogenous IκBNS p70 isoform is indeed identical with our IκBNS p70 aa-sequence as the antibody recognises an antigen located in the N-terminal portion that is unique for the IκBNS p70 isoform.

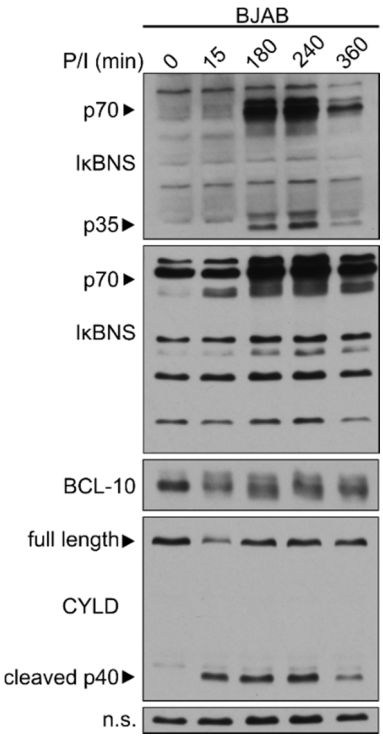

Figure 45. Testing the self-made anti-IκBNS p70 antibody for its detection capabilities for the larger IκBNS p70 isoform in comparison to the anti-IκBNS p35 and p70 antibody.
BJAB cells (GCB DLBCL) were stimulated by P/I for 0, 15, 240 and 360 min to induce endogenous IκBNS expression. Lysates were analysed for IκBNS expression with the anti-IκBNS p35 and p70 antibody (upper panel) and the anti-IκBNS p70 specific antibody (middle panel). Blotting against the MALT1 substrates BCL-10 and CYLD served as B-cell activation marker. An unspecific band (n.s.) indicates the equal loading of samples.

Since we expect different IκBNS isoforms not only to have mutual tasks and properties but also isoform specific and unique purposes and characteristics, we were next interested in the existence of differences between the IκBNS p35 and p70 isoform. Schuster et al. claimed in 2012 that in immunoblotting IκBNS appears within the first 4 h of P/I mediated stimulation of conventional mouse T-cells as a 35 kDa protein in the cytoplasm and as two 70 kDa IκBNS proteins in the nucleus. Moreover, Fiorini et al., found that IκBNS (most likely the p35 isoform) was selectively found in the nuclear fraction of thymocytes derived from mice treated 2 h with VSV8. Furthermore, they expressed an N-terminally eGFP-tagged IκBNS p35 in HeLa cells that was predominantly localised to the nucleus.

In turn to see where IκBNS p35 and p70 localise and if the isoforms would indeed differ in their spatial distribution also in B-cells we conducted cell fractionations with BJAB cells (GCB DLBCL) that were treated for 1 and 3 h with P/I to induce IκBNS (Figure 46.a) and with U2932 and HBL-1 (ABC DLBCL) cells, both expressing IκBNS under steady state conditions (Figure 46.b). Lamin A/C was considered as nuclear marker whereas ERK2 constituted the cytoplasmic marker protein. Western blot analysis showed that under inductive IκBNS expression conditions in BJAB cells the IκBNS p70 isoform emerges first in the nuclear fraction after 1 h of P/I stimulation whereas IκBNS p35 is not detectable in both, the cytoplasmic and nuclear fraction at that time point. After 3 h of P/I mediated B-cell stimulation both isoforms appear

in the cytosolic fraction in rather low but equal amounts. This is in contrast to the nuclear fraction where both isoforms were clearly enriched compared to the cytoplasmic fraction whereby IκBNS p70 was now obviously more abundant than the smaller IκBNS p35 isoform (Figure 46.a). The fractionation of ABC DLBCL cell lines expressing steady state IκBNS levels revealed that there is clearly more IκBNS p35 and p70 in the nucleus than in the cytoplasm (Figure 46.b). Thereby, the ratios of protein amounts between IκBNS p35 and p70 apparently remained the same no matter in which cellular compartment.

Taken together, from these results we draw the conclusion that there exists no cytoplasmic or nuclear specific IκBNS isoform. Furthermore, upon IκBNS expression induction by P/I, IκBNS p70 clearly appears first in the nucleus whereas IκBNS p35 is not present neither in the cytoplasm nor the nucleus. This could be caused simply by the fact that IκBNS p70 is generally higher expressed than IκBNS p35. Thus the smaller isoform is also expressed but in such little amounts that is not detectable by immunoblotting. Moreover, in general it can be said, that both isoforms are more abundant in the nucleus than in the cytoplasm after the induction by P/I and under steady state conditions, as well. Mentionable, the ratio of protein levels between IκBNS p35 and p70 always remains the same with only one exception. After 3 h of P/I stimulation the ratio between the levels of IκBNS p35 and p70 is equal in the cytoplasmic fraction and p70 is strikingly more abundant in the nuclear fraction than p35. This fact could be explained by different nuclear shuttling behaviours of the IκBNS isoforms. The larger isoform IκBNS p70 could probably bear a nuclear localisation sequence (NLS) in its unique N-terminal portion and could be therefore retained in the nucleus in contrast to IκBNS p35 for which no NLS was found so far. According to the cytoplasmic and nuclear marker, cell fractionations worked properly in all samples.

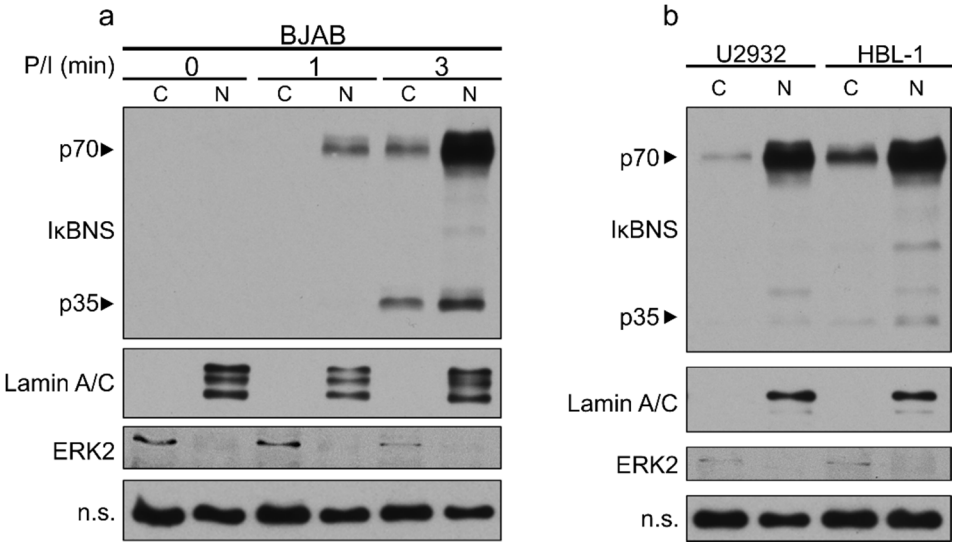

Figure 46. Fractionation of P/I stimulated one GCB DLBCL and two ABC DLBCL cell lines under steady state conditions to assess potential differences between the spatial distribution of IκBNS p35 and IκBNS p70. (a) The GCB DLBCL cell line BJAB was stimulated with P/I for 0, 1 and 3 h to induce IκBNS p35 and IκBNS p70 expression. Subsequently, cells were fractionated into cytoplasmic and nuclear moieties. **(b)** The ABC DLBCL cell lines U2932 and HBL-1 cells were harvested under steady state conditions. Afterwards, cytoplasmic and nuclear fractions were prepared. **(a, b)** Expression levels of IκBNS p35 and IκBNS p70, Lamin A/C and ERK2 were determined by immunoblotting. In both panels Lamin A/C detection served as a marker for the purity of the nuclear fraction whereas ERK2 levels indicate the purity of the cytoplasmic fraction. An unspecific band (n.s.) served as loading control.

3.5 Regulation of HLA-DR expression by IκBNS

IκBNS belongs to the group of atypical, nuclear residing NF-κB inhibitors. The members of this protein family were shown to contribute considerably to the modulation of NF-κB mediated transcription in immune cells. They accomplish this task by their capability to negatively or positively regulate the transcriptional activity of target genes together with DNA-associated NF-kB transcription factors (reviewed in Annemann et al., 2016). For this reason, we were interested which genes and in which direction these affected genes would be regulated by an IκBNS knockdown in ABC DLBCL. For this purpose, we conducted an inducible shRNA #1 mediated IκBNS knock down in HBL-1 cells for 96 h that was followed by an RNA-Seq. The approach revealed multiple MHC class II (MHCII) genes and moreover genes encoding accessory proteins that are needed for MHCII-restricted antigen presentation like CD74 (also known as invariant chain or Li) or Human Leucocyte Antigen-DM (HLA-DM) (LeibundGut-Landmann et al., 2004) among the top hits of genes that were negatively regulated by IκBNS (Table 2.). MHCII molecule

expression is restricted to the surface of professional antigen presenting cells such as B-cells and is crucial for presenting peptide antigens derived from extracellular pathogens to the TCR of $CD4^+$ T-cells. This MHCII:peptide complex engagement by the TCR in turn induces the activation and proliferation of the respective T-cell and is therefore pivotal for an antigen-specific response of the adaptive immune system. Moreover, MHC class II molecules are not only important for mounting an adaptive immune response directed against pathogens but also for the recognition of peptides specific for tumorigenic cells by tumor-specific T-cells. This feature indicates the important role of MHCII in immune surveillance (Wilkinson et al., 2012). The human MHCII protein family is subdivided into the classical MHCII (HLA-DP, -DQ, and –DR), the non-classical (HLA-DM and –DO) and the invariant chain molecules. Unlike their classical counterparts, non-classical MHCII are not located at the cell surface and do not present antigens. Instead, they regulate and promote the loading of peptide antigens to classical MHCII molecules (Alfonso and Karlsson 2000; Ting and Trowsdale, 2002; Reith and Mach., 2001; LeibundGut-Landmann et al., 2004; Wilkinson et al., 2009). Remarkably, also the class II major histocompatibility complex transactivator “CIITA” which is the essential master transcriptional regulator of the entire MHC class II genes and several associated genes like the membrane glycoprotein Li, was positively affected by IκBNS silencing (Table 2.). CIITA governs whether and in what extend MHC II proteins are expressed. Therefore, CIITA is expressed in MHCII positive professional antigen presenting cells such as B-cells, macrophages and DCs (Reith and Mach., 2001; LeibundGut-Landmann et al., 2004).

Based on the results we obtained by RNA-Seq., we were next interested to further examine the impact of IκBNS expression on MHC class II protein expression in DLBCL. As B-cells are professional antigen presenting cells, they usually express MHCII on the cell surface. Thus, we also expected to find MHC class II molecules on the surface of DLBCL cell lines. RNA-Seq. revealed the HLA-DRB1 gene which encodes the beta subunit of the HLA-DR isoform to be the most affected MHC class II gene by shRNA mediated IκBNS knockdown. In addition to that HLA-DR is known to be the highest expressed isoform in human (Landsverk et al., 2009). Accordingly, we decided to investigate this particular classical MHCII isoform on the surface of DLBCL cell lines in our experiments.

Gene	Fold change	P-value
LAG3;CD223	1,60	1,24E-17
HLA-DRB1	**1,51**	**9,37E-27**
ferritin heavy chain 1	1,44	2,46E-15
2'-5'-oligoadenylate synthetase 3	1,44	8,77E-11
CD52	1,42	8,85E-15
MX dynamin like GTPase 1	1,41	7,87E-11
HLA-DRA1	**1,40**	**1,67E-24**
Janus kinase 3	1,40	5,42E-17
HLA-DQA	**1,39**	**2,97E-11**
TNF alpha induced protein 2	1,39	1,14E-08
protein tyrosine phosphatase, non-receptor type 7	1,38	1,74E-13
transmembrane protein 160	1,38	3,69E-08
CD74 (invariant chain)	**1,37**	**9,59E-41**
BCL2 interacting killer	1,36	3,66E-08
heat shock protein family B (small) member 1	1,35	1,20E-08
MIR663A host gene	1,35	6,40E-08
fibromodulin	1,34	6,34E-10
parvin gamma	1,34	4,44E-07
HLA-DRB	**1,34**	**2,11E-07**
surfactant protein B	1,33	5,02E-09
class II major histocompatibility complex transactivator (CIITA)	**1,22**	**3,77E-07**
NFKB inhibitor delta (IκBNS)	0,76	3,29E-11

Table 2. Genes that were revealed by RNA-Seq. to be upregulated upon 96 h of inducible shRNA mediated IκBNS knock down in samples from the steady state IκBNS expressing ABC DLBCL cell line HBL-1. "Gene" designates the name of the gene found to exhibit an altered transcriptional activity upon IκBNS knock down; **"Fold change"** means the extent of the transcriptional activity change compared to the control; Highlighted in bold are genes that belong to MHC class II gene family.

Partial IκBNS knock-down can be easily achieved in a relative short time span by treating ABC DLBCL cell lines with the calcineurin inhibitors CsA and FK506. For this reason, we subjected the calcineurin inhibitor sensitive cell line HBL-1 and the insensitive cell line OCI-LY3 to a dilution series of CsA. After an incubation of two days we determined the amount of HLA-DR molecules displayed on the cell surface by flow cytometry. Indeed, the CsA mediated knock down of IκBNS led to an increase of HLA-DR proteins residing on cell surface of approximately 30 % for HBL-1 and more than 50% for OCI-LY3 cells in comparison to the untreated control (Figure 47.). This effect is dose dependent as there was an observable tendency of

elevating HLA-DR surface levels accompanied by increasing CsA concentrations. The highest HLA-DR surface levels could be therefore achieved in both cell lines with the highest applied concentration of CsA. In summary, these results indicate, that the partial IκBNS knock down caused by the pharmacological inhibition of calcineurin and resulting NFATc1 activity blockage is leading to the enhanced presentation of HLA-DR molecules on the cell surface of ABC DLBCL cell lines. Notably, this effect seems to be independent from whether the cell line is calcineurin inhibitor sensitive or not.

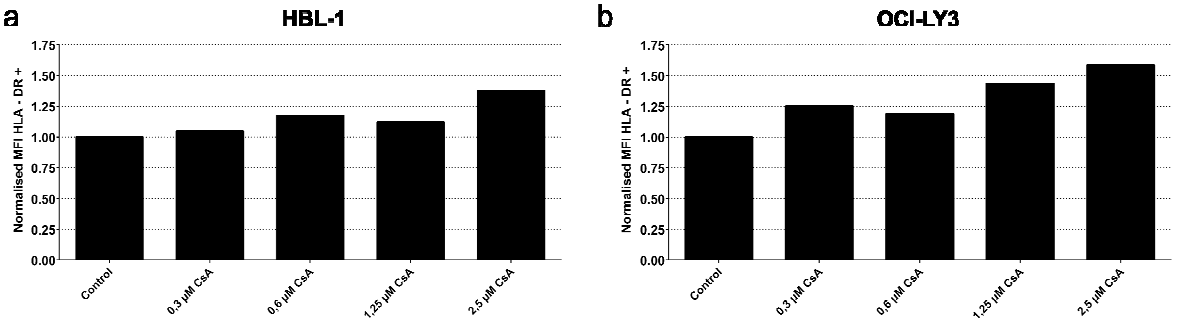

Figure 47. Measurement of HLA-DR surface levels on HBL-1 and OCI-LY3 cells (ABC DLBCL) upon two days of CsA mediated knock down of IκBNS. (a) HBL-1 and **(b)** OCI-LY3 cells were treated with solvent as control or the indicated concentrations of CsA for two days prior to flow cytometry analysis of HLA-DR surface levels. **(a, b)** Depicted is the mean fluorescence intensity (MFI) of HLA-DR$^+$ cells normalised to solvent treated cells (control).

Since we wanted to confirm the previously observed effect (Figure 47.), we consequently treated another ABC DLBCL with both available calcineurin inhibitors (CsA and FK506). Thus, we incubated TMD8 cells that also exhibit high expression levels of IκBNS with dilutions series of both inhibitors for two days and subsequently assessed HLA-DR surface levels by flow cytometry. The impact of CsA mediated IκBNS knock down on HLA-DR levels that we had already observed for HBL-1 and OCI-LY3 cells could clearly be reproduced for HLA-DR surface levels of TMD8 cells treated with CsA or FK506 (Figure 48.). Furthermore, the effect of raising HLA-DR surface levels going along with increasing concentrations of CsA was this time clearly dose dependent. It was possible to increase HLA-DR surface levels more than 3-fold compared to solvent control by treating TMD8 cells with 5 µM CsA (Figure 48.a). FK506 treatment of TMD8 cells clearly induced the elevation of HLA-DR surface levels, as well. Noteworthy, the mentioned dose dependent effect we have seen for CsA treatment was also present here, as the highest HLA-DR surface levels could be measured at the highest amounts of FK506

(Figure 48.b), but not that impressive as for CsA treatment of TMD8. Here, calcineurin inhibition by FK506 led to an HLA-DR surface expression up to 1,5 fold compared with the solvent control. In summary, the CsA and Fk506 mediated knock down of IκBNS in ABC DLBCL leads to clearly enhanced HLA-DR surface levels in a dose dependent manner.

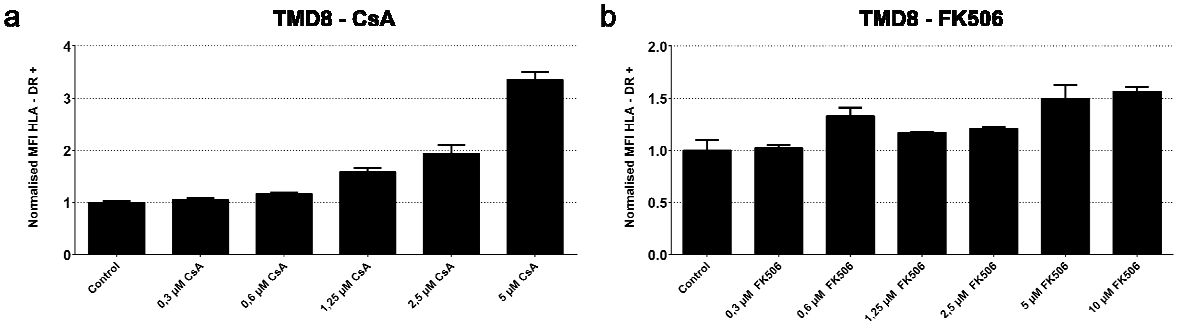

Figure 48. Assessment of HLA-DR surface levels upon treatment of TMD8 cells (ABC DLBCL) with dilutions series of the calcineurin inhibitors CsA and FK506 to knock down IκBNS expression. Cells were treated with solvent as control or **(a)** the indicated concentrations of CsA or **(b)** for two days ahead of flow cytometry analysis of HLA-DR surface levels. **(a, b)** Depicted is the mean fluorescence intensity (MFI) of HLA-DR$^+$ cells normalised to solvent treated cells (control).

To demonstrate that IκBNS itself directly causes the changes of HLA-DR surface levels on B-cells we overexpressed both IκBNS isoforms (FLAG-tagged p35 and V5-tagged p70) in B-cell lines that show high HLA-DR and no steady state IκBNS expression. RNA-Seq. revealed IκBNS as a negative regulator of HLA-DR. Therefore, the knock down of IκBNS by calcineurin inhibitors led to increased HLA-DR surface levels on ABC DLBCL cell lines (Figure 47. and 48.). For this reason, we expected diminished HLA-DR surface levels on B-cells overexpressing the IκBNS isoforms p35 and p70. In order to figure this out, we lentivirally transduced the GCB DLBCL cell line BJAB and the Burkitt's lymphoma cell line RAJI with either an empty vector as control or vectors coding for IκBNS p35 or p70 (Figure 49.a, b). Upon puromycin selection of successfully transduced cells, we measured HLA-DR surface levels of BJAB and RAJI cells that were properly expressing IκBNS p35 or p70 one week after lentiviral transduction (Figure 49.a, b). As assumed, BJAB and RAJI cells expressing IκBNS p35 or p70, showed indeed clearly diminished HLA-DR surface levels (Figure 49.a, b) compared to the empty vector transduced cells. In detail, HLA-DR surface levels were lowered up to roughly 30% for BJAB and 40% for RAJI cells by the expression of IκBNS p35, whereas the expression of IκBNS p70 caused a reduction of HLA-DR surface levels by approximately 40% on BJAB

and slightly more than 40% on RAJI cells (Figure 49.a, b). In summary, the overexpression of IκBNS p35 and p70 in B-cells deriving from GCB DLBCL and Burkitt's lymphoma origin caused a clear reduction of HLA-DR surface levels. Thereby was the extent of reduction independent from the overexpressed isoform albeit the effect was minimally more pronounced in cells expressing IκBNS p70.

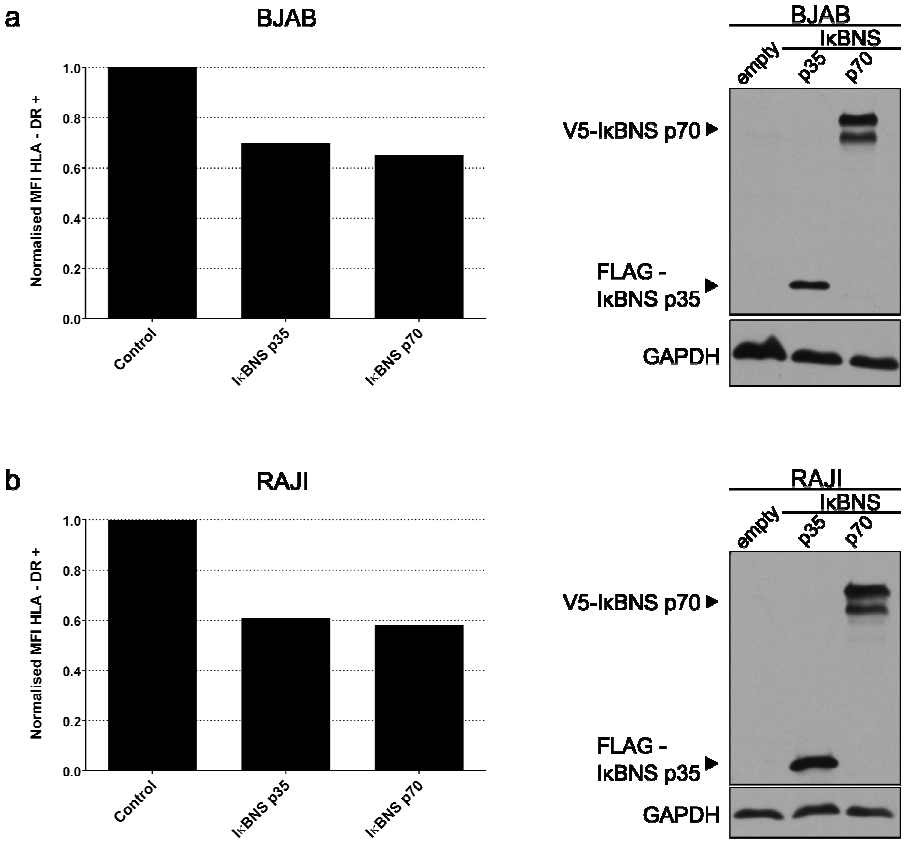

Figure 49. Determining HLA-DR surface levels of BJAB (GCB DLBCL) and RAJI (Burkitt's lymphoma) B-cells expressing IκBNS isoforms p35 and p70. (**a, b)** BJAB and RAJI cells were lentivirally transduced with an empty vector as control or vectors expressing a FLAG-tagged IκBNS p35 or a V5-tagged IκBNS p70. After puromycin mediated selection of successfully transduced cells, HLA-DR surface levels were determined by flow cytometry. (**a, b left)** Depicted is the mean fluorescence intensity (MFI) of HLA-DR$^+$ cells normalised to solvent treated cells (control). **(a ,b right)** On the day of flow cytometry measurement, cells were harvested and lysates were analysed by western blotting to assess IκBNS p35 and p70 expression. GAPDH served as control for equal loading of samples.

Taken together, this result approves that IκBNS is indeed a negative regulator of MHC class II genes e.g. from HLA-DR indicated by the change of surface levels on B-cells. Hence, the IκBNS knock down by pharmacological calcineurin inhibitors in naturally IκBNS expressing ABC DLBCL cell lines causes the elevation of HLA-DR surface levels. Whereas, the overexpression of one IκBNS isoform (either p35 or p70) in B-cells exhibiting no steady state IκBNS expression is sufficient to remarkably diminish HLA-DR surface display

3.6 CD Marker screen of GCB and ABC DLBCL

DLBCL represent a heterogeneous group of lymphoid malignancies in regard to clinical presentation and morphological aspects. Due to this there was an obvious need for having methods and algorithms that would help to stratify patients into distinct groups regarding prognosis and prediction to therapy response. An advanced approach in this respect was the classification of DLBCL according to gene expression profiling into three main molecular subtypes (GCB, ABC, PMBL) that exhibit different survival outcomes (Alizadeh et al.,200). But so far GEP is quite expensive, requires time for analysing huge amounts of data and is not available for a broad range of laboratories. Therefore, intensive efforts have been made during the last years to reveal reliable biological markers and to establish simpler, more broadly available clinical tools and methods that would provide improvements in risk stratification and in the development of new, more specific therapies. One such quite well validated and still commonly used tool is the so called International prognostic index (IPI) established in 1993 by the International Non-Hodgkin's Lymphoma Prognostic Factors Project. IPI remains the most robust predictive tool for DLBCL also after the introduction of the monoclonal anti-CD20 antibody rituximab complementing the conventional CHOP therapy, now R-CHOP (Vaidya and Witzig, 2014). However, this index is based on five clinical risk factors found in DLBCL that are quite subjective and a substantial amount of patients rated as “low” or “intermediate risk” by IPI show therapeutic failure (Linderoth et al., 2003). Several groups describe the usage of immunohistochemical profiling as a promising method to identify outcome predictors and deduced algorithms that are moreover relatively easy to apply and appropriate for daily routine in clinical laboratories. One of these immunohistochemical (IHC) approaches was proposed by Hans et al. in 2004. They suggested an algorithm including CD10, BCL6 and MUM1 as specific markers to distinguish between DLBCL subtypes and achieved a concordance of 80% with GEP classification (Hans et al., 2004). Furthermore, this immunostaining based Hans’ algorithm was improved in 2009 by Choi et al. using GCET1, CD10, BCL6, MUM1, and FOXP1 as biological markers for DLBCL subclassification and facilitating risk stratification. Although the used markers and the deduced algorithms described in literature for class prediction were quite similar, the results were inconsistent regarding accuracy of significant prognostic value. Considering the previously described points, there is still an obvious need for reliable, specific

biomarkers that are capable to differentiate DLBCL into GCB and ABC subgroups, predict the response to R-CHOP therapy and present targets for new antibody treatments. Among the potential candidates meeting these demands are cell surface molecules from which the majority is listed in the cluster of differentiation (CD) index. This is demonstrated for instance by the fact that CD10 was already used to differentiate between GCB and ABC DLBCL by several algorithms (Hans et al., 2004; Choi et al., 2009) and that CD20 serves as the target for the monoclonal Rituximab in the standard treatment of DLBCL and many other Non-Hodgkin-Lymphoma.

In order to reveal CD-markers that could serve as suitable biomarkers on GCB and ABC DLBCL, we performed an antibody based screen assessing the expression levels of 360 cell surface markers of three GCB (BJAB, SU-DHL-4, SU-DHL-6) and three ABC (HBL-1, TMD8, U2932) DLBCL cell lines. The CD-marker screen revealed that, there are indeed noticeable differences in the expression of multiple cell surface molecules between GCB and ABC DLBCL as depicted in Figure 50.a. Several of these markers can be regarded as indicators for the validity of the assay. IgM-BCR for instance is predominantly expressed by ABC DLBCL whereas GCB DLBCL usually exhibit an Ig class switch recombination (CSR) to IgG-BCR (Young et al., 2015). Indeed, high surface IgM was also observed on ABC DLBCL in the conducted screen whereas absent on GCB DLBCL cell lines (Figure 50.a). The ABC DLBCL characterising aberrant CSR causing high IgM-BCR is based on the finding of deletions in the switch μ (Sμ) region of the IgH gene by Lenz et al. (2007), which interfere with CSR. The group assumed that the high and persistent expression of AID in ABC DLBCL contributes in the formation of these high frequent Sμ deletions mutations leading to functionally impaired CSR. Moreover, also the common reliable GCB phenotype predictive marker, the 100 kDa neutral membrane metallo-endopeptidase CD10 which is implicated in the deactivation of numerous biologically active peptides (Dogan et al., 2000; Ohshima et al., 2001; Sezaki et al., 2003), was confirmed by our screen to be expressed primarily in the comprised GCB DLBCL cell lines (Figure 50. a). In general, CD10 is an antigen found on the surface of lymphoid precursor cells and B lymphoid cells arising from the germinal centre origin (McCluggage et al., 2001). Furthermore, GEP revealed CD10 mRNA expression to be strongly associated with the GCB subtype of DLBCL (Ohshima et al., 2001). On this basis CD10 positivity of cells was therefore demonstrated and

defined by several IHC based decision algorithms as the primary defining criterion for GCB classification e.g. the earlier described Hans' algorithm, an altered Hans' algorithm suggested by Muris et al. in 2006 or in a predictive IHC algorithm that classifies DLBCL in regard to the clinical prognosis into poor intermediate and good proposed by more by Anderson et al. in 2009.

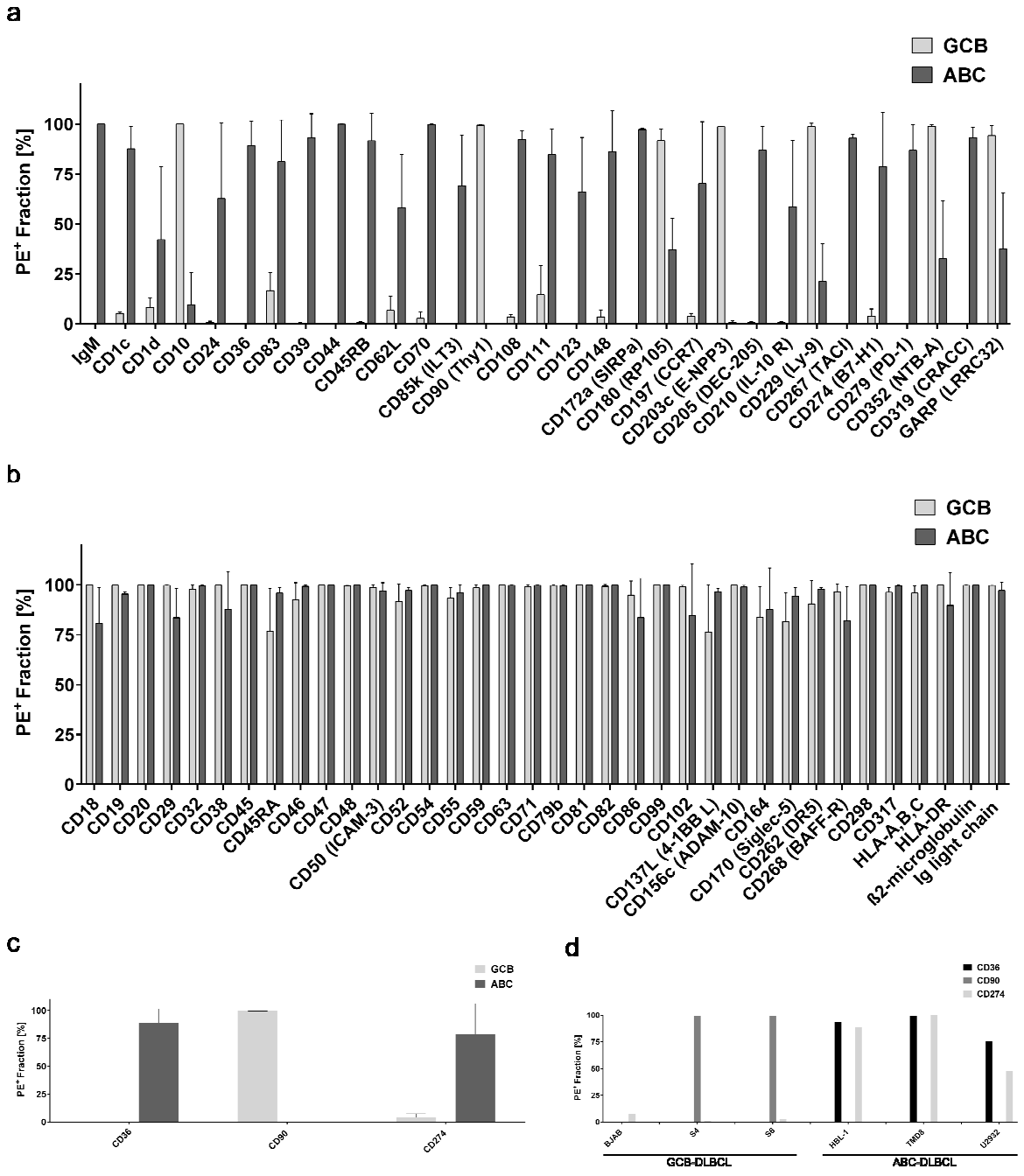

Figure 50. Surface marker screen determining 360 distinct molecules with GCB and ABC DLBCL. (a) Top hits of surface markers that were differentially or **(b)** equally expressed on the included cell lines of the GCB (BJAB, SU-DHL-4 and SUD-DHL-6) and ABC (HBL-1, TMD8 and U2932) subtype of DLBCL. **(c)** Illustration of the expression distribution of the selected surface markers CD36, CD90 and CD274 on the included GCB and ABC DLBCL cell lines. **(d)** Fractions of $CD36^+$, $CD90^+$ and $CD274^+$ of the indicated DLBCL cell lines. **(a-d)** Depicted are the fractions of

PE^+ cells in %. The LEGENDScreen™ assay was conducted according to the manufacturer's instructions.

According to the CD marker screen results we selected three surface proteins that were differentially expressed between GCB and ABC DLBCL for further, more detailed investigations (Figure 50.a). We decided to choose CD90 as particular GCB and two membrane proteins namely CD36 and CD274 as ABC DLBCL specific surface markers (Figure 50.a, c, d).

Since we were interested to confirm the expression pattern of CD36, CD90 and CD274 in DLBCL we recapitulated the assessment of those molecules on a broader range of GCB (BJAB, SU-DHL-4, SU-DHL-6, OCI-Ly1, OCI-Ly7 and OCI-Ly19) and ABC DLBCL (HBL-1, TMD8, U2932, OCI-Ly3 and OCI-Ly10) on both, the surface protein expression and the mRNA level (Figure 51.a-d). CD36 was indeed exclusively expressed at different fractions on all ABC DLBCL we investigated (Figure 51.a). Whereas on the mRNA levels also the GCB cell line OCI-Ly1 and OCI-L19 exhibit little presence of CD36 mRNA (Figure 51.b). The supposed GCB DLBCL marker CD90 was in fact expressed only on cell lines classified as the GCB subtype of DLBCL although not all of those cell lines were positive for CD90 (BJAB, OCI-Ly1, and OCI-Ly7) (Figure 51.c). This CD90 surface expression pattern is quite well reflected by CD90 mRNA levels. Only the GCB cell lines that also showed surface CD90 protein expression namely SU-DHL-4, SU-DHL-6 and OCI-Ly19 exhibit CD90 mRNA levels, remarkably in the same proportionality (Figure 51.d). Also the presumable specific ABC DLBCL indicator CD274 was as revealed by the CD marker screen actually expressed solely on DLBCL cell lines belonging to the ABC subtype. Here, the fractions of $CD274^+$ cells were quite different. Two cell lines ABC cell lines (U2932, OCI-LY3) did not show CD274 surface expression whereas TMD8 and OCI-Ly10 are characterised by considerable high fractions of $CD274^+$ cells (Figure 51.e). The CD274 mRNA levels also demonstrate a clear preference of CD274 expression by ABC DLBCL. All investigated ABC DLBCL cell lines express CD274 mRNA at different levels (Figure 51.f). Noteworthy, TMD8 which exhibits the highest fraction of $CD274^+$ cells also shows the highest CD274 mRNA expression among the ABC DLBCL cell lines tested. Remarkably, also the GCB cell line OCI-Ly1 shows slight expression of CD274 mRNA what is not reflected on the protein level.

Taken together, the results obtained by the surface molecule screen could be well reproduced by our array of GCB and DLBCL cell lines. Thereby, the protein expression extent of chosen surface markers correlated quite well with mRNA levels.

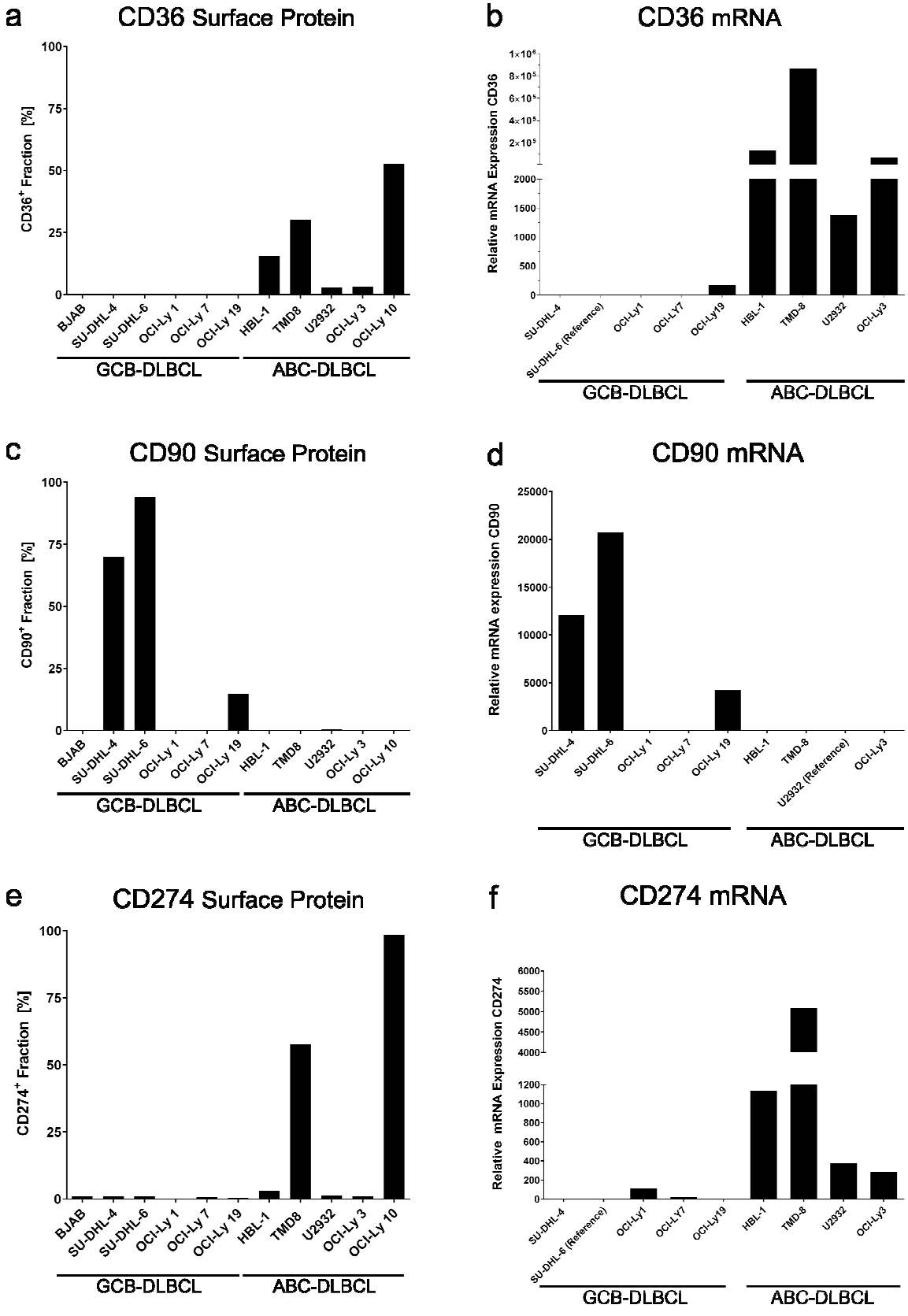

Figure 51. Assessment of surface protein and mRNA levels of selected surface markers specific for GCB and ABC DLBCL. (a, c , e) Fractions of **(a)** CD36 **(c)** CD90 and **(e)** CD274 positive cells of the indicated GCB and ABC DLBCL cell lines were determined by flow cytometry. **(b, d, f)** Relative **(b)** CD36, **(d)** CD90 and **(f)** CD274 mRNA expression levels of indicated DLBCL cell lines of the GCB and ABC subtype. mRNA levels were assessed by qPCR and analysed using the ΔΔCT method. In **(b)** and **(f)** the GCB DLBCL cell line SU-DHL-6 and in **(d)** the ABC cell line U2932 served as a reference for relative mRNA expression levels of the respective surface marker gene.

Next we were interested in functional aspects of the revealed DLBCL subtype specific surface markers in the context of DLBCL pathomechanisms. Many solid tumors exhibit an altered FA metabolism as well as increased utilisation of lipids via β-oxidation to gain energy. Multiple FA pathways were found to be constitutively activated in DLBCL and moreover cell survival seems to be strongly dependent on lipid metabolism (Dashnamoorthy et al., 2014). As earlier described, CD36 signaling coordinates the cellular fat metabolism by numerous functions. Recently, Samovski et al. unveiled a direct link between CD36 and β-oxidation in muscle cells. CD36 regulates the activation of the AMP-activated protein kinase (AMPK), a cellular metabolic and redox sensor. AMPK is activated upon energy deprivation and consequently inhibits energy-intensive metabolic pathways whereas on the other hand it concomitantly upregulates nutrient uptake and catabolic reactions. Thus, AMPK induces the recruitment of CD36 to the cytoplasma membrane and upregulates β-oxidation. CD36 inhibits AMPK under basal conditions. Whereas FA induced CD36 signaling promotes the activation of AMPK in turn leading to the increased activity of β-oxidation and the recruitment of more CD36 to the plasma membrane ending up in a feed forward cycle (Samovski et al., 2015). CD36 gene expression is regulated by the peroxisome proliferator-activated receptor γ (PPARγ), liver X receptor (LXR), and pregnane X receptor (PXR) (Tontonoz et al., 1998). Activating ligands of the transcription factor PPARγ are oxidized phospholipids which are also abundant within the oxLDL particle that is bound and transported into the cell by CD36 (Silverstein et al., 2010). Therefore, CD36 reinforces its own transcription by taking up lipoproteins such as oxLDL. CD36 binding and uptake of FA and oxLDL and subsequent intracellular signaling can be irreversibly blocked by the membrane-impermeable N-hydroxysuccinimidyl (NHS) esters of long chain FA (Harmon and Abumrad, 1993; Pepino et al., 2014). NHS esters of long-chain FA, were originally used to label and cross link proteins by their ability to covalently bind to the amino group of lysine side chains (Kuda et al., 2013;

Kalkhof and Sinz, 2008). The most commonly used CD36 inhibitor is sulfo-N-succinimidyl oleate (SSO), an oleate ester shown to efficiently inhibit CD36-mediated FA uptake and signaling in various cell types by binding to the lysine164, a residue lying within a predicted binding site for FA and oxLDL (Coort et al., 2002; Kuda et al.,2011, 2013).

Since ABC DLBCL cell lines show high CD36 mRNA and surface protein levels compared to GCB DLBCL cell lines, we next examined whether ABC DLBCL would as a consequence of this also exhibit higher β-oxidation activity. Thus also elevated mRNA levels of key β-oxidation enzymes in comparison to GCB DLBCL cell lines. To this end, we investigated the mRNA levels from genes coding for essential key-enzymes of β-oxidation in GCB (BJAB, SU-DHL-4, SU-DHL-6, OCI-Ly1, OCI-Ly7 and OCI-Ly19) and ABC (HBL-1, TMD8, U2932, OCI-Ly3 and OCI-Ly10) DLBCL cell lines (Figure 52.a). The **ACADM** gene codes for the medium-chain acyl-CoA dehydrogenase (MCAD) required for the metabolisation of medium chain fatty acids consisting of 4 to 12 carbonatoms (Bartlett and Eaton, 2004). The very long-chain acyl-CoA dehydrogenase (VLCAD) is encoded by the **ACADVL** gene. VCLAD catalyses the initial step of β-oxidation of long-chain fatty acids comprising 14 to 20 carbonatoms (Leslie et al 2009). The **HADHA** gene encodes the hydroxyacyl-CoA dehydrogenase α-subunit which is part of an enzyme complex called mitochondrial trifunctional protein. This complex contains three distinct enzymes and is essential for the metabolisation of long-chain fatty acids with chain lengths between 12 to 18 carbonatoms (Choi et al., 2007). Though ABC DLBCL show higher levels of CD36 mRNA and surface protein levels than GCB DLBCL cell lines, the mRNA levels of the selected β-oxidation key enzymes amongst the different DLBCL subtypes were comparable for all genes tested (Figure 52.a). This result indicates that the expression of genes regulating β-oxidation is not affected by the different degrees of CD36 expression in DLBCL.

In turn to investigate the importance of CD36 in respect of its FA and oxLDL uptaking properties and its resulting potential influence on β-oxidation activity in DLBCL in more detail we treated the GCB cell line SU-DHL-6, which showed only minimal CD36 mRNA levels and two ABC (HBL-1 and TMD8) DLBCL cell lines with the irreversible CD36 inhibitor SSO at different concentrations. Subsequently, we assessed the mRNA levels of ACADM, HADHA, ACADVL and CD36. As depicted in Figure 52.b, c, d the inhibition of CD36 by SSO had no remarkable effect on

neither the mRNA levels of the β-oxidation key enzyme coding genes nor the mRNA levels of CD36 itself. This was also independent from GCB and ABC subtype. Noticeable exceptions seem to be mRNA expression levels of ACADVL and CD36 in SU-DHL-6 cells treated with 250 µM SSO that exhibit a two fold increase compared to solvent control. In summary, these results indicate that although CD36 is substantially more expressed in the ABC subtype of DLBCL on both the mRNA and the surface protein level, β-oxidation is not affected by this obvious difference. This result also suggests that the level of β-oxidation activity is comparable between DLBCL subtypes. Additionally, from the treatment of GCB and ABC DLBCL cell lines with an irreversible CD36 inhibitor we can conclude that there is no impact on neither β-oxidation nor CD36 mRNA levels when CD36 FA and oxLDL uptake and associated (FA and oxLDL initiated) signaling is blocked. Taken together, this result suggests that CD36 might be a valid biomarker to differentiate between GCB and the more aggressive ABC DLBCL. However, CD36 seems not to be appropriate as a putative therapy target since CD36 blockage had no impact on the expression of genes coding for proteins regulating the activity of the vital β-oxidation which was found to be comparable between the GCB and ABC subtype of DLBCL.

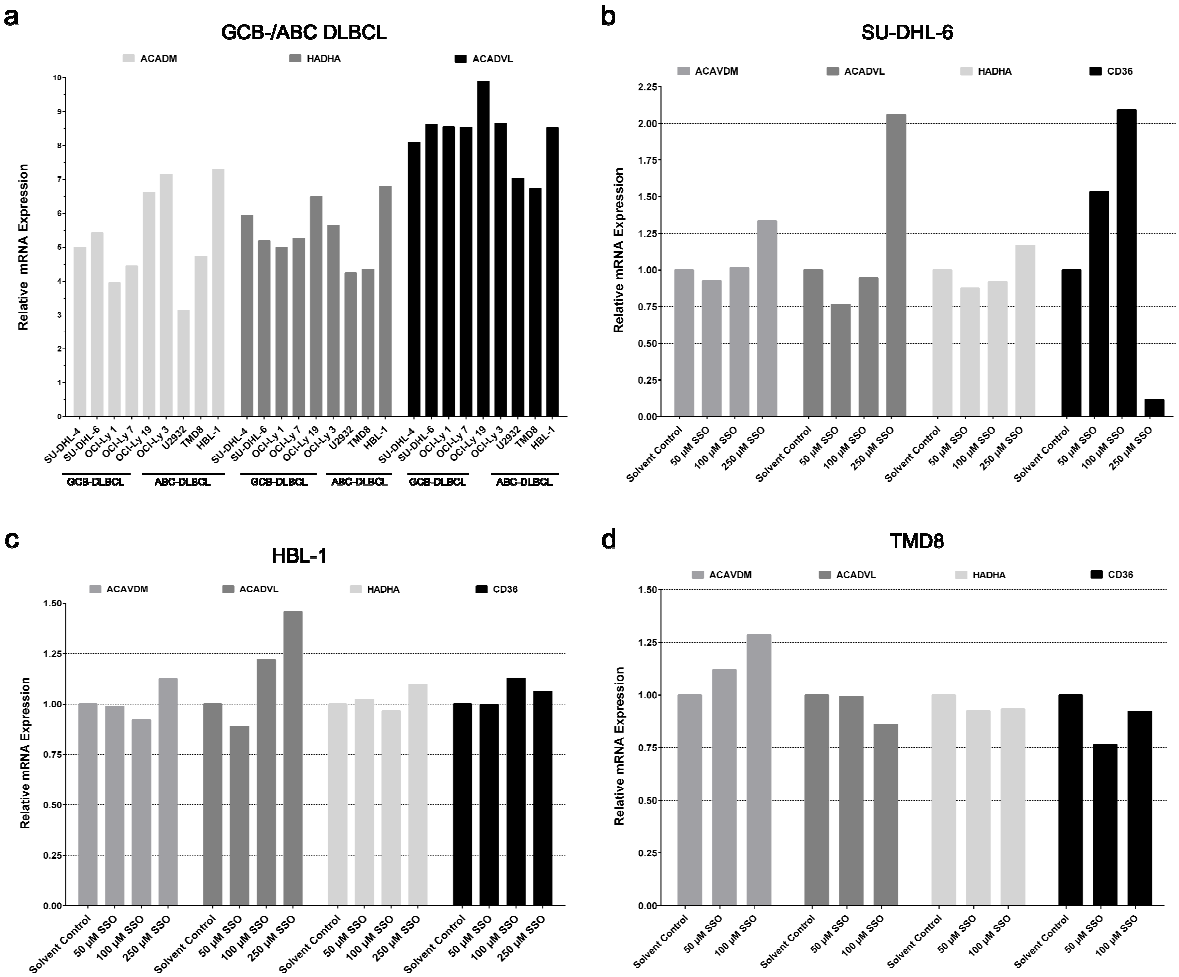

Figure 52. Determining mRNA expression levels of genes coding for β-oxidation key enzymes and CD36 in GCB and ABC DLBCL under steady state conditions and CD36 inhibition by SSO. a) Relative mRNA expression of ACAVDM, HADHA and ACADVL coding for β-oxidation key enzymes were assessed by qPCR in samples from the indicated GCB and ABC DLBCL cell lines and analysed using the ΔCT method. **(b-d)** The GCB cell line **(b)** SU-DHL-6 and two ABC DLBCL cell lines **(c)** HBL-1, **(d)** TMD8 were treated either with solvent as control or the indicated concentrations of the irreversible CD36 inhibitor SSO for 1 h. Subsequently, cells were harvested, RNA was isolated and reversely transcribed into cDNA. By qPCR mRNA levels from ACAVDM, HADHA, ACADVL and CD36 were assessed and analysed using the ΔΔCT method.

4. Discussion

4.1 Significance of DLBCL research

DLBCL are a highly heterogeneous and aggressive B-cell Non-Hodgkin-Lymphoma malignancy. The molecular era of disease characterisation led to steady advances in the development of disease tailored treatment approaches. This includes the establishment of biologicals such as target-directed monoclonal antibodies e.g. rituximab and small molecule drugs e.g. Ibrutinib that are designed to interfere with the effector functions of proteins in key positions of vital signal transduction pathways. These new therapies considerably improved patient overall survival (Link and Friedberg, 2008; Lenz et al., 2008).

In the context of DLBCL treatment, the addition of the anti-CD20 monoclonal antibody rituximab based immunotherapy to the established first-line chemotherapeutics based standard chemotherapy regimen CHOP in 2002, remarkably improved complete remissions by 15 to 20%. Despite the success of rituximab, when having a closer look at the distinct survival rates of the DLBCL molecular subtypes there is still a proportion of patients with advanced DLBCL disease stages who do not response to R-CHOP therapy or exhibit relapsed or refractory DLBCL in the aftermath of R-CHOP immuno- chemotherapy. In particular, patients suffering from the more favourable GCB subtype still exhibit a 3-year progression free survival (PFS) rate of 74% and a 3-year overall survival (OS) rate of approximately 80% upon R-CHOP treatment. Moreover, patients affected by the most aggressive DLBCL and thus less favourable ABC subtype which is often resistant to standard chemotherapies show a worse 3-year PFS rate of 40% and 3-year OS rate of approximately 45% following R-CHOP therapy. (Lenz et al., 2008; Young et al., 2015). Therefore, there is an obvious need for identifying new molecular targets and the further development of corresponding, more efficient novel agents in order to improve clinical outcome and prolong patient survival suffering from this hematopoietic cancer type, especially the adverse ABC subtype. To achieve this aim, understanding the underlying molecular pathological mechanisms characterising (ABC) DLBCL lymphomagenesis is of critical importance.

During the last years, investigation of ABC DLBCL by gene expression profiling revealed constitutive active canonical NF-κB signaling. By transduction of an IκBα super repressor and dominant negative forms of IKKβ as well as the application of IKKβ small molecule inhibitors the ABC DLBCL subtype was unveiled to be addicted to this chronically active NF-kB signaling that emerged to be the major hallmark of this lymphoma entity and a major criterion to distinguish the ABC from the GCB DLBCL subtype (Davis et al., 2001).The aberrant NF-kB signaling was found to be caused by various genetic abnormalities present in different NF-κB activity modulating signal elements constituting key drivers of this oncogenic signaling (e.g. CD79A/B; CARMA1, MYD88 or A20) (Davis et al., 2001; Ngo et al., 2006; Lenz et al., 2008, Compagno et al., 2009, Kato et al., 2009; Davis et al., 2010; Ngo et al., 2011). However, little is known about the role of typical and especially atypical IκBs like IκBNS concerning the oncogenic NF-κB signaling in ABC DLBCL. IκB protein family members are known to be implicated in negative and positive regulation of the NF-κB signaling network and consequently NF-κB target gene transcription. Due to this, investigating their function and importance in contributing to the oncogenic molecular signaling pathways present DLBCL is of great interest. A deeper and more comprehensive knowledge about the regulation and role of the atypical NF-κB inhibitor IκBNS in the context of the complex oncogenic DLBCL pathogenesis is a promising research issue in order to provide a basis for the development of future therapeutic agents.

4.2 The expression of IκBNS in DLBCL subtypes

Within the present study, we showed that in contrast to the GCB DLBCL subtype cell lines the atypical, nuclear IκB family protein IκBNS was constitutively expressed in all tested model cell lines of the ABC DLBCL subtype cell lines as proven by the assessment of mRNA and protein levels. The distribution of IκBNS expression according to DLBCL subtypes was confirmed at least on the mRNA level determined in 19 patient derived samples for each DLBCL subtype. Unfortunately, the background of this measurement was relatively high, most likely due to activated T-cells in the inflammatory tumor environment that also express IκBNS. Based on these findings, we suggest that the expression of IκBNS could be a further biomarker in order to classify the GCB and ABC DLBCL subtypes on the molecular level. This would help to improve stratifying patients into different risk groups and

thus survival prediction and to choose the most suitable therapy strategy. As already mentioned, DLBCL tumor surrounding cells like activated T-cells should also express IκBNS, as indicated by P/I and anti-CD3/28 mediated stimulation of Jurkat T-cells in this study. Thus, in case IκBNS would be applied as ABC DLBCL biomarker in immunohistochemistry, there would be an obvious need to increase the recognition specificity in order to clearly identify IκBNS expression that belongs to the B-cell derived tumor and to exclude IκBNS derived signals from cells present in the tumor environment. For this reason, we suggest that IκBNS staining of DLBCL tumor tissue should be correlated with other already well-established B-cell (e.g. CD20) and DLBCL markers that would in the first line identify DLBCL cells and second the distinct DLBCL subtype. For this purpose, IκBNS staining could be implemented in already established immunostaining based algorithms such as the Hans' algorithm (Hans et al., 2004) that defines the ABC DLBCL type as $CD10^-$, $BCL6^-$, and MUM^+ or an algorithm proposed by Choi et al (2009) that includes GCET1, CD10, BCL6, MUM1, and FOXP1 as staining markers for DLBCL and to distinguish subtypes. According to Choi et al., their proposed immunohistochemistry staining based algorithm has a concordance of 93% with gene expression profiling of DLBCL.

4.3 The mutual transcriptional regulation of IκBNS by NF-κB and NFAT

In addition to the NF-κB signaling addicted ABC DLBCL cell lines, IκBNS expression was also detected in several sotrastaurin (STN)/Ibrutinib sensitive, BCR-driven canonical NF-κB signaling exhibiting MCL cell lines and one STN/Ibrutinib insensitive MCL cell line that displays activation of the non-canonical NF-κB signaling (Rahal et al., 2014). In additional B- and T-cell lymphoma/leukemia model cell lines representing GCB DLBCLs, Burkitt's lymphoma and T-ALL we were able to induce IκBNS expression by the application of P/I or PMA alone albeit in a quite less extent within one hour. Furthermore, also TCR stimulation of a T-ALL cell line triggered the induction of IκBNS expression. The interference with NF-κB upstream signaling by LVSR and STN application under simultaneous cell stimulation by P/I completely abolished the induction of IκBNS expression. Moreover, siRNA mediated knock down of MALT1 in an ABC DLBCL cell line resulted in diminished IκBNS expression levels. Together, these results suggest that IκBNS is a target gene of

canonical NF-κB signaling in a couple of different lymphoma malignancies. The hypothesis of IκBNS expression to be controlled through NF-κB signaling in ABC DLBCL was further strengthened by the induction of its expression on the protein level by CARMA1 mutants found in roughly 10% of ABC DLBCL patient samples to activate the classical NF-κB pathway. Moreover, a putative IκBNS promoter sequence within intron one of the NFκBID gene, bearing NF-κB and NFAT recognition sites was discovered by the analysis of published CHIP-datasets. This promoter sequence showed transcriptional activity when RelA and canonical wild-type NF-κB, mutated upstream elements e.g. MALT1/BCL-10, CARMA1, MYD88 and combinations thereof, how they are commonly found in the context of oncogenic ABC DLBCL signaling, were added. Furthermore, also the noncanonical NF-κB signaling element BIRC3 in its wild-type and a MCL-derived mutant version induced promoter activity. These findings substantiated the hypothesis of IκBNS transcriptional regulation by canonical and noncanonical NF-κB signaling. Further studies of this IκBNS promoter sequence by CHIP and EMSA experiments should validate its capacity to bind NF-κB subunits.

Interestingly, the combination of the NF-κB subunit RelA with Ionomycin was able to induce IκBNS promoter activity more than twice as much as RelA alone. Ionomycin treatment alone however, was not able to induce IκBNS promoter activity. Thus, as anticipated, the addition of NFATc1 did not result in induction of the IκBNS promoter. On the contrary, similarly to the combination with Ionomycin, RelA in combination with NFATc1 caused a strong induction of IκBNS promoter activity compared to RelA alone. Our results therefore indicate that IκBNS transcription is driven by NF-κB signaling in synergy with Ca^{2+}-NFAT signaling as already indicated by the finding of NF-κB and NFAT sites within the IκBNS promoter sequence. Notably, each transcription factor family on its own was able to induce low IκBNS protein levels. Combined expression however, induced strong IκBNS promoter activity consistent with strong induction of IκBNS protein expression in GCB DLBCL cell lines stimulated by P/I.

The assumption that besides NF-kB also NFAT signaling is involved in IκBNS expression regulation was further substantiated by the treatment of constitutively IκBNS expressing ABC DLBCL cells for several days with calcineurin-NFAT signaling inhibitors what led to clearly diminished IκBNS protein levels. Furthermore, also the induction of IκBNS by P/I was obviously impeded by pre-treatment of cells

with calcineurin inhibitors. Moreover, lentiviral mediated expression of a dominant negative IκBα in combination with the application of CsA or FK506 had a clear impairing effect on P/I mediated induction of IκBNS expression in a T-ALL and a GCB DLBCL cell line. Notably, this effect was more pronounced than in cells in which either NF-kB or NFAT was inhibited. Thus, our findings suggest that high IκBNS levels as seen constitutively in ABC DLBCL or upon P/I induction in GCB DLBCL cell lines require the transcriptional activity of both, the NF-kB and NFAT transcription factor family.

In accordance with the previously described results, the treatment with the calcineurin inhibitor CsA revealed that except for the GCB DLBCL cell line SU-DHL-4, NFATc1 was found dephosphorylated in all investigated GCB and ABC DLBCL cell lines, indicating a transcriptionally active NFATc1 state. Notably, in consistence with this finding, nuclear localised and dephosphorylated NFATc1 and dephosphorylated NFATc2 were also reported to be observed in samples obtained from DLBCL patients (Fu et al., 2006; Medyouf et al., 2007). Furthermore, in line with our calcineurin inhibitor results, NFAT activity was shown to be calcineurin-dependent in cell lines derived from DLBCL and T-ALL patients, as their treatment resulted in the suppression of NFAT activation. In addition, NFATc1 activity in DLBCL was also indicated by an immunohistological evaluation of almost 300 lymphoma samples conducted by Marafioti et al. (2005) that revealed NFATc1 to be overexpressed in most lymphoid neoplasms. This overexpression could be at least in some ABC DLBCL cell lines the result of a genomic amplification affecting a 1,9 Mb region of chromosome 18q that includes the NFATc1 gene. This amplification was found in 5% of ABC DLBCL and could cause a gene dosage based overexpression of NFATc1 (Lenz et al., 2008; Müller et al., 2010). Marafioti et al. (2005) observed NFATc1 to exhibit a nuclear localisation in 30% of DLBCL and 70% of Burkitt's lymphoma samples, indicating in vivo activity of the NFAT pathway in those malignancies what is in accordance with our DLBCL cell line model results. In general, the expression of NFATc1 across the investigated DLBCL cell line panel in this study was highly variable and expression levels did not correlate with any particular lymphoma subgroup. Additionally, the sensitivity of DLBCL cell lines towards CsA seems to be independent of NFAT protein expression levels as both, the ABC DLBCL cell lines OCI-LY3 and SU-DHL-2 show very low NFATc1 levels but differ clearly in the sensitivity towards CsA treatment. Thus, the results

indicate that NFAT is of importance for both DLBCL subtypes. Furthermore, blotting against NFATc1 in samples derived from an array of GCB and ABC DLBCL cell lines also revealed three broad NFATc1 specific bands for each cell line. The close bands of each of the three band clusters are most likely different NFATc1 phosphorylation states, whereas the three main bands assumingly represent the different A, B and C NFATc1 isoforms. Considering the predicted NFATc1 isoform sizes, the lowest band represents most likely the NFAT c1/A α (716 aa) and β (703 aa) isoforms, the middle band the NFATc1/B α (825aa) and β (812aa) variants and the upper band the NFATc1/C α (943 aa) and β (930aa) isoforms (uniprot.org.; Entry O95644 (NFAC1_HUMAN)).

Why is NFATc1 dephosphorylated in GCB DLBCL cell lines?

NFATc1 activity in GCB DLBCL cell lines stands in contradiction to the finding that cells show up regulation and constitutively active NFATc1 signaling as a result of activated BCR signaling which can be triggered either by antigen engagement or aberrantly by acquired somatic mutations. Activated BCR signaling leads to the generation of IP3, causing the mobilisation of intracellular Ca^{2+} which in turn initiates the influx of extracellular Ca^{2+} resulting in the activation of calcium dependent signaling such as NFAT (Le Roy et al., 2012; Young et al., 2015). This suggests that NFATc1 activity in GCB DLBCL could be regulated by a mechanism other than BCR signaling. GCB DLBCL were unveiled to be insensitive against targeted knock-down of BCR components such as the mIg light and heavy chain and the associated signaling chains CD79A and B. Also the RNAi mediated knock-down of BCR downstream signaling elements such as SYK, BLNK, BTK, PLCγ2, PKCβ, CARD11 and the pharmacological inhibition of BTK by Ibrutinib, PKCβ by STN, MALT1 by z-VRPR-fmk and IKK by e.g. MLN120B were found to be selectively toxic to ABC DLBCL that do not harbour a CARD11 mutation, but not to GCB DLBCL. (Ngo et al., 2006; Lam et al., 2005; Hailfinger et al., 2009; Davis et al., 2010). Furthermore, this lymphoma subtype does not exhibit common mutations in elements of the BCR signaling cascade. Based on these result, it could be concluded that in contrast to ABC DLBCL, GCB DLBCL do not rely on active BCR and integrated downstream signaling pathways such as NF-kB for survival (Davis et al., 2001). The chronically active BCR signaling of ABC DLBCL encompasses the activation of the PI3K pathway which is a hallmark of multiple cancer types as it is important for cell

survival, growth and proliferation by for instance linking BCR signaling to the prosurvival NF-kB pathway (Pfeifer et al., 2013). Furthermore, the constitutive PI3K activity was found to be vital for two ABC DLBCL cell lines harbouring CD79B mutations (Kloo et al., 2011). However, albeit GCB DLBCL do not exhibit chronic active BCR signaling, Chen et al. (2013) revealed that also a subset of GCB DLBCL depend on SYK mediated activation of the PI3K/AKT pathway. In line with the previous, the GCB DLBCL subtype maintains normal BCR expression but exhibits higher relative SYK expression, contributing to the activation of the PI3K/AKT pathway (Srinivasan et al., 2009; Kenkre et al., 2012; Chen et al., 2013). In accordance with this, GCB DLBCL were also reported to show mutations in the PI3K/AKT pathway negative regulatory phosphatase PTEN, genetic deletions on chr.10q23 comprising the PTEN locus and amplifications of the mIR17-192 micro RNA cluster that result in the inactivation of PTEN in more than 55% of cases and only in 14% of ABC DLBCL (Lenz et al., 2008; Xiao et al., 2008; Song et al., 2012; Chen et al., 2013; Pfeifer et al., 2013). Moreover, Pfeifer et al. (2013) revealed an addiction of PTEN deficient GCB DLBCL cell lines to PI3K/AKT signaling by reexpressing functional PTEN. An investigation of the BCR on the surface of ABC and GCB DLBCL cells revealed that that in contrast to ABC, the GCB DLBCL subtype does not show BCR low diffusion clusters, as they are known for antigen-dependent stimulation of B-cells (Davis et al., 2010). The parallels of ABC DLBCL BCR signaling to antigen-stimulated active signaling in benign B-cells led to the assumption that the chronic active BCR signaling of ABC DLBCL may be driven by auto-antigens. These could be derived from various sources or even as reported in CLL, the ABC DLBCL BCR recognises its self, thereby acting as its own antigen ligand that triggers the intracellular signaling cascade. Considering these facts, it was suggested that the essential PI3K activity in GCB DLBCL cell lines is triggered by so called tonic BCR signaling, which is antigen-independent in contrast to the (auto)-antigen-dependent chronically active BCR signaling observed in ABC DLBCL. Tonic BCR signaling delivers antigen-independent “low level” survival signaling leading to low baseline NF-κB activity as it was shown in SU-DHL-4, SU-DHL-6 cells and enables long term survival of resting B-cells, independent from CARD11. (Gauld et al., 2002, Kraus et al., 2004; Monroe, 2004; Srinivasan et al., 2009; Rossi et al., 2013; Chen et al., 2013). Taking into account the above illustrated mechanism of GCB DLBCL BCR signaling it would be conceivable that the activity

of NFATc1 in the GCB DLBCL cell lines investigated by this study is based on antigen-independent tonic BCR signaling which could lead next to a low baseline NF-κB activity also to a base-line NFAT activity as revealed in BJAB and HT cells. Why SU-DHL-4 cells exhibit only very weakly or no dephosphorylated NFATc1 albeit they were shown to have base-line NF-κB activity remains unresolved and could be an issue for further investigation.

Whereas the GCB cell lines were entirely resistant, the inhibition of NFAT signaling by calcineurin inhibitors did not affect growth behaviour of all comprised ABC DLBCL cell lines in the same manner. Even though NFAT was seemingly active in all model cell lines and all of them expressed high IκBNS levels. Thus, calcineurin inhibition seemed to be selectively toxic and we could distinguish ABC DLBCL cell lines responding insensitively, medium sensitively and highly sensitively to calcineurin inhibitor treatment. In order to reveal the underlying reason why ABC DLBCL cell lines exhibit altered growth behaviour upon calcineurin inhibitor treatment, we found a clear correlation between increasing concentrations of calcineurin inhibitors and the reduced secretion of the survival promoting and pro-proliferative interleukins IL-6 and IL-10 and corresponding STAT3 phosphorylation levels. ABC DLBCL were described by earlier studies to be addicted to an autocrine/paracrine positive feedback loop including IL-6 and IL-10, that is driven by NF-κB signaling and interleukin receptor downstream STAT3 phosphorylation (Moore et al., 2001; Kishimoto et al., 2005; Lam et al., 2008). Furthermore, we excluded some well known NF-κB signaling targets to be affected by calcineurin inhibitor treatment by testing the expression levels and revealed a dose-dependent negative effect of CsA mediated calcineurin inhibition on STAT3 phosphorylation, indicating that only a subset of NF-κB targets such as IL-6 and IL-10 are affected by calcineurin inhibition (Libermann and Baltimore, 1990; Xu and Shu, 2002). The described impact of pharmacological calcineurin inhibition on ABC DLBCL growth was thus most pronounced in inhibitor highly sensitive cell lines that exhibited the strongest decrease in p-STAT3 levels and IL-6 and IL-10 amounts. Whereas no change in secreted interleukin levels and STAT3 phosphorylation was observed in calcineurin inhibitor insensitive ABC DLBCL cell lines. A recently published work proposed a model in which calcineurin is recruited to the TCR and acts there as positive modulator of TCR downstream signaling by removing an inhibitory TCR activation induced phosphorylation (Dutta et al., 2017). As TCR and BCR signaling

show many similarities we propose calcineurin to be involved in BCR signaling, as well. We therefore speculate that calcineurin participates in BCR signaling positive regulation in ABC DLBCL that leads to enhanced NF-κB and NFAT signaling. Either this occurs indirectly by removing an inhibitory phosphorylation from an unknown substrate which in turn, in its active state, positively regulates BCR downstream signaling or directly by dephosphorylation of substrates in the BCR signaling chain.

4.4 Calcineurin as positive regulator of BCR signaling

In order to find the assumed putative calcineurin substrate(s) in BCR signaling, we conducted a phosphoproteom analysis by SILAC with subsequent MS with samples derived from CsA or FK506 treated ABC DLBCL HBL-1 cells. Indeed, phosphoproteom analysis identified a couple of putative new substrates that are involved BCR signaling. The fact that the found possible direct and indirect calcineurin substrates were far upstream in BCR-signaling would explain why CD79 mutated ABC DLBCL cell lines were worst affected by calcineurin inhibitor treatment. Thus, it would be conceivable that NF-kB activating mutations of more downstream signaling elements such as CARMA1, TAK1 or A20 just compensate or mitigate the loss of the calcineurin mediated positive effect on BCR signaling as consequence of CsA or FK506 mediated calcineurin inhibition. This downstream mutation overwriting mechanism eventually leads to unaltered or only slightly declined NF-κB signaling and thus to an only minor impact on IL-6 and IL-10 secretion of cells bearing such mutations such as OCI-LY3 or SU-DHL-2. This in turn would explain the more insensitive effect on the growth of those cell lines when treated with calcineurin inhibitors.

Several putative calcineurin dependent dephosphorylation sites namely S197, T209, Y210, S215 in CD79A and S221 in CD79B were found hyperphosphorylated by phosphoproteom analysis in HBL-1 samples that were treated by the calcineurin inhibitors CsA and FK506. Except for S197, all putative calcineurin substrate sites found in CD79A are located C-terminally from the CD79A ITAM sequence (aa 185 - aa 202) which plays a central role in transmembrane signal transduction. Essential for the functionality of the CD79A ITAM are two tyrosine-residues Y188 and Y199. In the context of ABC DLBCL biology, Davis et al. (2010) found by sequencing that

2,9% of patient derived biopsies had a mutation affecting CD79A. The ABC DLBCL cell line OCI-LY10 for instance, exhibits a heterozygous CD79A splice donor site mutation leading to a deletion of 18 aa, eradicating almost the whole ITAM sequence. Remarkably, over 90% of the OCI-LY-10 CD79A mRNA derived from the mutated allele. Under resting conditions, the BCR is suggested to be already associated with a preformed transducer complex as a prerequisite for BCR signaling, including kinases, phosphatases and diverse adaptor proteins (Wienands et al., 1996). In particular, Clark et al. (1992) conclude from their results that the cytoplasmic domains of CD79 associate with the src-family tyrosine kinases LYN and FYN, the PI3K and one or more serine/threonine (S/T) kinases, putative antagonists of calcineurin.

Upon ligand binding of the IgM, a member of the src family protein-tyrosine kinase family, predominantly LYN initially catalyses, the phosphorylation of the first N-terminal ITAM tyrosine of CD79A and CD79B (see Figure 53.). Noteworthy, the ITAM tyrosines of CD79B are less efficiently phosphorylated than the corresponding CD79A tyrosines. This N-terminal p-tyrosine provides a docking site for the C-terminal SYK SH2-domain. SYK is described to be a vital component in BCR signaling and was shown by mouse knock out models to be indispensable for the majority of BCR signaling mediated responses to antigen binding (Takata et al., 1994; Turner et al., 1995; Cheng et al., 1995; Cornall et al., 2000). A structural NMR based study conducted by Gaul et al., 2000, suggests that the preference of LYN towards the first ITAM tyrosine is based on the interaction of LYN with a glutamate residue three positions C-terminally and a glycine residue two aa N-terminally from the acceptor tyrosine (see Figure 53.). In order to generate proper signal transduction by CD79A however, asymmetrical ITAM phosphorylation is insufficient. Therefore, the phosphorylation of both ITAM tyrosines is required. Most likely, SYK itself exerts this second ITAM phosphorylation at Y199 (Rolli et al., 2002). Only then an interaction of the CD79A ITAM with the SYK tandem-arranged pair of SH2 domains is possible and leads to SYK activation and further signal propagation. Long lasting SYK activity is needed by NFAT to remain active for more than one hour after the triggering of the BCR (Oh et al., 2007), indicating the importance of CD79 signaling for IκBNS expression. Not only CD79A and B ITAM tyrosine residues become phosphorylated upon BCR ligand binding but also several serine and threonine residues (Clark et al., 1992; Van Noesel et al., 1990; Leprince et al.,

1992). Serine/threonine residue phosphorylation was observed in the cytoplasmic portions of various receptors and conferred either negative or positive influence on downstream signal transduction (Mufson, 1997; Lim and Cao, 1999; Li et al., 1999). Hence, Müller et al. (2000) were keen to figure out which impact the S/T residues in the cytoplasmic tail of CD79A (aa 166-aa 226) would have on BCR signaling. For this purpose, they mutated two serines and the threonine of the CD79A cytoplasmic domain (see Figure 53.) to non-phosphorylatable alanines and a valine, respectively. Among the mutated residues were also our putative CD79A calcineurin dephosphorylation sites S197 and T209. By testing the signaling function of this unphosphorylatable CD79A they revealed that the phosphorylated S/T residues of CD79A negatively regulate BLNK and ITAM tyrosine phosphorylation. In particular, they observed a stronger and more prolonged ITAM tyrosine phosphorylation of the S/T unphosphorylatable CD79A compared to the S/T phosphorylatable wild-type CD79A. This finding indicates that CD79A S/T kinases negatively modulate BCR signaling output. This is in accordance with our assumption that the S/T phosphatase calcineurin seems to positively regulate BCR signaling for instance by removing CD79A ITAM signaling hampering phosphorylations on S197, T209 and S215 as unveiled by SILAC/MS. This would establish calcineurin as an antagonist of the CD79A S/T kinases that negatively regulate CD79 proximal signaling. Moreover, Müller et al. also investigated the impact of the unphosphorylatable CD79A variant on the phosphorylation of both CD79A ITAM tyrosines, Y188 and Y199, from which the phosphorylation of the former is more pronounced. To analyse this, they substituted either one of ITAM tyrosines or both tyrosines with phenylalanines with and without an additional unphosphorylatable CD79A background. This experimental setting unveiled that the mutation of the N-terminal CD79A ITAM tyrosine (Y188F) leads to an only weakly phosphorylated second C-terminal ITAM tyrosine in the context of a S/T phosphorylatable CD79A cytoplasmic tail. In contrast to that, a mutated N-terminal ITAM tyrosine in an S/T unphosphorylatable CD79A background results in an increase of the phosphorylation of the second ITAM tyrosine. On the other hand, the mutation of the C-terminal ITAM tyrosine (Y199F) in both CD79A backgrounds did not remarkably alter CD79A phosphorylation. From these outcomes the authors concluded that the phosphorylation of S/T residues in the cytoplasmic CD79A portion mainly regulates the phosphorylation of the C-terminal CD79A ITAM tyrosine

(Y199). This is also implicated as well by the fact that Y199 is situated in the proximity to three flanking serine residues (S197 and S203 and S215) and one threonine residue (T209). All of them except for S203 were found to be hyperphosphorylated in our SILAC/MS based phosphoproteom analysis conducted with samples derived from a calcineurin inhibitor treated ABC DLBCL cell line. Noteworthy, the binding of the second C-terminal ITAM tyrosine to SYK is stronger than that of the C-terminal SYK SH2 domain to the first N-terminal ITAM tyrosine (Fütterer et al., 1998). Considering the depicted facts, it's reasonable to assume that the balance between phosphorylation and dephosphorylation of CD79 by associated so far unidentified kinases and phosphatases of the putative calcineurin target sites S197, T209 and S215 in the cytoplasmic portion possibly modulates the binding of SYK to CD79A and thus further signal transduction as well. In this proposed model, phosphorylation of the S/T residues impedes proper high-affinity SYK CD79 binding and further signaling, establishing a negative feedback loop. Whereas dephosphorylation of distinct aa-residues in the cytoplasmic portion by e.g. the S/T phosophatase calcineurin promotes the phosphorylation of the ITAM tyrosines followed by high-affinity binding of both SYK SH2 domains and proximal BCR signaling. The same mechanism we propose for CD79B.

Why does calcineurin modulate upstream BCR signaling?

Considering our obtained results in the context of the depicted literature it is conceivable that under BCR unligated conditions, the cytoplasmic portions of CD79A and B are constitutively phosphorylated by S/T kinases at the introduced serine and threonine residues in order to prevent premature or non-specific activation of proximal BCR signaling. Furthermore, upon ligand binding the delicate balance between phosphorylated and unphosphorylated S/T residues in the CD79 cytoplasmic portion could represent a fine-tuning mechanism for the extent of BCR proximal signal propagation in order to adapt to external stimuli and to respond in adequate degree. Thus, when calcineurin is pharmacologically inhibited by the application of CsA or FK506, the phosphorylated CD79A/B state is predominant and BCR signal propagation to downstream pathways such as NF-κB, NFAT and AP-1 is dampened or completely ceased. Unless downstream activating mutations in proteins like CARMA1 as found in the CsA/FK506 insensitive cell line OCI-LY3 override this effect. Accordingly, the constitutive expression of NF-κB and NFAT

target genes such as IκBNS and IL-6 and IL-10 in ABC DLBCL in which calcineurin is constitutively active as indicated by dephosphorylated NFATc1, would be negatively affected by calcineurin inhibition, as well in turn leading to reduced growth and survival as seen in this study. Notably, this theory would be in line with the finding that T-cells that express an unphosphorylatable CD79A exhibit constitutive NFAT and thus calcineurin activity, as well (Müller et al., 2000).

In contrast, it is also imaginable that under non-stimulated conditions, the CD79A and B cytoplasmic tails are kept in an S/T unphosphorylated state with the participation of calcineurin and other phosphatases and become gradually or at once phosphorylated instantly or after a certain time upon BCR engagement. Thus, in case calcineurin is inhibited just prior to and during BCR stimulation, CD79A would be hyperphosphorylated at all time and signal propagation would be blocked as ITAM tyrosines were not efficiently phosphorylated by src kinases as LYN.

How the phosphorylated S/T residues in CD79A and B inhibit ITAM tyrosine phosphorylation by src kinases however remains elusive. Hypothetically, the phosphorylated serines and threonines could depict sites for protein-protein interactions providing binding platforms for proteins that consequently interfere with LYN and SYK binding and thus with further signal transduction, a mechanism that was already observed several times in other receptors (Yaffe and Cantley, 1999; Bünemann and Hosey, 1999; Levine, 1999). Another possibility is that the phosphorylated S/T residues just represent a steric hindrance for the binding of proximal signal transducers such as SYK and BLNK and thus disrupt the signaling cascade.

Contrary to its positive impact on BCR proximal signaling, the cytoplasmic ITAM bearing part of CD79A was also found to encompass a function in BCR signal inhibition. This was concluded from mouse B-cells, expressing a truncated CD79A molecule lacking a large part of the endoplasmic tail thus including only 21 instead of 61 aa and lacking the ITAM sequence. These murine B-cells were hyperactive and could be stimulated easier by BCR cross-linking and additionally show constitutive BCR signaling. (Kraus et al.1999, Torres et al., 1996; Torres and Hafen, 1999).

This resembles the ABC DLBCL cell line OCI-LY10 which lacks aa 191 to aa 208, affecting a large stretch of the ITAM of CD79A including the second ITAM tyrosine and the putative calcineurin site S197 and just flanks T209, another putative

calcineurin target site found by the phosphoproteom analysis. Taking into account the findings from Müller et al. (2000) and the B-cells bearing truncated CD79A, this deletion could cause enhanced and sustained BCR signaling, consequently leading to NF-kB and NFAT signaling as the inhibitory function of p-S197 is missing, conferring a positive modulation similar to calcineurin by S197 dephosphorylation. SYK would then nevertheless be able to bind the CD79A N-terminal phosphorylated tyrosine albeit in a lower affinity and promote downstream signaling. Alike CD79A, CD79B also contains two ITAM tyrosines that upon src kinase mediated phosphorylation recruit and bind SYK (Rowley et al., 1995). Likewise in CD79A the second ITAM tyrosine of CD79B is surrounded by several S/T residues.

As already mentioned earlier, the phosphoproteom analysis in HBL-1 also unveiled with S221 a putative calcineurin dephosphorylation site in CD79B in close proximity to the second ITAM tyrosine. Assuming that the theory of downstream signaling inhibitory S/T residues also applies for CD79B, the dephosphorylation of S221 by calcineurin could also result in enhanced CD79B ITAM tyrosine phosphorylation and lead to SYK recruitment and consequently to positive modulation of BCR signaling. Interestingly, the ABC DLBCL cell lines HBL-1 and TMD8 used in this study, harbour a heterozygous missense mutation leading to the substitution of the first CD79B ITAM tyrosine to a phenylalanine (HBL1-1: Y196F) or histidine (TMD8: Y196H), respectively, preventing their phosphorylation. However, though heterozygous, over 90% of total CD79B mRNA in HBL-1 was originating from the mutant allele according to Davis et al. (2010). The replacement of the BCR proximal signaling essential first CD79B ITAM tyrosine was found by Davis et al (2010) to occur in 18% of patient derived samples. The group also found that this substitution of the first CD79B ITAM tyrosine led to elevated BCR surface levels and decreased LYN kinase activity. In accordance with this, also GCB DLBCLs that were reconstituted with common ABC DLBCL CD79 A or B mutants were observed to have higher surface Ig levels than wild-type controls. Moreover, also ABC DLBCL that were transduced with mutant CD79B expressed increased BCR amounts in their surface compared to wild-type bearing controls. Furthermore, murine B-cells that bear mutations in CD79A or CD79B ITAM tyrosines were shown to exhibit increased surface BCR levels due to inhibited receptor clathrin-dependent endocytosis. The increased number of BCR on the cell surface leads to the amplification of BCR signaling which calcineurin activity could even further enhance by

dephosphorylating S221 of CD79B and thus promote the phosphorylation of the second C-terminal ITAM tyrosine (Y207) providing a docking site for SYK. The CD79 ITAMs are also needed for the controlled termination of BCR signaling as they mediate receptor internalisation. Notably, murine B-cells that harbour CD79A/B ITAM impairing mutations were observed to response more sensitive to antigen encounter (Gazumyan et al., 2006; Kraus et al., 1999; Torres et al., 1999). A study by Busman-Sahay (2013) who established a model system including both CD79 subunits, showed that the N-terminal CD79B ITAM tyrosine (Y196) is the only ITAM tyrosine needed for internalisation. In addition to that, they also unveiled that the CD79A cytoplasmic portion is required to activate CD79B's ability to trigger BCR receptor endocytosis. Thus, deletion mutations of CD79A as found in OCI-LY10 could interfere as well with proper BCR internalisation.

LYN is a further factor, needed for BCR internalisation that is as already mentioned above, less active in CD79B membrane-proximal ITAM tyrosine mutated cells (Ma et al., 2001; Niiro and Clark., 2002). LYN holds a dual role within BCR signaling since it promotes signaling by phosphorylating CD79 ITAM tyrosines but is also capable of attenuating BCR signaling by phosphorylating CD22 ITIMs leading to the recruitment of the protein tyrosine phosphatase SHP-1 (refer to: chapter BCR signaling). Conclusively, the mutation of the HBL-1 and TMD8 N-terminal ITAM tyrosine (Y196), the partial deletion of the CD79A ITAM as seen in OCI-LY10 cells or the deletion of the CD79A cytoplasmic portion would therefore result in declined LYN kinase activity mediated increased BCR surface presence, as a consequence of impaired endocytosis, promoting chronically active BCR signaling.

The mutation of the first N-terminal CD79A ITAM tyrosine to phenylalanine by Müller et al. led to decreased phosphorylation of the second ITAM tyrosine in an otherwise S/T phosphorylatable CD79A cytoplasmic tail. However, in a non-phosphorylatable CD79A background, mimicking the dephosphorylated state as sustained by S/T phosphatases such as calcineurin, Y188F mutation resulted in enhanced phosphorylation of the second C-terminal ITAM tyrosine (Y199). Transferring these observations to CD79B in the context of HBL-1 and TMD8 mutations, this would mean that CD79B bearing the somatically acquired Y196H or Y196F mutations would exhibit higher phosphorylation of the second ITAM tyrosine (Y207) assumingly mediated by a src family kinase in a S/T dephosphorylated background sustained by calcineurin enzymatic activity resulting in positive modulation of

chronic BCR signaling in ABC DLBCL. However, as soon as the phosphate activity of calcineurin is blocked by CsA or FK506, S221 would not be kept in its phosphorylated state anymore and as a consequence of this, the second ITAM tyrosine Y207 would be phosphorylated only weakly. This would lead to an attenuating impact on the binding of SYK and consequently BCR signaling transduction. CD79B does not harbour non-ITAM tyrosines that are crucial for binding BLNK. Consequently, only CD79A is able to recruit BLNK to the BCR signaling complex upon ligand binding, though both CD79 subunits can bind SYK by phosphorylated ITAM tyrosines (Rowley et al., 1995). However, the CD79B subunit exhibits only weak ITAM tyrosine phosphorylation (Clark et al., 1992; Flaswinkel and Reth, 1994). Furthermore, CD79A and CD79B induce different kinds of calcium signaling. Only CD79A induces transmembrane Ca^{2+} influx and a long-lasting single shot release of intracellular Ca^{2+} stores. Whereas CD79B induced emptying of intracellular Ca^{2+} stores is described to be brief and oscillatory (Choquet et al., 1993), indicating that CD79B alone does not have the competency to initiate proper primary BCR downstream signaling on its own. Luisiri et al. (1996) found that CD79B is able to enhance the tyrosine phosphorylation of CD79A by more than 10-fold associated with a reduction of the stimulation threshold for tyrosine kinase activation. Therefore, CD79B seems rather to regulate CD79A tyrosine phosphorylation and thus the signaling transducing capability of CD79A instead of inducing primary BCR-signaling itself. Considering the CD79B ITAM tyrosine phosphorylation promoting influence on CD79A, calcineurin phosphatase inhibition that leads to an increased CD79B S221 phosphorylation and assumingly to the inhibition of ITAM tyrosines phosphorylation and thus to the prevention of SYK binding to CD79B could therefore also interfere with the ability of CD79B to positively regulate CD79A ITAM tyrosine phosphorylation and thus to negatively regulate the proximal BCR signaling cascade.

Phosphoproteom analysis also revealed the CD79A non ITAM residue Y210 to be hyperphosphorylated under calcineurin inhibitory conditions in the ABC DLBCL cell line HBL-1. Kabak et al. (2002) all showed the corresponding ITAM flanking murine residue Y204 to be required, in its phosphorylated state, for the recruitment and direct binding to the linker protein BLNK by its SH2 domain. They also conclude from their findings that the murine Y176 (human Y182), which was not found to be phosphorylated, contributing to a functional coupling of BLNK to CD79A by a

phosphorylation independent mechanism. They suppose that this contribution to BLNK binding is achieved by the spatial orientation of BLNK to the kinase domain of SYK. The binding of BLNK to CD79A by phosphorylated Y210 brings BLNK into proximity of the CD79A ITAM tyrosine bound SYK. Consequently, SYK is capable of phosphorylating BLNK tyrosines that serve as binding partners for SH2 domains of different signaling proteins that integrate multiple downstream signaling pathways. In this manner, SYK activation is linked to downstream pathways. Moreover, Kabak et al. (2002) report that tyrosine-to-phenylalanine mutation of Y204 (corresponding to the human Y210) and to a lesser extent Y176 (corresponding to the human Y182) led to a reduction of BLNK phosphorylation and subsequent BLNK dependent pathways like JNK activation. Furthermore, CD79A Y176 and Y204 (human: Y182 and Y210) mutation and the consequent inability of BLNK to bind CD79A cannot be compensated by CD79B as it does not harbour any tyrosine residues outside of the ITAM in its cytoplasmic domain (Müller et al., 2000). The enhanced phosphorylation of the CD79A Y210 upon CsA and FK506 treatment of HBL-1 and the subsequent BLNK binding and SYK dependent phosphorylation assumingly results in the maintenance of BCR downstream signaling as suggested by Kabak and colleagues. This contradicts the proposed role of the S/T phosphatase as a positive modulator of BCR signaling. Moreover, it stands also in opposition to the suggestion of Kabak et al. that SYK recruitment by phosphorylated CD79A ITAM tyrosines is a prerequisite for the phosphorylation of Y204 (human Y210). On the other hand, Müller et al. (2000) assume based on their findings that the rapid phosphorylation of BLNK does not need prior ITAM phosphorylation and suggest that the phosphorylation of S/T residues in CD79A negatively regulates BLNK and ITAM phosphorylation. One possible explanation for this calcineurin inhibition induced Y210 hyperphosphorylation could be a mechanism in which after a certain time of calcineurin inhibition that leads to a negative impact on BCR-signaling by the above described mechanism, Y210 is phosphorylated e.g. by a certain src-kinase establishing some kind of bypass in order to maintain BCR signaling. This signaling is supposed to be of a small magnitude as BCR signaling addicted ABC DLBCL that do not harbour CD79 proximal BCR signaling or NF-kB and NFAT activating genetic alterations such as the mutation of CARD11 or the deletion of A20, respectively are impaired in growth. Moreover, as observed by the treatment of ABC DLBCL cell

lines with calcineurin inhibitors, the expression of mutual NF-kB and NFAT target genes such as IκBNS become clearly reduced.

Furthermore, also the scaffold protein BLNK was affected by the inhibition of calcineurin S/T phosphatase activity. The BLNK aa-residues S129; S213; S409 and S270 were found to be hypophosphorylated as a consequence of pharmacological calcineurin phosphatase activity inhibition by CsA and FK506. As calcineurin is a phosphatase, this hypophosphorylation has to be a secondary effect, assumingly caused by a kinase that is positively regulated by calcineurin. This result also suggests that these serine residues participate in positive regulation of BCR downstream signaling when they are phosphorylated. Their actual function(s) however remains elusive and should be an issue of future studies e.g. by assessing the effects on downstream signaling by replacing the serine residues through unphosphorylatable or phosphomimicking residues.

However, it also conceivable that the CD79A Y210 residue that was phosphorylated in the proposed bypass mechanism under calcineurin inhibition is bound by BLNK which is subsequently relieved of inhibitory phosphorylations by the activity of an unknown S/T phosphatase at S129; S213; S409 and S270, which are to the best of our knowledge undescribed in literature. Inhibition of those phosphorylations in turn would lead to an aberrant BLNK function because SYK does not phosphorylate the tyrosine residues that serve as binding platform for signaling elements. SYK would not be active due to the lacking phosphorylations of the CD79A/B ITAM tyrosines to which it normally binds and subsequently gets activated.

According to the conducted phosphoproteom analysis, also the BCL-10 residue S138 was affected by calcineurin inhibition as it was found to be present in a hyper-phosphorylated state, indicating that this particular phosphorylated BCL-10 serine residue is a substrate of calcineurin S/T phosphatase activity. This finding is in line with a study conducted by Palkowitsch et al. (2011). They report that calcium influx is essential for proper CBM complex formation as the calcium dependent catalytically active calcineurin subunit CnA in stimulated Jurkat T-cells and in vitro was found to positively affect the formation of the CBM complex by the dephosphorylation of BCL-10. Thus, they suggest that the calcium signaling dependent S/T phosphatase calcineurin is implicated in the assembly of the CBM complex. As the formation of the CBM complex is a prerequisite for NF-κB activity the calcineurin dependent BCL-10 dephosphorylation also positively regulates TCR

induced activity of NF-κB signaling. Also Zeng et al. (2007) conclude from their experiments that T-cell activation induces BCL-10 phosphorylation. BCL-10 S138 and the surrounding serine residues S134, S136, S141 and S144 in the serine/threonine rich C-terminal BCL-10 domain that contains about 20% S/T residues are known to be IKKβ targets (Wegener et al., 2006). Their phosphorylation by IKKβ was found to interfere with T-cell activation as it leads to a change in the structure of the MALT1-BCL-10 dimer that is present in the cytoplasm of unstimulated cells, resulting in the attenuation of CBM complex assembly when cells are stimulated (Wegener et al., 2006). Thus IKKβ acts also upstream of IκB phosphorylation by phosphorylating BCL-10 and is in this fashion able to negatively and positively regulate antigen receptor induced NF-kB activity, establishing a negative feedback mechanism by the phosphorylation of BCL-10 at S138. In accordance with this, studies conducted by Scharschmidt et al. (2004) and Hu et al. (2006) describe an ubiquitin mediated degradation of BCL-10 that is induced by T-cell activation. Palkowitsch and colleagues found that calcineurin acts as IKKβ antagonist since they observed calcineurin to reverse the IKKβ mediated BCL-10 hyperphosphorylation. Especially the phosphorylation of S138 is associated with a signal-induced degradation of BCL-10. Zeng et al. (2007) mutated S138 to an alanine and observed an impaired T-cell activation-induced phosphorylation of BCL-10, prevented activation-induced BCL-10 ubiquitination and thus a delayed BCL-10 degradation. Consequently, the replacement of serine 138 to an unphosphorylatable alanine results also in prolonged NF-κB signaling and consistent with that an increased IL-2 secretion. In consistency with this, the mutation of these BCL-10 serines by Wegener et al (2006) was also found to result in enhanced expression of the NF-kB target genes IL-2 and TNF-α upon activation of primary T-cells. These finding is in accordance with the revealed reduced expression of the NF-κB targets IL-6 and IL-10 in calcineurin inhibitor sensitive ABC DLBCL cell lines in this study. In summary, Zeng and colleagues conclude from these findings that the phosphorylation at the BCL-10 S138 is the trigger for BCL-10 ubiquitination and subsequent degradation upon cell activation. Furthermore, the phosphorylation of BCL-10 at S138 was found to negatively regulate the NF-κB pathway and subsequent IL-2 production, assumingly in order to properly terminate T-cell activation. By co-immunoprecipitation Palkowitsch et al. revealed that CnA obviously interacts constitutively with the CBM complex

components MALT1 and CARMA1. Moreover, they also demonstrate that the pharmacological calcineurin inhibitors (CsA and FK506) and in a weaker extent the siRNA mediated knockdown of CnA interferes with P/I or anti-CD3/28-induced CBM complex assembly in T-cells. This was indicated by a reduction of BCL-10-CARMA1 interaction. Moreover, Zeng et al. confirmed the impairing effect of the unphosphorylatable BCL-10 S138A mutation on cell activation-induced degradation of BCL-10, they had observed in Jurkat T-cells as well as in primary murine splenic B-cells. Due to this and because B-cells share many similarities with T-cell antigen-receptor signaling it is justified to transfer the results obtained by Zeng and Palkowitsch into the context of ABC DLBCL signaling. Thus we suggest, that the chronically active BCR and Ca^{2+} signaling induced calcineurin constitutively dephosphorylates BCL-10 at S138. This in turn results in a promotion of CBM complex formation and an inhibition of ubiquitin mediated BCL-10 degradation. This means that the inhibition of calcineurin by CsA or FK506 BCL-10 results in BCL-10 hyperphosphorylation at S138, assumingly mediated by IKKβ. This in turn leads to enhanced BCL-10 ubiquitination followed by BCL-10 degradation. The downregulation of BCL-10 has a negative regulatory effect on NF-κB signaling resulting in diminished transcriptional induction of respective NF-κB target genes such as IκBNS as well as IL-6 and IL-10. As a consequence of the proposed mechanism, especially ABC DLBCL cell lines like HBL-1 and TMD8 that do not harbour CBM complex formation promoting or CBM downstream NF-κB signaling activating mutations could therefore be very sensitive towards the treatment with pharmacological inhibitors of calcineurin.

Taken together, there exist several elements at different positions in antigen receptor signaling on which calcineurin S/T phosphatase activity could exert its positive regulatory influence on the signaling cascade. The different mutation pattern of ABC DLBCL are suggested to influence the consequences of calcineurin inhibition. Only ABC DLBCL cell lines harbouring signaling transduction activating mutations downstream of calcineurin engagement in proximal BCR signaling are supposed to compensate or mitigate the loss of calcineurin positive modulation and are thus less to non-sensitive towards CsA and FK506 treatment.

a CD79A amino-acid sequence

```
1          10          20          30          40          50
MPGGPGVLQA LPATIFLLFL LSAVYLGPGC QALWMHKVPA SLMVSLGEDA
          60          70          80          90         100
HFQCPHNSSN NANVTWWRVL HGNYTWPPEF LGPGEDPNGT LIIQNVNKSH
         110         120         130         140         150
GGIYVCRVQE GNESYQQSCG TYLRVRQPPP RPFLDMGEGT KNRIITAEGI
         160         170         180         190         200
ILLFCAVVPG TLLLFRKRWQ NEKLGLDAGD EYEDENLYEG LNLDDCSMYE
         210         220     226
DISRGLQGTY QDVGSLNIGD VQLEKP
```

b CD79B amino-acid sequence

```
1          10          20          30          40          50
MARLALSPVP SHWMVALLLL LSAEPVPAAR SEDRYRNPKG SACSRIWQSP
          60          70          80          90         100
RFIARKRGFT VKMHCYMNSA SGNVSWLWKQ EMDENPQQLK LEKGRMEESQ
         110         120         130         140         150
NESLATLTIQ GIRFEDNGIY FCQQKCNNTS EVYQGCGTEL RVMGFSTLAQ
         160         170         180         190         200
LKQRNTLKDG IIMIQTLLII LFIIVPIFLL LDKDDSKAGM EEDHTYEGLD
         210         220         229
IDQTATYEDI VTLRTGEVKW SVGEHPGQE
```

Figure 53. CD79A and B amino-acid sequences. (a, b) In bold: the CD79A/B cytoplasmic portions. Underlined: the CD79A/B ITAM sequences. ITAM regions were revealed to be affected by somatically acquired mutations in 2,9% of GCB DLBCLs and 21,1% of ABC DLBCL. Highlighted in red: ITAM tyrosines which are important in their phosphorylated state for SYK binding at the sequence positions **(a)** Y188 and Y199 in CD79A and **(b)** Y196 and Y207 in CD79B. The CD79B N-terminal ITAM tyrosine (Y196) was found to be substituted by multiple amino acids due to point mutations in 18% of ABC DLBCL as for instance in HBL-1 (Y196F) and TMD8 (Y196H) model cell lines. The ABC DLBCL cell line model OCI-LY10 has a heterozygous splice donor site mutation that leads to the deletion of 18 aa affecting the majority of the ITAM sequence. Highlighted in yellow: S/T/Y residues found hyperphosphorylated by phosphoproteom analysis upon CsA and FK506 treatment of HBL-1 cells. For further information see continuous text. Amino-acid sequences taken from uniprot.org: Entry name: CD79A_HUMAN; Entry P11912; Entry name: CD79B_HUMAN; Entry: P40259.

4.5 Characterisation of two IκBNS isoforms

RNAi mediated knockdown and the application of the CRISPR/Cas9 technique both, originally designed to target IκBNS p35, revealed the presence of a second IκBNS isoform sharing the respective target sequences and originating from the same gene locus. The new isoform was observed to be expressed always along with the IκBNS p35 protein in all tested cell lines and exhibits a size of approximately 70 kDa in

SDS-PAGE. Consequently, protein levels were affected by both gene expression editing techniques. This new IκBNS p70 isoform was observed to exhibit an endogenous expression level more than twice as high as IκBNS p35 under constitutive expression in ABC DLBCL and P/I and anti-CD3/28 triggered expression in GCB DLBCL, Burkitt's lymphoma and T-ALL cell lines. On the other hand, IκBNS p70 showed the same characteristics as IκBNS p35 regarding expression levels and subcellular distribution upon P/I mediated cell stimulation in GCB DLBCL cell lines and under constitutive expression in ABC DLBCL. The treatment of ABC DLBCL cell lines with cycloheximide revealed no difference between half-lifes of both IκBNS isoforms.

The 70 kDa IκBNS specific signal was already described by earlier studies in murine cells and was assumed to emanate from one gene locus but was suggested to be generated by a posttranslational modification (Schuster et al., 2012; Jeltsch et al., 2014). Deep sequencing comprising ABC DLBCL samples revealed that there exists only one Nfκbid mRNA that should be therefore the origin of both, the IκBNS p35 and p70 signal. Indeed, the usage of an ORF prediction tool applied on the Nfκbid mRNA sequence, unveiled the existence of a second ORF that was validated to be the origin of the IκBNS p70 protein. According to this analysis, IκBNS p70 is protein made up of 572 aa with a predicted molecular weight of 61 kDa. In particular, the newly established IκBNS p70 aa sequence includes the whole IκBNS p35 sequence, bearing six ankyrin repeats important for protein-protein interactions. Further, it exhibits an additional 259 aa counting unstructured N-terminal tail of so far unknown function. With this putative IκBNS p70 aa-sequence, we generated an expression construct comprising the above described aa-sequence and expressed it transiently in HEK293T and over a longer period of time, lentivirally mediated in Jurkat T-cells. By comparing the introduced IκBNS p70 with the endogenously expressed IκBNS p70 of ABC cell lines and the P/I induced IκBNS p70 of Jurkat T-cells by immunoblotting, we observed that the 61 kDa predicted sequence actually exhibits the same size and band pattern as the endogenous counterpart, indicating the validity of our IκBNS p70. The multiple bands that were observed to be specific for both IκBNS isoforms could constitute post translationally modified versions of the IκBNS p70 isoform of so far unknown function. The lentiviral expression of both isoforms in Jurkat T-cells revealed as well an autoinhibitory feedback loop of IκBNS. The expression of the endogenous IκBNS p35 and p70 isoform was remarkably

diminished upon P/I mediated cell stimulation under simultaneous lentiviral overexpression of IκBNS p35 and p70. This assumed autoinhibitory feedback loop is likely made to prevent a surplus of IκBNS expression what would also result in a dysregulation of putative IκBNS controlled target genes.

In order to further validate the existence of the predicted IκBNS p70, we generated an antibody against aa 215- aa 231 of the IκBNS p70 sequence, an epitope located within the additional N-terminal tail. By application of this antibody in immunoblotting we were indeed able to detect an upcoming band of approximately 70 kDa by P/I mediated stimulation of BJAB cells. As expected, the IκBNS p35 isoform was not detectable with this IκBNS p70 specific antibody. Unfortunately, the seemingly IκBNS specific 70 kDa band was partly covered by an unspecific band.

The difference in the protein sequences of the distinct IκBNS isoforms should have an impact on protein structure and function, as well. However, we could not assign any structure to the additional N-terminal portion of IκBNS p70 and thus no obvious function. It is conceivable that this unstructured region could represent some kind of autoinhibitory peptide domain that covers ankyrin repeats, keeping IκBNS p70 in an inactive state. Due to steric reasons, this would prevent interactions with unknown interaction partners and Rel family proteins IκBNS was shown to interact with (Fiorini et al., 2002; Hirotani et al., 2005; Schuster et al., 2012). However, by an unknown mechanism assumingly a phosphorylation event, the autoinhibitory portion could alter its spatial orientation and its autoinhibitory property could be abrogated and IκBNS p70 could become additionally to its smaller isoform active as transcriptional regulator. This mechanism would introduce a new layer of IκBNS controlled target gene regulation. Another possibility is that the additional N-terminal portion of the IκBNS p70 isoform comprises a yet unrecognised TAD. A comparable issue is known for the three described IκBζ splicing variants IκBζ (S, L and D) (Kitamura et al., 2000; Haruta et al., 2001; Ito et al., 2004). Whereas IκBζ(S) and IκBζ(L) are known to contain a TAD, IκBζ(D) misses such a domain. Regarding IκBζ, this difference between the isoforms became functionally obvious in an experiment in which a retroviral mediated expression of IκBζ (S) and (L) but not IκBζ(D) in a mouse fibroblast cell line resulted in increased IL-6 production (Motoyama et al., 2005). The presence of a TAD in the IκBNS p70 N-terminus would establish a dual system consisting of a putative transcriptional negative regulator namely IκBNS p35 that lacks a TAD and IκBNS p70 that possesses a TAD as transcriptional positive

regulator. Consequently, this would mean a fine tuning mechanism for IκBNS controlled target genes. Therefore, future experiments should shed light on the function of the of the additional N-terminal portion of IκBNS p70. For instance by targeted knockdown of only one isoform in ABC DLBCL or conducting GAL4 fusion protein reporter assays with the 259 aa IκBNS p70 N-terminal tail.

4.6 IκBNS is essential for ABC DLBCL survival and might promote immune escape of ABC DLBCL by regulating MHCII surface expression

The importance of constitutive IκBNS expression for ABC DLBCL biology was demonstrated by the induction of toxicity selectively in ABC DLBCL cell lines by shRNA mediated knock-down of IκBNS within one week. In contrast, overexpression of IκBNS p35 did neither impair nor confer a growth advantage to neither GCB nor ABC DLBCL cell lines. This indicates that putative targets genes controlled by IκBNS are critical for ABC DLBCL survival and a further increase of the IκBNS p35 protein amount in ABC DLBCL does not affect cell growth. In summary, our results suggest that IκBNS is a crucial mediator of canonical NF-κB activity in the NF-κB signaling addicted ABC subtype of DLBCL. As IκBNS expression seems to be vital for ABC DLBCL survival, IκBNS could represent a promising suitable molecular target in the therapy of ABC DLBCL. Since IκBNS does not exhibit enzyme activity, a negative impact on its functionality should rather interfere with its function as transcriptional inducer and repressor. This could be achieved by designing small peptides/molecules mimicking the binding sites from NF-κB interaction partners of IκBNS. In this manner, IκBNS would not be able anymore to associate with NF-κB subunits and as a consequence of this not having transcriptional control neither positively nor negatively over its target genes.

shRNA mediated knock-down of IκBNS in the ABC DLBCL cell line HBL-1 followed by RNAseq revealed several genes encoding classical MHCII molecules such as HLA-DRA1, HLA-DRB, HLA-DRB1,HLA-DQA, the invariant chain (CD74) and also the class II major histocompatibility complex transactivator “CIITA” which represents the essential master regulator of MHCII expression to be negatively regulated IκBNS target genes. The treatment of HBL-1, OCI-LY3 and TMD8 cells with calcineurin inhibitors, which was known to us to cause IκBNS knock-down, actually resulted in

a calcineurin inhibitor dose dependent increase of HLA-DR surface presentation as previously indicated by RNAseq results. To substantiate that IκBNS has indeed a direct negative regulating impact on HLA-DR surface levels, both IκBNS isoforms were lentivirally expressed in the GCB DLBCL cell line BJAB and the Burkitt's lymphoma cell line RAJI that do not express endogenous IκBNS. Indeed, as expected, the overexpression of IκBNS p35 or p70 in the mentioned B-cell lines caused a clear reduction of HLA-DR surface expression at a comparable, suggesting that IκBNS is indeed a MHCII negative regulator. This finding is from interest in respect of possible DLBCL treatment options. Clinical studies with DLBCL patients conducted by Rimsza et al. in 2007 show that low levels of MHC class II HLA-DR molecules on DLBCL are associated with a remarkable poor survival outcome of patients. This association is most likely based on the finding that decreased levels or also even the loss of MHCII on DLBCL cells causes an impaired tumor-infiltrating T-cell response and as consequence of this a compromised immunosurveillance of the tumorigenic cells (List et al., 1993; Rimsza et al., 2004; Roberts et al., 2006; Kendrick et al., 2017). Efficient and sustained anti-tumor response in the priming and effector phase needs the assistance from $CD4^+$ T-cells that recognise MHCII molecules displayed on the surface of professional APCs such as B-cells (Toes et al., 1998; Ossendrop et al., 2000). Accordingly, the loss of MHCII is commonly observed in oncogenic diseases and represents a mechanism with which malignant cells are capable of editing the immune system to their advantage by preventing their detection and subsequent elimination. This mechanism is also called "immune escape" (Khong et al., 2002; Dunn et al., 2002; Beatty and Gladney 2015). Furthermore, our RNAseq results are consistent with the finding of Rimsza et al. (2006) that show that the expression of classical and non-classical MHCII molecules as well as CD74 in DLBCL is associated with the expression of CIITA. This non-DNA-binding MHCII expression master transcriptional factor was found in this study by RNAseq to be increased upon IκBNS knock down in HBL-1 cells. Thus, it can be assumed that IκBNS is a negative regulator of CIITA function. Further experiments should therefore investigate the interaction between IκBNS and the transcriptional regulation of the CIITA encoding gene MHC2TA and moreover the "CIITA enhanceosome complex" that serves as CIITA docking platform and thus regulates CIITA target gene transcription. MHC2TA transcription is controlled by four distinct not-coregulated promoters (pI to IV). In B-cells transcription of MHC2TA

was found to be initiated from pIII (LeibundGut-Landmann et al., 2004). As GCB DLBCL cell lines were found during this study not to express IκBNS, the finding by Wilkinson et al. (2012) that in general MHCII expression of GCB DLBCL is significantly higher than in ABC DLBCL is in accordance with our results. This could be one reason why the ABC DLBCL subtype exhibits a more aggressive clinical course and decreased patient survival than the GCB subtype. Remarkably reduced MHCII surface levels were for instance observed by Cycon et al. (2009) in OCI-LY3 cells that were caused by a dyscoordinated downregulation of the MHCII β-chain for an unknown reason. However, they are also other reasons that are clearly independent from IκBNS expression why some ABC DLBCL do express reduced or not express MHCII molecules. Cycon et al. (2009) found that the ABC DLBCL cell line OCI-LY10 harbours a homozygous deletion in the MHCII locus and thus the cell line has no detectable HLA-DR and HLA-DQ expression. According to our results, it can be said that the low levels of MHCII molecules on the surface of ABC DLBCL, that are characterised by adverse survival under treatment is caused by a steady state expression of IκBNS that conveys a clear survival advantage over GCB DLBCL in respect of immune evasion. Taking into account the previously mentioned facts and that we have shown that artificial IκBNS p35 and p70 overexpression in B-cell lines causes decreased HLA-DR surface levels, it is valid to claim that one reason why ABC DLBCL cell lines were selected to express high levels of endogenous IκBNS p35 and p70 could be its capability to repress HLA-DR surface levels by a so far unknown mechanism. This in turn leads to decreased immunogenicity of the cells and therefore augmented immune escape and thus survival of ABC DLBCL.

4.7 Calcineurin inhibitor administration as additional therapeutic option to R-CHOP in the treatment of ABC DLBCL

Considering the findings regarding the impact of calcineurin inhibitor treatment on certain ABC DLBCLs in this study, the inhibition of calcineurin seems to hold a not negligible therapeutic potential in the treatment of ABC DLBCL. The calcineurin inhibitors CsA and FK506 are commonly used as potent immunosuppressive especially in preventing transplant rejection and in the therapy of autoimmune diseases. CsA and FK506 mediated calcineurin inhibition was found by this study to clearly impair the growth of ABC DLBCL with a certain mutation pattern. This growth impairing effect was revealed to be caused by reduced NFAT and NF-kB signaling the consequently resulted in decreased secretion levels of the pro-proliferative IL-6 and IL-10 and reduced IκBNS expression. For this reason, we suppose that calcineurin inhibitor treatment could be suitable for ABC DLBCL that harbour mutations which are upstream of MALT1. CsA or FK506 treatment could thus be applied prior to the R-CHOP regimen in order to weaken the cells by interfering with the BCR antigen-receptor signaling cascade and Ca^{2+}/NFAT signaling. This interference in turn results in a reduction of the aberrant pro-proliferative and anti-apoptotic NF-kB signaling in ABC DLBCL. As a consequence of this, also the expression of (mutual) NF-kB and NFAT target genes such as the vital IκBNS would be affected by this R-CHOP complementary pre-treatment. Moreover, calcineurin inhibitor treatment of ABC DLBCL cell lines study was found by this study to lead to increased surface expression of MHCII molecules most likely by the down-regulation of IκBNS. The MHCII down regulating impact of IκBNS could be exploited as well by a R-CHOP complementary pre-treatment of ABC DLBCL with calcineurin inhibitory compounds. Increased MHCII surface levels would enhance the immunogenicity of the ABC DLBCL cells in turn leading to a better immunosurveillance and finally a more effective anti-tumor immune response.

4.8 IκBNS and its relative IκBζ

According to our results, constitutive IκBNS expression represents an intrinsic advantage for ABC DLBCL tumor survival as its shRNA mediated knock down led to the induction of toxicity in ABC DLBCL. We elucidated one possible mechanism why IκBNS expression is a survival advantage for ABC DLBCL. We showed IκBNS expression to negatively regulate MHCII surface presentation assumingly leading to reduced immunosurveillance of the oncogenic cell. But is this mechanism the only reason why ABC DLBCL were selected to express IκBNS steady state levels?

The human atypical IκB proteins IκBNS and its relative IκBζ share a sequence similarity of 26% (their murine counterparts 43%) and were shown to share characteristics regarding effector functions in several cell types and also in respect of their regulation and role in the pathogenesis of the ABC subtype of DLBCL.

Both IκBs were revealed to be upregulated by constitutive NF-κB signaling and thus to be overexpressed in the ABC DLBCL subtype. Furthermore, the shRNA mediated downregulation of IκBNS and IκBζ had a toxic effect on ABC DLBCL cell lines indicating that the target genes under their transcriptional control are critical for the survival of ABC DLBCL (This study; Nogai et al., 2013). Moreover, as found by Nogai et al. (2013) shRNA mediated knock-down of IκBζ downregulates the expression of IL-6 and IL-10 in ABC DLBCL cell lines. An investigation of IκBζ lacking B-cells by Hanihara et al., 2013 revealed that IκBζ is essential for the induction of several genes such as IL-10 upon BCR or TLR stimulation. In addition to that, IκBζ was described by several studies to positively regulate IL-6 in various cell types. In human monocytes for instance, the expression of IL-6 depends on the binding of p50/IκBζ heterodimers to its promoter. This finding could be confirmed by monocytes that exhibit higher IκBζ expression than monocyte-derived macrophages as their IL-6 expression reflected the distinct IκBζ expression levels (Seshadri et al., 2009). Furthermore, in murine macrophages, IκBζ/p50/p50 complexes bind to the IL-6 locus and increase transcription when the cells were stimulated with TLR ligands and IL-1 (Yamamoto, 2004; Eto, 2003). In consistence with this, overexpression of IκBζ leads to increased IL-6 expression, whereas a lack of IκBζ results in reduced IL-6 expression (Yamamoto et al., 2004; Kitamura et al., 2000). Additionally, IκBζ regulates IL-12p40 expression by binding to its promoter and in line with this, IκBζ deficient cells were observed to express less IL-12p40 (Yamamoto et al., 2004; Kayama et al., 2008). Moreover, also IκBζ-defective

conventional DCs were shown to express less LPS-induced IL-6 (Okamoto et al., 2010). Also IκBNS was shown to be involved in the regulation of IL-6, IL-10 and IL12p40. IκBNS is described to be crucial for the expression of IL-6 and IL-12p40 in bone marrow derived DCs (Kuwata et al., 2006). However, in macrophages and DCs lacking IκBNS, LPS induced a prolonged and increased IL-6 and IL-12p40 expression. This suggested that IκBNS is a negative regulator of LPS induced IL-6 and IL-12p40 expression in macrophages. It was supposed that an IκBNS/p50 complex is needed to end IL-6 expression (Hirotani et al., 2005; Kuwata et al., 2006). Annemann et al, (2015) observed a reduced secretion of IL-10 in IκBNS deficient TH17 cells. They revealed IκBNS to bind to the IL-10 gene locus in stimulated TH17 cells and found decreased expression of IL-10 in IκBNS lacking TH17 cells, indicating IL-10 to be a direct positively regulated target of IκBNS in this T-cell subset. This means that IκBζ and IκBNS share the regulation of certain target genes such as IL-6, IL-10 and IL-12p40. Furthermore, both atypical IκBs seem to have an essential positive regulator function on IFN-γ gene expression. Mature CD4+ T-cells deficient for IκBNS for example show reduced IFN-γ expression upon anti-CD3/28 antibody mediated TCR stimulation (Touma et al., 2007). Furthermore, decreased IFN-γ production was also observed by IκBNS knock-out lymphocytes and $CD8^+$ T-cells derived from lymph nodes (Touma et al., 2007). IκBζ was like IκBNS found to be indispensable for IFN-γ production by NK cells. In this respect, IκBζ was shown to be induced by IL-12 or IL-18 stimulation of NK cells and subsequently recruited to the IFN-γ gene promoter region (Miyake et al., 2010). In accordance with the previous, IκBζ was found to associated with the IFN-γ promoter in a complex including p50/p65 (Kannan et al., 2011). IκBζ deficient mice were observed to exhibit impaired TH17 development resulting in resistance to experimental autoimmune encephalomyelitis (EAE) when they were immunised with the myelin oligodendrocyte glycoprotein (MOG)-peptide (Okamoto et al., 2010). Also a mouse model lacking IκBNS expression was found to be more resistant to EAE induction (Kobayashi et al., 2014). In addition, IκBζ and IκBNS deficient mice exhibit a deregulated humoral immune response as indicated by markedly reduced IgM and IgG3 serum levels (Touma et al., 2011; Arnold et al., 2012; Hanihara et al., 2013). In case of IκBNS deficiency this could be illustrated in the production of less antigen-specific antibodies against influenza viruses. Moreover, B-cells from IκBNS deficient mice also exhibit a defective IgG3 class switch (Touma et al., 2011).

Both atypical NF-kB inhibitors were also reported by several studies to be implicated in TH17 development and proliferation whereby IκBζ seems to play more important role than IκBNS. Mice deficient for IκBNS showed a clearly reduced number of IL-17$^+$ T-cells under *C.rodentium* infection, induced EAE and colitis. Furthermore, TH17-cells lacking IκBNS exhibited impaired expression of IL-10, IL-17A, IL-17F and GM-CSF (Annemann et al., 2015; Kobayashi et al., 2014). Notably, also GM-CSF mRNA expression of LPS stimulated peritoneal macrophages was found to be dependent from IκBζ (Yamamoto et al., 2004). Also described is a defective TH17-related RORγt and CCR6 expression in CD4$^+$ IκBNS-deficient cells what could represent a possible explanation for the above mentioned cytokine secretion defect. The direct transcriptional control of IκBNS over the TH17 characteristic interleukin IL-17A could be excluded by Kobayashi et al. (2014). According to Okamoto et al. (2010), IκBζ seems to play a crucial regulatory role in TH17 development by cooperating with ROR nuclear receptors. In more detail, in contrast to IκBNS, IκBζ could be unveiled to bind in a RORγt and RORα-dependent manner to the IL17A promoter and was suggested to positively regulate IL17A expression by the increased binding of transcriptional co-activators (Okamoto et al., 2010). In consistence with that, IκBζ knock-out TH17 cells show decreased mRNA levels of IL17A and other TH17-related genes like IL-21, IL-22 and IL-23r. As a consequence of this TH17 phenotype promoting impact of IκBζ, corresponding IκBζ knock-out mice are completely resistant to EAE due to the lack of IL-17 producing TH17 cell (Okamoto et al., 2010).

As depicted above, IκBζ and IκBNS seem to share multiple functional similarities and to have partially redundant roles in different cellular processes. Therefore, it is conceivable that the found steady state expression of IκBNS in ABC DLBCL as it was already shown for IκBζ shown by Nogai et al. (2013) also represents an intrinsic advantage for ABC DLBCL cells for several reasons that led to the selective pressure to express IκBNS. These reasons are assumingly at least partially redundant for IκBζ. First, IκBNS in ABC DLBCL could directly control, as IκBζ, the expression of IL-6 and IL-10 and thus sustain the autocrine/paracrine pro-proliferative cytokine signaling loop. Second, IκBζ was suggested by Nogai and colleagues to play a central role in the regulation of NF-κB target genes and thus to be required for proper functionality of the NF-κB signaling network in ABC DLBCL. The same function could be true for IκBNS, which could partially regulate the same

NF-κB target genes as IκBζ does in ABC DLBCL. However, the knock-down of IκBNS induced toxicity in all IκBNS and IκBζ expressing ABC DLBCL cell lines tested. This experimental outcome is similar to the result of an IκBζ knock-down experiment conducted by Nogai et al. (2013). This suggests that the observed toxic effects that were induced by the individual knock-down of both atypical IκBs are based on non-redundant functions of IκBNS and IκBζ that cannot be mutually adopted.

4.9 Seeking new surface markers and molecular targets for classifying and combat DLBCL

We were conducting the LEGENDScreen™ assay with 3 cell lines of the GCB DLBCL subtype (BJAB, SU-DHL-4, SU-DHL-6) and 3 cell lines classified as ABC DLBCL (HBL-1, TMD8, U2932) with the intention to reveal new biomarkers which could be useful to differentiate between the GCB and ABC DLBCL subtypes and moreover that could be potentially exploited as molecular targets in future DLBCL treatment approaches. The screen unveiled surface markers that were expressed on both DLBCL subtypes and also markers that were mainly or even exclusively expressed by only one, the GCB or the ABC DLBCL subtype.

Understandably, among the surface markers that were mutually expressed by the GCB and the ABC DLBCL subtype cell lines, the screen unveiled plenty of surface molecules that are known to be generally expressed on the surface of B-cells and are thus also shared by both DLBCL entities such as the pan B-cell marker CD20 and CD79B.

CD20 is a non-glycosylated surface protein of 33-37 kDa that is expressed in B-cell development from the early pre-B to the stage of mature B-cells and is down regulated during the transition to plasma blasts (Cragg et al., 2005; Rehnberg et al., 2009). CD20 can be found in approximately 95% of B-cell lymphoma, is not present on precursor B-cells or stem cells and at low levels on plasma cells (Cragg et al., 2005; (Boye, Elter and Engert, 2003). It was found to localise with MHCII and the BCR ahead to antigen engagement (Cragg et al., 2005). It is the target of several antibodies in the therapy of $CD20^+$ B-cell Non-Hodgkin Lymphoma and autoimmune disorders (Boye, Elter and Engert, 2003; Randall, 2016). The functionality of CD20 is not yet understood but in respect of cancer treatment it contributes to complement

and effector-cell mediated lysis, apoptosis induction and interferes with calcium influx (Boye, Elter and Engert, 2003).

CD79B and CD79A make up the heterodimer CD79 and together with the surface Ig it forms the BCR-complex, the characteristic feature of B-cells (Chu and Arber 2001; Naeim et al., 2013). It is crucial for the transport of mIg to the cell surface and the propagation of proximal BCR signaling (Torres et al., 2008). Thus, CD79 is already expressed in prior to Ig heavy chain rearrangement and also CD20 in the course of B-cell maturation. It is therefore a convenient pan-B-cell marker to e.g. classify leukemia and hence to identify B-cell neoplasms such as DLBCL, as well.

From the CD markers that were revealed to be differentially distributed between the GCB and ABC DLBCL subtypes, we chose CD90 which was revealed to be exclusively expressed by GCB DLBCL cell lines and CD36 as well as CD274 that were both found to be associated with the ABC DLBCL subtype for more detailed investigations.

CD90 which is also called Thy-1 is a 25-37 kDa GPI-anchored membrane protein lacking an intracellular domain. The core protein exhibits 25 kDa, whereas the fully N-glycosylated protein displayed on the cell surface comprises 37 kDa (Pont, 1987; Kumar et al., 2016). With a carbohydrate content of up to 30% of its molecular mass it is one of the most heavily glycosylated proteins (Pont, 1987). Thy-1 exerts tasks in cell-cell and cell-matrix interactions, apoptosis, migration, fibrosis (Rege and Hagood, 2006) and was recently found to be implicated in several kinds of neoplasia were it has a binary role in tumor facilitation and containment dependent on the cancer type (Kumar et al., 2016). Moreover, Thy-1 expression was found in the highly invasive cancer cell microenvironment in prostate and pancreatic cancer, determining their aggressive and metastatic abilities (Pascal et al., 2011; Zhu et al., 2014). This is from importance since the altered tumor stroma plays in general a considerable role in cancer progression and metastasis (Barron and Rowley, 2012; Ungefroren et al., 2011). Furthermore, Thy-1 is also discussed as cancer stem cell (CSC) marker candidate as Thy-1 was revealed to be co-expressed with other CSC markers and $CD90^+$ cells were isolated from various tumor types such as breast cancer (Lobba et al., 2012). These $CD90^+$ cells showed the characteristic traits of CSCs in regard to spheroid forming abilities, proliferation, differentiation, metastatic properties and the capability to grow as tumor xenograft in mice (Shaikh et al., 2016). Interestingly, in line with our results, Thy-1 was also identified at high

expression levels by Ishiura et al. (2010) in B-cell lymphoma cell lines such as BJAB (GCB DLBCL). The treatment of those cell lines with an anti-Thy-1 antibody revealed an inhibitory effect on proliferation contributed partially by apoptosis and necrosis. The antibody caused caspase activation and additional down regulation of anti-apoptotic BCL-2 family members. This proliferation inhibitory effect that was observed by Ishiura et al. seemed to be even stronger than that facilitated by rituximab. As we found CD90 to be highly expressed by the GCB subtype of DLBCL treatment with bi-specific anti-CD20/CD90 antibodies could be therefore indeed a promising approach in the therapy of GCB DLBCL.

CD36 (alternative names: FAT, GPIV, GPIIIb, PAS IV) is an 88 kDa integral membrane glycoprotein and member of the scavenger receptor family of pattern recognition receptors (Silverstein and Febbraio, 2009; Danilova et al., 2013; Park, 2014).CD36 is made up of two transmembrane domains, two short intracytoplasmic domains containing both termini, lacking known intracellular signaling domains and a larger extracellular extensively glycosylated domain (Febbraio et al., 2001; Park, 2014). CD36 is expressed on numerous cells types like monocytes, macrophages, dendritic cells, microvascular endothelial cells, adipocytes and platelets (Pepino et al., 2014). It is known to interact with other membrane receptors like integrins, TLRs and tetraspanins. (Miao et al., 2001; Akira, 2003 Lawler et al., 2012). CD36 binds a multitude of different ligands at different binding sites such as thrombospondin-1, oxidized phospholipids, DAG, cholesterol, native lipoproteins (HDL, LDL and VLDL), oxidized lipoproteins (oxLDL and oxHDL) and long-chain fatty acids (Lawler et al., 2012; Park 2014; Pepin et al., 2014). Concerning functionality, CD36 plays among others a role in fat metabolism as it acts as a high affinity fatty acid translocase (FAT) by binding long chain free fatty acids (FA) and transporting them into the cell, thereby providing an energy source for β-oxidation (Harmon et al., 1993; Glatz et al., 2010; Abumrad and Davidson, 2012; Park 2014). Moreover, CD36 is also reported to be implicated in FA metabolism related issues including fat taste perception, fat uptake and absorption and FA exploitation by muscle and adipose tissues (Glatz et al., 2010; Abumrad and Davidson, 2012; Pepino et al., 2014). Despite the negligible intracellular presence and lacking a common intracellular signaling domain, CD36 was reported to have diverse downstream ligand-dependent signaling pathways (Moore et al., 2002; Chen et al., 2008; Silverstein and Febbraio, 2009). It interacts for example directly with src-kinases like FYN, LYN

and YES (Huang et al., 1991). This for instance occurs in macrophages upon engagement of oxLDL leading to LYN phosphorylation and the subsequent activation of downstream signaling molecules. Amongst them are e.g. JNK1 & 2 which in turn facilitate oxLDL inward transport (Silverstein and Febbraio, 2009; Park, 2014). Moreover, CD36 downstream signaling also comprises the activation of NF-κB (Janabi et al., 2000). This was concluded from the finding that macrophages from CD36 deficient patients exhibit attenuated NF-κB activity and decreased secretion of IL-1β and TNF-α (Yamashita et al., 2007). Patients suffering from a CD36 deficiency show high incidences of cardiomyopathy, hyperlipidemia and insulin resistance (Yamashita et al., 2007). Furthermore, it functions as endogenous angiogenesis negative regulator of microvascular endothelial cells (Dawson et al., 1997). This is achieved by inhibiting proangiogenic signals inducing proliferation and tube formation, generating instead signals leading to apoptosis by activating caspase 3 and the secretion of FasL and TNF-α (Jiménez et al., 2000). Furthermore, CD36 activation that was mediated by an N-terminal recombinant thrombospondin-2 fragment was recently shown to inhibit growth and metastasis of breast cancer by endothelial cell apoptosis (Koch et al., 2011). Thus, CD36 is also considered to play an important role in tumor growth and other processes that involve neovascularisation. Regarding B-cell malignancies, CD36 was revealed to be transcriptionally regulated by Oct-2, a commonly known B-cell differentiation regulator (Corcoran et al., 1993; Pfisterer et al., 1997). Additionally, the expression of CD36 in chronic B-cell lymphoproliferative diseases was linked to metastasis (Rutella et al., 1997). In B-CLLs CD36 is described as an indicator for tumor cell dissemination (Rutella et al., 1999). In respect of DLBCL context, CD36 was described to be a predictor for the non-GCB DLBCL subtype (Danilova et al., 2013). This result is in line with the results of our CD-marker screen that revealed CD36 to be selectively expressed in ABC DLBCL on both the mRNA as well as the protein level. Moreover, the overexpression of CD36 was reported as a protective factor, since it improved overall and progression-free survival in DLBCL patients under R-CHOP therapy (Danilova et al., 2013).

A study by Kobayashi et al. (2003), reports that CD36 together with Integrin β1 was overexpressed in most cases of $CD5^+$ DLBCL, a unique de novo DLBCL subtype that has been identified based on CD5 expression. As demonstrated by genome profiling and immunohistochemistry, the majority of $CD5^+$ DLBCL belongs to the

ABC DLBCL subgroup. This is in accordance with our finding of CD36 to be specifically expressed in ABC DLBCL. This $CD5^+$ DLBCL entity accounts for 5-10% of all DLBCL cases and exhibits an aggressive disease course and thus a poorer prognosis (Jain et al., 2013). Whereas Integrin β1 was exclusively expressed on lymphoma cells, CD36 was overexpressed only on vascular endothelia cells from $CD5^+$ DLBCL (Kobayashi et al., 2003). Therefore, the authors assumed an interaction between the Integrin β1 bearing lymphoma cells and the CD36 expressing endothelial cells residing in the $CD5^+$ DLBCL tumor, also because both proteins were shown to interact with each other by Thorne et al. in 2000. Considering the previously described findings and conclusions from literature and our observation that CD36 seems to be selectively expressed in the ABC subtype of DLBCL, CD36 could indeed represent a promising surface molecule to identify ABC DLBCL cells and could also be a target molecule of future ABC DLBCL therapy approaches. However, the blockage of CD36 by SSO in this study did not affect mRNA expression levels of GCB and ABC DLBCL encoding enzymes implicated in the regulation of β-oxidation. This suggests that CD36 is not an essential element in the lipid metabolism of DLBCL and is therefore at least in this regard not a promising target molecule in the treatment of ABC DLBCL. Additionally, it could serve as prognostic marker to predict therapy response and survival outcome of DLBCL patients, as well.

CD274 (PD-1L; B7-H1) is a 33 kDa immunomodulatory glycoprotein mainly expressed on the cell surface of antigen-presenting cells like activated T-cells, natural killer (NK), T-cells, B-cells, DCs, and macrophages (Agata et al.1996; Andorsky et al., 2011; Krempski et al., 2011; Fang et al., 2017). It is also common on a broad range of solid tumors including breast, lung, colon, melanoma, liver, thymus or head (Konishi et al., 2004; Keir et al., 2008). In B-cell malignancies, however PD-L1 and its cognate inhibitory receptor PD-1 are rarely expressed (Brown et al., 2003; Andorsky et al., 2011). PD-L1 was also found to be expressed on selected DLBCL and on non-cancerous cells infiltrating the tumor such as macrophages (Chen et al., 2013; Georgiou et al., 2016). In addition to that, the number of DLBCL tumor infiltrating $PD\text{-}1^+$ lymphocytes correlates with favourable overall survival (Muenst et al., 2010; Ahearne et al., 2014). This finding however contradicts the suppressing role of PD-1 in immune response. Fang et al. (2017) assume that the correlation between the increase of $PD\text{-}1^+$ lymphocytes and

beneficial outcome might reflect previous active immune response. Moreover, PD-1L is also reported to be expressed on several primary T-cell lymphoma like anaplastic large T-cell lymphoma (Brown et al., 2003). Engagement of PD-1L with PD-1, which is expressed on the surface of activated T-cells, transmits a negative regulatory signal leading to the inhibition of cell cycle progression and cytokine production of activated T-cells transforming them into the reversible "T-cell exhaustion" phenotype (Freeman et al., 2000). As PD-L1 inhibits local antitumor T-cell responses by this mechanism, the expression of PD-L1 is strongly connected to tumor progression and poor outcome in many types of cancers (Kim et al., 2013; Kiyasu et al., 2015). Thus, the expression of PD-1L by tumor cells or APCs neighbouring the tumor constitutes an important factor for various cancers to achieve immune evasion (Iwai et al., 2002; Chen et al., 2013; Akbay et al., 2013; Georgiou et al., 2016). Dong et al. showed in 2002 that melanoma cells of mice expressing PD-1L avoid immune system mediated elimination by inhibiting the activation of tumor specific T-cells or even promote apoptosis of tumor specific T-cells. In consistence with this, the treatment of mice with anti-PD-1L-antibodies (Hirano et al., 2005) and PD-1 knockout mice that were treated with tumor cells mice showed enhanced anti-tumor responses indicated by cytotoxicity and cytokine secretion (Iwai et al., 2002 and 2005). Hence, PD-1L blockage is able to augment immunotherapies. Consequently, therapies targeting PD1 and PD-1L approved to be from clinical efficacy in patients with different types of solid cancers, and Hodgkin/Non-Hodgkin lymphoma (Topalian et al., 2012; Bachy et al., 2014; Ansell et al., 2015). Moreover, the utility of this therapy approach is further underscored by the recent promising treatment of lymphoid malignancies including DLBCL using the anti-PD-1 receptor antibody nivolumab (Lesokhin et al., 2016; Ansell et al., 2015). A further remarkable example in this regard is the therapy approach with anti PD-1/PD-1L antibodies of the so far immunotherapy non-responsive NSCLC which led to an enhanced anti-tumor immune response and therefore markedly improved clinical therapeutic effects (Gettinger et al., 2016). The antibody based therapy targeting the PD-1/PD-1L axis was also found to enhance the proliferation of tumor-derived T-cells and supported the activation of NKT cells (Chu et al., 2009). Moreover, the extent of PD-1L expression is associated with treatment response in several tumor subsets (Brahmer et al., 2012; Topalian et al., 2012). In accordance with our CD-marker screen Chen et al. reported in 2013 that the investigation of 61

DLBCL cases, amongst them 27 ABC DLBCL cases, for PD-1L expression revealed the association between the ABC subtype and PD-1L expression as statistically significant. Moreover, also Kiyasu et al. found in a retrospective study of 1253 patient DLBCL biopsies that PD-1L expression was significantly associated with the non-GCB subtype, EBV positivity and hence poor prognosis. They also report that patients with PD-1L$^+$ DLBCL exhibit an inferior overall survival compared to cases with PD-L1$^-$ DLBCL. A statistical tendency of PD-1L expression to be linked to ABC DLBCL was also observed by Kwiecinska et al. in 2016. This correlation between PD-1L expression and the ABC DLBCL subtype was also observed by Andorsky et al. in 2011. This group also described that the blockage of PD-1L in DLBCL by antagonising antibodies results in increased activation of nearby T-cells. Overall, PD-1L could be thus considered as a potential reliable biomarker of the aggressive ABC subtype of DLBCL and the associated adverse clinical prognosis. Moreover, PD-1L could also constitute a promising therapy target in antibody based immunotherapy of PD-1L$^+$ DLBCL in order to reduce immune escape capabilities of this lymphoma type.

4.10 Summary: The pivotal role of calcineurin and IκBNS in ABC DLBCL biology

In summary, we propose a model in which calcineurin and IκBNS play an essential role in the survival and immune evasion of ABC DLBCL, exhibiting chronically active BCR signaling due to somatically acquired mutations upstream of CARD11. BCR signaling leads by the increase of intracellular calcium levels to the activation of calcineurin which in turn has versatile tasks. It dephosphorylates NFAT which in turn migrates to the nucleus where it positively regulates together with NF-kB the expression of IκBNS p35 and p70. Constitutive IκBNS p35 and p70 results in reduced MHCII molecule surface expression levels, assumingly by modulating CIITA expression or transcriptional activity on target genes probably resulting in enhanced immune escape. Furthermore, as revealed by phosphoproteom analysis and supported by literature (Müller et al., 2000; Palkowitsch et al., 2011; Zeng et al., 2007), most notably a reported comparable mechanism unveiled in TCR signaling (Dutta et al., 2017), the S/T phosphate activity of calcineurin seems to act as a positive regulator of BCR signaling. Calcineurin accomplishes this as indicated by

phosphoproteom analysis by the dephosphorylation of several putative BCR proximal signaling elements such as CD79A/B, BLNK or BCL-10. The positive impact of calcineurin activity on BCR signaling consequently leads to the enhancement of the prosurvival and anti-apoptotic NF-kB and NFAT signaling networks and hence to the maintenance of the vital IL-6 and IL-10 autocrine/paracrine positive feedback loop as well as to a further reinforcement of IκBNS expression. Together, these findings suggest that a deeper investigation of the calcineurin and IκBNS function in the context of aberrant NF-kB signaling in ABC DLBCL seems to be a promising issue in order to lay the foundation for future therapy approaches. For an overview see Figure 54.

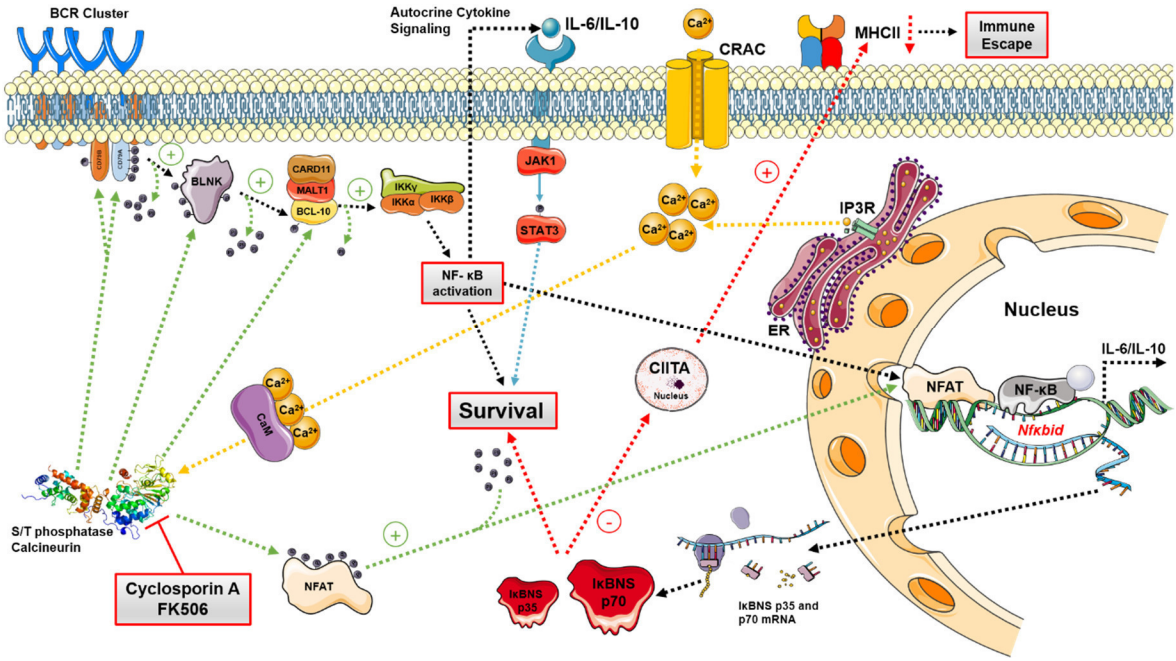

Figure 54. Illustrative overview of the proposed model in which calcineurin acts at different positions as BCR signaling positive regulator and promotes the expression of IκBNS by activating and enhancing NFAT and NF-kB signaling in ABC DLBCL. IκBNS p35 and p70 were found to be under the mutual transcriptional control of NFAT and NF-kB. IκBNS p35 and p70 expression leads to reduced MHCII surface expression in B-cells most likely by interfering with the expression or transcriptional activity of CIITA and thus could contribute to immune escape of ABC DLBCL and was moreover found to be essential for ABC DLBCL survival. Cyclosporin A and FK506 are structurally unrelated inhibitors of calcineurin phosphatase activity. Yellow dashed arrows: Ca^{2+} signaling; Green dashed arrows: direct effects of calcineurin activity; Red dashed arrows: IκBNS p35 and p70 caused effects; Blue dashed arrows: IL-6 and IL-10 autocrine/paracrine cytokine signaling; Black dashed arrows: BCR and NF-kB signaling. Abbreviations: BCR, B-cell receptor; S/T, Serine/Threonine; BLNK, B-cell linker protein; NFAT, Nuclear Factor of activated T-cells; CARD11, Caspase recruitment domain-containing protein 11 ;MALT1, Mucosa-associated lymphoid tissue lymphoma translocation protein 1; BCL-10, B-cell lymphoma/leukemia 10; JAK1, Janus kinase 1; STAT3; Signal transducer and activator of transcription 3; CRAC, Calcium release-activated channels; MHCII major histocompatibility

complex; CIITA class II, major histocompatibility complex, transactivator; ER, endoplasmic reticulum; IP3R, Inositol 1,4,5-trisphosphate receptor; CaM; Calmodulin; IKKα, β, γ, nuclear factor kappa-B kinase subunit alpha, beta, gamma. The figure was generated using *Servier Medical Art.* The human calcineurin heterodimer protein structure was taken from the protein data bank "PDB"; DOI:10.2210/pdb1aui/pdb

5. References

Abumrad, N. A., and N. O. Davidson. 2012. Role of the gut in lipid homeostasis. Physiol Rev 92: 1061-1085.

Agata, Y., A. Kawasaki, H. Nishimura, Y. Ishida, T. Tsubata, H. Yagita, and T. Honjo. 1996. Expression of the PD-1 antigen on the surface of stimulated mouse T and B lymphocytes. Int Immunol 8: 765-772.

Ahearne, M. J., K. Bhuller, R. Hew, H. Ibrahim, K. Naresh, and S. D. Wagner. 2014. Expression of PD-1 (CD279) and FoxP3 in diffuse large B-cell lymphoma. Virchows Arch 465: 351-358.

Akbay, E. A., S. Koyama, J. Carretero, A. Altabef, J. H. Tchaicha, C. L. Christensen, O. R. Mikse, A. D. Cherniack, E. M. Beauchamp, T. J. Pugh, M. D. Wilkerson, P. E. Fecci, M. Butaney, J. B. Reibel, M. Soucheray, T. J. Cohoon, P. A. Janne, M. Meyerson, D. N. Hayes, G. I. Shapiro, T. Shimamura, L. M. Sholl, S. J. Rodig, G. J. Freeman, P. S. Hammerman, G. Dranoff, and K. K. Wong. 2013. Activation of the PD-1 pathway contributes to immune escape in EGFR-driven lung tumors. Cancer Discov 3: 1355-1363.

Akira, S. 2003. Toll-like receptor signaling. J Biol Chem 278: 38105-38108.

Alfonso, C., and L. Karlsson. 2000. Nonclassical MHC class II molecules. Annu Rev Immunol 18: 113-142.

Alizadeh, A. A., M. B. Eisen, R. E. Davis, C. Ma, I. S. Lossos, A. Rosenwald, J. C. Boldrick, H. Sabet, T. Tran, X. Yu, J. I. Powell, L. Yang, G. E. Marti, T. Moore, J. Hudson, Jr., L. Lu, D. B. Lewis, R. Tibshirani, G. Sherlock, W. C. Chan, T. C. Greiner, D. D. Weisenburger, J. O. Armitage, R. Warnke, R. Levy, W. Wilson, M. R. Grever, J. C. Byrd, D. Botstein, P. O. Brown, and L. M. Staudt. 2000. Distinct types of diffuse large B-cell lymphoma identified by gene expression profiling. Nature 403: 503-511.

Amasaki, Y., E. S. Masuda, R. Imamura, K. Arai, and N. Arai. 1998. Distinct NFAT family proteins are involved in the nuclear NFAT-DNA binding complexes from human thymocyte subsets. J Immunol 160: 2324-2333.

Amato, S. F., K. Nakajima, T. Hirano, and T. C. Chiles. 1996. Transcriptional regulation of the junB promoter in mature B lymphocytes. Activation through a cyclic adenosine 3',5'-monophosphate-like binding site. J Immunol 157: 146-155.

Amiot, L., M. Onno, T. Lamy, C. Dauriac, P. Y. Le Prise, R. Fauchet, and B. Drenou. 1998. Loss of HLA molecules in B lymphomas is associated with an aggressive clinical course. Br J Haematol 100: 655-663.

Anderson, J. R., J. O. Armitage, and D. D. Weisenburger. 1998. Epidemiology of the non-Hodgkin's lymphomas: distributions of the major subtypes differ by geographic locations. Non-Hodgkin's Lymphoma Classification Project. Ann Oncol 9: 717-720.

Anderson, J. J., S. Fordham, L. Overman, H. Dignum, K. Wood, S. J. Proctor, S. Crosier, B. Angus, R. E. Culpin, and T. Mainou-Fowler. 2009. Immunophenotyping of diffuse large B-cell lymphoma (DLBCL) defines multiple sub-groups of germinal centre-like tumours displaying different survival characteristics. Int J Oncol 35: 961-971.

Andorsky, D. J., R. E. Yamada, J. Said, G. S. Pinkus, D. J. Betting, and J. M. Timmerman. 2011. Programmed death ligand 1 is expressed by non-hodgkin lymphomas and inhibits the activity of tumor-associated T cells. Clin Cancer Res 17: 4232-4244.

Annemann, M., C. Plaza-Sirvent, M. Schuster, K. Katsoulis-Dimitriou, S. Kliche, B. Schraven, and I. Schmitz. 2016. Atypical IkappaB proteins in immune cell differentiation and function. Immunol Lett 171: 26-35.

Annemann, M., Z. Wang, C. Plaza-Sirvent, R. Glauben, M. Schuster, F. Ewald Sander, P. Mamareli, A. A. Kuhl, B. Siegmund, M. Lochner, and I. Schmitz. 2015. IkappaBNS regulates murine Th17 differentiation during gut inflammation and infection. J Immunol 194: 2888-2898.

Ansell, S. M., L. S. Hodge, F. J. Secreto, M. Manske, E. Braggio, T. Price-Troska, S. Ziesmer, Y. Li, S. H. Johnson, S. N. Hart, J. P. Kocher, G. Vasmatzis, A. Chanan-Kahn, M. Gertz, R. Fonseca, A. Dogan, J. R. Cerhan, and A. J. Novak. 2014. Activation of TAK1 by MYD88 L265P drives malignant B-cell Growth in non-Hodgkin lymphoma. Blood Cancer J 4: e183.

Ansell, S. M., A. M. Lesokhin, I. Borrello, A. Halwani, E. C. Scott, M. Gutierrez, S. J. Schuster, M. M. Millenson, D. Cattry, G. J. Freeman, S. J. Rodig, B. Chapuy, A. H. Ligon, L. Zhu, J. F. Grosso, S. Y. Kim, J. M. Timmerman, M. A. Shipp, and P. Armand. 2015. PD-1 blockade with nivolumab in relapsed or refractory Hodgkin's lymphoma. N Engl J Med 372: 311-319.

Armitage, J. O., and D. D. Weisenburger. 1998. New approach to classifying non-Hodgkin's lymphomas: clinical features of the major histologic subtypes. Non-Hodgkin's Lymphoma Classification Project. J Clin Oncol 16: 2780-2795.

Arnold, C. N., E. Pirie, P. Dosenovic, G. M. McInerney, Y. Xia, N. Wang, X. Li, O. M. Siggs, G. B. Karlsson Hedestam, and B. Beutler. 2012. A forward genetic screen reveals roles for Nfkbid, Zeb1, and Ruvbl2 in humoral immunity. Proc Natl Acad Sci U S A 109: 12286-12293.

Bachy, E., and B. Coiffier. 2014. Anti-PD1 antibody: a new approach to treatment of lymphomas. Lancet Oncol

15: 7-8.

Baeuerle, P. A., and T. Henkel. 1994. Function and activation of NF-kappa B in the immune system. Annu Rev Immunol 12: 141-179.

Baldwin, A. S., Jr. 1996. The NF-kappa B and I kappa B proteins: new discoveries and insights. Annu Rev Immunol 14: 649-683.

Barbulescu, K., K. H. Meyer zum Buschenfelde, and M. F. Neurath. 1997. Constitutive and inducible protein/DNA interactions of the interferon-gamma promoter in vivo in [corrected] CD45RA and CD45R0 T helper subsets. Eur J Immunol 27: 1098-1107.

Barron, D. A., and D. R. Rowley. 2012. The reactive stroma microenvironment and prostate cancer progression. Endocr Relat Cancer 19: R187-204.

Bartee, E., M. Mansouri, B. T. Hovey Nerenberg, K. Gouveia, and K. Fruh. 2004. Downregulation of major histocompatibility complex class I by human ubiquitin ligases related to viral immune evasion proteins. J Virol 78: 1109-1120.

Bartlett, K., and S. Eaton. 2004. Mitochondrial beta-oxidation. Eur J Biochem 271: 462-469.

Barton, K., N. Muthusamy, M. Chanyangam, C. Fischer, C. Clendenin, and J. M. Leiden. 1996. Defective thymocyte proliferation and IL-2 production in transgenic mice expressing a dominant-negative form of CREB. Nature 379: 81-85.

Bea, S., F. Tort, M. Pinyol, X. Puig, L. Hernandez, S. Hernandez, P. L. Fernandez, M. van Lohuizen, D. Colomer, and E. Campo. 2001. BMI-1 gene amplification and overexpression in hematological malignancies occur mainly in mantle cell lymphomas. Cancer Res 61: 2409-2412.

Beals, C. R., C. M. Sheridan, C. W. Turck, P. Gardner, and G. R. Crabtree. 1997. Nuclear export of NF-ATc enhanced by glycogen synthase kinase-3. Science 275: 1930-1934.

Beatty, G. L., and W. L. Gladney. 2015. Immune escape mechanisms as a guide for cancer immunotherapy. Clin Cancer Res 21: 687-692.

Beg, A. A., and A. S. Baldwin, Jr. 1993. The I kappa B proteins: multifunctional regulators of Rel/NF-kappa B transcription factors. Genes Dev 7: 2064-2070.

Beguelin, W., R. Popovic, M. Teater, Y. Jiang, K. L. Bunting, M. Rosen, H. Shen, S. N. Yang, L. Wang, T. Ezponda, E. Martinez-Garcia, H. Zhang, Y. Zheng, S. K. Verma, M. T. McCabe, H. M. Ott, G. S. Van Aller, R. G. Kruger, Y. Liu, C. F. McHugh, D. W. Scott, Y. R. Chung, N. Kelleher, R. Shaknovich, C. L. Creasy, R. D. Gascoyne, K. K. Wong, L. Cerchietti, R. L. Levine, O. Abdel-Wahab, J. D. Licht, O. Elemento, and A. M. Melnick. 2013. EZH2 is required for germinal center formation and somatic EZH2 mutations promote lymphoid transformation. Cancer Cell 23: 677-692.

Beinke, S., and S. C. Ley. 2004. Functions of NF-kappaB1 and NF-kappaB2 in immune cell biology. Biochem J 382: 393-409.

Ben-Neriah, Y. 2002. Regulatory functions of ubiquitination in the immune system. Nat Immunol 3: 20-26.

Benoist, C., and D. Mathis. 1990. Regulation of major histocompatibility complex class-II genes: X, Y and other letters of the alphabet. Annu Rev Immunol 8: 681-715.

Bertoni, F., and M. Ponzoni. 2007. The cellular origin of mantle cell lymphoma. Int J Biochem Cell Biol 39: 1747-1753.

Blasioli, J., S. Paust, and M. L. Thomas. 1999. Definition of the sites of interaction between the protein tyrosine phosphatase SHP-1 and CD22. J Biol Chem 274: 2303-2307.

Blonska, M., Y. Zhu, H. H. Chuang, M. J. You, K. Kunkalla, F. Vega, and X. Lin. 2015. Jun-regulated genes promote interaction of diffuse large B-cell lymphoma with the microenvironment. Blood 125: 981-991.

Bodmer, H., S. Viville, C. Benoist, and D. Mathis. 1994. Diversity of endogenous epitopes bound to MHC class II molecules limited by invariant chain. Science 263: 1284-1286.

Bonizzi, G., and M. Karin. 2004. The two NF-kappaB activation pathways and their role in innate and adaptive immunity. Trends Immunol 25: 280-288.

Bonner, J. M., and G. L. Boulianne. 2017. Diverse structures, functions and uses of FK506 binding proteins. Cell Signal 38: 97-105.

Booman, M., K. Szuhai, A. Rosenwald, E. Hartmann, H. Kluin-Nelemans, D. de Jong, E. Schuuring, and P. Kluin. 2008. Genomic alterations and gene expression in primary diffuse large B-cell lymphomas of immune-privileged sites: the importance of apoptosis and immunomodulatory pathways. J Pathol 216: 209-217.

Bours, V., P. R. Burd, K. Brown, J. Villalobos, S. Park, R. P. Ryseck, R. Bravo, K. Kelly, and U. Siebenlist. 1992. A novel mitogen-inducible gene product related to p50/p105-NF-kappa B participates in transactivation through a kappa B site. Mol Cell Biol 12: 685-695.

Bouvier, M., and D. C. Wiley. 1994. Importance of peptide amino and carboxyl termini to the stability of MHC class I molecules. Science 265: 398-402.

Boye, J., T. Elter, and A. Engert. 2003. An overview of the current clinical use of the anti-CD20 monoclonal

antibody rituximab. Ann Oncol 14: 520-535.

Brahmer, J. R., S. S. Tykodi, L. Q. Chow, W. J. Hwu, S. L. Topalian, P. Hwu, C. G. Drake, L. H. Camacho, J. Kauh, K. Odunsi, H. C. Pitot, O. Hamid, S. Bhatia, R. Martins, K. Eaton, S. Chen, T. M. Salay, S. Alaparthy, J. F. Grosso, A. J. Korman, S. M. Parker, S. Agrawal, S. M. Goldberg, D. M. Pardoll, A. Gupta, and J. M. Wigginton. 2012. Safety and activity of anti-PD-L1 antibody in patients with advanced cancer. N Engl J Med 366: 2455-2465.

Brennan, P., J. W. Babbage, B. M. Burgering, B. Groner, K. Reif, and D. A. Cantrell. 1997. Phosphatidylinositol 3-kinase couples the interleukin-2 receptor to the cell cycle regulator E2F. Immunity 7: 679-689.

Brown, K., S. Gerstberger, L. Carlson, G. Franzoso, and U. Siebenlist. 1995. Control of I kappa B-alpha proteolysis by site-specific, signal-induced phosphorylation. Science 267: 1485-1488.

Brown, J. A., D. M. Dorfman, F. R. Ma, E. L. Sullivan, O. Munoz, C. R. Wood, E. A. Greenfield, and G. J. Freeman. 2003. Blockade of programmed death-1 ligands on dendritic cells enhances T cell activation and cytokine production. J Immunol 170: 1257-1266.

Brummelkamp, T. R., S. M. Nijman, A. M. Dirac, and R. Bernards. 2003. Loss of the cylindromatosis tumour suppressor inhibits apoptosis by activating NF-kappaB. Nature 424: 797-801.

Brunet, A., A. Bonni, M. J. Zigmond, M. Z. Lin, P. Juo, L. S. Hu, M. J. Anderson, K. C. Arden, J. Blenis, and M. E. Greenberg. 1999. Akt promotes cell survival by phosphorylating and inhibiting a Forkhead transcription factor. Cell 96: 857-868.

Buchholz, M., A. Schatz, M. Wagner, P. Michl, T. Linhart, G. Adler, T. M. Gress, and V. Ellenrieder. 2006. Overexpression of c-myc in pancreatic cancer caused by ectopic activation of NFATc1 and the Ca2+/calcineurin signaling pathway. EMBO J 25: 3714-3724.

Buhl, A. M., and J. C. Cambier. 1999. Phosphorylation of CD19 Y484 and Y515, and linked activation of phosphatidylinositol 3-kinase, are required for B cell antigen receptor-mediated activation of Bruton's tyrosine kinase. J Immunol 162: 4438-4446.

Bunemann, M., and M. M. Hosey. 1999. G-protein coupled receptor kinases as modulators of G-protein signalling. J Physiol 517 (Pt 1): 5-23.

Bunnell, S. C., M. Diehn, M. B. Yaffe, P. R. Findell, L. C. Cantley, and L. J. Berg. 2000. Biochemical interactions integrating Itk with the T cell receptor-initiated signaling cascade. J Biol Chem 275: 2219-2230.

Busman-Sahay, K., L. Drake, A. Sitaram, M. Marks, and J. R. Drake. 2013. Cis and trans regulatory mechanisms control AP2-mediated B cell receptor endocytosis via select tyrosine-based motifs. PLoS One 8: e54938.

Caganova, M., C. Carrisi, G. Varano, F. Mainoldi, F. Zanardi, P. L. Germain, L. George, F. Alberghini, L. Ferrarini, A. K. Talukder, M. Ponzoni, G. Testa, T. Nojima, C. Doglioni, D. Kitamura, K. M. Toellner, I. H. Su, and S. Casola. 2013. Germinal center dysregulation by histone methyltransferase EZH2 promotes lymphomagenesis. J Clin Invest 123: 5009-5022.

Calaminici, M., K. Piper, A. M. Lee, and A. J. Norton. 2004. CD23 expression in mediastinal large B-cell lymphomas. Histopathology 45: 619-624.

Carbone, A., A. Gloghini, Y. L. Kwong, and A. Younes. 2014. Diffuse large B cell lymphoma: using pathologic and molecular biomarkers to define subgroups for novel therapy. Ann Hematol 93: 1263-1277.

Castillo, J. J., E. S. Winer, and A. J. Olszewski. 2014. Sites of extranodal involvement are prognostic in patients with diffuse large B-cell lymphoma in the rituximab era: an analysis of the Surveillance, Epidemiology and End Results database. Am J Hematol 89: 310-314.

Chan, V. W., C. A. Lowell, and A. L. DeFranco. 1998. Defective negative regulation of antigen receptor signaling in Lyn-deficient B lymphocytes. Curr Biol 8: 545-553.

Chen, L. F., and W. C. Greene. 2004. Shaping the nuclear action of NF-kappaB. Nat Rev Mol Cell Biol 5: 392-401.

Chen, C., L. C. Edelstein, and C. Gelinas. 2000. The Rel/NF-kappaB family directly activates expression of the apoptosis inhibitor Bcl-x(L). Mol Cell Biol 20: 2687-2695.

Chen, K., M. Febbraio, W. Li, and R. L. Silverstein. 2008. A specific CD36-dependent signaling pathway is required for platelet activation by oxidized low-density lipoprotein. Circ Res 102: 1512-1519.

Chen, L., J. N. Glover, P. G. Hogan, A. Rao, and S. C. Harrison. 1998. Structure of the DNA-binding domains from NFAT, Fos and Jun bound specifically to DNA. Nature 392: 42-48.

Chen, J., V. Stewart, G. Spyrou, F. Hilberg, E. F. Wagner, and F. W. Alt. 1994. Generation of normal T and B lymphocytes by c-jun deficient embryonic stem cells. Immunity 1: 65-72.

Chen, Z., J. Hagler, V. J. Palombella, F. Melandri, D. Scherer, D. Ballard, and T. Maniatis. 1995. Signal-induced site-specific phosphorylation targets I kappa B alpha to the ubiquitin-proteasome pathway. Genes Dev 9: 1586-1597.

Chen, B. J., B. Chapuy, J. Ouyang, H. H. Sun, M. G. Roemer, M. L. Xu, H. Yu, C. D. Fletcher, G. J. Freeman,

M. A. Shipp, and S. J. Rodig. 2013. PD-L1 expression is characteristic of a subset of aggressive B-cell lymphomas and virus-associated malignancies. Clin Cancer Res 19: 3462-3473.

Chen, L., S. Monti, P. Juszczynski, J. Ouyang, B. Chapuy, D. Neuberg, J. G. Doench, A. M. Bogusz, T. M. Habermann, A. Dogan, T. E. Witzig, J. L. Kutok, S. J. Rodig, T. Golub, and M. A. Shipp. 2013. SYK inhibition modulates distinct PI3K/AKT- dependent survival pathways and cholesterol biosynthesis in diffuse large B cell lymphomas. Cancer Cell 23: 826-838.

Cheng, A. M., B. Rowley, W. Pao, A. Hayday, J. B. Bolen, and T. Pawson. 1995. Syk tyrosine kinase required for mouse viability and B-cell development. Nature 378: 303-306.

Chiles, T. C., and T. L. Rothstein. 1992. Surface Ig receptor-induced nuclear AP-1-dependent gene expression in B lymphocytes. J Immunol 149: 825-831.

Chiu, C. W., M. Dalton, M. Ishiai, T. Kurosaki, and A. C. Chan. 2002. BLNK: molecular scaffolding through 'cis'-mediated organization of signaling proteins. EMBO J 21: 6461-6472.

Choi, J. H., H. R. Yoon, G. H. Kim, S. J. Park, Y. L. Shin, and H. W. Yoo. 2007. Identification of novel mutations of the HADHA and HADHB genes in patients with mitochondrial trifunctional protein deficiency. Int J Mol Med 19: 81-87.

Choi, W. W., D. D. Weisenburger, T. C. Greiner, M. A. Piris, A. H. Banham, J. Delabie, R. M. Braziel, H. Geng, J. Iqbal, G. Lenz, J. M. Vose, C. P. Hans, K. Fu, L. M. Smith, M. Li, Z. Liu, R. D. Gascoyne, A. Rosenwald, G. Ott, L. M. Rimsza, E. Campo, E. S. Jaffe, D. L. Jaye, L. M. Staudt, and W. C. Chan. 2009. A new immunostain algorithm classifies diffuse large B-cell lymphoma into molecular subtypes with high accuracy. Clin Cancer Res 15: 5494-5502.

Choquet, D., M. Partiseti, S. Amigorena, C. Bonnerot, W. H. Fridman, and H. Korn. 1993. Cross-linking of IgG receptors inhibits membrane immunoglobulin-stimulated calcium influx in B lymphocytes. J Cell Biol 121: 355-363.

Chu, P. G., and D. A. Arber. 2001. CD79: a review. Appl Immunohistochem Mol Morphol 9: 97-106.

Chu, D. H., C. T. Morita, and A. Weiss. 1998. The Syk family of protein tyrosine kinases in T-cell activation and development. Immunol Rev 165: 167-180.

Chu Fuliang , M. F., Hong Qin, Rakesh Sharma, Qing Yi, Galina Rodionov, Rinat Rotem-Yehudar and Sattva Neelapu. 2009. In Vitro and In Vivo Effects of CT-011, a Humanized Anti–PD-1 Monoclonal Antibody, in Combination with Rituximab against Human B-Cell Lymphomas. Blood 114:724.

Chuvpilo, S., C. Schomberg, R. Gerwig, A. Heinfling, R. Reeves, F. Grummt, and E. Serfling. 1993. Multiple closely-linked NFAT/octamer and HMG I(Y) binding sites are part of the interleukin-4 promoter. Nucleic Acids Res 21: 5694-5704.

Chuvpilo, S., A. Avots, F. Berberich-Siebelt, J. Glockner, C. Fischer, A. Kerstan, C. Escher, I. Inashkina, F. Hlubek, E. Jankevics, T. Brabletz, and E. Serfling. 1999. Multiple NF-ATc isoforms with individual transcriptional properties are synthesized in T lymphocytes. J Immunol 162: 7294-7301.

Ci, W., J. M. Polo, L. Cerchietti, R. Shaknovich, L. Wang, S. N. Yang, K. Ye, P. Farinha, D. E. Horsman, R. D. Gascoyne, O. Elemento, and A. Melnick. 2009. The BCL6 transcriptional program features repression of multiple oncogenes in primary B cells and is deregulated in DLBCL. Blood 113: 5536-5548.

Clark, M. R., K. S. Campbell, A. Kazlauskas, S. A. Johnson, M. Hertz, T. A. Potter, C. Pleiman, and J. C. Cambier. 1992. The B cell antigen receptor complex: association of Ig-alpha and Ig-beta with distinct cytoplasmic effectors. Science 258: 123-126.

Claudio, E., K. Brown, S. Park, H. Wang, and U. Siebenlist. 2002. BAFF-induced NEMO-independent processing of NF-kappa B2 in maturing B cells. Nat Immunol 3: 958-965.

Coiffier, B. 1997. Non-Hodgkin's lymphomas., pp. 265-287. In M. Dunitz (ed.), Textbook of medical oncology., London.

Coiffier, B., E. Lepage, J. Briere, R. Herbrecht, H. Tilly, R. Bouabdallah, P. Morel, E. Van Den Neste, G. Salles, P. Gaulard, F. Reyes, P. Lederlin, and C. Gisselbrecht. 2002. CHOP chemotherapy plus rituximab compared with CHOP alone in elderly patients with diffuse large-B-cell lymphoma. N Engl J Med 346: 235-242.

Colotta, F., N. Polentarutti, M. Sironi, and A. Mantovani. 1992. Expression and involvement of c-fos and c-jun protooncogenes in programmed cell death induced by growth factor deprivation in lymphoid cell lines. J Biol Chem 267: 18278-18283.

Compagno, M., W. K. Lim, A. Grunn, S. V. Nandula, M. Brahmachary, Q. Shen, F. Bertoni, M. Ponzoni, M. Scandurra, A. Califano, G. Bhagat, A. Chadburn, R. Dalla-Favera, and L. Pasqualucci. 2009. Mutations of multiple genes cause deregulation of NF-kappaB in diffuse large B-cell lymphoma. Nature 459: 717-721.

Consortium, T. M. s. 1999. Complete sequence and gene map of a human major histocompatibility complex. . Nature 401: 921-923.

Coope, H. J., P. G. Atkinson, B. Huhse, M. Belich, J. Janzen, M. J. Holman, G. G. Klaus, L. H. Johnston, and

S. C. Ley. 2002. CD40 regulates the processing of NF-kappaB2 p100 to p52. EMBO J 21: 5375-5385.

Coornaert, B., M. Baens, K. Heyninck, T. Bekaert, M. Haegman, J. Staal, L. Sun, Z. J. Chen, P. Marynen, and R. Beyaert. 2008. T cell antigen receptor stimulation induces MALT1 paracaspase-mediated cleavage of the NF-kappaB inhibitor A20. Nat Immunol 9: 263-271.

Coort, S. L., J. Willems, W. A. Coumans, G. J. van der Vusse, A. Bonen, J. F. Glatz, and J. J. Luiken. 2002. Sulfo-N-succinimidyl esters of long chain fatty acids specifically inhibit fatty acid translocase (FAT/CD36)-mediated cellular fatty acid uptake. Mol Cell Biochem 239: 213-219.

Corcoran, L. M., M. Karvelas, G. J. Nossal, Z. S. Ye, T. Jacks, and D. Baltimore. 1993. Oct-2, although not required for early B-cell development, is critical for later B-cell maturation and for postnatal survival. Genes Dev 7: 570-582.

Cornall, R. J., A. M. Cheng, T. Pawson, and C. C. Goodnow. 2000. Role of Syk in B-cell development and antigen-receptor signaling. Proc Natl Acad Sci U S A 97: 1713-1718.

Cornall, R. J., J. G. Cyster, M. L. Hibbs, A. R. Dunn, K. L. Otipoby, E. A. Clark, and C. C. Goodnow. 1998. Polygenic autoimmune traits: Lyn, CD22, and SHP-1 are limiting elements of a biochemical pathway regulating BCR signaling and selection. Immunity 8: 497-508.

Crabtree, G. R., and E. N. Olson. 2002. NFAT signaling: choreographing the social lives of cells. Cell 109 Suppl: S67-79.

Cragg, M. S., C. A. Walshe, A. O. Ivanov, and M. J. Glennie. 2005. The biology of CD20 and its potential as a target for mAb therapy. Curr Dir Autoimmun 8: 140-174.

Cresswell, P. 1994. Antigen presentation. Getting peptides into MHC class II molecules. Curr Biol 4: 541-543.

Cresswell, P. 1994. Assembly, transport, and function of MHC class II molecules. Annu Rev Immunol 12: 259-293.

Cross, D. A., D. R. Alessi, P. Cohen, M. Andjelkovich, and B. A. Hemmings. 1995. Inhibition of glycogen synthase kinase-3 by insulin mediated by protein kinase B. Nature 378: 785-789.

Cycon, K. A., L. M. Rimsza, and S. P. Murphy. 2009. Alterations in CIITA constitute a common mechanism accounting for downregulation of MHC class II expression in diffuse large B-cell lymphoma (DLBCL). Exp Hematol 37: 184-194.

Cyster, J. G., and C. C. Goodnow. 1995. Protein tyrosine phosphatase 1C negatively regulates antigen receptor signaling in B lymphocytes and determines thresholds for negative selection. Immunity 2: 13-24.

Cyster, J. G., and C. C. Goodnow. 1997. Tuning antigen receptor signaling by CD22: integrating cues from antigens and the microenvironment. Immunity 6: 509-517.

Dal Porto, J. M., S. B. Gauld, K. T. Merrell, D. Mills, A. E. Pugh-Bernard, and J. Cambier. 2004. B cell antigen receptor signaling 101. Mol Immunol 41: 599-613.

D'Ambrosio, D., K. L. Hippen, and J. C. Cambier. 1996. Distinct mechanisms mediate SHC association with the activated and resting B cell antigen receptor. Eur J Immunol 26: 1960-1965.

Danilova, O. V., L. J. Dumont, N. B. Levy, F. Lansigan, W. B. Kinlaw, A. V. Danilov, and P. Kaur. 2013. FASN and CD36 predict survival in rituximab-treated diffuse large B-cell lymphoma. J Hematop 6: 11-18.

Dashnamoorthy Ravi , N. A., Afshin Behesti, Paige Kozlowski, Frederick Lansigan, William B Kinlaw, Ronald Gartenhaus, Graham Jones, Lynn Hlatky and Andrew M. Evens. 2014. The Lipid Addiction of Diffuse Large B-Cell Lymphoma (DLBCL) and Potential Treatment Strategies with Novel Fatty Acid Synthase (FASN) Small Molecule Inhibitors. Blood 2014 124: 4490.

Datta, S. R., H. Dudek, X. Tao, S. Masters, H. Fu, Y. Gotoh, and M. E. Greenberg. 1997. Akt phosphorylation of BAD couples survival signals to the cell-intrinsic death machinery. Cell 91: 231-241.

Davis, R. E., K. D. Brown, U. Siebenlist, and L. M. Staudt. 2001. Constitutive nuclear factor kappaB activity is required for survival of activated B cell-like diffuse large B cell lymphoma cells. J Exp Med 194: 1861-1874.

Davis, R. E., V. N. Ngo, G. Lenz, P. Tolar, R. M. Young, P. B. Romesser, H. Kohlhammer, L. Lamy, H. Zhao, Y. Yang, W. Xu, A. L. Shaffer, G. Wright, W. Xiao, J. Powell, J. K. Jiang, C. J. Thomas, A. Rosenwald, G. Ott, H. K. Muller-Hermelink, R. D. Gascoyne, J. M. Connors, N. A. Johnson, L. M. Rimsza, E. Campo, E. S. Jaffe, W. H. Wilson, J. Delabie, E. B. Smeland, R. I. Fisher, R. M. Braziel, R. R. Tubbs, J. R. Cook, D. D. Weisenburger, W. C. Chan, S. K. Pierce, and L. M. Staudt. 2010. Chronic active B-cell-receptor signalling in diffuse large B-cell lymphoma. Nature 463: 88-92.

Dawson, D. W., S. F. Pearce, R. Zhong, R. L. Silverstein, W. A. Frazier, and N. P. Bouck. 1997. CD36 mediates the In vitro inhibitory effects of thrombospondin-1 on endothelial cells. J Cell Biol 138: 707-717.

De Gassart, A., V. Camosseto, J. Thibodeau, M. Ceppi, N. Catalan, P. Pierre, and E. Gatti. 2008. MHC class II stabilization at the surface of human dendritic cells is the result of maturation-dependent MARCH I down-regulation. Proc Natl Acad Sci U S A 105: 3491-3496.

Dejardin, E., N. M. Droin, M. Delhase, E. Haas, Y. Cao, C. Makris, Z. W. Li, M. Karin, C. F. Ware, and D. R. Green. 2002. The lymphotoxin-beta receptor induces different patterns of gene expression via two NF-

kappaB pathways. Immunity 17: 525-535.

del Peso, L., M. Gonzalez-Garcia, C. Page, R. Herrera, and G. Nunez. 1997. Interleukin-3-induced phosphorylation of BAD through the protein kinase Akt. Science 278: 687-689.

DiDonato, J., F. Mercurio, C. Rosette, J. Wu-Li, H. Suyang, S. Ghosh, and M. Karin. 1996. Mapping of the inducible IkappaB phosphorylation sites that signal its ubiquitination and degradation. Mol Cell Biol 16: 1295-1304.

Dobrzanski, P., R. P. Ryseck, and R. Bravo. 1994. Differential interactions of Rel-NF-kappa B complexes with I kappa B alpha determine pools of constitutive and inducible NF-kappa B activity. EMBO J 13: 4608-4616.

Dogan, A., E. Bagdi, P. Munson, and P. G. Isaacson. 2000. CD10 and BCL-6 expression in paraffin sections of normal lymphoid tissue and B-cell lymphomas. Am J Surg Pathol 24: 846-852.

Dong, H., S. E. Strome, D. R. Salomao, H. Tamura, F. Hirano, D. B. Flies, P. C. Roche, J. Lu, G. Zhu, K. Tamada, V. A. Lennon, E. Celis, and L. Chen. 2002. Tumor-associated B7-H1 promotes T-cell apoptosis: a potential mechanism of immune evasion. Nat Med 8: 793-800.

Douek, D. C., and D. M. Altmann. 1997. HLA-DO is an intracellular class II molecule with distinctive thymic expression. Int Immunol 9: 355-364.

Dubois, S. M., C. Alexia, Y. Wu, H. M. Leclair, C. Leveau, E. Schol, T. Fest, K. Tarte, Z. J. Chen, J. Gavard, and N. Bidere. 2014. A catalytic-independent role for the LUBAC in NF-kappaB activation upon antigen receptor engagement and in lymphoma cells. Blood 123: 2199-2203.

Dunleavy, K., and W. H. Wilson. 2015. Primary mediastinal B-cell lymphoma and mediastinal gray zone lymphoma: do they require a unique therapeutic approach? Blood 125: 33-39.

Dunn, G. P., A. T. Bruce, H. Ikeda, L. J. Old, and R. D. Schreiber. 2002. Cancer immunoediting: from immunosurveillance to tumor escape. Nat Immunol 3: 991-998.

Dutta, D., V. A. Barr, I. Akpan, P. R. Mittelstadt, L. I. Singha, L. E. Samelson, and J. D. Ashwell. 2017. Recruitment of calcineurin to the TCR positively regulates T cell activation. Nat Immunol 18: 196-204.

Eferl, R., and E. F. Wagner. 2003. AP-1: a double-edged sword in tumorigenesis. Nat Rev Cancer 3: 859-868.

Eto, A., T. Muta, S. Yamazaki, and K. Takeshige. 2003. Essential roles for NF-kappa B and a Toll/IL-1 receptor domain-specific signal(s) in the induction of I kappa B-zeta. Biochem Biophys Res Commun 301: 495-501.

Fagerlund, R., M. Behar, K. T. Fortmann, Y. E. Lin, J. D. Vargas, and A. Hoffmann. 2015. Anatomy of a negative feedback loop: the case of IkappaBalpha. J R Soc Interface 12: 0262.

Famiglietti, S. J., K. Nakamura, and J. C. Cambier. 1999. Unique features of SHIP, SHP-1 and SHP-2 binding to FcgammaRIIb revealed by surface plasmon resonance analysis. Immunol Lett 68: 35-40.

Fang, X., B. Xiu, Z. Yang, W. Qiu, L. Zhang, S. Zhang, Y. Wu, X. Zhu, X. Chen, S. Xie, X. Yi, A. Liang, and Y. Zeng. 2017. The expression and clinical relevance of PD-1, PD-L1, and TP63 in patients with diffuse large B-cell lymphoma. Medicine (Baltimore) 96: e6398.

Febbraio, M., D. P. Hajjar, and R. L. Silverstein. 2001. CD36: a class B scavenger receptor involved in angiogenesis, atherosclerosis, inflammation, and lipid metabolism. J Clin Invest 108: 785-791.

Feugier, P. 2015. A review of rituximab, the first anti-CD20 monoclonal antibody used in the treatment of B non-Hodgkin's lymphomas. Future Oncol 11: 1327-1342.

Fiala, G. J., D. Kaschek, B. Blumenthal, M. Reth, J. Timmer, and W. W. Schamel. 2013. Pre-clustering of the B cell antigen receptor demonstrated by mathematically extended electron microscopy. Front Immunol 4: 427.

Fiorini, E., I. Schmitz, W. E. Marissen, S. L. Osborn, M. Touma, T. Sasada, P. A. Reche, E. V. Tibaldi, R. E. Hussey, A. M. Kruisbeek, E. L. Reinherz, and L. K. Clayton. 2002. Peptide-induced negative selection of thymocytes activates transcription of an NF-kappa B inhibitor. Mol Cell 9: 637-648.

Flaswinkel, H., and M. Reth. 1994. Dual role of the tyrosine activation motif of the Ig-alpha protein during signal transduction via the B cell antigen receptor. EMBO J 13: 83-89.

Flockhart, R. J., J. L. Armstrong, N. J. Reynolds, and P. E. Lovat. 2009. NFAT signalling is a novel target of oncogenic BRAF in metastatic melanoma. Br J Cancer 101: 1448-1455.

Fong, D. C., A. Brauweiler, S. A. Minskoff, P. Bruhns, I. Tamir, I. Mellman, M. Daeron, and J. C. Cambier. 2000. Mutational analysis reveals multiple distinct sites within Fc gamma receptor IIB that function in inhibitory signaling. J Immunol 165: 4453-4462.

Fontan, L., C. Yang, V. Kabaleeswaran, L. Volpon, M. J. Osborne, E. Beltran, M. Garcia, L. Cerchietti, R. Shaknovich, S. N. Yang, F. Fang, R. D. Gascoyne, J. A. Martinez-Climent, J. F. Glickman, K. Borden, H. Wu, and A. Melnick. 2012. MALT1 small molecule inhibitors specifically suppress ABC-DLBCL in vitro and in vivo. Cancer Cell 22: 812-824.

Francis, D. A., J. G. Karras, X. Y. Ke, R. Sen, and T. L. Rothstein. 1995. Induction of the transcription factors NF-kappa B, AP-1 and NF-AT during B cell stimulation through the CD40 receptor. Int Immunol 7: 151-

161.

Franzoso, G., V. Bours, S. Park, M. Tomita-Yamaguchi, K. Kelly, and U. Siebenlist. 1992. The candidate oncoprotein Bcl-3 is an antagonist of p50/NF-kappa B-mediated inhibition. Nature 359: 339-342.

Franzoso, G., L. Carlson, T. Scharton-Kersten, E. W. Shores, S. Epstein, A. Grinberg, T. Tran, E. Shacter, A. Leonardi, M. Anver, P. Love, A. Sher, and U. Siebenlist. 1997. Critical roles for the Bcl-3 oncoprotein in T cell-mediated immunity, splenic microarchitecture, and germinal center reactions. Immunity 6: 479-490.

Freeman, G. J., A. J. Long, Y. Iwai, K. Bourque, T. Chernova, H. Nishimura, L. J. Fitz, N. Malenkovich, T. Okazaki, M. C. Byrne, H. F. Horton, L. Fouser, L. Carter, V. Ling, M. R. Bowman, B. M. Carreno, M. Collins, C. R. Wood, and T. Honjo. 2000. Engagement of the PD-1 immunoinhibitory receptor by a novel B7 family member leads to negative regulation of lymphocyte activation. J Exp Med 192: 1027-1034.

Frick, M., B. Dorken, and G. Lenz. 2011. The molecular biology of diffuse large B-cell lymphoma. Ther Adv Hematol 2: 369-379.

Friedberg, J. W., J. Sharman, J. Sweetenham, P. B. Johnston, J. M. Vose, A. Lacasce, J. Schaefer-Cutillo, S. De Vos, R. Sinha, J. P. Leonard, L. D. Cripe, S. A. Gregory, M. P. Sterba, A. M. Lowe, R. Levy, and M. A. Shipp. 2010. Inhibition of Syk with fostamatinib disodium has significant clinical activity in non-Hodgkin lymphoma and chronic lymphocytic leukemia. Blood 115: 2578-2585.

Fu, L., Y. C. Lin-Lee, L. V. Pham, A. Tamayo, L. Yoshimura, and R. J. Ford. 2006. Constitutive NF-kappaB and NFAT activation leads to stimulation of the BLyS survival pathway in aggressive B-cell lymphomas. Blood 107: 4540-4548.

Fuchs, S. Y., V. Adler, T. Buschmann, Z. Yin, X. Wu, S. N. Jones, and Z. Ronai. 1998. JNK targets p53 ubiquitination and degradation in nonstressed cells. Genes Dev 12: 2658-2663.

Fujimoto, M., Y. Fujimoto, J. C. Poe, P. J. Jansen, C. A. Lowell, A. L. DeFranco, and T. F. Tedder. 2000. CD19 regulates Src family protein tyrosine kinase activation in B lymphocytes through processive amplification. Immunity 13: 47-57.

Fujita, S., K. Seino, K. Sato, Y. Sato, K. Eizumi, N. Yamashita, M. Taniguchi, and K. Sato. 2006. Regulatory dendritic cells act as regulators of acute lethal systemic inflammatory response. Blood 107: 3656-3664.

Futterer, K., J. Wong, R. A. Grucza, A. C. Chan, and G. Waksman. 1998. Structural basis for Syk tyrosine kinase ubiquity in signal transduction pathways revealed by the crystal structure of its regulatory SH2 domains bound to a dually phosphorylated ITAM peptide. J Mol Biol 281: 523-537.

Gachet, S., and J. Ghysdael. 2009. Calcineurin/NFAT signaling in lymphoid malignancies. Gen Physiol Biophys 28 Spec No Focus: F47-54.

Gajate, C., M. T. Alonso, T. Schimmang, and F. Mollinedo. 1996. C-Fos is not essential for apoptosis. Biochem Biophys Res Commun 218: 267-272.

Gaul, B. S., M. L. Harrison, R. L. Geahlen, R. A. Burton, and C. B. Post. 2000. Substrate recognition by the Lyn protein-tyrosine kinase. NMR structure of the immunoreceptor tyrosine-based activation motif signaling region of the B cell antigen receptor. J Biol Chem 275: 16174-16182.

Gauld, S. B., J. M. Dal Porto, and J. C. Cambier. 2002. B cell antigen receptor signaling: roles in cell development and disease. Science 296: 1641-1642.

Gazumyan, A., A. Reichlin, and M. C. Nussenzweig. 2006. Ig beta tyrosine residues contribute to the control of B cell receptor signaling by regulating receptor internalization. Journal of Experimental Medicine 203: 1785-1794.

Georgiou, K., L. Chen, M. Berglund, W. Ren, N. F. de Miranda, S. Lisboa, M. Fangazio, S. Zhu, Y. Hou, K. Wu, W. Fang, X. Wang, B. Meng, L. Zhang, Y. Zeng, G. Bhagat, M. Nordenskjold, C. Sundstrom, G. Enblad, R. Dalla-Favera, H. Zhang, M. R. Teixeira, L. Pasqualucci, R. Peng, and Q. Pan-Hammarstrom. 2016. Genetic basis of PD-L1 overexpression in diffuse large B-cell lymphomas. Blood 127: 3026-3034.

Gerondakis, S., R. Grumont, I. Rourke, and M. Grossmann. 1998. The regulation and roles of Rel/NF-kappa B transcription factors during lymphocyte activation. Curr Opin Immunol 10: 353-359.

Gerondakis, S., M. Grossmann, Y. Nakamura, T. Pohl, and R. Grumont. 1999. Genetic approaches in mice to understand Rel/NF-kappaB and IkappaB function: transgenics and knockouts. Oncogene 18: 6888-6895.

Gerondakis, S., R. Grumont, R. Gugasyan, L. Wong, I. Isomura, W. Ho, and A. Banerjee. 2006. Unravelling the complexities of the NF-kappaB signalling pathway using mouse knockout and transgenic models. Oncogene 25: 6781-6799.

Gettinger, S., N. A. Rizvi, L. Q. Chow, H. Borghaei, J. Brahmer, N. Ready, D. E. Gerber, F. A. Shepherd, S. Antonia, J. W. Goldman, R. A. Juergens, S. A. Laurie, F. E. Nathan, Y. Shen, C. T. Harbison, and M. D. Hellmann. 2016. Nivolumab Monotherapy for First-Line Treatment of Advanced Non-Small-Cell

Lung Cancer. J Clin Oncol 34: 2980-2987.

Ghielmini, M., and E. Zucca. 2009. How I treat mantle cell lymphoma. Blood 114: 1469-1476.

Ghosh, S., and M. S. Hayden. 2008. New regulators of NF-kappaB in inflammation. Nat Rev Immunol 8: 837-848.

Ghosh, S., M. J. May, and E. B. Kopp. 1998. NF-kappa B and Rel proteins: evolutionarily conserved mediators of immune responses. Annu Rev Immunol 16: 225-260.

Giffin, M. J., J. C. Stroud, D. L. Bates, K. D. von Koenig, J. Hardin, and L. Chen. 2003. Structure of NFAT1 bound as a dimer to the HIV-1 LTR kappa B element. Nat Struct Biol 10: 800-806.

Glatz, J. F., J. J. Luiken, and A. Bonen. 2010. Membrane fatty acid transporters as regulators of lipid metabolism: implications for metabolic disease. Physiol Rev 90: 367-417.

Glimcher, L. H., and C. J. Kara. 1992. Sequences and factors: a guide to MHC class-II transcription. Annu Rev Immunol 10: 13-49.

Glud, S. Z., A. B. Sorensen, M. Andrulis, B. Wang, E. Kondo, R. Jessen, L. Krenacs, E. Stelkovics, M. Wabl, E. Serfling, A. Palmetshofer, and F. S. Pedersen. 2005. A tumor-suppressor function for NFATc3 in T-cell lymphomagenesis by murine leukemia virus. Blood 106: 3546-3552.

Graef, I. A., F. Chen, L. Chen, A. Kuo, and G. R. Crabtree. 2001. Signals transduced by Ca(2+)/calcineurin and NFATc3/c4 pattern the developing vasculature. Cell 105: 863-875.

Grant, P. A., C. B. Thompson, and S. Pettersson. 1995. IgM receptor-mediated transactivation of the IgH 3' enhancer couples a novel Elf-1-AP-1 protein complex to the developmental control of enhancer function. EMBO J 14: 4501-4513.

Green, M. R., S. Monti, S. J. Rodig, P. Juszczynski, T. Currie, E. O'Donnell, B. Chapuy, K. Takeyama, D. Neuberg, T. R. Golub, J. L. Kutok, and M. A. Shipp. 2010. Integrative analysis reveals selective 9p24.1 amplification, increased PD-1 ligand expression, and further induction via JAK2 in nodular sclerosing Hodgkin lymphoma and primary mediastinal large B-cell lymphoma. Blood 116: 3268-3277.

Gregory, M. A., T. L. Phang, P. Neviani, F. Alvarez-Calderon, C. A. Eide, T. O'Hare, V. Zaberezhnyy, R. T. Williams, B. J. Druker, D. Perrotti, and J. Degregori. 2010. Wnt/Ca2+/NFAT signaling maintains survival of Ph+ leukemia cells upon inhibition of Bcr-Abl. Cancer Cell 18: 74-87.

Grigoriadis, A. E., K. Schellander, Z. Q. Wang, and E. F. Wagner. 1993. Osteoblasts are target cells for transformation in c-fos transgenic mice. J Cell Biol 122: 685-701.

Grimm, S., M. K. Bauer, P. A. Baeuerle, and K. Schulze-Osthoff. 1996. Bcl-2 down-regulates the activity of transcription factor NF-kappaB induced upon apoptosis. J Cell Biol 134: 13-23.

Grody, F. N. N. R. X. S. W. 2013. pp. 25-46, Atlas of Hematopathology. Elsevier.

Guan, Y., H. Yao, Z. Zheng, G. Qiu, and K. Sun. 2011. MiR-125b targets BCL3 and suppresses ovarian cancer proliferation. Int J Cancer 128: 2274-2283.

Guy, K., L. J. Docherty, and A. E. Dewar. 1986. Deficient expression of MHC class II antigens in some cases of human B cell leukaemia. Clin Exp Immunol 63: 290-297.

Hachmann, J., L. E. Edgington-Mitchell, M. Poreba, L. E. Sanman, M. Drag, M. Bogyo, and G. S. Salvesen. 2015. Probes to monitor activity of the paracaspase MALT1. Chem Biol 22: 139-147.

Hacker, H., and M. Karin. 2006. Regulation and function of IKK and IKK-related kinases. Sci STKE 2006: re13.

Haddad, E. M., V. C. McAlister, E. Renouf, R. Malthaner, M. S. Kjaer, and L. L. Gluud. 2006. Cyclosporin versus tacrolimus for liver transplanted patients. Cochrane Database Syst Rev: CD005161.

Hailfinger, S., G. Lenz, V. Ngo, A. Posvitz-Fejfar, F. Rebeaud, M. Guzzardi, E. M. Penas, J. Dierlamm, W. C. Chan, L. M. Staudt, and M. Thome. 2009. Essential role of MALT1 protease activity in activated B cell-like diffuse large B-cell lymphoma. Proc Natl Acad Sci U S A 106: 19946-19951.

Halazonetis, T. D., K. Georgopoulos, M. E. Greenberg, and P. Leder. 1988. c-Jun dimerizes with itself and with c-Fos, forming complexes of different DNA binding affinities. Cell 55: 917-924.

Handel-Fernandez, M. E., and V. Vincek. 1999. Sequence analysis and expression of a mouse homolog of human IkappaBL gene. Biochim Biophys Acta 1444: 306-310.

Hanihara, F., Y. Takahashi, A. Okuma, T. Ohba, and T. Muta. 2013. Transcriptional and post-transcriptional regulation of IkappaB-zeta upon engagement of the BCR, TLRs and FcgammaR. Int Immunol 25: 531-544.

Hans, C. P., D. D. Weisenburger, T. C. Greiner, R. D. Gascoyne, J. Delabie, G. Ott, H. K. Muller-Hermelink, E. Campo, R. M. Braziel, E. S. Jaffe, Z. Pan, P. Farinha, L. M. Smith, B. Falini, A. H. Banham, A. Rosenwald, L. M. Staudt, J. M. Connors, J. O. Armitage, and W. C. Chan. 2004. Confirmation of the molecular classification of diffuse large B-cell lymphoma by immunohistochemistry using a tissue microarray. Blood 103: 275-282.

Harmon, C. M., and N. A. Abumrad. 1993. Binding of sulfosuccinimidyl fatty acids to adipocyte membrane proteins: isolation and amino-terminal sequence of an 88-kD protein implicated in transport of long-chain fatty acids. J Membr Biol 133: 43-49.

Hartenstein, B., S. Teurich, J. Hess, J. Schenkel, M. Schorpp-Kistner, and P. Angel. 2002. Th2 cell-specific cytokine expression and allergen-induced airway inflammation depend on JunB. EMBO J 21: 6321-6329.

Haruta, H., A. Kato, and K. Todokoro. 2001. Isolation of a novel interleukin-1-inducible nuclear protein bearing ankyrin-repeat motifs. J Biol Chem 276: 12485-12488.

Hashimoto, A., H. Okada, A. Jiang, M. Kurosaki, S. Greenberg, E. A. Clark, and T. Kurosaki. 1998. Involvement of guanosine triphosphatases and phospholipase C-gamma2 in extracellular signal-regulated kinase, c-Jun NH2-terminal kinase, and p38 mitogen-activated protein kinase activation by the B cell antigen receptor. J Exp Med 188: 1287-1295.

Hata, A., H. Sabe, T. Kurosaki, M. Takata, and H. Hanafusa. 1994. Functional analysis of Csk in signal transduction through the B-cell antigen receptor. Mol Cell Biol 14: 7306-7313.

Hatada, E. N., A. Nieters, F. G. Wulczyn, M. Naumann, R. Meyer, G. Nucifora, T. W. McKeithan, and C. Scheidereit. 1992. The ankyrin repeat domains of the NF-kappa B precursor p105 and the protooncogene bcl-3 act as specific inhibitors of NF-kappa B DNA binding. Proc Natl Acad Sci U S A 89: 2489-2493.

Hatem, J., A. M. Schrank-Hacker, C. D. Watt, J. J. Morrissette, A. I. Rubin, E. J. Kim, S. D. Nasta, M. A. Wasik, and A. M. Bogusz. 2016. Marginal zone lymphoma-derived interfollicular diffuse large B-cell lymphoma harboring 20q12 chromosomal deletion and missense mutation of BIRC3 gene: a case report. Diagn Pathol 11: 137.

Hayden, M. S., and S. Ghosh. 2004. Signaling to NF-kappaB. Genes Dev 18: 2195-2224.

Hayden, M. S., and S. Ghosh. 2008. Shared principles in NF-kappaB signaling. Cell 132: 344-362.

Hayden, M. S., and S. Ghosh. 2012. NF-kappaB, the first quarter-century: remarkable progress and outstanding questions. Genes Dev 26: 203-234.

Heit, J. J., A. A. Apelqvist, X. Gu, M. M. Winslow, J. R. Neilson, G. R. Crabtree, and S. K. Kim. 2006. Calcineurin/NFAT signalling regulates pancreatic beta-cell growth and function. Nature 443: 345-349.

Henkel, T., T. Machleidt, I. Alkalay, M. Kronke, Y. Ben-Neriah, and P. A. Baeuerle. 1993. Rapid proteolysis of I kappa B-alpha is necessary for activation of transcription factor NF-kappa B. Nature 365: 182-185.

Hermann-Kleiter, N., and G. Baier. 2010. NFAT pulls the strings during CD4+ T helper cell effector functions. Blood 115: 2989-2997.

Herrmann, A., E. Hoster, T. Zwingers, G. Brittinger, M. Engelhard, P. Meusers, M. Reiser, R. Forstpointner, B. Metzner, N. Peter, B. Wormann, L. Trumper, M. Pfreundschuh, H. Einsele, W. Hiddemann, M. Unterhalt, and M. Dreyling. 2009. Improvement of overall survival in advanced stage mantle cell lymphoma. J Clin Oncol 27: 511-518.

Hinz, M., S. C. Arslan, and C. Scheidereit. 2012. It takes two to tango: IkappaBs, the multifunctional partners of NF-kappaB. Immunol Rev 246: 59-76.

Hippen, K. L., A. M. Buhl, D. D'Ambrosio, K. Nakamura, C. Persin, and J. C. Cambier. 1997. Fc gammaRIIB1 inhibition of BCR-mediated phosphoinositide hydrolysis and Ca2+ mobilization is integrated by CD19 dephosphorylation. Immunity 7: 49-58.

Hirano, F., K. Kaneko, H. Tamura, H. Dong, S. Wang, M. Ichikawa, C. Rietz, D. B. Flies, J. S. Lau, G. Zhu, K. Tamada, and L. Chen. 2005. Blockade of B7-H1 and PD-1 by monoclonal antibodies potentiates cancer therapeutic immunity. Cancer Res 65: 1089-1096.

Hirotani, T., P. Y. Lee, H. Kuwata, M. Yamamoto, M. Matsumoto, I. Kawase, S. Akira, and K. Takeda. 2005. The nuclear IkappaB protein IkappaBNS selectively inhibits lipopolysaccharide-induced IL-6 production in macrophages of the colonic lamina propria. J Immunol 174: 3650-3657.

Hodge, M. R., A. M. Ranger, F. Charles de la Brousse, T. Hoey, M. J. Grusby, and L. H. Glimcher. 1996. Hyperproliferation and dysregulation of IL-4 expression in NF-ATp-deficient mice. Immunity 4: 397-405.

Hoffmann, A., A. Levchenko, M. L. Scott, and D. Baltimore. 2002. The IkappaB-NF-kappaB signaling module: temporal control and selective gene activation. Science 298: 1241-1245.

Hogan, P. G., L. Chen, J. Nardone, and A. Rao. 2003. Transcriptional regulation by calcium, calcineurin, and NFAT. Genes Dev 17: 2205-2232.

Honma, K., S. Tsuzuki, M. Nakagawa, H. Tagawa, S. Nakamura, Y. Morishima, and M. Seto. 2009. TNFAIP3/A20 functions as a novel tumor suppressor gene in several subtypes of non-Hodgkin lymphomas. Blood 114: 2467-2475.

Horsley, V., A. O. Aliprantis, L. Polak, L. H. Glimcher, and E. Fuchs. 2008. NFATc1 balances quiescence and proliferation of skin stem cells. Cell 132: 299-310.

Hoyos, B., D. W. Ballard, E. Bohnlein, M. Siekevitz, and W. C. Greene. 1989. Kappa B-specific DNA binding proteins: role in the regulation of human interleukin-2 gene expression. Science 244: 457-460.

Hsing, L. C., and A. Y. Rudensky. 2005. The lysosomal cysteine proteases in MHC class II antigen presentation. Immunol Rev 207: 229-241.

Hu, C. M., S. Y. Jang, J. C. Fanzo, and A. B. Pernis. 2002. Modulation of T cell cytokine production by interferon regulatory factor-4. J Biol Chem 277: 49238-49246.

Hu, S., M. Q. Du, S. M. Park, A. Alcivar, L. Qu, S. Gupta, J. Tang, M. Baens, H. Ye, T. H. Lee, P. Marynen, J. L. Riley, and X. Yang. 2006. cIAP2 is a ubiquitin protein ligase for BCL10 and is dysregulated in mucosa-associated lymphoid tissue lymphomas. J Clin Invest 116: 174-181.

Huang, T. T., N. Kudo, M. Yoshida, and S. Miyamoto. 2000. A nuclear export signal in the N-terminal regulatory domain of IkappaBalpha controls cytoplasmic localization of inactive NF-kappaB/IkappaBalpha complexes. Proc Natl Acad Sci U S A 97: 1014-1019.

Huang, M. M., J. B. Bolen, J. W. Barnwell, S. J. Shattil, and J. S. Brugge. 1991. Membrane glycoprotein IV (CD36) is physically associated with the Fyn, Lyn, and Yes protein-tyrosine kinases in human platelets. Proc Natl Acad Sci U S A 88: 7844-7848.

Huang, G. N., D. L. Huso, S. Bouyain, J. Tu, K. A. McCorkell, M. J. May, Y. Zhu, M. Lutz, S. Collins, M. Dehoff, S. Kang, K. Whartenby, J. Powell, D. Leahy, and P. F. Worley. 2008. NFAT binding and regulation of T cell activation by the cytoplasmic scaffolding Homer proteins. Science 319: 476-481.

Hunt, K. E., and K. K. Reichard. 2008. Diffuse large B-cell lymphoma. Arch Pathol Lab Med 132: 118-124.

Huo, L., and T. L. Rothstein. 1995. Receptor-specific induction of individual AP-1 components in B lymphocytes. J Immunol 154: 3300-3309.

Huo, L., and T. L. Rothstein. 1996. Isolation and characterization of murine fra-1: induction mediated by CD40 and surface Ig is protein kinase C dependent. J Immunol 157: 3812-3818.

Huxford, T., D. B. Huang, S. Malek, and G. Ghosh. 1998. The crystal structure of the IkappaBalpha/NF-kappaB complex reveals mechanisms of NF-kappaB inactivation. Cell 95: 759-770.

Ikeda, S., S. Kishida, H. Yamamoto, H. Murai, S. Koyama, and A. Kikuchi. 1998. Axin, a negative regulator of the Wnt signaling pathway, forms a complex with GSK-3beta and beta-catenin and promotes GSK-3beta-dependent phosphorylation of beta-catenin. EMBO J 17: 1371-1384.

Imamura, R., E. S. Masuda, Y. Naito, S. Imai, T. Fujino, T. Takano, K. Arai, and N. Arai. 1998. Carboxyl-terminal 15-amino acid sequence of NFATx1 is possibly created by tissue-specific splicing and is essential for transactivation activity in T cells. J Immunol 161: 3455-3463.

Inomata, M., H. Tagawa, Y. M. Guo, Y. Kameoka, N. Takahashi, and K. Sawada. 2009. MicroRNA-17-92 down-regulates expression of distinct targets in different B-cell lymphoma subtypes. Blood 113: 396-402.

Iqbal, J., T. C. Greiner, K. Patel, B. J. Dave, L. Smith, J. Ji, G. Wright, W. G. Sanger, D. L. Pickering, S. Jain, D. E. Horsman, Y. Shen, K. Fu, D. D. Weisenburger, C. P. Hans, E. Campo, R. D. Gascoyne, A. Rosenwald, E. S. Jaffe, J. Delabie, L. Rimsza, G. Ott, H. K. Muller-Hermelink, J. M. Connors, J. M. Vose, T. McKeithan, L. M. Staudt, W. C. Chan, and P. Leukemia/Lymphoma Molecular Profiling. 2007. Distinctive patterns of BCL6 molecular alterations and their functional consequences in different subgroups of diffuse large B-cell lymphoma. Leukemia 21: 2332-2343.

Isakov, N., and A. Altman. 2002. Protein kinase C(theta) in T cell activation. Annu Rev Immunol 20: 761-794.

Ishiai, M., M. Kurosaki, R. Pappu, K. Okawa, I. Ronko, C. Fu, M. Shibata, A. Iwamatsu, A. C. Chan, and T. Kurosaki. 1999. BLNK required for coupling Syk to PLC gamma 2 and Rac1-JNK in B cells. Immunity 10: 117-125.

Ishiai, M., M. Kurosaki, R. Pappu, K. Okawa, I. Ronko, C. Fu, M. Shibata, A. Iwamatsu, A. C. Chan, and T. Kurosaki. 1999. BLNK required for coupling Syk to PLC gamma 2 and Rac1-JNK in B cells. Immunity 10: 117-125.

Ishiura, Y., N. Kotani, R. Yamashita, H. Yamamoto, Y. Kozutsumi, and K. Honke. 2010. Anomalous expression of Thy1 (CD90) in B-cell lymphoma cells and proliferation inhibition by anti-Thy1 antibody treatment. Biochem Biophys Res Commun 396: 329-334.

Ito, C. Y., A. G. Kazantsev, and A. S. Baldwin, Jr. 1994. Three NF-kappa B sites in the I kappa B-alpha promoter are required for induction of gene expression by TNF alpha. Nucleic Acids Res 22: 3787-3792.

Ito, T., M. Morimatsu, T. Oonuma, T. Shiina, H. Kitamura, and B. Syuto. 2004. Transcriptional regulation of the MAIL gene in LPS-stimulated RAW264 mouse macrophages. Gene 342: 137-143.

Iwai, Y., S. Terawaki, and T. Honjo. 2005. PD-1 blockade inhibits hematogenous spread of poorly immunogenic tumor cells by enhanced recruitment of effector T cells. Int Immunol 17: 133-144.

Iwai, Y., M. Ishida, Y. Tanaka, T. Okazaki, T. Honjo, and N. Minato. 2002. Involvement of PD-L1 on tumor cells in the escape from host immune system and tumor immunotherapy by PD-L1 blockade. Proc Natl Acad Sci U S A 99: 12293-12297.

Jacobs, M. D., and S. C. Harrison. 1998. Structure of an IkappaBalpha/NF-kappaB complex. Cell 95: 749-758.

Jain, J., V. E. Valge-Archer, and A. Rao. 1992. Analysis of the AP-1 sites in the IL-2 promoter. J Immunol 148: 1240-1250.

Jain, J., Z. Miner, and A. Rao. 1993. Analysis of the preexisting and nuclear forms of nuclear factor of activated

T cells. J Immunol 151: 837-848.

Jain, J., C. Loh, and A. Rao. 1995. Transcriptional regulation of the IL-2 gene. Curr Opin Immunol 7: 333-342.

Jain, J., P. G. McCaffrey, V. E. Valge-Archer, and A. Rao. 1992. Nuclear factor of activated T cells contains Fos and Jun. Nature 356: 801-804.

Jain, P., L. E. Fayad, A. Rosenwald, K. H. Young, and S. O'Brien. 2013. Recent advances in de novo CD5+ diffuse large B cell lymphoma. Am J Hematol 88: 798-802.

Jain, J., E. A. Nalefski, P. G. McCaffrey, R. S. Johnson, B. M. Spiegelman, V. Papaioannou, and A. Rao. 1994. Normal peripheral T-cell function in c-Fos-deficient mice. Mol Cell Biol 14: 1566-1574.

Janabi, M., S. Yamashita, K. Hirano, N. Sakai, H. Hiraoka, K. Matsumoto, Z. Zhang, S. Nozaki, and Y. Matsuzawa. 2000. Oxidized LDL-induced NF-kappa B activation and subsequent expression of proinflammatory genes are defective in monocyte-derived macrophages from CD36-deficient patients. Arterioscler Thromb Vasc Biol 20: 1953-1960.

Jauliac, S., C. Lopez-Rodriguez, L. M. Shaw, L. F. Brown, A. Rao, and A. Toker. 2002. The role of NFAT transcription factors in integrin-mediated carcinoma invasion. Nat Cell Biol 4: 540-544.

Jeltsch, K. M., D. Hu, S. Brenner, J. Zoller, G. A. Heinz, D. Nagel, K. U. Vogel, N. Rehage, S. C. Warth, S. L. Edelmann, R. Gloury, N. Martin, C. Lohs, M. Lech, J. E. Stehklein, A. Geerlof, E. Kremmer, A. Weber, H. J. Anders, I. Schmitz, M. Schmidt-Supprian, M. Fu, H. Holtmann, D. Krappmann, J. Ruland, A. Kallies, M. Heikenwalder, and V. Heissmeyer. 2014. Cleavage of roquin and regnase-1 by the paracaspase MALT1 releases their cooperatively repressed targets to promote T(H)17 differentiation. Nat Immunol 15: 1079-1089.

Jimenez, B., O. V. Volpert, S. E. Crawford, M. Febbraio, R. L. Silverstein, and N. Bouck. 2000. Signals leading to apoptosis-dependent inhibition of neovascularization by thrombospondin-1. Nat Med 6: 41-48.

Johnson, C., D. Van Antwerp, and T. J. Hope. 1999. An N-terminal nuclear export signal is required for the nucleocytoplasmic shuttling of IkappaBalpha. EMBO J 18: 6682-6693.

Joos, S., M. I. Otano-Joos, S. Ziegler, S. Bruderlein, S. du Manoir, M. Bentz, P. Moller, and P. Lichter. 1996. Primary mediastinal (thymic) B-cell lymphoma is characterized by gains of chromosomal material including 9p and amplification of the REL gene. Blood 87: 1571-1578.

Jordanova, E. S., S. A. Riemersma, K. Philippo, M. Giphart-Gassler, E. Schuuring, and P. M. Kluin. 2002. Hemizygous deletions in the HLA region account for loss of heterozygosity in the majority of diffuse large B-cell lymphomas of the testis and the central nervous system. Genes Chromosomes Cancer 35: 38-48.

Juilland, M., M. Gonzalez, T. Erdmann, Y. Banz, Z. Jevnikar, S. Hailfinger, A. Tzankov, M. Grau, G. Lenz, U. Novak, and M. Thome. 2016. CARMA1- and MyD88-dependent activation of Jun/ATF-type AP-1 complexes is a hallmark of ABC diffuse large B-cell lymphomas. Blood 127: 1780-1789.

Kabak, S., B. J. Skaggs, M. R. Gold, M. Affolter, K. L. West, M. S. Foster, K. Siemasko, A. C. Chan, R. Aebersold, and M. R. Clark. 2002. The direct recruitment of BLNK to immunoglobulin alpha couples the B-cell antigen receptor to distal signaling pathways. Mol Cell Biol 22: 2524-2535.

Kalkhof, S., and A. Sinz. 2008. Chances and pitfalls of chemical cross-linking with amine-reactive N-hydroxysuccinimide esters. Anal Bioanal Chem 392: 305-312.

Kane, L. P., V. S. Shapiro, D. Stokoe, and A. Weiss. 1999. Induction of NF-kappaB by the Akt/PKB kinase. Curr Biol 9: 601-604.

Kannan, Y., J. Yu, R. M. Raices, S. Seshadri, M. Wei, M. A. Caligiuri, and M. D. Wewers. 2011. IkappaBzeta augments IL-12- and IL-18-mediated IFN-gamma production in human NK cells. Blood 117: 2855-2863.

Karlen, S., V. A. Mordvinov, and C. J. Sanderson. 1996. How is expression of the interleukin-5 gene regulated? Immunol Cell Biol 74: 218-223.

Kasof, G. M., L. Goyal, and E. White. 1999. Btf, a novel death-promoting transcriptional repressor that interacts with Bcl-2-related proteins. Mol Cell Biol 19: 4390-4404.

Kato, M., M. Sanada, I. Kato, Y. Sato, J. Takita, K. Takeuchi, A. Niwa, Y. Chen, K. Nakazaki, J. Nomoto, Y. Asakura, S. Muto, A. Tamura, M. Iio, Y. Akatsuka, Y. Hayashi, H. Mori, T. Igarashi, M. Kurokawa, S. Chiba, S. Mori, Y. Ishikawa, K. Okamoto, K. Tobinai, H. Nakagama, T. Nakahata, T. Yoshino, Y. Kobayashi, and S. Ogawa. 2009. Frequent inactivation of A20 in B-cell lymphomas. Nature 459: 712-716.

Kawakami, Z., I. Kitabayashi, T. Matsuoka, G. Gachelin, and K. Yokoyama. 1992. Conserved structural motifs among mammalian junB genes. Nucleic Acids Res 20: 914.

Kayama, H., V. R. Ramirez-Carrozzi, M. Yamamoto, T. Mizutani, H. Kuwata, H. Iba, M. Matsumoto, K. Honda, S. T. Smale, and K. Takeda. 2008. Class-specific regulation of pro-inflammatory genes by MyD88 pathways and IkappaBzeta. J Biol Chem 283: 12468-12477.

Kearns, J. D., S. Basak, S. L. Werner, C. S. Huang, and A. Hoffmann. 2006. IkappaBepsilon provides negative feedback to control NF-kappaB oscillations, signaling dynamics, and inflammatory gene expression. J

Cell Biol 173: 659-664.

Keir, M. E., M. J. Butte, G. J. Freeman, and A. H. Sharpe. 2008. PD-1 and its ligands in tolerance and immunity. Annu Rev Immunol 26: 677-704.

Kendrick, S., L. M. Rimsza, D. W. Scott, G. W. Slack, P. Farinha, K. L. Tan, D. Persky, S. Puvvada, J. M. Connors, L. Sehn, R. D. Gascoyne, and M. Schmelz. 2017. Aberrant cytoplasmic expression of MHCII confers worse progression free survival in diffuse large B-cell lymphoma. Virchows Arch 470: 113-117.

Kenkre, V. P., and B. S. Kahl. 2012. The future of B-cell lymphoma therapy: the B-cell receptor and its downstream pathways. Curr Hematol Malig Rep 7: 216-220.

Khan, S., R. de Giuli, G. Schmidtke, M. Bruns, M. Buchmeier, M. van den Broek, and M. Groettrup. 2001. Cutting edge: neosynthesis is required for the presentation of a T cell epitope from a long-lived viral protein. J Immunol 167: 4801-4804.

Khong, H. T., and N. P. Restifo. 2002. Natural selection of tumor variants in the generation of "tumor escape" phenotypes. Nat Immunol 3: 999-1005.

Kiani, A., J. P. Viola, A. H. Lichtman, and A. Rao. 1997. Down-regulation of IL-4 gene transcription and control of Th2 cell differentiation by a mechanism involving NFAT1. Immunity 7: 849-860.

Kiani, A., I. Habermann, M. Haase, S. Feldmann, S. Boxberger, M. A. Sanchez-Fernandez, C. Thiede, M. Bornhauser, and G. Ehninger. 2004. Expression and regulation of NFAT (nuclear factors of activated T cells) in human CD34+ cells: down-regulation upon myeloid differentiation. J Leukoc Biol 76: 1057-1065.

Kim, J. R., Y. J. Moon, K. S. Kwon, J. S. Bae, S. Wagle, K. M. Kim, H. S. Park, H. Lee, W. S. Moon, M. J. Chung, M. J. Kang, and K. Y. Jang. 2013. Tumor infiltrating PD1-positive lymphocytes and the expression of PD-L1 predict poor prognosis of soft tissue sarcomas. PLoS One 8: e82870.

Kishimoto, T. 2005. Interleukin-6: from basic science to medicine--40 years in immunology. Annu Rev Immunol 23: 1-21.

Kitamura, H., K. Kanehira, K. Okita, M. Morimatsu, and M. Saito. 2000. MAIL, a novel nuclear I kappa B protein that potentiates LPS-induced IL-6 production. FEBS Lett 485: 53-56.

Kiyasu, J., H. Miyoshi, A. Hirata, F. Arakawa, A. Ichikawa, D. Niino, Y. Sugita, Y. Yufu, I. Choi, Y. Abe, N. Uike, K. Nagafuji, T. Okamura, K. Akashi, R. Takayanagi, M. Shiratsuchi, and K. Ohshima. 2015. Expression of programmed cell death ligand 1 is associated with poor overall survival in patients with diffuse large B-cell lymphoma. Blood 126: 2193-2201.

Klemsz, M. J., L. B. Justement, E. Palmer, and J. C. Cambier. 1989. Induction of c-fos and c-myc expression during B cell activation by IL-4 and immunoglobulin binding ligands. J Immunol 143: 1032-1039.

Kloo B, N. D., Pfeifer M, Grau M, Düwel M, Vincendeau M, Dörken B, Lenz P, Lenz G, Krappmann D. 2011. Critical role of PI3K signaling for NF-kappaB-dependent survival in a subset of activated B-cell-like diffuse large B-cell lymphoma cells. Proc Natl Acad Sci U S A 108(1).

Knies, N., B. Alankus, A. Weilemann, A. Tzankov, K. Brunner, T. Ruff, M. Kremer, U. B. Keller, G. Lenz, and J. Ruland. 2015. Lymphomagenic CARD11/BCL10/MALT1 signaling drives malignant B-cell proliferation via cooperative NF-kappaB and JNK activation. Proc Natl Acad Sci U S A 112: E7230-7238.

Kobayashi, S., A. Hara, T. Isagawa, I. Manabe, K. Takeda, and T. MaruYama. 2014. The nuclear IkappaB family protein IkappaBNS influences the susceptibility to experimental autoimmune encephalomyelitis in a murine model. PLoS One 9: e110838.

Kobayashi, K., J. Phuchareon, K. Inada, Y. Tomita, T. Koizumi, M. Hatano, S. Miyatake, and T. Tokuhisa. 1997. Overexpression of c-fos inhibits down-regulation of a cyclin-dependent kinase-2 inhibitor p27Kip1 in splenic B cells activated by surface Ig cross-linking. J Immunol 158: 2050-2056.

Kobayashi, T., M. Yamaguchi, S. Kim, J. Morikawa, S. Ogawa, S. Ueno, E. Suh, E. Dougherty, I. Shmulevich, H. Shiku, and W. Zhang. 2003. Microarray reveals differences in both tumors and vascular specific gene expression in de novo CD5+ and CD5- diffuse large B-cell lymphomas. Cancer Res 63: 60-66.

Koch, M., F. Hussein, A. Woeste, C. Grundker, K. Frontzek, G. Emons, and T. Hawighorst. 2011. CD36-mediated activation of endothelial cell apoptosis by an N-terminal recombinant fragment of thrombospondin-2 inhibits breast cancer growth and metastasis in vivo. Breast Cancer Res Treat 128: 337-346.

Koenig, A., T. Linhart, K. Schlengemann, K. Reutlinger, J. Wegele, G. Adler, G. Singh, L. Hofmann, S. Kunsch, T. Buch, E. Schafer, T. M. Gress, M. E. Fernandez-Zapico, and V. Ellenrieder. 2010. NFAT-induced histone acetylation relay switch promotes c-Myc-dependent growth in pancreatic cancer cells. Gastroenterology 138: 1189-1199 e1181-1182.

Kolodziejski, P. J., M. B. Rashid, and N. T. Eissa. 2003. Intracellular formation of "undisruptable" dimers of inducible nitric oxide synthase. Proc Natl Acad Sci U S A 100: 14263-14268.

Kong, S., S. J. Kim, B. Sandal, S. M. Lee, B. Gao, D. D. Zhang, and D. Fang. 2011. The type III histone deacetylase Sirt1 protein suppresses p300-mediated histone H3 lysine 56 acetylation at Bclaf1

promoter to inhibit T cell activation. J Biol Chem 286: 16967-16975.

Konishi, J., K. Yamazaki, M. Azuma, I. Kinoshita, H. Dosaka-Akita, and M. Nishimura. 2004. B7-H1 expression on non-small cell lung cancer cells and its relationship with tumor-infiltrating lymphocytes and their PD-1 expression. Clin Cancer Res 10: 5094-5100.

Koopmann, J. O., J. Albring, E. Huter, N. Bulbuc, P. Spee, J. Neefjes, G. J. Hammerling, and F. Momburg. 2000. Export of antigenic peptides from the endoplasmic reticulum intersects with retrograde protein translocation through the Sec61p channel. Immunity 13: 117-127.

Kops, G. J., N. D. de Ruiter, A. M. De Vries-Smits, D. R. Powell, J. L. Bos, and B. M. Burgering. 1999. Direct control of the Forkhead transcription factor AFX by protein kinase B. Nature 398: 630-634.

Krappmann, D. 2013. Shaping oncogenic NF-kappaB activity in the nucleus. Blood 122: 2146-2147.

Kraus, M., K. Saijo, R. M. Torres, and K. Rajewsky. 1999. Ig-alpha cytoplasmic truncation renders immature B cells more sensitive to antigen contact. Immunity 11: 537-545.

Kraus, M., M. B. Alimzhanov, N. Rajewsky, and K. Rajewsky. 2004. Survival of resting mature B lymphocytes depends on BCR signaling via the Igalpha/beta heterodimer. Cell 117: 787-800.

Krempski, J., L. Karyampudi, M. D. Behrens, C. L. Erskine, L. Hartmann, H. Dong, E. L. Goode, K. R. Kalli, and K. L. Knutson. 2011. Tumor-infiltrating programmed death receptor-1+ dendritic cells mediate immune suppression in ovarian cancer. J Immunol 186: 6905-6913.

Krikos, A., C. D. Laherty, and V. M. Dixit. 1992. Transcriptional activation of the tumor necrosis factor alpha-inducible zinc finger protein, A20, is mediated by kappa B elements. J Biol Chem 267: 17971-17976.

Kropshofer, H., A. B. Vogt, G. Moldenhauer, J. Hammer, J. S. Blum, and G. J. Hammerling. 1996. Editing of the HLA-DR-peptide repertoire by HLA-DM. EMBO J 15: 6144-6154.

Kuda, O., C. M. Jenkins, J. R. Skinner, S. H. Moon, X. Su, R. W. Gross, and N. A. Abumrad. 2011. CD36 protein is involved in store-operated calcium flux, phospholipase A2 activation, and production of prostaglandin E2. J Biol Chem 286: 17785-17795.

Kuda, O., T. A. Pietka, Z. Demianova, E. Kudova, J. Cvacka, J. Kopecky, and N. A. Abumrad. 2013. Sulfo-N-succinimidyl oleate (SSO) inhibits fatty acid uptake and signaling for intracellular calcium via binding CD36 lysine 164: SSO also inhibits oxidized low density lipoprotein uptake by macrophages. J Biol Chem 288: 15547-15555.

Kulkarni, S., R. Savan, Y. Qi, X. Gao, Y. Yuki, S. E. Bass, M. P. Martin, P. Hunt, S. G. Deeks, A. Telenti, F. Pereyra, D. Goldstein, S. Wolinsky, B. Walker, H. A. Young, and M. Carrington. 2011. Differential microRNA regulation of HLA-C expression and its association with HIV control. Nature 472: 495-498.

Kumar, A., A. Bhanja, J. Bhattacharyya, and B. G. Jaganathan. 2016. Multiple roles of CD90 in cancer. Tumour Biol 37: 11611-11622.

Kuppers, R. 2005. Mechanisms of B-cell lymphoma pathogenesis. Nat Rev Cancer 5: 251-262.

Kurosaki, T., and S. Tsukada. 2000. BLNK: connecting Syk and Btk to calcium signals. Immunity 12: 1-5.

Kurts, C., B. W. Robinson, and P. A. Knolle. 2010. Cross-priming in health and disease. Nat Rev Immunol 10: 403-414.

Kuwata, H., M. Matsumoto, K. Atarashi, H. Morishita, T. Hirotani, R. Koga, and K. Takeda. 2006. IkappaBNS inhibits induction of a subset of Toll-like receptor-dependent genes and limits inflammation. Immunity 24: 41-51.

Kwiecinska, A., N. Tsesmetzis, M. Ghaderi, L. Kis, L. Saft, and G. Z. Rassidakis. 2016. CD274 (PD-L1)/PDCD1 (PD-1) expression in de novo and transformed diffuse large B-cell lymphoma. Br J Haematol.

Lam, L. T., G. Wright, R. E. Davis, G. Lenz, P. Farinha, L. Dang, J. W. Chan, A. Rosenwald, R. D. Gascoyne, and L. M. Staudt. 2008. Cooperative signaling through the signal transducer and activator of transcription 3 and nuclear factor-{kappa}B pathways in subtypes of diffuse large B-cell lymphoma. Blood 111: 3701-3713.

Lam, L. T., R. E. Davis, J. Pierce, M. Hepperle, Y. Xu, M. Hottelet, Y. Nong, D. Wen, J. Adams, L. Dang, and L. M. Staudt. 2005. Small molecule inhibitors of IkappaB kinase are selectively toxic for subgroups of diffuse large B-cell lymphoma defined by gene expression profiling. Clin Cancer Res 11: 28-40.

Lamy, L., V. N. Ngo, N. C. Emre, A. L. Shaffer, 3rd, Y. Yang, E. Tian, V. Nair, M. J. Kruhlak, A. Zingone, O. Landgren, and L. M. Staudt. 2013. Control of autophagic cell death by caspase-10 in multiple myeloma. Cancer Cell 23: 435-449.

Landsverk, O. J., O. Bakke, and T. F. Gregers. 2009. MHC II and the endocytic pathway: regulation by invariant chain. Scand J Immunol 70: 184-193.

Lawler, P. R., and J. Lawler. 2012. Molecular basis for the regulation of angiogenesis by thrombospondin-1 and -2. Cold Spring Harb Perspect Med 2: a006627.

Le Gros, G., S. Z. Ben-Sasson, R. Seder, F. D. Finkelman, and W. E. Paul. 1990. Generation of interleukin 4 (IL-4)-producing cells in vivo and in vitro: IL-2 and IL-4 are required for in vitro generation of IL-4-producing cells. J Exp Med 172: 921-929.

Le Roy, C., P. A. Deglesne, N. Chevallier, T. Beitar, V. Eclache, M. Quettier, M. Boubaya, R. Letestu, V. Levy, F. Ajchenbaum-Cymbalista, and N. Varin-Blank. 2012. The degree of BCR and NFAT activation predicts clinical outcomes in chronic lymphocytic leukemia. Blood 120: 356-365.

Lee, W., P. Mitchell, and R. Tjian. 1987. Purified transcription factor AP-1 interacts with TPA-inducible enhancer elements. Cell 49: 741-752.

Lee, H. J., E. S. Masuda, N. Arai, K. Arai, and T. Yokota. 1995. Definition of cis-regulatory elements of the mouse interleukin-5 gene promoter. Involvement of nuclear factor of activated T cell-related factors in interleukin-5 expression. J Biol Chem 270: 17541-17550.

Lee, H. H., H. Dadgostar, Q. Cheng, J. Shu, and G. Cheng. 1999. NF-kappaB-mediated up-regulation of Bcl-x and Bfl-1/A1 is required for CD40 survival signaling in B lymphocytes. Proc Natl Acad Sci U S A 96: 9136-9141.

Lehen'kyi, V., M. Flourakis, R. Skryma, and N. Prevarskaya. 2007. TRPV6 channel controls prostate cancer cell proliferation via Ca(2+)/NFAT-dependent pathways. Oncogene 26: 7380-7385.

LeibundGut-Landmann, S., J. M. Waldburger, M. Krawczyk, L. A. Otten, T. Suter, A. Fontana, H. Acha-Orbea, and W. Reith. 2004. Mini-review: Specificity and expression of CIITA, the master regulator of MHC class II genes. Eur J Immunol 34: 1513-1525.

Lennert, K., H. Stein, and E. Kaiserling. 1975. Cytological and functional criteria for the classification of malignant lymphomata. Br J Cancer Suppl 2: 29-43.

Lenz, G., I. Nagel, R. Siebert, A. V. Roschke, W. Sanger, G. W. Wright, S. S. Dave, B. Tan, H. Zhao, A. Rosenwald, H. K. Muller-Hermelink, R. D. Gascoyne, E. Campo, E. S. Jaffe, E. B. Smeland, R. I. Fisher, W. M. Kuehl, W. C. Chan, and L. M. Staudt. 2007. Aberrant immunoglobulin class switch recombination and switch translocations in activated B cell-like diffuse large B cell lymphoma. J Exp Med 204: 633-643.

Lenz, G., R. E. Davis, V. N. Ngo, L. Lam, T. C. George, G. W. Wright, S. S. Dave, H. Zhao, W. Xu, A. Rosenwald, G. Ott, H. K. Muller-Hermelink, R. D. Gascoyne, J. M. Connors, L. M. Rimsza, E. Campo, E. S. Jaffe, J. Delabie, E. B. Smeland, R. I. Fisher, W. C. Chan, and L. M. Staudt. 2008. Oncogenic CARD11 mutations in human diffuse large B cell lymphoma. Science 319: 1676-1679.

Lenz, G., G. W. Wright, N. C. Emre, H. Kohlhammer, S. S. Dave, R. E. Davis, S. Carty, L. T. Lam, A. L. Shaffer, W. Xiao, J. Powell, A. Rosenwald, G. Ott, H. K. Muller-Hermelink, R. D. Gascoyne, J. M. Connors, E. Campo, E. S. Jaffe, J. Delabie, E. B. Smeland, L. M. Rimsza, R. I. Fisher, D. D. Weisenburger, W. C. Chan, and L. M. Staudt. 2008. Molecular subtypes of diffuse large B-cell lymphoma arise by distinct genetic pathways. Proc Natl Acad Sci U S A 105: 13520-13525.

Lenz, G., G. Wright, S. S. Dave, W. Xiao, J. Powell, H. Zhao, W. Xu, B. Tan, N. Goldschmidt, J. Iqbal, J. Vose, M. Bast, K. Fu, D. D. Weisenburger, T. C. Greiner, J. O. Armitage, A. Kyle, L. May, R. D. Gascoyne, J. M. Connors, G. Troen, H. Holte, S. Kvaloy, D. Dierickx, G. Verhoef, J. Delabie, E. B. Smeland, P. Jares, A. Martinez, A. Lopez-Guillermo, E. Montserrat, E. Campo, R. M. Braziel, T. P. Miller, L. M. Rimsza, J. R. Cook, B. Pohlman, J. Sweetenham, R. R. Tubbs, R. I. Fisher, E. Hartmann, A. Rosenwald, G. Ott, H. K. Muller-Hermelink, D. Wrench, T. A. Lister, E. S. Jaffe, W. H. Wilson, W. C. Chan, L. M. Staudt, and P. Lymphoma/Leukemia Molecular Profiling. 2008. Stromal gene signatures in large-B-cell lymphomas. N Engl J Med 359: 2313-2323.

Leprince, C., K. E. Draves, J. A. Ledbetter, R. M. Torres, and E. A. Clark. 1992. Characterization of molecular components associated with surface immunoglobulin M in human B lymphocytes: presence of tyrosine and serine/threonine protein kinases. Eur J Immunol 22: 2093-2099.

Lernbecher, T., B. Kistler, and T. Wirth. 1994. Two distinct mechanisms contribute to the constitutive activation of RelB in lymphoid cells. EMBO J 13: 4060-4069.

Leslie, N. D., C. A. Valencia, A. W. Strauss, J. A. Connor, and K. Zhang. 1993. Very Long-Chain Acyl-Coenzyme A Dehydrogenase Deficiency. In M. P. Adam, H. H. Ardinger, R. A. Pagon, S. E. Wallace, L. J. H. Bean, H. C. Mefford, K. Stephens, A. Amemiya and N. Ledbetter (eds.), GeneReviews(R), Seattle (WA).

Lesokhin, A. M., S. M. Ansell, P. Armand, E. C. Scott, A. Halwani, M. Gutierrez, M. M. Millenson, A. D. Cohen, S. J. Schuster, D. Lebovic, M. Dhodapkar, D. Avigan, B. Chapuy, A. H. Ligon, G. J. Freeman, S. J. Rodig, D. Cattry, L. Zhu, J. F. Grosso, M. B. Bradley Garelik, M. A. Shipp, I. Borrello, and J. Timmerman. 2016. Nivolumab in Patients With Relapsed or Refractory Hematologic Malignancy: Preliminary Results of a Phase Ib Study. J Clin Oncol 34: 2698-2704.

LeVine, H., 3rd. 1999. Structural features of heterotrimeric G-protein-coupled receptors and their modulatory proteins. Mol Neurobiol 19: 111-149.

Li, Z., and G. J. Nabel. 1997. A new member of the I kappaB protein family, I kappaB epsilon, inhibits RelA (p65)-mediated NF-kappaB transcription. Mol Cell Biol 17: 6184-6190.

Li, Q., and I. M. Verma. 2002. NF-kappaB regulation in the immune system. Nat Rev Immunol 2: 725-734.

Li, J., K. DeFea, and R. A. Roth. 1999. Modulation of insulin receptor substrate-1 tyrosine phosphorylation by

an Akt/phosphatidylinositol 3-kinase pathway. J Biol Chem 274: 9351-9356.

Li, N., S. Banin, H. Ouyang, G. C. Li, G. Courtois, Y. Shiloh, M. Karin, and G. Rotman. 2001. ATM is required for IkappaB kinase (IKKk) activation in response to DNA double strand breaks. J Biol Chem 276: 8898-8903.

Li, Z., X. Wang, R. Y. Yu, B. B. Ding, J. J. Yu, X. M. Dai, A. Naganuma, E. R. Stanley, and B. H. Ye. 2005. BCL-6 negatively regulates expression of the NF-kappaB1 p105/p50 subunit. J Immunol 174: 205-214.

Liang, M., X. Han, S. Vadhan-Raj, M. Nguyen, Y. H. Zhang, M. Fernandez, E. Drakos, S. N. Konoplev, C. C. Yin, R. N. Miranda, T. J. McDonnell, L. J. Medeiros, and C. E. Bueso-Ramos. 2010. HDM4 is overexpressed in mantle cell lymphoma and its inhibition induces p21 expression and apoptosis. Mod Pathol 23: 381-391.

Libermann, T. A., and D. Baltimore. 1990. Activation of interleukin-6 gene expression through the NF-kappa B transcription factor. Mol Cell Biol 10: 2327-2334.

Liljedahl, M., T. Kuwana, W. P. Fung-Leung, M. R. Jackson, P. A. Peterson, and L. Karlsson. 1996. HLA-DO is a lysosomal resident which requires association with HLA-DM for efficient intracellular transport. EMBO J 15: 4817-4824.

Lim, C. P., and X. Cao. 1999. Serine phosphorylation and negative regulation of Stat3 by JNK. J Biol Chem 274: 31055-31061.

Lin, L., and S. Ghosh. 1996. A glycine-rich region in NF-kappaB p105 functions as a processing signal for the generation of the p50 subunit. Mol Cell Biol 16: 2248-2254.

Lindenblatt, C., K. Schulze-Osthoff, and G. Totzke. 2009. IkappaBzeta expression is regulated by miR-124a. Cell Cycle 8: 2019-2023.

Linderoth, J., M. Jerkeman, E. Cavallin-Stahl, S. Kvaloy, E. Torlakovic, and S. Nordic Lymphoma Group. 2003. Immunohistochemical expression of CD23 and CD40 may identify prognostically favorable subgroups of diffuse large B-cell lymphoma: a Nordic Lymphoma Group Study. Clin Cancer Res 9: 722-728.

Link, B. K., and J. W. Friedberg. 2008. Monoclonal antibodies in lymphoma: the first decade. Semin Hematol 45: 71-74.

List, A. F., C. M. Spier, T. P. Miller, and T. M. Grogan. 1993. Deficient tumor-infiltrating T-lymphocyte response in malignant lymphoma: relationship to HLA expression and host immunocompetence. Leukemia 7: 398-403.

Liu, H., Z. G. Lu, Y. Miki, and K. Yoshida. 2007. Protein kinase C delta induces transcription of the TP53 tumor suppressor gene by controlling death-promoting factor Btf in the apoptotic response to DNA damage. Mol Cell Biol 27: 8480-8491.

Liu, J., J. D. Farmer, Jr., W. S. Lane, J. Friedman, I. Weissman, and S. L. Schreiber. 1991. Calcineurin is a common target of cyclophilin-cyclosporin A and FKBP-FK506 complexes. Cell 66: 807-815.

Li-Weber, M., P. Salgame, C. Hu, and P. H. Krammer. 1997. Characterization of constitutive and inducible transcription factors binding to the P2 NF-AT site in the human interleukin-4 promoter. Gene 188: 253-260.

Li-Weber, M., M. Giaisi, S. Baumann, K. Palfi, and P. H. Krammer. 2004. NF-kappa B synergizes with NF-AT and NF-IL6 in activation of the IL-4 gene in T cells. Eur J Immunol 34: 1111-1118.

Lo Coco, F., B. H. Ye, F. Lista, P. Corradini, K. Offit, D. M. Knowles, R. S. Chaganti, and R. Dalla-Favera. 1994. Rearrangements of the BCL6 gene in diffuse large cell non-Hodgkin's lymphoma. Blood 83: 1757-1759.

Lobba, A. R., M. F. Forni, A. C. Carreira, and M. C. Sogayar. 2012. Differential expression of CD90 and CD14 stem cell markers in malignant breast cancer cell lines. Cytometry A 81: 1084-1091.

Lopez-Rodriguez, C., J. Aramburu, A. S. Rakeman, and A. Rao. 1999. NFAT5, a constitutively nuclear NFAT protein that does not cooperate with Fos and Jun. Proc Natl Acad Sci U S A 96: 7214-7219.

Lopez-Rodriguez, C., J. Aramburu, L. Jin, A. S. Rakeman, M. Michino, and A. Rao. 2001. Bridging the NFAT and NF-kappaB families: NFAT5 dimerization regulates cytokine gene transcription in response to osmotic stress. Immunity 15: 47-58.

Lucas, P. C., M. Yonezumi, N. Inohara, L. M. McAllister-Lucas, M. E. Abazeed, F. F. Chen, S. Yamaoka, M. Seto, and G. Nunez. 2001. Bcl10 and MALT1, independent targets of chromosomal translocation in malt lymphoma, cooperate in a novel NF-kappa B signaling pathway. J Biol Chem 276: 19012-19019.

Luisiri, P., Y. J. Lee, B. J. Eisfelder, and M. R. Clark. 1996. Cooperativity and segregation of function within the Ig-alpha/beta heterodimer of the B cell antigen receptor complex. J Biol Chem 271: 5158-5163.

Luo, C., E. Burgeon, and A. Rao. 1996. Mechanisms of transactivation by nuclear factor of activated T cells-1. J Exp Med 184: 141-147.

Ma, H., T. M. Yankee, J. Hu, D. J. Asai, M. L. Harrison, and R. L. Geahlen. 2001. Visualization of Syk-antigen receptor interactions using green fluorescent protein: differential roles for Syk and Lyn in the regulation

of receptor capping and internalization. J Immunol 166: 1507-1516.

Ma, J., W. Xing, G. Coffey, K. Dresser, K. Lu, A. Guo, G. Raca, A. Pandey, P. Conley, H. Yu, and Y. L. Wang. 2015. Cerdulatinib, a novel dual SYK/JAK kinase inhibitor, has broad anti-tumor activity in both ABC and GCB types of diffuse large B cell lymphoma. Oncotarget 6: 43881-43896.

Macian, F. 2005. NFAT proteins: key regulators of T-cell development and function. Nat Rev Immunol 5: 472-484.

Macian, F., C. Lopez-Rodriguez, and A. Rao. 2001. Partners in transcription: NFAT and AP-1. Oncogene 20: 2476-2489.

Macian, F., F. Garcia-Cozar, S. H. Im, H. F. Horton, M. C. Byrne, and A. Rao. 2002. Transcriptional mechanisms underlying lymphocyte tolerance. Cell 109: 719-731.

Majeti, R., Z. Xu, T. G. Parslow, J. L. Olson, D. I. Daikh, N. Killeen, and A. Weiss. 2000. An inactivating point mutation in the inhibitory wedge of CD45 causes lymphoproliferation and autoimmunity. Cell 103: 1059-1070.

Malek, S., Y. Chen, T. Huxford, and G. Ghosh. 2001. IkappaBbeta, but not IkappaBalpha, functions as a classical cytoplasmic inhibitor of NF-kappaB dimers by masking both NF-kappaB nuclear localization sequences in resting cells. J Biol Chem 276: 45225-45235.

Malek, S., D. B. Huang, T. Huxford, S. Ghosh, and G. Ghosh. 2003. X-ray crystal structure of an IkappaBbeta x NF-kappaB p65 homodimer complex. J Biol Chem 278: 23094-23100.

Mancini, M., and A. Toker. 2009. NFAT proteins: emerging roles in cancer progression. Nat Rev Cancer 9: 810-820.

Marafioti, T., M. Pozzobon, M. L. Hansmann, R. Ventura, S. A. Pileri, H. Roberton, S. Gesk, P. Gaulard, T. F. Barth, M. Q. Du, L. Leoncini, P. Moller, Y. Natkunam, R. Siebert, and D. Y. Mason. 2005. The NFATc1 transcription factor is widely expressed in white cells and translocates from the cytoplasm to the nucleus in a subset of human lymphomas. Br J Haematol 128: 333-342.

Marson, A., K. Kretschmer, G. M. Frampton, E. S. Jacobsen, J. K. Polansky, K. D. MacIsaac, S. S. Levine, E. Fraenkel, H. von Boehmer, and R. A. Young. 2007. Foxp3 occupancy and regulation of key target genes during T-cell stimulation. Nature 445: 931-935.

Martin, C. A., and M. E. Dorf. 1991. Differential regulation of interleukin-6, macrophage inflammatory protein-1, and JE/MCP-1 cytokine expression in macrophage cell lines. Cell Immunol 135: 245-258.

Mathas, S., M. Hinz, I. Anagnostopoulos, D. Krappmann, A. Lietz, F. Jundt, K. Bommert, F. Mechta-Grigoriou, H. Stein, B. Dorken, and C. Scheidereit. 2002. Aberrantly expressed c-Jun and JunB are a hallmark of Hodgkin lymphoma cells, stimulate proliferation and synergize with NF-kappa B. EMBO J 21: 4104-4113.

Mathey-Prevot, B., N. C. Andrews, H. S. Murphy, S. G. Kreissman, and D. G. Nathan. 1990. Positive and negative elements regulate human interleukin 3 expression. Proc Natl Acad Sci U S A 87: 5046-5050.

Matsumura, M., D. H. Fremont, P. A. Peterson, and I. A. Wilson. 1992. Emerging principles for the recognition of peptide antigens by MHC class I molecules. Science 257: 927-934.

McCaffrey, P. G., C. Luo, T. K. Kerppola, J. Jain, T. M. Badalian, A. M. Ho, E. Burgeon, W. S. Lane, J. N. Lambert, T. Curran, and et al. 1993. Isolation of the cyclosporin-sensitive T cell transcription factor NFATp. Science 262: 750-754.

McCluggage, W. G., V. P. Sumathi, and P. Maxwell. 2001. CD10 is a sensitive and diagnostically useful immunohistochemical marker of normal endometrial stroma and of endometrial stromal neoplasms. Histopathology 39: 273-278.

Medyouf, H., H. Alcalde, C. Berthier, M. C. Guillemin, N. R. dos Santos, A. Janin, D. Decaudin, H. de The, and J. Ghysdael. 2007. Targeting calcineurin activation as a therapeutic strategy for T-cell acute lymphoblastic leukemia. Nat Med 13: 736-741.

Meixner, A., F. Karreth, L. Kenner, and E. F. Wagner. 2004. JunD regulates lymphocyte proliferation and T helper cell cytokine expression. EMBO J 23: 1325-1335.

Miao, W. M., E. Vasile, W. S. Lane, and J. Lawler. 2001. CD36 associates with CD9 and integrins on human blood platelets. Blood 97: 1689-1696.

Migliazza, A., S. Martinotti, W. Chen, C. Fusco, B. H. Ye, D. M. Knowles, K. Offit, R. S. Chaganti, and R. Dalla-Favera. 1995. Frequent somatic hypermutation of the 5' noncoding region of the BCL6 gene in B-cell lymphoma. Proc Natl Acad Sci U S A 92: 12520-12524.

Miyakawa, H., S. K. Woo, S. C. Dahl, J. S. Handler, and H. M. Kwon. 1999. Tonicity-responsive enhancer binding protein, a rel-like protein that stimulates transcription in response to hypertonicity. Proc Natl Acad Sci U S A 96: 2538-2542.

Miyake, T., T. Satoh, H. Kato, K. Matsushita, Y. Kumagai, A. Vandenbon, T. Tani, T. Muta, S. Akira, and O. Takeuchi. 2010. IkappaBzeta is essential for natural killer cell activation in response to IL-12 and IL-18. Proc Natl Acad Sci U S A 107: 17680-17685.

Mizuno, K., Y. Tagawa, K. Mitomo, Y. Arimura, N. Hatano, T. Katagiri, M. Ogimoto, and H. Yakura. 2000. Src homology region 2 (SH2) domain-containing phosphatase-1 dephosphorylates B cell linker protein/SH2 domain leukocyte protein of 65 kDa and selectively regulates c-Jun NH2-terminal kinase activation in B cells. J Immunol 165: 1344-1351.

Mohan, N., and M. L. Meltz. 1994. Induction of nuclear factor kappa B after low-dose ionizing radiation involves a reactive oxygen intermediate signaling pathway. Radiat Res 140: 97-104.

Molkentin, J. D., J. R. Lu, C. L. Antos, B. Markham, J. Richardson, J. Robbins, S. R. Grant, and E. N. Olson. 1998. A calcineurin-dependent transcriptional pathway for cardiac hypertrophy. Cell 93: 215-228.

Moller, P., B. Lammler, B. Herrmann, H. F. Otto, G. Moldenhauer, and F. Momburg. 1986. The primary mediastinal clear cell lymphoma of B-cell type has variable defects in MHC antigen expression. Immunology 59: 411-417.

Moller, P., G. Moldenhauer, F. Momburg, B. Lammler, M. Eberlein-Gonska, S. Kiesel, and B. Dorken. 1987. Mediastinal lymphoma of clear cell type is a tumor corresponding to terminal steps of B cell differentiation. Blood 69: 1087-1095.

Momburg, F., B. Herrmann, G. Moldenhauer, and P. Moller. 1987. B-cell lymphomas of high-grade malignancy frequently lack HLA-DR, -DP and -DQ antigens and associated invariant chain. Int J Cancer 40: 598-603.

Monroe, J. G. 2004. Ligand-independent tonic signaling in B-cell receptor function. Curr Opin Immunol 16: 288-295.

Moore, K. W., R. de Waal Malefyt, R. L. Coffman, and A. O'Garra. 2001. Interleukin-10 and the interleukin-10 receptor. Annu Rev Immunol 19: 683-765.

Moore, K. J., J. El Khoury, L. A. Medeiros, K. Terada, C. Geula, A. D. Luster, and M. W. Freeman. 2002. A CD36-initiated signaling cascade mediates inflammatory effects of beta-amyloid. J Biol Chem 277: 47373-47379.

Moreno-Garcia, M. E., K. Sommer, H. Rincon-Arano, M. Brault, J. Ninomiya-Tsuji, L. E. Matesic, and D. J. Rawlings. 2013. Kinase-independent feedback of the TAK1/TAB1 complex on BCL10 turnover and NF-kappaB activation. Mol Cell Biol 33: 1149-1163.

Morin, R. D., N. A. Johnson, T. M. Severson, A. J. Mungall, J. An, R. Goya, J. E. Paul, M. Boyle, B. W. Woolcock, F. Kuchenbauer, D. Yap, R. K. Humphries, O. L. Griffith, S. Shah, H. Zhu, M. Kimbara, P. Shashkin, J. F. Charlot, M. Tcherpakov, R. Corbett, A. Tam, R. Varhol, D. Smailus, M. Moksa, Y. Zhao, A. Delaney, H. Qian, I. Birol, J. Schein, R. Moore, R. Holt, D. E. Horsman, J. M. Connors, S. Jones, S. Aparicio, M. Hirst, R. D. Gascoyne, and M. A. Marra. 2010. Somatic mutations altering EZH2 (Tyr641) in follicular and diffuse large B-cell lymphomas of germinal-center origin. Nat Genet 42: 181-185.

Motoyama, M., S. Yamazaki, A. Eto-Kimura, K. Takeshige, and T. Muta. 2005. Positive and negative regulation of nuclear factor-kappaB-mediated transcription by IkappaB-zeta, an inducible nuclear protein. J Biol Chem 280: 7444-7451.

Muenst, S., S. Hoeller, N. Willi, S. Dirnhofera, and A. Tzankov. 2010. Diagnostic and prognostic utility of PD-1 in B cell lymphomas. Dis Markers 29: 47-53.

Mufson, R. A. 1997. The role of serine/threonine phosphorylation in hematopoietic cytokine receptor signal transduction. FASEB J 11: 37-44.

Muller, M. R., and A. Rao. 2010. NFAT, immunity and cancer: a transcription factor comes of age. Nat Rev Immunol 10: 645-656.

Muller, R., J. Wienands, and M. Reth. 2000. The serine and threonine residues in the Ig-alpha cytoplasmic tail negatively regulate immunoreceptor tyrosine-based activation motif-mediated signal transduction. Proc Natl Acad Sci U S A 97: 8451-8454.

Muris, J. J., C. J. Meijer, W. Vos, J. H. van Krieken, N. M. Jiwa, G. J. Ossenkoppele, and J. J. Oudejans. 2006. Immunohistochemical profiling based on Bcl-2, CD10 and MUM1 expression improves risk stratification in patients with primary nodal diffuse large B cell lymphoma. J Pathol 208: 714-723.

Musti, A. M., M. Treier, and D. Bohmann. 1997. Reduced ubiquitin-dependent degradation of c-Jun after phosphorylation by MAP kinases. Science 275: 400-402.

Naeim Faramarz, P. N. R., Sophie X., Song, Wayne W. Grody. 2013. pp. 25-46, Atlas of Hematopathology. Elsevier.

Nagai, K., M. Takata, H. Yamamura, and T. Kurosaki. 1995. Tyrosine phosphorylation of Shc is mediated through Lyn and Syk in B cell receptor signaling. J Biol Chem 270: 6824-6829.

Nakamura, K., A. Brauweiler, and J. C. Cambier. 2000. Effects of Src homology domain 2 (SH2)-containing inositol phosphatase (SHIP), SH2-containing phosphotyrosine phosphatase (SHP)-1, and SHP-2 SH2 decoy proteins on Fc gamma RIIB1-effector interactions and inhibitory functions. J Immunol 164: 631-638.

Narimatsu, M., H. Maeda, S. Itoh, T. Atsumi, T. Ohtani, K. Nishida, M. Itoh, D. Kamimura, S. J. Park, K. Mizuno, J. Miyazaki, M. Hibi, K. Ishihara, K. Nakajima, and T. Hirano. 2001. Tissue-specific autoregulation of the stat3 gene and its role in interleukin-6-induced survival signals in T cells. Mol Cell Biol 21: 6615-6625.

Nayak, A., J. Glockner-Pagel, M. Vaeth, J. E. Schumann, M. Buttmann, T. Bopp, E. Schmitt, E. Serfling, and F. Berberich-Siebelt. 2009. Sumoylation of the transcription factor NFATc1 leads to its subnuclear relocalization and interleukin-2 repression by histone deacetylase. J Biol Chem 284: 10935-10946.

Naylor, T. L., H. Tang, B. A. Ratsch, A. Enns, A. Loo, L. Chen, P. Lenz, N. J. Waters, W. Schuler, B. Dorken, Y. M. Yao, M. Warmuth, G. Lenz, and F. Stegmeier. 2011. Protein kinase C inhibitor sotrastaurin selectively inhibits the growth of CD79 mutant diffuse large B-cell lymphomas. Cancer Res 71: 2643-2653.

Neefjes, J. J., and H. L. Ploegh. 1988. Allele and locus-specific differences in cell surface expression and the association of HLA class I heavy chain with beta 2-microglobulin: differential effects of inhibition of glycosylation on class I subunit association. Eur J Immunol 18: 801-810.

Neefjes, J., M. L. Jongsma, P. Paul, and O. Bakke. 2011. Towards a systems understanding of MHC class I and MHC class II antigen presentation. Nat Rev Immunol 11: 823-836.

Ngo, V. N., R. E. Davis, L. Lamy, X. Yu, H. Zhao, G. Lenz, L. T. Lam, S. Dave, L. Yang, J. Powell, and L. M. Staudt. 2006. A loss-of-function RNA interference screen for molecular targets in cancer. Nature 441: 106-110.

Ngo, V. N., R. M. Young, R. Schmitz, S. Jhavar, W. Xiao, K. H. Lim, H. Kohlhammer, W. Xu, Y. Yang, H. Zhao, A. L. Shaffer, P. Romesser, G. Wright, J. Powell, A. Rosenwald, H. K. Muller-Hermelink, G. Ott, R. D. Gascoyne, J. M. Connors, L. M. Rimsza, E. Campo, E. S. Jaffe, J. Delabie, E. B. Smeland, R. I. Fisher, R. M. Braziel, R. R. Tubbs, J. R. Cook, D. D. Weisenburger, W. C. Chan, and L. M. Staudt. 2011. Oncogenically active MYD88 mutations in human lymphoma. Nature 470: 115-119.

Niemann, C. U., and A. Wiestner. 2013. B-cell receptor signaling as a driver of lymphoma development and evolution. Semin Cancer Biol 23: 410-421.

Niiro, H., and E. A. Clark. 2002. Regulation of B-cell fate by antigen-receptor signals. Nat Rev Immunol 2: 945-956.

Nogai, H., S. S. Wenzel, S. Hailfinger, M. Grau, E. Kaergel, V. Seitz, B. Wollert-Wulf, M. Pfeifer, A. Wolf, M. Frick, K. Dietze, H. Madle, A. Tzankov, M. Hummel, B. Dorken, C. Scheidereit, M. Janz, P. Lenz, M. Thome, and G. Lenz. 2013. IkappaB-zeta controls the constitutive NF-kappaB target gene network and survival of ABC DLBCL. Blood 122: 2242-2250.

Noguchi, H., M. Matsushita, T. Okitsu, A. Moriwaki, K. Tomizawa, S. Kang, S. T. Li, N. Kobayashi, S. Matsumoto, K. Tanaka, N. Tanaka, and H. Matsui. 2004. A new cell-permeable peptide allows successful allogeneic islet transplantation in mice. Nat Med 10: 305-309.

Nolan, G. P., T. Fujita, K. Bhatia, C. Huppi, H. C. Liou, M. L. Scott, and D. Baltimore. 1993. The bcl-3 proto-oncogene encodes a nuclear I kappa B-like molecule that preferentially interacts with NF-kappa B p50 and p52 in a phosphorylation-dependent manner. Mol Cell Biol 13: 3557-3566.

Novack, D. V., L. Yin, A. Hagen-Stapleton, R. D. Schreiber, D. V. Goeddel, F. P. Ross, and S. L. Teitelbaum. 2003. The IkappaB function of NF-kappaB2 p100 controls stimulated osteoclastogenesis. J Exp Med 198: 771-781.

Ochi, Y., T. Koizumi, S. Kobayashi, J. Phuchareon, M. Hatano, M. Takada, Y. Tomita, and T. Tokuhisa. 1994. Analysis of IL-2 gene regulation in c-fos transgenic mice. Evidence for an enhancement of IL-2 expression in splenic T cells stimulated via TCR/CD3 complex. J Immunol 153: 3485-3490.

Oeckinghaus, A., and S. Ghosh. 2009. The NF-kappaB family of transcription factors and its regulation. Cold Spring Harb Perspect Biol 1: a000034.

Oeckinghaus, A., M. S. Hayden, and S. Ghosh. 2011. Crosstalk in NF-kappaB signaling pathways. Nat Immunol 12: 695-708.

Oh, H., E. Ozkirimli, K. Shah, M. L. Harrison, and R. L. Geahlen. 2007. Generation of an analog-sensitive Syk tyrosine kinase for the study of signaling dynamics from the B cell antigen receptor. J Biol Chem 282: 33760-33768.

Ohno, H., G. Takimoto, and T. W. McKeithan. 1990. The candidate proto-oncogene bcl-3 is related to genes implicated in cell lineage determination and cell cycle control. Cell 60: 991-997.

Ohshima, K., C. Kawasaki, H. Muta, K. Muta, V. Deyev, S. Haraoka, J. Suzumiya, E. R. Podack, and M. Kikuchi. 2001. CD10 and Bcl10 expression in diffuse large B-cell lymphoma: CD10 is a marker of improved prognosis. Histopathology 39: 156-162.

Okamoto, K., Y. Iwai, M. Oh-Hora, M. Yamamoto, T. Morio, K. Aoki, K. Ohya, A. M. Jetten, S. Akira, T. Muta, and H. Takayanagi. 2010. IkappaBzeta regulates T(H)17 development by cooperating with ROR nuclear receptors. Nature 464: 1381-1385.

Okuma, A., K. Hoshino, T. Ohba, S. Fukushi, S. Aiba, S. Akira, M. Ono, T. Kaisho, and T. Muta. 2013. Enhanced apoptosis by disruption of the STAT3-IkappaB-zeta signaling pathway in epithelial cells induces Sjogren's syndrome-like autoimmune disease. Immunity 38: 450-460.

Olive, M., D. Krylov, D. R. Echlin, K. Gardner, E. Taparowsky, and C. Vinson. 1997. A dominant negative to activation protein-1 (AP1) that abolishes DNA binding and inhibits oncogenesis. J Biol Chem 272: 18586-18594.

Olive, V., M. J. Bennett, J. C. Walker, C. Ma, I. Jiang, C. Cordon-Cardo, Q. J. Li, S. W. Lowe, G. J. Hannon, and L. He. 2009. miR-19 is a key oncogenic component of mir-17-92. Genes Dev 23: 2839-2849.

Orian, A., A. L. Schwartz, A. Israel, S. Whiteside, C. Kahana, and A. Ciechanover. 1999. Structural motifs involved in ubiquitin-mediated processing of the NF-kappaB precursor p105: roles of the glycine-rich region and a downstream ubiquitination domain. Mol Cell Biol 19: 3664-3673.

Ossendorp, F., R. E. Toes, R. Offringa, S. H. van der Burg, and C. J. Melief. 2000. Importance of CD4(+) T helper cell responses in tumor immunity. Immunol Lett 74: 75-79.

Oukka, M., I. C. Ho, F. C. de la Brousse, T. Hoey, M. J. Grusby, and L. H. Glimcher. 1998. The transcription factor NFAT4 is involved in the generation and survival of T cells. Immunity 9: 295-304.

Pahl, H. L. 1999. Activators and target genes of Rel/NF-kappaB transcription factors. Oncogene 18: 6853-6866.

Palkowitsch, L., U. Marienfeld, C. Brunner, A. Eitelhuber, D. Krappmann, and R. B. Marienfeld. 2011. The Ca2+-dependent phosphatase calcineurin controls the formation of the Carma1-Bcl10-Malt1 complex during T cell receptor-induced NF-kappaB activation. J Biol Chem 286: 7522-7534.

Pan, M. G., Y. Xiong, and F. Chen. 2013. NFAT gene family in inflammation and cancer. Curr Mol Med 13: 543-554.

Pan, M., M. M. Winslow, L. Chen, A. Kuo, D. Felsher, and G. R. Crabtree. 2007. Enhanced NFATc1 nuclear occupancy causes T cell activation independent of CD28 costimulation. J Immunol 178: 4315-4321.

Pao, L. I., S. J. Famiglietti, and J. C. Cambier. 1998. Asymmetrical phosphorylation and function of immunoreceptor tyrosine-based activation motif tyrosines in B cell antigen receptor signal transduction. J Immunol 160: 3305-3314.

Pao, L. I., W. D. Bedzyk, C. Persin, and J. C. Cambier. 1997. Molecular targets of CD45 in B cell antigen receptor signal transduction. J Immunol 158: 1116-1124.

Parcej, D., and R. Tampe. 2010. ABC proteins in antigen translocation and viral inhibition. Nat Chem Biol 6: 572-580.

Park, Y. M. 2014. CD36, a scavenger receptor implicated in atherosclerosis. Exp Mol Med 46: e99.

Park, J. H., K. Kaushansky, and L. Levitt. 1993. Transcriptional regulation of interleukin 3 (IL3) in primary human T lymphocytes. Role of AP-1- and octamer-binding proteins in control of IL3 gene expression. J Biol Chem 268: 6299-6308.

Park, J., A. Takeuchi, and S. Sharma. 1996. Characterization of a new isoform of the NFAT (nuclear factor of activated T cells) gene family member NFATc. J Biol Chem 271: 20914-20921.

Pascal, L. E., J. Ai, R. Z. Vencio, E. F. Vencio, Y. Zhou, L. S. Page, L. D. True, Z. Wang, and A. Y. Liu. 2011. Differential Inductive Signaling of CD90 Prostate Cancer-Associated Fibroblasts Compared to Normal Tissue Stromal Mesenchyme Cells. Cancer Microenviron 4: 51-59.

Pasparakis, M., T. Luedde, and M. Schmidt-Supprian. 2006. Dissection of the NF-kappaB signalling cascade in transgenic and knockout mice. Cell Death Differ 13: 861-872.

Pasqualucci, L., M. Compagno, J. Houldsworth, S. Monti, A. Grunn, S. V. Nandula, J. C. Aster, V. V. Murty, M. A. Shipp, and R. Dalla-Favera. 2006. Inactivation of the PRDM1/BLIMP1 gene in diffuse large B cell lymphoma. J Exp Med 203: 311-317.

Pattenden, S. G., R. Klose, E. Karaskov, and R. Bremner. 2002. Interferon-gamma-induced chromatin remodeling at the CIITA locus is BRG1 dependent. EMBO J 21: 1978-1986.

Peng, S. L., A. J. Gerth, A. M. Ranger, and L. H. Glimcher. 2001. NFATc1 and NFATc2 together control both T and B cell activation and differentiation. Immunity 14: 13-20.

Penix, L. A., M. T. Sweetser, W. M. Weaver, J. P. Hoeffler, T. K. Kerppola, and C. B. Wilson. 1996. The proximal regulatory element of the interferon-gamma promoter mediates selective expression in T cells. J Biol Chem 271: 31964-31972.

Pepino, M. Y., O. Kuda, D. Samovski, and N. A. Abumrad. 2014. Structure-function of CD36 and importance of fatty acid signal transduction in fat metabolism. Annu Rev Nutr 34: 281-303.

Pepino, M. Y., O. Kuda, D. Samovski, and N. A. Abumrad. 2014. Structure-function of CD36 and importance of fatty acid signal transduction in fat metabolism. Annu Rev Nutr 34: 281-303.

Perez-Galan, P., M. Dreyling, and A. Wiestner. 2011. Mantle cell lymphoma: biology, pathogenesis, and the molecular basis of treatment in the genomic era. Blood 117: 26-38.

Perez-Galan, P., H. Mora-Jensen, M. A. Weniger, A. L. Shaffer, 3rd, E. G. Rizzatti, C. M. Chapman, C. C. Mo, L. S. Stennett, C. Rader, P. Liu, N. Raghavachari, M. Stetler-Stevenson, C. Yuan, S. Pittaluga, I.

Maric, K. M. Dunleavy, W. H. Wilson, L. M. Staudt, and A. Wiestner. 2011. Bortezomib resistance in mantle cell lymphoma is associated with plasmacytic differentiation. Blood 117: 542-552.

Pfeifer, M., M. Grau, D. Lenze, S. S. Wenzel, A. Wolf, B. Wollert-Wulf, K. Dietze, H. Nogai, B. Storek, H. Madle, B. Dorken, M. Janz, S. Dirnhofer, P. Lenz, M. Hummel, A. Tzankov, and G. Lenz. 2013. PTEN loss defines a PI3K/AKT pathway-dependent germinal center subtype of diffuse large B-cell lymphoma. Proc Natl Acad Sci U S A 110: 12420-12425.

Pfisterer, P., J. Hess, and T. Wirth. 1997. Identification of target genes of the lymphoid-specific transcription factor Oct2. Immunobiology 198: 217-226.

Pham, L. V., A. T. Tamayo, L. C. Yoshimura, Y. C. Lin-Lee, and R. J. Ford. 2005. Constitutive NF-kappaB and NFAT activation in aggressive B-cell lymphomas synergistically activates the CD154 gene and maintains lymphoma cell survival. Blood 106: 3940-3947.

Phan, R. T., and R. Dalla-Favera. 2004. The BCL6 proto-oncogene suppresses p53 expression in germinal-centre B cells. Nature 432: 635-639.

Phan, R. T., M. Saito, K. Basso, H. Niu, and R. Dalla-Favera. 2005. BCL6 interacts with the transcription factor Miz-1 to suppress the cyclin-dependent kinase inhibitor p21 and cell cycle arrest in germinal center B cells. Nat Immunol 6: 1054-1060.

Plas, D. R., and C. B. Thompson. 2003. Akt activation promotes degradation of tuberin and FOXO3a via the proteasome. J Biol Chem 278: 12361-12366.

Pober, J. S., M. A. Gimbrone, Jr., R. S. Cotran, C. S. Reiss, S. J. Burakoff, W. Fiers, and K. A. Ault. 1983. Ia expression by vascular endothelium is inducible by activated T cells and by human gamma interferon. J Exp Med 157: 1339-1353.

Pont, S. 1987. Thy-1: a lymphoid cell subset marker capable of delivering an activation signal to mouse T lymphocytes. Biochimie 69: 315-320.

Project, T. N.-H. s. L. C. 1997. A clinical evaluation of the International Lymphoma Study Group classification of non-Hodgkin's lymphoma. . Blood 89: 3909-3918.

Rahal, R., M. Frick, R. Romero, J. M. Korn, R. Kridel, F. C. Chan, B. Meissner, H. E. Bhang, D. Ruddy, A. Kauffmann, A. Farsidjani, A. Derti, D. Rakiec, T. Naylor, E. Pfister, S. Kovats, S. Kim, K. Dietze, B. Dorken, C. Steidl, A. Tzankov, M. Hummel, J. Monahan, M. P. Morrissey, C. Fritsch, W. R. Sellers, V. G. Cooke, R. D. Gascoyne, G. Lenz, and F. Stegmeier. 2014. Pharmacological and genomic profiling identifies NF-kappaB-targeted treatment strategies for mantle cell lymphoma. Nat Med 20: 87-92.

Ramakrishnan, P., W. Wang, and D. Wallach. 2004. Receptor-specific signaling for both the alternative and the canonical NF-kappaB activation pathways by NF-kappaB-inducing kinase. Immunity 21: 477-489.

Randall, K. L. 2016. Rituximab in autoimmune diseases. Aust Prescr 39: 131-134.

Ranger, A. M., M. Oukka, J. Rengarajan, and L. H. Glimcher. 1998. Inhibitory function of two NFAT family members in lymphoid homeostasis and Th2 development. Immunity 9: 627-635.

Ranger, A. M., M. R. Hodge, E. M. Gravallese, M. Oukka, L. Davidson, F. W. Alt, F. C. de la Brousse, T. Hoey, M. Grusby, and L. H. Glimcher. 1998. Delayed lymphoid repopulation with defects in IL-4-driven responses produced by inactivation of NF-ATc. Immunity 8: 125-134.

Rao, A., C. Luo, and P. G. Hogan. 1997. Transcription factors of the NFAT family: regulation and function. Annu Rev Immunol 15: 707-747.

Rassidakis, G. Z., A. Thomaides, C. Atwell, R. Ford, D. Jones, F. X. Claret, and L. J. Medeiros. 2005. JunB expression is a common feature of CD30+ lymphomas and lymphomatoid papulosis. Mod Pathol 18: 1365-1370.

Razani, B., A. D. Reichardt, and G. Cheng. 2011. Non-canonical NF-kappaB signaling activation and regulation: principles and perspectives. Immunol Rev 244: 44-54.

Rebeaud, F., S. Hailfinger, A. Posevitz-Fejfar, M. Tapernoux, R. Moser, D. Rueda, O. Gaide, M. Guzzardi, E. M. Iancu, N. Rufer, N. Fasel, and M. Thome. 2008. The proteolytic activity of the paracaspase MALT1 is key in T cell activation. Nat Immunol 9: 272-281.

Rege, T. A., and J. S. Hagood. 2006. Thy-1 as a regulator of cell-cell and cell-matrix interactions in axon regeneration, apoptosis, adhesion, migration, cancer, and fibrosis. FASEB J 20: 1045-1054.

Rehnberg, M., S. Amu, A. Tarkowski, M. I. Bokarewa, and M. Brisslert. 2009. Short- and long-term effects of anti-CD20 treatment on B cell ontogeny in bone marrow of patients with rheumatoid arthritis. Arthritis Res Ther 11: R123.

Reith, W., and B. Mach. 2001. The bare lymphocyte syndrome and the regulation of MHC expression. Annu Rev Immunol 19: 331-373.

Rengarajan, J., K. A. Mowen, K. D. McBride, E. D. Smith, H. Singh, and L. H. Glimcher. 2002. Interferon regulatory factor 4 (IRF4) interacts with NFATc2 to modulate interleukin 4 gene expression. J Exp Med 195: 1003-1012.

Riemann, M., R. Endres, S. Liptay, K. Pfeffer, and R. M. Schmid. 2005. The IkappaB protein Bcl-3 negatively regulates transcription of the IL-10 gene in macrophages. J Immunol 175: 3560-3568.

Riemersma, S. A., E. S. Jordanova, R. F. Schop, K. Philippo, L. H. Looijenga, E. Schuuring, and P. M. Kluin. 2000. Extensive genetic alterations of the HLA region, including homozygous deletions of HLA class II genes in B-cell lymphomas arising in immune-privileged sites. Blood 96: 3569-3577.

Rimsza, L. M., P. Farinha, D. A. Fuchs, H. Masoudi, J. M. Connors, and R. D. Gascoyne. 2007. HLA-DR protein status predicts survival in patients with diffuse large B-cell lymphoma treated on the MACOP-B chemotherapy regimen. Leuk Lymphoma 48: 542-546.

Rimsza, L. M., R. A. Roberts, T. P. Miller, J. M. Unger, M. LeBlanc, R. M. Braziel, D. D. Weisenberger, W. C. Chan, H. K. Muller-Hermelink, E. S. Jaffe, R. D. Gascoyne, E. Campo, D. A. Fuchs, C. M. Spier, R. I. Fisher, J. Delabie, A. Rosenwald, L. M. Staudt, and T. M. Grogan. 2004. Loss of MHC class II gene and protein expression in diffuse large B-cell lymphoma is related to decreased tumor immunosurveillance and poor patient survival regardless of other prognostic factors: a follow-up study from the Leukemia and Lymphoma Molecular Profiling Project. Blood 103: 4251-4258.

Rimsza, L. M., R. A. Roberts, E. Campo, T. M. Grogan, S. Bea, I. Salaverria, A. Zettl, A. Rosenwald, G. Ott, H. K. Muller-Hermelink, J. Delabie, R. I. Fisher, J. M. Unger, M. Leblanc, L. M. Staudt, E. S. Jaffe, R. D. Gascoyne, W. C. Chan, D. D. Weisenburger, T. Greiner, R. M. Braziel, and T. P. Miller. 2006. Loss of major histocompatibility class II expression in non-immune-privileged site diffuse large B-cell lymphoma is highly coordinated and not due to chromosomal deletions. Blood 107: 1101-1107.

Rincon, M., H. Enslen, J. Raingeaud, M. Recht, T. Zapton, M. S. Su, L. A. Penix, R. J. Davis, and R. A. Flavell. 1998. Interferon-gamma expression by Th1 effector T cells mediated by the p38 MAP kinase signaling pathway. EMBO J 17: 2817-2829.

Ritz, O., K. Rommel, K. Dorsch, E. Kelsch, J. Melzner, M. Buck, K. Leroy, V. Papadopoulou, S. Wagner, R. Marienfeld, S. Bruderlein, J. K. Lennerz, and P. Moller. 2013. STAT6-mediated BCL6 repression in primary mediastinal B-cell lymphoma (PMBL). Oncotarget 4: 1093-1102.

Robbs, B. K., A. L. Cruz, M. B. Werneck, G. P. Mognol, and J. P. Viola. 2008. Dual roles for NFAT transcription factor genes as oncogenes and tumor suppressors. Mol Cell Biol 28: 7168-7181.

Roberts, R. A., G. Wright, A. R. Rosenwald, M. A. Jaramillo, T. M. Grogan, T. P. Miller, Y. Frutiger, W. C. Chan, R. D. Gascoyne, G. Ott, H. K. Muller-Hermelink, L. M. Staudt, and L. M. Rimsza. 2006. Loss of major histocompatibility class II gene and protein expression in primary mediastinal large B-cell lymphoma is highly coordinated and related to poor patient survival. Blood 108: 311-318.

Roelse, J., M. Gromme, F. Momburg, G. Hammerling, and J. Neefjes. 1994. Trimming of TAP-translocated peptides in the endoplasmic reticulum and in the cytosol during recycling. J Exp Med 180: 1591-1597.

Roffler-Tarlov, S., J. J. Brown, E. Tarlov, J. Stolarov, D. L. Chapman, M. Alexiou, and V. E. Papaioannou. 1996. Programmed cell death in the absence of c-Fos and c-Jun. Development 122: 1-9.

Rolli, V., M. Gallwitz, T. Wossning, A. Flemming, W. W. Schamel, C. Zurn, and M. Reth. 2002. Amplification of B cell antigen receptor signaling by a Syk/ITAM positive feedback loop. Mol Cell 10: 1057-1069.

Rooney, J. W., T. Hoey, and L. H. Glimcher. 1995. Coordinate and cooperative roles for NF-AT and AP-1 in the regulation of the murine IL-4 gene. Immunity 2: 473-483.

Roschewski, M., L. M. Staudt, and W. H. Wilson. 2014. Diffuse large B-cell lymphoma-treatment approaches in the molecular era. Nat Rev Clin Oncol 11: 12-23.

Rosenwald, A., G. Wright, K. Leroy, X. Yu, P. Gaulard, R. D. Gascoyne, W. C. Chan, T. Zhao, C. Haioun, T. C. Greiner, D. D. Weisenburger, J. C. Lynch, J. Vose, J. O. Armitage, E. B. Smeland, S. Kvaloy, H. Holte, J. Delabie, E. Campo, E. Montserrat, A. Lopez-Guillermo, G. Ott, H. K. Muller-Hermelink, J. M. Connors, R. Braziel, T. M. Grogan, R. I. Fisher, T. P. Miller, M. LeBlanc, M. Chiorazzi, H. Zhao, L. Yang, J. Powell, W. H. Wilson, E. S. Jaffe, R. Simon, R. D. Klausner, and L. M. Staudt. 2003. Molecular diagnosis of primary mediastinal B cell lymphoma identifies a clinically favorable subgroup of diffuse large B cell lymphoma related to Hodgkin lymphoma. J Exp Med 198: 851-862.

Rosenwald, A., G. Wright, W. C. Chan, J. M. Connors, E. Campo, R. I. Fisher, R. D. Gascoyne, H. K. Muller-Hermelink, E. B. Smeland, J. M. Giltnane, E. M. Hurt, H. Zhao, L. Averett, L. Yang, W. H. Wilson, E. S. Jaffe, R. Simon, R. D. Klausner, J. Powell, P. L. Duffey, D. L. Longo, T. C. Greiner, D. D. Weisenburger, W. G. Sanger, B. J. Dave, J. C. Lynch, J. Vose, J. O. Armitage, E. Montserrat, A. Lopez-Guillermo, T. M. Grogan, T. P. Miller, M. LeBlanc, G. Ott, S. Kvaloy, J. Delabie, H. Holte, P. Krajci, T. Stokke, L. M. Staudt, and P. Lymphoma/Leukemia Molecular Profiling. 2002. The use of molecular profiling to predict survival after chemotherapy for diffuse large-B-cell lymphoma. N Engl J Med 346: 1937-1947.

Rossi, D., C. Ciardullo, and G. Gaidano. 2013. Genetic aberrations of signaling pathways in lymphomagenesis: revelations from next generation sequencing studies. Semin Cancer Biol 23: 422-430.

Rowley, R. B., A. L. Burkhardt, H. G. Chao, G. R. Matsueda, and J. B. Bolen. 1995. Syk protein-tyrosine kinase

is regulated by tyrosine-phosphorylated Ig alpha/Ig beta immunoreceptor tyrosine activation motif binding and autophosphorylation. J Biol Chem 270: 11590-11594.

Roy, S., R. Charboneau, K. Cain, S. DeTurris, D. Melnyk, and R. A. Barke. 1999. Deficiency of the transcription factor c-fos increases lipopolysaccharide-induced macrophage interleukin 12 production. Surgery 126: 239-247.

Ruan, Q., S. J. Zheng, S. Palmer, R. J. Carmody, and Y. H. Chen. 2010. Roles of Bcl-3 in the pathogenesis of murine type 1 diabetes. Diabetes 59: 2549-2557.

Rueda, D., O. Gaide, L. Ho, E. Lewkowicz, F. Niedergang, S. Hailfinger, F. Rebeaud, M. Guzzardi, B. Conne, M. Thelen, J. Delon, U. Ferch, T. W. Mak, J. Ruland, J. Schwaller, and M. Thome. 2007. Bcl10 controls TCR- and FcgammaR-induced actin polymerization. J Immunol 178: 4373-4384.

Ruefli-Brasse, A. A., D. M. French, and V. M. Dixit. 2003. Regulation of NF-kappaB-dependent lymphocyte activation and development by paracaspase. Science 302: 1581-1584.

Rui, L., N. C. Emre, M. J. Kruhlak, H. J. Chung, C. Steidl, G. Slack, G. W. Wright, G. Lenz, V. N. Ngo, A. L. Shaffer, W. Xu, H. Zhao, Y. Yang, L. Lamy, R. E. Davis, W. Xiao, J. Powell, D. Maloney, C. J. Thomas, P. Moller, A. Rosenwald, G. Ott, H. K. Muller-Hermelink, K. Savage, J. M. Connors, L. M. Rimsza, E. Campo, E. S. Jaffe, J. Delabie, E. B. Smeland, D. D. Weisenburger, W. C. Chan, R. D. Gascoyne, D. Levens, and L. M. Staudt. 2010. Cooperative epigenetic modulation by cancer amplicon genes. Cancer Cell 18: 590-605.

Ruland, J., G. S. Duncan, A. Wakeham, and T. W. Mak. 2003. Differential requirement for Malt1 in T and B cell antigen receptor signaling. Immunity 19: 749-758.

Rutella, S., C. Rumi, A. Di Mario, and G. Leone. 1997. Expression of thrombospondin receptor (CD36) in chronic B-cell lymphoproliferative disorders: a role in tumor metastasis? Eur J Histochem 41 Suppl 2: 53-54.

Rutella, S., C. Rumi, P. Puggioni, T. Barberi, A. Di Mario, L. M. Larocca, and G. Leone. 1999. Expression of thrombospondin receptor (CD36) in B-cell chronic lymphocytic leukemia as an indicator of tumor cell dissemination. Haematologica 84: 419-424.

Ryseck, R. P., P. Bull, M. Takamiya, V. Bours, U. Siebenlist, P. Dobrzanski, and R. Bravo. 1992. RelB, a new Rel family transcription activator that can interact with p50-NF-kappa B. Mol Cell Biol 12: 674-684.

Saito, M., U. Novak, E. Piovan, K. Basso, P. Sumazin, C. Schneider, M. Crespo, Q. Shen, G. Bhagat, A. Califano, A. Chadburn, L. Pasqualucci, and R. Dalla-Favera. 2009. BCL6 suppression of BCL2 via Miz1 and its disruption in diffuse large B cell lymphoma. Proc Natl Acad Sci U S A 106: 11294-11299.

Saitoh, T., M. Nakayama, H. Nakano, H. Yagita, N. Yamamoto, and S. Yamaoka. 2003. TWEAK induces NF-kappaB2 p100 processing and long lasting NF-kappaB activation. J Biol Chem 278: 36005-36012.

Salama, M. E., M. Rajan Mariappan, K. Inamdar, S. R. Tripp, and S. L. Perkins. 2010. The value of CD23 expression as an additional marker in distinguishing mediastinal (thymic) large B-cell lymphoma from Hodgkin lymphoma. Int J Surg Pathol 18: 121-128.

Sales, K. J., V. Grant, I. H. Cook, D. Maldonado-Perez, R. A. Anderson, A. R. Williams, and H. N. Jabbour. 2010. Interleukin-11 in endometrial adenocarcinoma is regulated by prostaglandin F2alpha-F-prostanoid receptor interaction via the calcium-calcineurin-nuclear factor of activated T cells pathway and negatively regulated by the regulator of calcineurin-1. Am J Pathol 176: 435-445.

Sales, K. J., D. Maldonado-Perez, V. Grant, R. D. Catalano, M. R. Wilson, P. Brown, A. R. Williams, R. A. Anderson, E. A. Thompson, and H. N. Jabbour. 2009. Prostaglandin F(2alpha)-F-prostanoid receptor regulates CXCL8 expression in endometrial adenocarcinoma cells via the calcium-calcineurin-NFAT pathway. Biochim Biophys Acta 1793: 1917-1928.

Samovski, D., J. Sun, T. Pietka, R. W. Gross, R. H. Eckel, X. Su, P. D. Stahl, and N. A. Abumrad. 2015. Regulation of AMPK activation by CD36 links fatty acid uptake to beta-oxidation. Diabetes 64: 353-359.

Saric, T., S. C. Chang, A. Hattori, I. A. York, S. Markant, K. L. Rock, M. Tsujimoto, and A. L. Goldberg. 2002. An IFN-gamma-induced aminopeptidase in the ER, ERAP1, trims precursors to MHC class I-presented peptides. Nat Immunol 3: 1169-1176.

Savage, K. J., S. Monti, J. L. Kutok, G. Cattoretti, D. Neuberg, L. De Leval, P. Kurtin, P. Dal Cin, C. Ladd, F. Feuerhake, R. C. Aguiar, S. Li, G. Salles, F. Berger, W. Jing, G. S. Pinkus, T. Habermann, R. Dalla-Favera, N. L. Harris, J. C. Aster, T. R. Golub, and M. A. Shipp. 2003. The molecular signature of mediastinal large B-cell lymphoma differs from that of other diffuse large B-cell lymphomas and shares features with classical Hodgkin lymphoma. Blood 102: 3871-3879.

Saveanu, L., O. Carroll, V. Lindo, M. Del Val, D. Lopez, Y. Lepelletier, F. Greer, L. Schomburg, D. Fruci, G. Niedermann, and P. M. van Endert. 2005. Concerted peptide trimming by human ERAP1 and ERAP2 aminopeptidase complexes in the endoplasmic reticulum. Nat Immunol 6: 689-697.

Schanke, J. T., A. Marcuzzi, R. P. Podzorski, and B. Van Ness. 1994. An AP1 binding site upstream of the kappa immunoglobulin intron enhancer binds inducible factors and contributes to expression. Nucleic

Acids Res 22: 5425-5432.

Scharenberg, A. M., O. El-Hillal, D. A. Fruman, L. O. Beitz, Z. Li, S. Lin, I. Gout, L. C. Cantley, D. J. Rawlings, and J. P. Kinet. 1998. Phosphatidylinositol-3,4,5-trisphosphate (PtdIns-3,4,5-P3)/Tec kinase-dependent calcium signaling pathway: a target for SHIP-mediated inhibitory signals. EMBO J 17: 1961-1972.

Scharschmidt, E., E. Wegener, V. Heissmeyer, A. Rao, and D. Krappmann. 2004. Degradation of Bcl10 induced by T-cell activation negatively regulates NF-kappa B signaling. Mol Cell Biol 24: 3860-3873.

Schmidlin, H., S. A. Diehl, M. Nagasawa, F. A. Scheeren, R. Schotte, C. H. Uittenbogaart, H. Spits, and B. Blom. 2008. Spi-B inhibits human plasma cell differentiation by repressing BLIMP1 and XBP-1 expression. Blood 112: 1804-1812.

Schmitz, R., M. L. Hansmann, V. Bohle, J. I. Martin-Subero, S. Hartmann, G. Mechtersheimer, W. Klapper, I. Vater, M. Giefing, S. Gesk, J. Stanelle, R. Siebert, and R. Kuppers. 2009. TNFAIP3 (A20) is a tumor suppressor gene in Hodgkin lymphoma and primary mediastinal B cell lymphoma. J Exp Med 206: 981-989.

Schubert, U., L. C. Anton, J. Gibbs, C. C. Norbury, J. W. Yewdell, and J. R. Bennink. 2000. Rapid degradation of a large fraction of newly synthesized proteins by proteasomes. Nature 404: 770-774.

Schuetz, J. M., N. A. Johnson, R. D. Morin, D. W. Scott, K. Tan, S. Ben-Nierah, M. Boyle, G. W. Slack, M. A. Marra, J. M. Connors, A. R. Brooks-Wilson, and R. D. Gascoyne. 2012. BCL2 mutations in diffuse large B-cell lymphoma. Leukemia 26: 1383-1390.

Schuh, K., B. Kneitz, J. Heyer, U. Bommhardt, E. Jankevics, F. Berberich-Siebelt, K. Pfeffer, H. K. Muller-Hermelink, A. Schimpl, and E. Serfling. 1998. Retarded thymic involution and massive germinal center formation in NF-ATp-deficient mice. Eur J Immunol 28: 2456-2466.

Schuster, M., M. Annemann, C. Plaza-Sirvent, and I. Schmitz. 2013. Atypical IkappaB proteins - nuclear modulators of NF-kappaB signaling. Cell Commun Signal 11: 23.

Schuster, M., R. Glauben, C. Plaza-Sirvent, L. Schreiber, M. Annemann, S. Floess, A. A. Kuhl, L. K. Clayton, T. Sparwasser, K. Schulze-Osthoff, K. Pfeffer, J. Huehn, B. Siegmund, and I. Schmitz. 2012. IkappaB(NS) protein mediates regulatory T cell development via induction of the Foxp3 transcription factor. Immunity 37: 998-1008.

Schwarz, E. M., P. Krimpenfort, A. Berns, and I. M. Verma. 1997. Immunological defects in mice with a targeted disruption in Bcl-3. Genes Dev 11: 187-197.

Sen, R., and D. Baltimore. 1986. Multiple nuclear factors interact with the immunoglobulin enhancer sequences. Cell 46: 705-716.

Serwold, T., F. Gonzalez, J. Kim, R. Jacob, and N. Shastri. 2002. ERAAP customizes peptides for MHC class I molecules in the endoplasmic reticulum. Nature 419: 480-483.

Seshadri, S., Y. Kannan, S. Mitra, J. Parker-Barnes, and M. D. Wewers. 2009. MAIL regulates human monocyte IL-6 production. J Immunol 183: 5358-5368.

Sezaki, N., F. Ishimaru, T. Tabayashi, I. Kataoka, K. Nakase, K. Fujii, T. Kozuka, H. Nakayama, M. Harada, and M. Tanimoto. 2003. The type 1 CD10/neutral endopeptidase 24.11 promoter: functional characterization of the 5'-untranslated region. Br J Haematol 123: 177-183.

Shaffer, A. L., 3rd, R. M. Young, and L. M. Staudt. 2012. Pathogenesis of human B cell lymphomas. Annu Rev Immunol 30: 565-610.

Shaffer, A. L., X. Yu, Y. He, J. Boldrick, E. P. Chan, and L. M. Staudt. 2000. BCL-6 represses genes that function in lymphocyte differentiation, inflammation, and cell cycle control. Immunity 13: 199-212.

Shaffer, A. L., K. I. Lin, T. C. Kuo, X. Yu, E. M. Hurt, A. Rosenwald, J. M. Giltnane, L. Yang, H. Zhao, K. Calame, and L. M. Staudt. 2002. Blimp-1 orchestrates plasma cell differentiation by extinguishing the mature B cell gene expression program. Immunity 17: 51-62.

Shaikh, M. V., M. Kala, and M. Nivsarkar. 2016. CD90 a potential cancer stem cell marker and a therapeutic target. Cancer Biomark 16: 301-307.

Shao, A. W., H. Sun, Y. Geng, Q. Peng, P. Wang, J. Chen, T. Xiong, R. Cao, and J. Tang. 2016. Bclaf1 is an important NF-kappaB signaling transducer and C/EBPbeta regulator in DNA damage-induced senescence. Cell Death Differ 23: 865-875.

Shapiro-Shelef, M., K. I. Lin, D. Savitsky, J. Liao, and K. Calame. 2005. Blimp-1 is required for maintenance of long-lived plasma cells in the bone marrow. J Exp Med 202: 1471-1476.

Shaw, J., K. Meerovitch, R. C. Bleackley, and V. Paetkau. 1988. Mechanisms regulating the level of IL-2 mRNA in T lymphocytes. J Immunol 140: 2243-2248.

Shenoy, P. J., N. Malik, A. Nooka, R. Sinha, K. C. Ward, O. W. Brawley, J. Lipscomb, and C. R. Flowers. 2011. Racial differences in the presentation and outcomes of diffuse large B-cell lymphoma in the United States. Cancer 117: 2530-2540.

Shinohara, H., T. Yasuda, Y. Aiba, H. Sanjo, M. Hamadate, H. Watarai, H. Sakurai, and T. Kurosaki. 2005.

PKC beta regulates BCR-mediated IKK activation by facilitating the interaction between TAK1 and CARMA1. J Exp Med 202: 1423-1431.

Shirane, M., S. Hatakeyama, K. Hattori, K. Nakayama, and K. Nakayama. 1999. Common pathway for the ubiquitination of IkappaBalpha, IkappaBbeta, and IkappaBepsilon mediated by the F-box protein FWD1. J Biol Chem 274: 28169-28174.

Sica, A., L. Dorman, V. Viggiano, M. Cippitelli, P. Ghosh, N. Rice, and H. A. Young. 1997. Interaction of NF-kappaB and NFAT with the interferon-gamma promoter. J Biol Chem 272: 30412-30420.

Siggers, T., A. B. Chang, A. Teixeira, D. Wong, K. J. Williams, B. Ahmed, J. Ragoussis, I. A. Udalova, S. T. Smale, and M. L. Bulyk. 2011. Principles of dimer-specific gene regulation revealed by a comprehensive characterization of NF-kappaB family DNA binding. Nat Immunol 13: 95-102.

Silverstein, R. L., and M. Febbraio. 2009. CD36, a scavenger receptor involved in immunity, metabolism, angiogenesis, and behavior. Sci Signal 2: re3.

Silverstein, R. L., W. Li, Y. M. Park, and S. O. Rahaman. 2010. Mechanisms of cell signaling by the scavenger receptor CD36: implications in atherosclerosis and thrombosis. Trans Am Clin Climatol Assoc 121: 206-220.

Sinha, N., L. Lantigua, M. Niazi, and G. Diaz-Fuentes. 2013. An elderly lady with Fever of unknown etiology and severe pulmonary hypertension: intravascular lymphoma-an elusive diagnosis. Case Rep Med 2013: 153798.

Snow, A. L., W. Xiao, J. R. Stinson, W. Lu, B. Chaigne-Delalande, L. Zheng, S. Pittaluga, H. F. Matthews, R. Schmitz, S. Jhavar, S. Kuchen, L. Kardava, W. Wang, I. T. Lamborn, H. Jing, M. Raffeld, S. Moir, T. A. Fleisher, L. M. Staudt, H. C. Su, and M. J. Lenardo. 2012. Congenital B cell lymphocytosis explained by novel germline CARD11 mutations. J Exp Med 209: 2247-2261.

Sommer, K., B. Guo, J. L. Pomerantz, A. D. Bandaranayake, M. E. Moreno-Garcia, Y. L. Ovechkina, and D. J. Rawlings. 2005. Phosphorylation of the CARMA1 linker controls NF-kappaB activation. Immunity 23: 561-574.

Song, M. S., L. Salmena, and P. P. Pandolfi. 2012. The functions and regulation of the PTEN tumour suppressor. Nat Rev Mol Cell Biol 13: 283-296.

Sonneveld, P., M. de Ridder, H. van der Lelie, K. Nieuwenhuis, H. Schouten, A. Mulder, I. van Reijswoud, W. Hop, and B. Lowenberg. 1995. Comparison of doxorubicin and mitoxantrone in the treatment of elderly patients with advanced diffuse non-Hodgkin's lymphoma using CHOP versus CNOP chemotherapy. J Clin Oncol 13: 2530-2539.

Srahna, M., J. E. Remacle, K. Annamalai, S. Pype, D. Huylebroeck, M. A. Boogaerts, and P. Vandenberghe. 2001. NF-kappaB is involved in the regulation of CD154 (CD40 ligand) expression in primary human T cells. Clin Exp Immunol 125: 229-236.

Srinivasan, L., Y. Sasaki, D. P. Calado, B. Zhang, J. H. Paik, R. A. DePinho, J. L. Kutok, J. F. Kearney, K. L. Otipoby, and K. Rajewsky. 2009. PI3 kinase signals BCR-dependent mature B cell survival. Cell 139: 573-586.

Staal, J., Y. Driege, T. Bekaert, A. Demeyer, D. Muyllaert, P. Van Damme, K. Gevaert, and R. Beyaert. 2011. T-cell receptor-induced JNK activation requires proteolytic inactivation of CYLD by MALT1. EMBO J 30: 1742-1752.

Stark GR, K. I., Williams BR, Silverman RH, Schreiber RD. 1998. How cells respond to interferons. Annu Rev Biochem. 67: 227–264.

Steidl, C., and R. D. Gascoyne. 2011. The molecular pathogenesis of primary mediastinal large B-cell lymphoma. Blood 118: 2659-2669.

Steimle, V., L. A. Otten, M. Zufferey, and B. Mach. 1993. Complementation cloning of an MHC class II transactivator mutated in hereditary MHC class II deficiency (or bare lymphocyte syndrome). Cell 75: 135-146.

Stein, B., A. S. Baldwin, Jr., D. W. Ballard, W. C. Greene, P. Angel, and P. Herrlich. 1993. Cross-coupling of the NF-kappa B p65 and Fos/Jun transcription factors produces potentiated biological function. EMBO J 12: 3879-3891.

Steinbach, W. J., J. L. Reedy, R. A. Cramer, Jr., J. R. Perfect, and J. Heitman. 2007. Harnessing calcineurin as a novel anti-infective agent against invasive fungal infections. Nat Rev Microbiol 5: 418-430.

Stroud, J. C., and L. Chen. 2003. Structure of NFAT bound to DNA as a monomer. J Mol Biol 334: 1009-1022.

Sun, S. C. 2011. Non-canonical NF-kappaB signaling pathway. Cell Res 21: 71-85.

Sun, S. C. 2012. The noncanonical NF-kappaB pathway. Immunol Rev 246: 125-140.

Sun, L., L. Deng, C. K. Ea, Z. P. Xia, and Z. J. Chen. 2004. The TRAF6 ubiquitin ligase and TAK1 kinase mediate IKK activation by BCL10 and MALT1 in T lymphocytes. Mol Cell 14: 289-301.

Swerdlow SH, C. E., Harris NL. 2008. WHO classification of tumours of haematopoietic and lymphoid tissues. , IARC, Lyon, France: .

Takao, S., N. Sakai, M. Hatano, T. Koizumi, K. Hanioka, U. Ruther, and T. Tokuhisa. 1991. IgG response is impaired in H2-c-fos transgenic mice. Int Immunol 3: 369-375.

Takata, M., H. Sabe, A. Hata, T. Inazu, Y. Homma, T. Nukada, H. Yamamura, and T. Kurosaki. 1994. Tyrosine kinases Lyn and Syk regulate B cell receptor-coupled Ca2+ mobilization through distinct pathways. EMBO J 13: 1341-1349.

Tam, W., M. Gomez, A. Chadburn, J. W. Lee, W. C. Chan, and D. M. Knowles. 2006. Mutational analysis of PRDM1 indicates a tumor-suppressor role in diffuse large B-cell lymphomas. Blood 107: 4090-4100.

Tamir, I., J. M. Dal Porto, and J. C. Cambier. 2000. Cytoplasmic protein tyrosine phosphatases SHP-1 and SHP-2: regulators of B cell signal transduction. Curr Opin Immunol 12: 307-315.

Tanguay, D. A., J. A. Dickinson, B. J. McManus, L. Huo, T. L. Rothstein, and T. C. Chiles. 1994. Activation of AP-1 in primary B lymphocytes by surface immunoglobulin requires de novo Jun-B synthesis. Cell Immunol 158: 281-291.

Tassi, I., E. Claudio, H. Wang, W. Tang, H. L. Ha, S. Saret, A. Sher, D. Jankovic, and U. Siebenlist. 2015. Adaptive immune-mediated host resistance to Toxoplasma gondii is governed by the NF-kappaB regulator Bcl-3 in dendritic cells. Eur J Immunol 45: 1972-1979.

Tergaonkar, V., R. G. Correa, M. Ikawa, and I. M. Verma. 2005. Distinct roles of IkappaB proteins in regulating constitutive NF-kappaB activity. Nat Cell Biol 7: 921-923.

Terui, Y., N. Saad, S. Jia, F. McKeon, and J. Yuan. 2004. Dual role of sumoylation in the nuclear localization and transcriptional activation of NFAT1. J Biol Chem 279: 28257-28265.

Thibodeau, J., M. C. Bourgeois-Daigneault, G. Huppe, J. Tremblay, A. Aumont, M. Houde, E. Bartee, A. Brunet, M. E. Gauvreau, A. de Gassart, E. Gatti, M. Baril, M. Cloutier, S. Bontron, K. Fruh, D. Lamarre, and V. Steimle. 2008. Interleukin-10-induced MARCH1 mediates intracellular sequestration of MHC class II in monocytes. Eur J Immunol 38: 1225-1230.

Thome, M., J. E. Charton, C. Pelzer, and S. Hailfinger. 2010. Antigen receptor signaling to NF-kappaB via CARMA1, BCL10, and MALT1. Cold Spring Harb Perspect Biol 2: a003004.

Thompson, J. E., R. J. Phillips, H. Erdjument-Bromage, P. Tempst, and S. Ghosh. 1995. I kappa B-beta regulates the persistent response in a biphasic activation of NF-kappa B. Cell 80: 573-582.

Thorne, R. F., J. F. Marshall, D. R. Shafren, P. G. Gibson, I. R. Hart, and G. F. Burns. 2000. The integrins alpha3beta1 and alpha6beta1 physically and functionally associate with CD36 in human melanoma cells. Requirement for the extracellular domain OF CD36. J Biol Chem 275: 35264-35275.

Tiemann, M., C. Schrader, W. Klapper, M. H. Dreyling, E. Campo, A. Norton, F. Berger, P. Kluin, G. Ott, S. Pileri, E. Pedrinis, A. C. Feller, H. Merz, D. Janssen, M. L. Hansmann, H. Krieken, P. Moller, H. Stein, M. Unterhalt, W. Hiddemann, R. Parwaresch, and M. C. L. N. European. 2005. Histopathology, cell proliferation indices and clinical outcome in 304 patients with mantle cell lymphoma (MCL): a clinicopathological study from the European MCL Network. Br J Haematol 131: 29-38.

Tilzey, J. F., T. C. Chiles, and T. L. Rothstein. 1991. Jun-B gene expression mediated by the surface immunoglobulin receptor of primary B lymphocytes. Biochem Biophys Res Commun 175: 77-83.

Ting, J. P., and J. Trowsdale. 2002. Genetic control of MHC class II expression. Cell 109 Suppl: S21-33.

Toes, R. E., S. P. Schoenberger, E. I. van der Voort, R. Offringa, and C. J. Melief. 1998. CD40-CD40Ligand interactions and their role in cytotoxic T lymphocyte priming and anti-tumor immunity. Semin Immunol 10: 443-448.

Toney, L. M., G. Cattoretti, J. A. Graf, T. Merghoub, P. P. Pandolfi, R. Dalla-Favera, B. H. Ye, and A. L. Dent. 2000. BCL-6 regulates chemokine gene transcription in macrophages. Nat Immunol 1: 214-220.

Tontonoz, P., L. Nagy, J. G. Alvarez, V. A. Thomazy, and R. M. Evans. 1998. PPARgamma promotes monocyte/macrophage differentiation and uptake of oxidized LDL. Cell 93: 241-252.

Topalian, S. L., C. G. Drake, and D. M. Pardoll. 2012. Targeting the PD-1/B7-H1(PD-L1) pathway to activate anti-tumor immunity. Curr Opin Immunol 24: 207-212.

Torres, R. M., and K. Hafen. 1999. A negative regulatory role for Ig-alpha during B cell development. Immunity 11: 527-536.

Torres, R. M., H. Flaswinkel, M. Reth, and K. Rajewsky. 1996. Aberrant B cell development and immune response in mice with a compromised BCR complex. Science 272: 1804-1808.

Torres Raul M. , J. I., Harry W. Schroeder. 2008. pp. 53-77, Clinical Immunology. Elsevier.

Touma, M., D. B. Keskin, F. Shiroki, I. Saito, S. Koyasu, E. L. Reinherz, and L. K. Clayton. 2011. Impaired B cell development and function in the absence of IkappaBNS. J Immunol 187: 3942-3952.

Touma, M., V. Antonini, M. Kumar, S. L. Osborn, A. M. Bobenchik, D. B. Keskin, J. E. Connolly, M. J. Grusby, E. L. Reinherz, and L. K. Clayton. 2007. Functional role for I kappa BNS in T cell cytokine regulation as revealed by targeted gene disruption. J Immunol 179: 1681-1692.

Troen, G., V. Nygaard, T. K. Jenssen, I. M. Ikonomou, A. Tierens, E. Matutes, A. Gruszka-Westwood, D.

Catovsky, O. Myklebost, G. Lauritzsen, E. Hovig, and J. Delabie. 2004. Constitutive expression of the AP-1 transcription factors c-jun, junD, junB, and c-fos and the marginal zone B-cell transcription factor Notch2 in splenic marginal zone lymphoma. J Mol Diagn 6: 297-307.

Tsai, E. Y., J. Yie, D. Thanos, and A. E. Goldfeld. 1996. Cell-type-specific regulation of the human tumor necrosis factor alpha gene in B cells and T cells by NFATp and ATF-2/JUN. Mol Cell Biol 16: 5232-5244.

Tsai, E. Y., J. Jain, P. A. Pesavento, A. Rao, and A. E. Goldfeld. 1996. Tumor necrosis factor alpha gene regulation in activated T cells involves ATF-2/Jun and NFATp. Mol Cell Biol 16: 459-467.

Tunyaplin, C., A. L. Shaffer, C. D. Angelin-Duclos, X. Yu, L. M. Staudt, and K. L. Calame. 2004. Direct repression of prdm1 by Bcl-6 inhibits plasmacytic differentiation. J Immunol 173: 1158-1165.

Turner, M., P. J. Mee, P. S. Costello, O. Williams, A. A. Price, L. P. Duddy, M. T. Furlong, R. L. Geahlen, and V. L. Tybulewicz. 1995. Perinatal lethality and blocked B-cell development in mice lacking the tyrosine kinase Syk. Nature 378: 298-302.

Twa, D. D., F. C. Chan, S. Ben-Neriah, B. W. Woolcock, A. Mottok, K. L. Tan, G. W. Slack, J. Gunawardana, R. S. Lim, A. W. McPherson, R. Kridel, A. Telenius, D. W. Scott, K. J. Savage, S. P. Shah, R. D. Gascoyne, and C. Steidl. 2014. Genomic rearrangements involving programmed death ligands are recurrent in primary mediastinal large B-cell lymphoma. Blood 123: 2062-2065.

Ungefroren, H., S. Sebens, D. Seidl, H. Lehnert, and R. Hass. 2011. Interaction of tumor cells with the microenvironment. Cell Commun Signal 9: 18.

Vaidya, R., and T. E. Witzig. 2014. Prognostic factors for diffuse large B-cell lymphoma in the R(X)CHOP era. Ann Oncol 25: 2124-2133.

Vallabhapurapu, S., A. Matsuzawa, W. Zhang, P. H. Tseng, J. J. Keats, H. Wang, D. A. Vignali, P. L. Bergsagel, and M. Karin. 2008. Nonredundant and complementary functions of TRAF2 and TRAF3 in a ubiquitination cascade that activates NIK-dependent alternative NF-kappaB signaling. Nat Immunol 9: 1364-1370.

van Ham, S. M., E. P. Tjin, B. F. Lillemeier, U. Gruneberg, K. E. van Meijgaarden, L. Pastoors, D. Verwoerd, A. Tulp, B. Canas, D. Rahman, T. H. Ottenhoff, D. J. Pappin, J. Trowsdale, and J. Neefjes. 1997. HLA-DO is a negative modulator of HLA-DM-mediated MHC class II peptide loading. Curr Biol 7: 950-957.

Van Noesel, C. J., J. Borst, E. F. De Vries, and R. A. Van Lier. 1990. Identification of two distinct phosphoproteins as components of the human B cell antigen receptor complex. Eur J Immunol 20: 2789-2793.

Wang, J. K., T. X. Li, Y. F. Bai, and Z. H. Lu. 2003. Evaluating the binding affinities of NF-kappaB p50 homodimer to the wild-type and single-nucleotide mutant Ig-kappaB sites by the unimolecular dsDNA microarray. Anal Biochem 316: 192-201.

Wang, Z. E., S. L. Reiner, S. Zheng, D. K. Dalton, and R. M. Locksley. 1994. CD4+ effector cells default to the Th2 pathway in interferon gamma-deficient mice infected with Leishmania major. J Exp Med 179: 1367-1371.

Wang, C., L. Deng, M. Hong, G. R. Akkaraju, J. Inoue, and Z. J. Chen. 2001. TAK1 is a ubiquitin-dependent kinase of MKK and IKK. Nature 412: 346-351.

Wearsch, P. A., and P. Cresswell. 2008. The quality control of MHC class I peptide loading. Curr Opin Cell Biol 20: 624-631.

Wegener, E., A. Oeckinghaus, N. Papadopoulou, L. Lavitas, M. Schmidt-Supprian, U. Ferch, T. W. Mak, J. Ruland, V. Heissmeyer, and D. Krappmann. 2006. Essential role for IkappaB kinase beta in remodeling Carma1-Bcl10-Malt1 complexes upon T cell activation. Mol Cell 23: 13-23.

Whiteside, S. T., J. C. Epinat, N. R. Rice, and A. Israel. 1997. I kappa B epsilon, a novel member of the I kappa B family, controls RelA and cRel NF-kappa B activity. EMBO J 16: 1413-1426.

Wieczorek, M., E. T. Abualrous, J. Sticht, M. Alvaro-Benito, S. Stolzenberg, F. Noe, and C. Freund. 2017. Major Histocompatibility Complex (MHC) Class I and MHC Class II Proteins: Conformational Plasticity in Antigen Presentation. Front Immunol 8: 292.

Wienands, J., O. Larbolette, and M. Reth. 1996. Evidence for a preformed transducer complex organized by the B cell antigen receptor. Proc Natl Acad Sci U S A 93: 7865-7870.

Wilkinson, S. T., K. A. Vanpatten, D. R. Fernandez, P. Brunhoeber, K. E. Garsha, B. J. Glinsmann-Gibson, T. M. Grogan, J. Teruya-Feldstein, and L. M. Rimsza. 2012. Partial plasma cell differentiation as a mechanism of lost major histocompatibility complex class II expression in diffuse large B-cell lymphoma. Blood 119: 1459-1467.

Wilkinson, S. T., D. R. Fernandez, S. P. Murphy, R. M. Braziel, E. Campo, W. C. Chan, J. Delabie, R. D. Gascoyne, L. M. Staudt, E. S. Jaffe, A. Rosenwald, and L. M. Rimsza. 2009. Decreased major histocompatibility complex class II expression in diffuse large B-cell lymphoma does not correlate with CpG methylation of class II transactivator promoters III and IV. Leuk Lymphoma 50: 1875-1878.

Willingham, A. T., A. P. Orth, S. Batalov, E. C. Peters, B. G. Wen, P. Aza-Blanc, J. B. Hogenesch, and P. G. Schultz. 2005. A strategy for probing the function of noncoding RNAs finds a repressor of NFAT. Science 309: 1570-1573.

Wingfield, P. T. 2016. Use of protein folding reagents. Curr. Protoc. Protein Sci. 84: A.3A.1-A.3A.8.

Winslow, M. M., E. M. Gallo, J. R. Neilson, and G. R. Crabtree. 2006. The calcineurin phosphatase complex modulates immunogenic B cell responses. Immunity 24: 141-152.

Winston, J. T., P. Strack, P. Beer-Romero, C. Y. Chu, S. J. Elledge, and J. W. Harper. 1999. The SCFbeta-TRCP-ubiquitin ligase complex associates specifically with phosphorylated destruction motifs in IkappaBalpha and beta-catenin and stimulates IkappaBalpha ubiquitination in vitro. Genes Dev 13: 270-283.

Wong, D., A. Teixeira, S. Oikonomopoulos, P. Humburg, I. N. Lone, D. Saliba, T. Siggers, M. Bulyk, D. Angelov, S. Dimitrov, I. A. Udalova, and J. Ragoussis. 2011. Extensive characterization of NF-kappaB binding uncovers non-canonical motifs and advances the interpretation of genetic functional traits. Genome Biol 12: R70.

Wright, K. L., and J. P. Ting. 2006. Epigenetic regulation of MHC-II and CIITA genes. Trends Immunol 27: 405-412.

Wu, H., B. Rothermel, S. Kanatous, P. Rosenberg, F. J. Naya, J. M. Shelton, K. A. Hutcheson, J. M. DiMaio, E. N. Olson, R. Bassel-Duby, and R. S. Williams. 2001. Activation of MEF2 by muscle activity is mediated through a calcineurin-dependent pathway. EMBO J 20: 6414-6423.

Wu, Y., M. J. Nadler, L. A. Brennan, G. D. Gish, J. F. Timms, N. Fusaki, J. Jongstra-Bilen, N. Tada, T. Pawson, J. Wither, B. G. Neel, and N. Hozumi. 1998. The B-cell transmembrane protein CD72 binds to and is an in vivo substrate of the protein tyrosine phosphatase SHP-1. Curr Biol 8: 1009-1017.

Wulczyn, F. G., M. Naumann, and C. Scheidereit. 1992. Candidate proto-oncogene bcl-3 encodes a subunit-specific inhibitor of transcription factor NF-kappa B. Nature 358: 597-599.

Xanthoudakis, S., J. P. Viola, K. T. Shaw, C. Luo, J. D. Wallace, P. T. Bozza, D. C. Luk, T. Curran, and A. Rao. 1996. An enhanced immune response in mice lacking the transcription factor NFAT1. Science 272: 892-895.

Xiao, C., L. Srinivasan, D. P. Calado, H. C. Patterson, B. Zhang, J. Wang, J. M. Henderson, J. L. Kutok, and K. Rajewsky. 2008. Lymphoproliferative disease and autoimmunity in mice with increased miR-17-92 expression in lymphocytes. Nat Immunol 9: 405-414.

Xu, L. G., and H. B. Shu. 2002. TNFR-associated factor-3 is associated with BAFF-R and negatively regulates BAFF-R-mediated NF-kappa B activation and IL-10 production. J Immunol 169: 6883-6889.

Yaffe, M. B., and L. C. Cantley. 1999. Signal transduction. Grabbing phosphoproteins. Nature 402: 30-31.

Yamamoto, M., S. Yamazaki, S. Uematsu, S. Sato, H. Hemmi, K. Hoshino, T. Kaisho, H. Kuwata, O. Takeuchi, K. Takeshige, T. Saitoh, S. Yamaoka, N. Yamamoto, S. Yamamoto, T. Muta, K. Takeda, and S. Akira. 2004. Regulation of Toll/IL-1-receptor-mediated gene expression by the inducible nuclear protein IkappaBzeta. Nature 430: 218-222.

Yamashita, S., K. Hirano, T. Kuwasako, M. Janabi, Y. Toyama, M. Ishigami, and N. Sakai. 2007. Physiological and pathological roles of a multi-ligand receptor CD36 in atherogenesis; insights from CD36-deficient patients. Mol Cell Biochem 299: 19-22.

Yamauchi, S., H. Ito, and A. Miyajima. 2010. IkappaBeta, a nuclear IkappaB protein, positively regulates the NF-kappaB-mediated expression of proinflammatory cytokines. Proc Natl Acad Sci U S A 107: 11924-11929.

Yang, J., and M. Reth. 2010. Oligomeric organization of the B-cell antigen receptor on resting cells. Nature 467: 465-469.

Yang, X. Y., L. H. Wang, T. Chen, D. R. Hodge, J. H. Resau, L. DaSilva, and W. L. Farrar. 2000. Activation of human T lymphocytes is inhibited by peroxisome proliferator-activated receptor gamma (PPARgamma) agonists. PPARgamma co-association with transcription factor NFAT. J Biol Chem 275: 4541-4544.

Yang, Y., A. L. Shaffer, 3rd, N. C. Emre, M. Ceribelli, M. Zhang, G. Wright, W. Xiao, J. Powell, J. Platig, H. Kohlhammer, R. M. Young, H. Zhao, Y. Yang, W. Xu, J. J. Buggy, S. Balasubramanian, L. A. Mathews, P. Shinn, R. Guha, M. Ferrer, C. Thomas, T. A. Waldmann, and L. M. Staudt. 2012. Exploiting synthetic lethality for the therapy of ABC diffuse large B cell lymphoma. Cancer Cell 21: 723-737.

Yang, Y., R. Schmitz, J. Mitala, A. Whiting, W. Xiao, M. Ceribelli, G. W. Wright, H. Zhao, Y. Yang, W. Xu, A. Rosenwald, G. Ott, R. D. Gascoyne, J. M. Connors, L. M. Rimsza, E. Campo, E. S. Jaffe, J. Delabie, E. B. Smeland, R. M. Braziel, R. R. Tubbs, J. R. Cook, D. D. Weisenburger, W. C. Chan, A. Wiestner, M. J. Kruhlak, K. Iwai, F. Bernal, and L. M. Staudt. 2014. Essential role of the linear ubiquitin chain assembly complex in lymphoma revealed by rare germline polymorphisms. Cancer Discov 4: 480-493.

Yao, J., N. Mackman, T. S. Edgington, and S. T. Fan. 1997. Lipopolysaccharide induction of the tumor necrosis

factor-alpha promoter in human monocytic cells. Regulation by Egr-1, c-Jun, and NF-kappaB transcription factors. J Biol Chem 272: 17795-17801.

Yaron, A., H. Gonen, I. Alkalay, A. Hatzubai, S. Jung, S. Beyth, F. Mercurio, A. M. Manning, A. Ciechanover, and Y. Ben-Neriah. 1997. Inhibition of NF-kappa-B cellular function via specific targeting of the I-kappa-B-ubiquitin ligase. EMBO J 16: 6486-6494.

Yoeli-Lerner, M., Y. R. Chin, C. K. Hansen, and A. Toker. 2009. Akt/protein kinase b and glycogen synthase kinase-3beta signaling pathway regulates cell migration through the NFAT1 transcription factor. Mol Cancer Res 7: 425-432.

Yoeli-Lerner, M., G. K. Yiu, I. Rabinovitz, P. Erhardt, S. Jauliac, and A. Toker. 2005. Akt blocks breast cancer cell motility and invasion through the transcription factor NFAT. Mol Cell 20: 539-550.

Yoshida, H., H. Nishina, H. Takimoto, L. E. Marengere, A. C. Wakeham, D. Bouchard, Y. Y. Kong, T. Ohteki, A. Shahinian, M. Bachmann, P. S. Ohashi, J. M. Penninger, G. R. Crabtree, and T. W. Mak. 1998. The transcription factor NF-ATc1 regulates lymphocyte proliferation and Th2 cytokine production. Immunity 8: 115-124.

Young, R. M., and L. M. Staudt. 2013. Targeting pathological B cell receptor signalling in lymphoid malignancies. Nat Rev Drug Discov 12: 229-243.

Young, R. M., A. L. Shaffer, 3rd, J. D. Phelan, and L. M. Staudt. 2015. B-cell receptor signaling in diffuse large B-cell lymphoma. Semin Hematol 52: 77-85.

Zacharias, M., and S. Springer. 2004. Conformational flexibility of the MHC class I alpha1-alpha2 domain in peptide bound and free states: a molecular dynamics simulation study. Biophys J 87: 2203-2214.

Zarnegar, B. J., Y. Wang, D. J. Mahoney, P. W. Dempsey, H. H. Cheung, J. He, T. Shiba, X. Yang, W. C. Yeh, T. W. Mak, R. G. Korneluk, and G. Cheng. 2008. Noncanonical NF-kappaB activation requires coordinated assembly of a regulatory complex of the adaptors cIAP1, cIAP2, TRAF2 and TRAF3 and the kinase NIK. Nat Immunol 9: 1371-1378.

Zeng, H., L. Di, G. Fu, Y. Chen, X. Gao, L. Xu, X. Lin, and R. Wen. 2007. Phosphorylation of Bcl10 negatively regulates T-cell receptor-mediated NF-kappaB activation. Mol Cell Biol 27: 5235-5245.

Zhang, J., M. L. Billingsley, R. L. Kincaid, and R. P. Siraganian. 2000. Phosphorylation of Syk activation loop tyrosines is essential for Syk function. An in vivo study using a specific anti-Syk activation loop phosphotyrosine antibody. J Biol Chem 275: 35442-35447.

Zhang, F., F. P. Xu, Y. H. Liu, and H. G. Zhuang. 2011. [Signaling pathways in pathogenesis of diffuse large B-cell lymphoma]. Zhonghua Bing Li Xue Za Zhi 40: 282-285.

Zhang, H. W., N. L. Cheng, Z. W. Chen, J. F. Wang, S. H. Li, and W. Bai. 2011. Clinical Impact of t(14;18) in Diffuse Large B-cell Lymphoma. Chin J Cancer Res 23: 160-164.

Zhou, Y., H. Wang, W. Fang, J. E. Romaguer, Y. Zhang, K. B. Delasalle, L. Kwak, Q. Yi, X. L. Du, and M. Wang. 2008. Incidence trends of mantle cell lymphoma in the United States between 1992 and 2004. Cancer 113: 791-798.

Zhu, J., S. Thakolwiboon, X. Liu, M. Zhang, and D. M. Lubman. 2014. Overexpression of CD90 (Thy-1) in pancreatic adenocarcinoma present in the tumor microenvironment. PLoS One 9: e115507.

Zhu, Y. X., L. Y. Kang, W. Luo, C. C. Li, L. Yang, and Y. C. Yang. 1996. Multiple transcription factors are required for activation of human interleukin 9 gene in T cells. J Biol Chem 271: 15815-15822.

Zucca, E., E. Roggero, G. Pinotti, E. Pedrinis, C. Cappella, A. Venco, and F. Cavalli. 1995. Patterns of survival in mantle cell lymphoma. Ann Oncol 6: 257-262.

6. List of Figures

7. List of Tables

Danksagungen/Acknowledgements

Herzlich möchte ich mich bei **Dr. Stephan Hailfinger** bedanken, der mir die Möglichkeit gab in seiner Arbeitsgruppe meine Promotion zu machen und mir immer eine große Unterstützung bei allen Fragen rund um den Laboralltag war. Seine lockere und ermutigende Art hat mir in vielen Situationen wieder neue Motivation gegeben. Auch danke ich ihm für die sorgfältige Begutachtung dieser Arbeit.

Prof. Klaus Schulze-Osthoff danke ich für die Möglichkeit in seinen Labors den experimentellen Teil meiner Arbeit durchzuführen und dass er die Begutachtung dieser Arbeit übernommen hat.

PD Dr. Frank Essmann danke ich für die häufigen Aufmunterungen und spaßigen Momente und nicht zuletzt die Versorgung mit Stimmungsaufhellern in Form verschiedenster Fressalien.

Von Herzen möchte ich meinen **Eltern** danken, die mir immer ein zuverlässiger Rückhalt waren und sind.

Anna Schill danke ich für ihre aufmunternden Worte und Taten, ihren emotionalen Beistand und Verständnis.

Sebastian Lieb danke ich für die Hilfe bei der Durchführung des „BioLegend® LEGENDScreen™“.